Applications of SCET to the pair production of supersymmetric particles at hadron colliders

Dissertation
zur Erlangung des Grades "Doktor der Naturwissenschaften"
am Fachbereich Physik, Mathematik und Informatik
der Johannes Gutenberg-Universität
in Mainz

Alessandro Broggio
geboren in Bassano del Grappa

Mainz, 2013

Date of the oral exam: 4 February 2013
Dissertation submitted to the Johannes Gutenberg-Universität (Angabe D77)

Abstract

In this thesis we investigate the phenomenology of supersymmetric particles at hadron colliders beyond next-to-leading order (NLO) in perturbation theory. We discuss the foundations of Soft-Collinear Effective Theory (SCET) and, in particular, we explicitly construct the SCET Lagrangian for QCD. As an example, we discuss factorization and resummation for the Drell-Yan process in SCET. We use techniques from SCET to improve existing calculations of the production cross sections for slepton-pair production and top-squark-pair production at hadron colliders. As a first application, we implement soft-gluon resummation at next-to-next-to-next-to-leading logarithmic order (NNNLL) for slepton-pair production in the minimal supersymmetric extension of the Standard Model (MSSM). This approach resums large logarithmic corrections arising from the dynamical enhancement of the partonic threshold region caused by steeply falling parton luminosities. We evaluate the resummed invariant-mass distribution and total cross section for slepton-pair production at the Tevatron and LHC and we match these results, in the threshold region, onto NLO fixed-order calculations. As a second application we present the most precise predictions available for top-squark-pair production total cross sections at the LHC. These results are based on approximate NNLO formulas in fixed-order perturbation theory, which completely determine the coefficients multiplying the singular plus distributions. The analysis of the threshold region is carried out in pair invariant mass (PIM) kinematics and in single-particle inclusive (1PI) kinematics. We then match our results in the threshold region onto the exact fixed-order NLO results and perform a detailed numerical analysis of the total cross section.

Zusammenfassung

In dieser Arbeit untersuchen wir die Phänomenologie von supersymmetrischen Teilchen an Hadronbeschleunigern jenseits der nächstführenden Ordnung (NLO) in der Störungstheorie. Zuerst diskutieren wir die Grundlagen der Soft-Kollinearen Effektiven Theorie (SCET) und konstruieren explizit den SCET Lagrangian der Quantenchromodynamik (QCD). Als spezielle Anwendung diskutieren wir die Faktorisierung und die Resummierung von weichen Gluonen für den Drell-Yan Produktionsprozess. Danach benutzen wir die SCET-Techniken, um bereits bestehende Berechnungen des Produktionsquerschnittes der Sleptonpaarproduktion und der Topsquarkpaarproduktion an Hadronbeschleunigern zu verbessern. Als erste Anwendung implementieren wir die Resummation weicher Gluonen in nächst-zu-nächst-zu-nächstführender logarithmischer Ordnung (NNNLL) für die Sleptonpaarproduktion in der minimalen supersymmetrischen Erweiterung des Standardmodells (MSSM). Mit diesem Ansatz werden große logarithmische Korrekturen, die von einer dynamischen Erhöhung im "partonischen Grenzbereich" hervorgerufen werden und durch stark fallende Partonluminositätsfunktionen ausgelöst werden, resummiert. Wir berechnen die resummierte invariante Massenverteilung und den resummierten totalen Wirkungsquerschnitt der Sleptonpaarproduktion am Tevatron und am LHC. Für diese Berechnung stimmen wir unser resummiertes Ergebnis im partonischen Grenzbereich auf das exakte NLO Ergebnis ab. Als zweite Anwendung präsentieren wir die präzisesten Vorhersagen für den totalen Wirkungsquerschnitt der Topsquarkpaarproduktion am LHC. Diese Ergebnisse basieren auf einer Näherung der störungstheoretischen NNLO Formeln, welche jedoch vollständig die Koeffizienten der singulären Plusdistributionen bestimmen. Die Analyse des partonischen Grenzbereiches wird zum einen für die Kinematik der invarianten Masse des produzierten Teilchenpaares (PIM) und zum anderen für die Einteilchen-inklusive Kinematik (1PI) ausgeführt. Danach stimmen wir wieder unsere Ergebnisse des partonischen Grenzbereichs auf das exakte NLO Ergebnis ab und führen eine detaillierte numerischen Analyse des totalen Wirkungsquerschnitts durch.

Contents

1. Introduction

One of the main goals of the physics program at the Large Hadron Collider (LHC) is to investigate the existence of supersymmetric (SUSY) partners of the known Standard Model (SM) particles. If the masses of the SUSY partners are in the TeV range, they could soon be accessible by the LHC. At hadron colliders, squarks and gluinos, the superpartners of quarks and gluons respectively, are expected to be more abundantly produced relative to the other supersymmetric particles since they carry a color charge. For this reason, their experimental signatures will be affected by huge Quantum Chromodynamics (QCD) backgrounds. An attractive alternative is to look for simple signatures coming from non-colored partners. Good candidates are the leptonic superpartners (sleptons), which are expected to be among the lightest supersymmetric particles. Furthermore, in many scenarios, they decay directly into their SM partners and the stable lightest supersymmetric particle (LSP).

In order to put stringent bounds on the masses of SUSY particles at the LHC, it is crucial to obtain precise theoretical predictions for physical observables such as the total cross section and relevant differential distributions. In case of a discovery these observables are even more important for investigating the properties of these particles. Reducing the theoretical scale uncertainty by computing higher-order terms in the pertubative expansion is a task which soon becomes prohibitive. A good alternative for improving the theoretical predictions is to use soft-gluon resummation methods, which allow one to take into account the dominant contributions of the higher-order terms [1, 2]. These contributions arise from large Sudakov logarithms, which originate as a left-over from the cancellation of virtual and real soft divergences in a kinematic configuration where the invariant mass M is close to the partonic center of mass energy $\sqrt{\hat{s}}$, and hence there is little energy left for additional real radiation. These logarithms must be resummed to all orders to improve the convergence of the perturbative expansion.

In the last few years, a formalism based on Soft-Collinear Effective Theory (SCET), which allows one to resum soft-gluon emissions directly in momentum space, was developed in [3, 4] and applied to QCD corrections for several processes of interest in collider phenomenology, such as Drell-Yan scattering [5], Higgs production [6, 7], direct photon production [8] and top-pair production [9, 10]. A similar approach was developed independently in [11], where methods of SCET and Non-Relativistic QCD were used to resum simultaneously soft and Coulomb gluons [11–13].

In this thesis, we use techniques from SCET to improve existing calculations of the production cross sections for slepton-pair production and top-squark-pair production at hadron colliders, taking into account higher order contributions. Currently, for slepton-pair production, complete next-to-leading order (NLO) calculations are available in supersymmetric QCD for the total cross section and for the differential distributions [14–16]. Expressions for the resummed invariant mass distribution and total cross section were obtained in Mellin-moment space at next-to-leading logarithmic (NLL) accuracy [17]. In this thesis we extend these results to next-to-next-to-next-to-leading logarithmic (NNNLL) accuracy by means of SCET methods.

The steeply falling parton luminosities at large x dynamically enhance the contribution of the partonic threshold region, $z = M^2/\hat{s} \to 1$, which corresponds to the kinematic region where the partonic center of mass energy is just sufficient to produce the slepton-pair with invariant mass M. As a consequence, the gluon radiation in the final state is soft. In this particular limit, it can be proven that the hard-scattering kernel factorizes into a product of an hard function H and a soft function S. The hard function H is related to virtual corrections, while the soft function S originates from the real emission of soft gluons. At n-th order in perturbation theory the soft function involves singular plus distributions of the form $\alpha_s^n \left[\ln^m(1-z)/(1-z)\right]_+$, where $m = 0, \ldots, 2n-1$. The resummation of singular threshold logarithms can be accomplished by solving Renormalization Group (RG) equations for the hard and the soft function in the effective theory. To obtain the best possible predictions for the cross sections, we perform resummation at NNNLL accuracy and then match the results onto NLO calculations.

The top-squarks (stops) belong to the third family of squarks and they are expected to be the lightest colored supersymmetric particles. For this reason, they are likely to be the first supersymmetric particles discovered at the LHC. The NLO total cross section for stop-pair production has been available for more than ten years [18], but the associated theoretical uncertainties are quite large. A more precise prediction is certainly welcome and, indeed, is actually required for certain experimental analyses at the LHC. In this thesis we present approximate NNLO formulas for the stop-pair production total cross-section. These expressions are obtained by re-expanding the resummed formulas up to $\mathcal{O}(\alpha_s^4)$ in fixed-order perturbation theory. Moreover, we are able to completely determine the coefficients multiplying the singular plus distributions in the hard-scattering kernels up to NNLO. We perform a detailed analysis of the higher order corrections in two different kinematic schemes: pair invariant mass (PIM) and single-particle inclusive (1PI) kinematics. Finally we match our results in the threshold region with the exact results at NLO in fixed-order perturbation theory and perform a detailed numerical analysis of the total cross section.

The organization of the thesis is as follows. In Chapter 2 we give an introduction to supersymmetry. We discuss the basic formalism and in particular we focus on the general structure of SUSY Lagrangians. We also briefly discuss the particle content and interactions of the Minimal Supersymmetric Standard Model (MSSM). In Chapter 3 we give an extensive introduction to SCET. We first discuss the *strategy of regions* in order to expand Feynman integrals in different momentum regions and, as a first example, we introduce the SCET scalar Lagrangian which reproduces the results of the different terms of the expanded scalar integrals. Then, in analogy to the scalar case, we derive the SCET Lagrangian for the more complicated case of QCD. In Chapter 4 we explain the salient ingredients of factorization and resummation in the effective theory by discussing the relevant theorems for Drell-Yan [5]. We apply these methods to the production of supersymmetric particles at hadron colliders, and we present the most precise available results for slepton-pair production and stop-pair production. In Chapter 5 we perform a numerical analysis of the resummed invariant mass distribution and total cross section for slepton-pair production. We analyze the impact of resummation on these observables. We also study the impact of SUSY virtual corrections on the cross sections. In Chapter 6 we review the kinematics of stop-pair production in hadronic collisions and define the threshold region in PIM and 1PI kinematics. We present the calculation of the stop-pair production hard functions at NLO. The expressions for the soft functions are already known at NLO, they were computed in [9, 10] for top-pair production. By re-expanding the resummed formulas at fixed-order in perturbation theory, we obtain the coefficients of the singular plus distributions at NNLO. Finally, we present a detailed numerical analysis of the total cross section, including scale uncertainties, kinematic scheme uncertainties, Parton Distribution Functions (PDFs) and α_s uncertainties. Our conclusions are presented in Chapter 7.

2. Supersymmetry

2.1. Introduction

The Standard Model of particle physics works extremely well in describing the known phenomena in high-energy physics and, so far, no experimental signal in neat contrast with the SM predictions has been found.

On July 4$^{\text{th}}$ 2012, CMS and ATLAS, the two general purpose experiments operating at the LHC, announced to the world the discovery of a new boson with a mass in the range 125-126 GeV, compatible with the hypothesis of a SM Higgs boson. As a consequence of the Landau-Yang theorem, since the new boson decays into two photons, it cannot be a vector (spin one) particle. If, as many people expect, it turns out that the new particle has spin zero, this would be the first time that a fundamental scalar has ever been observed. Certainly a lot of work has to be done in order to understand the properties of the new boson, in particular to clarify whether this particle is really the SM Higgs boson or not. In the first case we could ask ourselves what is the particle content of the Higgs sector, namely if several other Higgs bosons are present. In the second case we will have to explain the nature of the emerging new physics.

A major theoretical issue of the SM, known as the "gauge hierarchy problem", is directly related to the existence of scalar particles. The Higgs boson of the SM (and in general any scalar particle) is not protected by any symmetry and it is radiatively unstable due to the large discrepancy between the electroweak scale (~ 246 GeV) and the new physics scale which could be the Planck scale ($\sim 10^{19}$ GeV). A conventional way to achieve the stabilization of the electroweak scale is to invoke a new symmetry, Supersymmetry [19, 20], to protect scalar particles from acquiring masses of order the cutoff scale. Supersymmetry predicts the existence of "supersymmetric partners" for all of the SM particles. These are expected to have masses of the order of a TeV, and therefore, they could be soon observed at the LHC.

Before the start of the LHC data taking, physicists were very optimistic about Supersymmetry. But after almost three years of LHC running, with 5 fb^{-1} of data collected at 7 TeV of center of mass energy and 19 fb^{-1} collected at 8 TeV, still there is no direct signal of SUSY. On the other hand, we know that the SM is incomplete and we need to include new physics at higher energy scales.

Between the several extensions of the SM, SUSY turned out to be extremely appealing to many physicists since it has a number of positive features:

1. it provides a solution to the gauge hierarchy problem,

2. it foresees the gauge coupling unification at the GUT scale, Fig. 2.1,

3. if R-parity is conserved, it provides an excellent dark matter candidate.

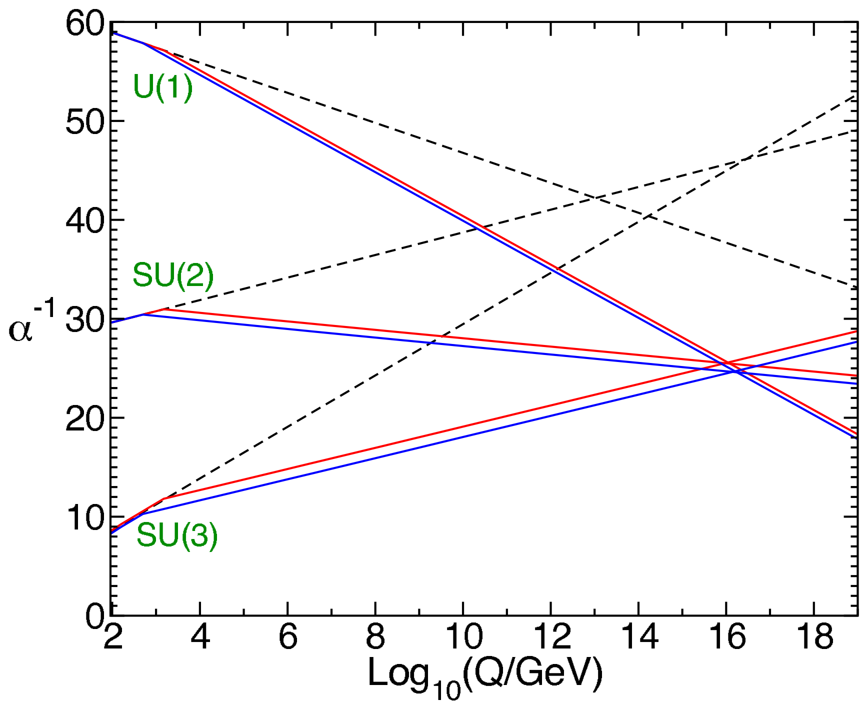

Figure 2.1.: Two loop RG evolution of the inverse of the couplings $\alpha_a^{-1}(Q)$ in the SM (dashed lines) and in the MSSM (solid lines). In the MSSM, the sparticles masses are varied between 500 GeV and 1.5 TeV and $\alpha_3(m_Z)$ is varied between 0.117 and 0.121. Figure taken from [21].

In the next paragraph we explain the origin of the "gauge hierarchy problem" [22] and how this problem is resolved with the introduction of supersymmetry.

If we compute the radiative corrections to the Higgs boson mass, m_h, we obtain quadratic divergences in the cut-off scale $\Lambda_{\rm UV}$ at which the theory stops to be valid and new physics should appear. We first consider the fermionic contribution in Fig. 1.2 (left), with n_f different types of fermions of mass m_f and λ_f as Yukawa coupling. If we consider the fermion to be heavy, and as a first approximation we neglect the external Higgs momentum squared, we find:

$$\Delta_f\, m_h^2 = n_f \frac{\lambda_f^2}{8\pi^2}\left(-\Lambda_{\rm UV}^2 + 6m_f^2 \log\frac{\Lambda_{\rm UV}}{m_f} - 2m_f^2\right) + \mathcal{O}\left(1/\Lambda_{\rm UV}^2\right)\,, \tag{2.1}$$

where the quadratic divergence appears as $\Delta m_h^2 \propto \Lambda_{\rm UV}^2$. The cut-off scale scale $\Lambda_{\rm UV}$ is assumed to be of the order the GUT scale, $M_{\rm GUT} \sim 10^{16}$ GeV, or the Planck scale,

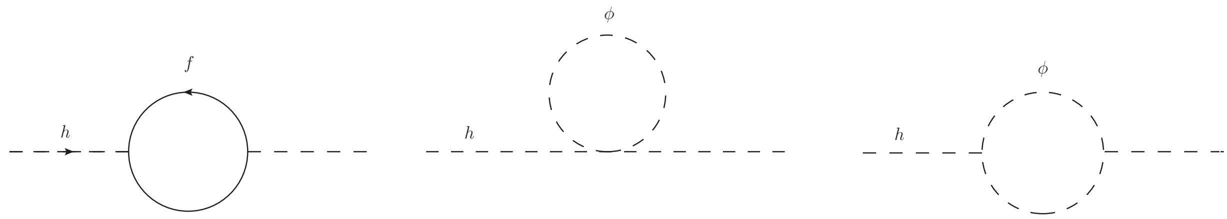

Figure 2.2.: Diagrams contributing to the Higgs boson mass at one-loop. Fermionic contribution (left) and scalar contributions (center, right).

$M_{\mathrm{P}} \sim 10^{19}$ GeV. As a consequence, the Higgs field is sensitive to the highest scale present in the theory, and therefore its mass, which should be in the elecroweak scale range, is unstable under radiative corrections. In the SM the Higgs boson is expected to be relatively light and it would be always possible to renormalize the theory by choosing appropriate counter-terms in order to get a Higgs mass around the electroweak scale. But this would need an unjustifiable tuning of the parameters of the order $\mathcal{O}(10^{-34})$ which seems very unnatural. Only scalar particles are affected by this problem. In the case of fermions the chiral symmetry is protecting their masses from large radiative corrections (the divergence is only logarithmic), while the local gauge symmetry prevents the photon to get a mass. For scalar particles, like the Higgs boson, these symmetries are not present. However, all the fermions and the electroweak gauge bosons of the SM obtain their masses from the Higgs Vacuum Expectation Value (VEV), $\langle H \rangle$, therefore all the mass spectrum of the SM is directly or indirectly sensitive to the highest scale in the theory.

If we consider the existence of a number n_S of complex scalar particles with masses m_S, where their trilinear and quadrilinear couplings to the Higgs boson are given by $v\lambda_S$ and λ_S respectively, we can compute their contributions to the Higgs mass in Fig. 1.2 (center, right) and we get

$$\Delta_S\, m_h^2 = \frac{\lambda_S n_S}{16\pi^2}\left(-\Lambda_{\mathrm{UV}}^2 + 2m_S^2 \log\frac{\Lambda_{\mathrm{UV}}}{m_S}\right) - \frac{\lambda_S^2 n_S v^2}{16\pi^2}\left(-1 + 2\log\frac{\Lambda_{\mathrm{UV}}}{m_S}\right) . \tag{2.2}$$

We observe that the quadratic divergence is present again. If we now make the assumption that the Higgs-scalar couplings and the Higgs-fermion couplings are related in the following way

$$\lambda_f^2 = -\lambda_S\,, \tag{2.3}$$

and that the number of scalars is the double of the number of fermions, $n_S = 2n_f$, we then obtain as a total contribution to the Higgs mass:

$$\Delta m_h^2 = \frac{\lambda_f^2 n_f}{4\pi^2}\left(\left(m_f^2 - m_S^2\right)\log\frac{\Lambda_{\mathrm{UV}}}{m_S} + 3m_f^2 \log\frac{m_S}{m_f}\right) + \mathcal{O}\left(1/\Lambda_{\mathrm{UV}}^2\right)\,, \tag{2.4}$$

where the quadratic divergence is now cancelled in the sum and we are left with a logarithmic divergence that also cancels out if we assume $m_S = m_f$.

The systematic cancellation of the dangerous contributions to the Higgs boson mass can be implemented through the introduction of a symmetry which relates the couplings of the new scalars to the couplings of the standard fermions. Therefore the "hierarchy problem" is finally stabilized. If supersymmetry is exact, $m_f = m_S$, the cancellation between fermionic and bosonic contribution is complete and the logarithmic divergence disappears. In the SM, one should also include in the radiative corrections to m_h the contributions of the Higgs boson itself and the ones of W/Z gauge bosons. By introducing fermionic partners for these SM particles and by adjusting their couplings to the Higgs boson, all the quadratically divergent corrections to the Higgs boson mass are canceled.

Since no supersymmetric partner with the same mass as the standard particles has been observed, we conclude that supersymmetry has to be broken. Therefore the new particles should be much heavier than the known particles. As a consequence of this mass splitting, the hierarchy problem would be reintroduced again in the theory via $\Delta m_h^2 \propto (m_f^2 - m_S^2)\log(\Lambda_{\rm UV}/m_S)$. To keep the Higgs mass at the order of the electroweak scale we need that the difference, $m_f^2 - m_S^2$, is relatively small. Hence the new particles should not be much heavier than 1 TeV.

2.2. Global N=1 supersymmetry

2.2.1. Supersymmetry algebra

In this section we will introduce the supersymmetry formalism following the discussion and the notation of [23]. Supersymmetry is a symmetry transformation which turns fermions into bosons and vice versa. For this reason, the supersymmetry generators $\mathcal{Q}_\alpha$ ($\alpha = 1, 2$) and their Hermitian adjoint operators $\bar{\mathcal{Q}}_{\dot\beta}$ ($\dot\beta = 1, 2$) should have a fermionic character and carry spin angular momentum 1/2. From this follows that supersymmetry is a spacetime symmetry, and therefore one needs to extend the Poincaré algebra to include the new symmetry generators. The structures for such symmetries are restricted by the Haag-Lopuszanski-Sohnius theorem for graded algebras [24] (as an extension of the Coleman-Mandula theorem [25]) which states that supersymmetry algebras are the only graded Lie algebras of symmetries of the S-matrix that are consistent with relativistic quantum field theory.

The $N = 1$ supersymmetry algebra, usually called "superalgebra" is defined by the following commuting and anti-commuting relations:

$$[\mathcal{Q}_\alpha, P_\mu] = \left[\bar{\mathcal{Q}}_{\dot\beta}, P_\mu\right] = 0\,, \tag{2.5}$$

$$\{\mathcal{Q}_\alpha, \mathcal{Q}_\beta\} = \left\{\bar{\mathcal{Q}}_{\dot\alpha}, \bar{\mathcal{Q}}_{\dot\beta}\right\} = 0\,, \tag{2.6}$$

$$\left\{\mathcal{Q}_\alpha, \bar{\mathcal{Q}}_{\dot\beta}\right\} = 2\sigma^\mu_{\alpha\dot\beta} P_\mu\,, \tag{2.7}$$

$$[P_\mu, P_\nu] = 0\,, \tag{2.8}$$

where σ denotes the Pauli matrices, $\mathcal{Q}_\alpha$, $\bar{\mathcal{Q}}_{\dot\beta}$ are the supersymmetry generators and P_μ is the four-momentum generator of spacetime translations. The Greek indices $(\alpha, \beta, \ldots, \dot\alpha, \dot\beta, \ldots)$ run from one to two, where the undotted indices refer to the components of left-handed Weyl spinors while the dotted indices refer to the components of right-handed Weyl spinors. Equation (2.5) for the component $\mu = 0$ implies that $\mathcal{Q}_\alpha$ commutes with the Hamiltonian $H = P^0$, $[\mathcal{Q}_\alpha, H] = 0$. If we apply the Hamiltonian to the bosonic ground state we get $H|\phi\rangle = m|\phi\rangle$. Since we know that the supersymmetry transformation acts on a bosonic state to obtain a fermionic state in the following way, $\mathcal{Q}_\alpha|\phi\rangle = |\psi_\alpha\rangle$, we get

$$H|\psi_\alpha\rangle = H\mathcal{Q}_\alpha|\phi\rangle = \mathcal{Q}_\alpha H|\phi\rangle = m|\psi_\alpha\rangle\,, \tag{2.9}$$

showing that we have mass degenerate multiplets with spin difference 1/2: ϕ has spin 0 while $|\psi_\alpha\rangle$ has spin 1/2.

Equation (2.7), using the relation $\sigma^\mu_{\alpha\dot\beta}\sigma^{\alpha\dot\beta}_\nu = 2g^\mu_\nu$, directly implies that

$$H = P^0 = \frac{1}{4}\left(\bar{\mathcal{Q}}_1\mathcal{Q}_1 + \mathcal{Q}_1\bar{\mathcal{Q}}_1 + \bar{\mathcal{Q}}_2\mathcal{Q}_2 + \mathcal{Q}_2\bar{\mathcal{Q}}_2\right)\,. \tag{2.10}$$

Since $\bar{\mathcal{Q}}_{\dot\alpha}$ are the Hermitian adjoint operators of $\mathcal{Q}_\alpha$, the eigenvalues of H are positive semidefinite, $H \geq 0$. This implies that for supersymmetric theories the vacuum energy is well defined.

2.2.2. Superfields

Before discussing the construction of a simple supersymmetric Lagrangian we have to define a formalism where supersymmetry is manifest. It is convenient to define the superspace as the set of coordinates/parameters of the extended symmetry group (which include the Poincaré group and the supersymmetry generators $\mathcal{Q}_\alpha$, $\bar{\mathcal{Q}}_{\dot\beta}$). The superspace coordinates contain the usual spacetime coordinates (t, x, y, z) and, in addition, the Grassmann parameters θ^α $(\alpha = 1, 2)$, $\bar\theta^{\dot\beta}$ $(\dot\beta = 1, 2)$ which fulfill the algebra:

$$\{\theta^\alpha, \theta^\beta\} = \{\bar\theta^{\dot\alpha}, \bar\theta^{\dot\beta}\} = \{\theta^\alpha, \bar\theta^{\dot\beta}\} = 0\,. \tag{2.11}$$

A finite supersymmetry transformation is a geometric operation on the superspace and it depends on $(x^\mu, \theta, \bar\theta)$. It is defined as follows:

$$S(x, \theta, \bar\theta) = e^{i(\theta^\alpha\mathcal{Q}_\alpha + \bar{\mathcal{Q}}_{\dot\beta}\bar\theta^{\dot\beta} - x_\mu P^\mu)}\,. \tag{2.12}$$

By multiplying two group elements using the Baker-Campbell-Hausdorff formula, one finds

$$S(x, \theta, \bar\theta)S(y, \alpha, \bar\alpha) = S(x + y - i\alpha\sigma_\mu\bar\theta + i\theta\sigma_\mu\bar\alpha, \theta + \alpha, \bar\theta + \bar\alpha)\,, \tag{2.13}$$

where the multiplication of group elements induces a translation on the parameter space:

$$g(x, \theta, \bar\theta) : (y, \alpha, \bar\alpha) \to (x + y - i\alpha\sigma_\mu\bar\theta + i\theta\sigma_\mu\bar\alpha, \theta + \alpha, \bar\theta + \bar\alpha)\,. \tag{2.14}$$

A superfield $\Phi(x,\theta,\bar{\theta})$ is defined as a function of the superspace coordinates which transforms under a supersymmetry transformation in the following way:

$$S(y,\alpha,\bar{\alpha})\left[\Phi(x,\theta,\bar{\theta})\right]=\Phi(x+y-i\alpha\sigma_\mu\bar{\theta}+i\theta\sigma_\mu\bar{\alpha},\theta+\alpha,\bar{\theta}+\bar{\alpha})\,. \tag{2.15}$$

By considering infinitesimal transformations of $S(x,\theta,\bar{\theta})$ on a superfield Φ:

$$\delta_S\Phi=\left[\alpha\frac{\partial}{\partial\theta}+\bar{\alpha}\frac{\partial}{\partial\bar{\theta}}-i(\alpha\sigma_\mu\bar{\theta}-\theta\sigma_\mu\bar{\alpha})\partial^\mu\right]\Phi\,, \tag{2.16}$$

it is possible to find an explicit representation for the generators P_μ, $\mathcal{Q}_\alpha$ and $\bar{\mathcal{Q}}_{\dot{\beta}}$ in terms of differential operators. One finds:

$$P_\mu = i\frac{\partial}{\partial x^\mu}\,, \tag{2.17}$$

$$\mathcal{Q}_\alpha = \frac{\partial}{\partial\theta^\alpha}-i\sigma^\mu_{\alpha\dot{\beta}}\bar{\theta}^{\dot{\beta}}\partial_\mu\,, \tag{2.18}$$

$$\bar{\mathcal{Q}}_{\dot{\alpha}} = -\frac{\partial}{\partial\bar{\theta}^{\dot{\alpha}}}+i\theta^\beta\sigma^\mu_{\beta\dot{\alpha}}\partial_\mu\,. \tag{2.19}$$

We are now ready to define the covariant derivative. As we have seen before, a supersymmetry transformation acts as a coordinate transformation in the superspace:

$$\begin{aligned}\theta' &= \theta+\alpha\,,\\ \bar{\theta}' &= \bar{\theta}+\bar{\alpha}\,,\\ x' &= x+y-i\alpha\sigma_\mu\bar{\theta}+i\theta\sigma_\mu\bar{\alpha}\,.\end{aligned} \tag{2.20}$$

If we consider $\partial_\mu=\frac{\partial}{\partial x^\mu}=\frac{\partial x'^\nu}{\partial x^\mu}\frac{\partial}{\partial x'^\nu}$, given that $\frac{\partial x'^\nu}{\partial x^\mu}=\delta^\nu_\mu$ we obtain $\partial_\mu=\partial'_\mu$. On the contrary, by considering

$$\partial_\alpha=\frac{\partial}{\partial\theta^\alpha}=\frac{\partial\theta'^\beta}{\partial\theta^\alpha}\frac{\partial}{\partial\theta'^\beta}+\frac{\partial x'^\mu}{\partial\theta^\alpha}\frac{\partial}{\partial x'^\mu}\,, \tag{2.21}$$

where $\frac{\partial\theta'^\beta}{\partial\theta^\alpha}=\delta^\beta_\alpha$ and $\frac{\partial x'^\mu}{\partial\theta^\alpha}=i\sigma^\mu_{\alpha\dot{\beta}}\bar{\alpha}^{\dot{\beta}}$, one finds

$$\partial_\alpha=\partial'_\alpha+i\sigma^\mu_{\alpha\dot{\beta}}\bar{\alpha}^{\dot{\beta}}\partial_\mu\,. \tag{2.22}$$

Therefore ∂_α does not transform covariantly. We define a (super)covariant derivative as

$$\mathcal{D}_\alpha=\partial_\alpha+i\sigma^\mu_{\alpha\dot{\beta}}\bar{\theta}^{\dot{\beta}}\partial_\mu\,, \tag{2.23}$$

and looking at our previous calculation we get:

$$\mathcal{D}'_\alpha = \partial'_\alpha+i\sigma^\mu_{\alpha\dot{\beta}}(\bar{\theta}^{\dot{\beta}}+\bar{\alpha}^{\dot{\beta}})\partial_\mu\,,$$

$$= \quad \partial'_\alpha + i\sigma^\mu_{\alpha\dot\beta}\bar\theta'^{\dot\beta}\partial'_\mu \,, \tag{2.24}$$

which has the same form in the transformed coordinates. In analogy one defines

$$\bar{\mathcal{D}}_{\dot\alpha} = -\partial_{\dot\alpha} - i\sigma^\mu_{\beta\dot\alpha}\theta^\beta\partial_\mu \,. \tag{2.25}$$

Moreover, by explicit computation, it can be shown that the covariant derivatives anti-commute with the supersymmetry variation

$$\mathcal{D}_\alpha(\delta_S\Phi) = -\delta_S(\mathcal{D}_\alpha\Phi) \,. \tag{2.26}$$

It is convenient to introduce two different representations of the superalgebra; these will be useful to simplify some expressions later. Instead of Eq. (2.12) we can consider

$$S_L = e^{i(\theta\mathcal{Q}-xP)}e^{i(\bar{\mathcal{Q}}\bar\theta)} \,, \tag{2.27}$$

and

$$S_R = e^{i(\bar{\mathcal{Q}}\bar\theta-xP)}e^{i(\theta\mathcal{Q})} \,. \tag{2.28}$$

By applying the supersymmetry transformation $S(y,\alpha,\bar\alpha)$ to S_L, S_R we get

$$S_L(x+y+2i\theta\sigma_\mu\bar\alpha + i\alpha\sigma_\mu\bar\alpha, \theta+\alpha, \bar\theta+\bar\alpha) \,, \tag{2.29}$$

$$S_R(x+y-2i\alpha\sigma_\mu\bar\theta - i\alpha\sigma_\mu\bar\alpha, \theta+\alpha, \bar\theta+\bar\alpha) \,. \tag{2.30}$$

We also introduce left (L) and right (R) representations for the superfields in analogy to (2.15), they transform under an infinitesimal supersymmetry transformation as

$$\delta\Phi_L \quad = \quad (\alpha\partial_\theta + \bar\alpha\partial_{\bar\theta} + 2i\theta\sigma^\mu\bar\alpha\partial_\mu)\Phi_L \,, \tag{2.31}$$

$$\delta\Phi_R \quad = \quad (\alpha\partial_\theta + \bar\alpha\partial_{\bar\theta} - 2i\alpha\sigma^\mu\bar\theta\partial_\mu)\Phi_R \,. \tag{2.32}$$

This leads to the left and right representations of the superalgebra generators

$$\mathcal{Q}_L = \partial_\theta \,, \qquad \bar{\mathcal{Q}}_L = -\partial_{\bar\theta} + 2i\theta\sigma_\mu\partial^\mu \,, \tag{2.33}$$

$$\mathcal{Q}_R = \partial_\theta - 2i\sigma_\mu\bar\theta\partial_\mu \,, \qquad \bar{\mathcal{Q}}_R = -\partial_{\bar\theta} \,, \tag{2.34}$$

and one can define as follows the corresponding covariant derivatives:

$$\mathcal{D}_L = \partial_\theta + 2i\sigma_\mu\bar\theta\partial_\mu \,, \qquad \bar{\mathcal{D}}_L = -\partial_{\bar\theta} \,, \tag{2.35}$$

$$\mathcal{D}_R = \partial_\theta \,, \qquad \bar{\mathcal{D}}_R = -\partial_{\bar\theta} - 2i\theta\sigma_\mu\partial^\mu \,. \tag{2.36}$$

There is a simple relation between the three representations of the superfields that we have introduced so far:

$$\Phi(x_\mu, \theta, \bar\theta) = \Phi_L(x_\mu + i\theta\sigma_\mu\bar\theta, \theta, \bar\theta)\,, \tag{2.37}$$

$$= \Phi_R(x_\mu - i\theta\sigma_\mu\bar\theta, \theta, \bar\theta)\,, \tag{2.38}$$

since they transform in the same way under supersymmetry transformations.

Here we discuss some specific examples of superfields. Superfields that fulfill the condition $\bar{\mathcal{D}}\Phi = 0$ or $\mathcal{D}\Phi = 0$ are called scalar (or chiral) superfields. In particular a superfield $\Phi(x, \theta, \bar\theta)$ which satisfies the first condition is called a left-handed chiral (L) superfield, while one which satisfies the second condition is usually called right-handed chiral (R) superfield. As an example, we consider a left chiral superfield ϕ_L where $\bar{\mathcal{D}}\phi_L = 0$. In the L representation $\bar{\mathcal{D}}$ simplifies to $\bar{\mathcal{D}} = -\partial/\partial\bar\theta$, this implies that ϕ_L is independent on $\bar\theta$. Therefore if we expand $\phi_L(x,\theta)$ as a Taylor series in θ only a finite number of terms survives since θ^α ($\alpha = 1, 2$) are anticommuting variables. We find:

$$\phi_L(x,\theta) = \varphi(x) + \theta^\alpha\psi_\alpha(x) + \theta^\alpha\theta^\beta\epsilon_{\alpha\beta}F(x)\,, \tag{2.39}$$

where $\varphi(x)$, $F(x)$ are complex scalar fields and $\psi_\alpha(x)$ is a left-handed Weyl spinor. We compute the effect of a supersymmetry transformation on the component fields of ϕ_L:

$$\delta_S\phi_L = (\alpha\mathcal{Q} + \bar{\mathcal{Q}}\bar\alpha - iy_\mu P^\mu)\phi_L\,, \tag{2.40}$$

taking $y_\mu = 0$ and substituting the expressions for $\mathcal{Q}_L$ and $\bar{\mathcal{Q}}_L$ we obtain

$$\delta_S\phi_L = \left[\alpha^\beta\partial_\beta + (-\partial_{\dot\alpha} + 2i\theta^\beta\sigma^\mu_{\beta\dot\alpha}\partial_\mu\bar\alpha^{\dot\alpha})\right]\phi_L(x,\theta)\,, \tag{2.41}$$

and after rewriting ϕ_L in components, we get:

$$\begin{aligned}\delta_S\phi_L &= \alpha^\beta\left[\partial_\beta\theta^\alpha\psi_\alpha + \partial_\beta\theta^\alpha\theta_\alpha F\right] + 2i\theta^\beta\sigma^\mu_{\beta\dot\alpha}\partial_\mu\left[\varphi + \theta^\gamma\psi_\gamma\right]\bar\alpha^{\dot\alpha} \\ &= \alpha^\beta\psi_\beta + 2\alpha^\beta\theta_\beta F + 2i\theta^\beta\sigma^\mu_{\beta\dot\alpha}\bar\alpha^{\dot\alpha}\partial_\mu\varphi + 2i\theta^\beta\sigma^\mu_{\beta\dot\alpha}\theta^\gamma(\partial_\mu\psi_\gamma)\bar\alpha^{\dot\alpha}\,.\end{aligned} \tag{2.42}$$

Comparing this expression to

$$\delta\phi_L(x,\theta) = \delta\varphi + \theta\delta\psi + \theta^2\delta F\,, \tag{2.43}$$

where $\theta^2 \equiv \theta^\alpha\theta_\alpha$, we can extract the infinitesimal transformations of the component fields of a left chiral superfield:

$$\delta\varphi = \alpha^\beta\psi_\beta\,, \tag{2.44}$$

$$\delta\psi_\beta = 2\alpha_\beta F + 2i\sigma^\mu_{\beta\dot\alpha}\bar\alpha^{\dot\alpha}\partial_\mu\varphi\,, \tag{2.45}$$

$$\delta F = -i(\partial_\mu\psi^\beta)\sigma^\mu_{\beta\dot\alpha}\bar\alpha^{\dot\alpha}\,. \tag{2.46}$$

The relations in Eqs. (2.44), (2.45) explicitly show that supersymmetry transforms fermions into bosons and vice versa. Eq. (2.46) describes the transformation low for the auxiliary field F.

As we have just seen, scalar superfields contain spin 0 bosons and spin 1/2 fermions. We would like to introduce superfields which contain spin 1 bosons, this is indeed needed to describe gauge interactions. We require for the vector (or gauge) superfield $V(x,\theta,\bar{\theta})$ to be a real field, $V^\dagger = V$. The expansion in components can be written as:

$$\begin{aligned} V(x,\theta,\bar{\theta}) &= \left(1+\frac{1}{4}\theta^2\bar{\theta}^2\Box\right)C+\left(i\theta+\frac{1}{2}\theta^2\sigma^\mu\bar{\theta}\partial_\mu\right)\chi \\ &+ \frac{1}{2}i\theta^2(M+iN)+(-i\bar{\theta}+\frac{1}{2}\bar{\theta}^2\theta\sigma_\mu\partial^\mu)\bar{\chi}-\frac{1}{2}\bar{\theta}^2(M-iN) \\ &- \theta\sigma_\mu\bar{\theta}V^\mu+i\theta^2\bar{\theta}\bar{\lambda}-i\bar{\theta}^2\theta\lambda+\frac{1}{2}\theta^2\bar{\theta}^2D\,, \end{aligned} \tag{2.47}$$

where C, M, N, D are real scalar fields (spin 0), λ, $\bar{\lambda}$ are Weyl spinors and V^μ is a real spin 1 field. The superpartner of the photon field V^μ is identified with the spin 1/2 field λ called photino.

2.2.3. Basic structure of supersymmetric Lagrangians

We are ready to discuss the general structure of supersymmetric Lagrangians. Looking at Eq. (2.46), one can notice that the supersymmetry variation of the highest component (F-term) of the chiral superfield is a total derivative. It can be also shown similarly that the highest component (D-term) of a vector superfield transforms as a total derivative. This means that a spacetime integral $\int d^4x$ of these quantities is invariant under supersymmetry transformations (assuming that the fields fall off at infinity fast enough). The Lagrangian density is a sum of superfields which are itself products of the elementary superfields that we have just introduced: the scalar and vector superfields. An invariant action can be thus obtained by

$$S=\int \mathrm{d}^4x\left[\int \mathrm{d}^2\theta\mathrm{d}^2\bar{\theta}\,\mathcal{K}+\int \mathrm{d}^2\theta\,\mathcal{W}+\text{h.c.}\right]. \tag{2.48}$$

$\mathcal{K}$ is usually called *Kähler potential*, while $\mathcal{W}$ is called *superpotential*. $\mathcal{K}$ and $\mathcal{W}$ usually contain products of superfields, therefore it is important to observe that any power ϕ^n of a generic left chiral superfield ($\bar{\mathcal{D}}\phi = 0$) automatically satisfy the condition $\bar{\mathcal{D}}\phi^n = 0$, which means that the multiplication of left chiral superfields is again a left chiral superfield. The same holds for right chiral superfields. These are candidates for the terms in the superpotential $\mathcal{W}$. As an example we can compute the contribution of $\mathcal{W} = m\phi^2$ to the F-term in the Lagrangian density[1]. It is easier to work in the left handed representation

[1]The integration over $\mathrm{d}^2\theta = -\frac{1}{4}\mathrm{d}\theta^\alpha\mathrm{d}\theta^\beta\varepsilon_{\alpha\beta}$ projects out the F component (or F-term) of $\mathcal{W}$.

$\phi_L = \varphi + \theta^\alpha \psi_\alpha + \theta^2 F$, and by squaring ϕ_L we get

$$\phi_L^2 = \varphi^2 + 2\varphi\theta^\alpha\psi_\alpha + \theta^2 \left(2\varphi F - \frac{1}{2}\psi^\alpha\psi_\alpha\right) , \tag{2.49}$$

hence we can read from Eq. (2.49) the F-term contribution to $\mathcal{W} = m\phi^2$:

$$\left[m\phi^2\right]_F = \int \mathrm{d}^2\theta\, \mathcal{W} = m\left[2\varphi F - \frac{1}{2}\psi^\alpha\psi_\alpha\right] . \tag{2.50}$$

The superpotential does not contain any derivative and in particular it does not contain kinetic terms. For the kinetic terms we need the bilinear combinations contained in $\mathcal{K}$. The terms contained in $\mathcal{K}$ have the structure of a product between left haded and right-handed superfields. For example we can consider the multiplication of ϕ with its complex conjugate $\phi^\dagger$. The superfield $\phi_L = \varphi + \theta^\alpha\psi_\alpha + \theta^2 F$ belongs to the L-representation, and taking the complex conjugate $\phi_L^\dagger$ we have that

$$(\phi_L)^\dagger = \varphi^* + \bar\theta\bar\psi + \bar\theta^2 F^* , \tag{2.51}$$

which is in the R-representation, $(\phi_L^\dagger)_R$, since it is independent of θ and satisfies $\mathcal{D}_R\phi_L^\dagger = 0$. In order to multiply ϕ and $\phi^\dagger$ we have to bring $(\phi_L)^\dagger$ back to the L-representation. This can be simply done with the translation in Eqs. (2.37), (2.38):

$$(\phi_L^\dagger)_L(x,\theta,\bar\theta) = (\phi_L^\dagger)_R(x - 2i\theta\sigma_\mu\bar\theta, \bar\theta) , \tag{2.52}$$

where we added a second subscript (L, R) to clarify the representation. By expanding $(\phi_L^\dagger)_R$ in components one gets

$$\begin{aligned}(\phi_L^\dagger)_R(x - 2i\theta\sigma_\mu\bar\theta, \bar\theta) \quad &= \quad \varphi^* - 2i(\theta\sigma_\mu\bar\theta)\partial^\mu\varphi^* - 2(\theta\sigma_\mu\bar\theta)(\theta\sigma_\nu\bar\theta)\partial^\mu\partial^\nu\varphi^* + \bar\theta\bar\psi \\ &- \quad 2i(\theta\sigma_\mu\bar\theta)\partial^\mu(\bar\theta\bar\psi) + \bar\theta^2 F^* . \end{aligned} \tag{2.53}$$

Finally we multiply ϕ and $\phi^\dagger$ and find

$$\phi\phi^\dagger(x,\theta,\bar\theta) = \phi(x,\theta)\phi^\dagger(x - 2i\theta\sigma\bar\theta) = \phi(x,\theta)e^{(-2i\theta\sigma^\mu\bar\theta\partial_\mu)}\phi^\dagger(x,\bar\theta) . \tag{2.54}$$

After a long but straightforward calculation, extracting the D-term contribution, namely the coefficient of $\theta^2\bar\theta^2$, we obtain

$$\int \mathrm{d}^2\theta \mathrm{d}^2\bar\theta(\phi\phi^\dagger) = FF^* - \varphi\partial_\mu\partial^\mu\varphi^* - \frac{i}{2}\psi^\beta\sigma^\mu_{\beta\dot\gamma}\partial_\mu\bar\psi^{\dot\gamma} . \tag{2.55}$$

Now we have all the elements to construct a simple example of a supersymmetric Lagrangian for chiral superfields. The D-term contribution include the kinetics terms for the scalar and the Weyl spinor, but we still have to add the mass term and the interactions.

This is done by specifying the superpotential. We give a closer look to the *Wess-Zumino Model*, where the superpotential is given by

$$\mathcal{W} = \left[m\phi^2 + \lambda\phi^3\right] . \tag{2.56}$$

We already computed the F-term contribution of ϕ^2 in Eq. 2.50, but we still need to expand ϕ^3 in components and take the coefficient of the highest component:

$$\int \mathrm{d}^2\theta\phi^3 = 3\varphi^2 F - \frac{3}{2}\varphi(\psi\psi) . \tag{2.57}$$

Putting everything together we find:

$$\begin{aligned} \mathcal{L} &= \left[\phi\phi^\dagger\right]_D + \left[m\phi^2 + \lambda\phi^3\right]_F , & (2.58) \\ &= (\partial_\mu\varphi)(\partial^\mu\varphi^*) + FF^* - \frac{i}{2}\psi^\beta\sigma^\mu_{\beta\dot{\gamma}}\partial_\mu\bar{\psi}^{\dot{\gamma}} \\ &+ m\left[2\varphi F - \frac{1}{2}(\psi\psi) + \text{h.c.}\right] + \lambda\left[3\varphi^2 F - \frac{3}{2}\varphi(\psi\psi) + \text{h.c.}\right] . & (2.59) \end{aligned}$$

We can eliminate the field F in favor of the scalar field φ using the Euler-Lagrange equations:

$$\frac{\partial\mathcal{L}}{\partial\phi} = \partial_\mu\frac{\partial\mathcal{L}}{\partial(\partial_\mu\phi)} , \tag{2.60}$$

since the derivatives of F do not appear in the expression in Eq. (2.59), we have

$$\frac{\partial\mathcal{L}}{\partial F} = 0 = F^* + 2m\varphi - 3\lambda\varphi^2 . \tag{2.61}$$

F is an auxiliary field and by substituting $F^* = -2m\varphi + 3\lambda\varphi^2$ in Eq. (2.59) one gets

$$\begin{aligned} \mathcal{L} &= |\partial_\mu\varphi|^2 - \frac{i}{2}\psi\sigma^\mu\partial_\mu\bar{\psi} + |2m\varphi + 3\lambda\varphi^2|^2 \\ &- m\left[2\varphi(2m\varphi^* + 3\lambda\varphi^{*2}) + \frac{1}{2}\psi\psi + \text{h.c.}\right] \\ &- \lambda\left[3\varphi^2(2m\varphi^* + 3\lambda\varphi^{*2}) + \frac{3}{2}\varphi(\psi\psi) + \text{h.c.}\right] . \end{aligned} \tag{2.62}$$

This Lagrangian describes the interaction of a complex scalar field with a Weyl spinor both with the same mass $2m$.

2.2.4. Brief discussion on vector superfields

In Subsection 2.2.3 we have focused our discussion on chiral multiplets and how to build simple Lagrangians for this type of superfields. Obviously, it is also possible to write down a Kähler potential and a superpotential for vector superfields, this is indeed needed to construct gauge theories with spin 1 gauge bosons.

The main ingredient needed for the discussion of gauge interactions is the vector superfield in Eq. (2.47) which satisfies the reality condition $V = V^\dagger$. V^μ is the candidate for the spin 1 gauge field and in an Abelian gauge theory like QED, it transforms under a gauge transformation as

$$V_\mu \to V_\mu + \partial_\mu \eta\,, \tag{2.63}$$

where η is a real scalar field.

We need to rephrase gauge transformations into a superfield terminology. It can be shown that the correct generalization is obtained by considering the transformation

$$V \to V + i(\Lambda - \Lambda^\dagger)\,, \tag{2.64}$$

where V is a vector superfield and Λ is a chiral superfield. The combination $i(\Lambda - \Lambda^\dagger)$ is also a vector superfield. Using again the relations in Eqs. (2.37), (2.38):

$$\begin{aligned}\Lambda - \Lambda^\dagger &= \varphi_\Lambda(x + i\theta\sigma_\mu\bar\theta, \theta) + \theta\psi_\Lambda(x + i\theta\sigma_\mu\bar\theta, \theta) + \theta^2 F_\Lambda(x + i\theta\sigma_\mu\bar\theta, \theta)\\ &- \varphi^*_\lambda(x - i\theta\sigma_\mu\bar\theta, \bar\theta) - \bar\theta\bar\psi_\Lambda(x - i\theta\sigma_\mu\bar\theta, \bar\theta) - \bar\theta^2 F^*_\Lambda(x - i\theta\sigma_\mu\bar\theta, \bar\theta)\,,\end{aligned} \tag{2.65}$$

and after Taylor expanding φ_λ, φ^*_λ we find

$$\Lambda - \Lambda^\dagger = i\theta\sigma_\mu\bar\theta\partial^\mu(\varphi_\Lambda + \varphi^*_\Lambda) + \ldots \tag{2.66}$$

We observe that V_μ transforms as in Eq. (2.63) by defining the real field $\eta = -(\varphi_\Lambda + \varphi^*_\Lambda)$. If one would consider all the remaining terms of the expansion in components in Eq. (2.66), it is possible to show that the fields M, N, χ, C in Eq. (2.47) can be gauged away by making an appropriate choice for $(\varphi_\Lambda + \varphi^*_\Lambda)$, ψ, F, F^*. The remaining fields λ and D are gauge invariant. This particular choice of the gauge is called the *Wess-Zumino gauge* and the vector superfield assumes a simple form:

$$V_{WZ}(x, \theta, \bar\theta) = -\theta\sigma_\mu\bar\theta V^\mu + i\theta^2\bar\theta\bar\lambda - i\bar\theta^2\theta\lambda + \frac{1}{2}\theta^2\bar\theta^2 D\,, \tag{2.67}$$

where it only contains V^μ, λ and D.

We define a spinor chiral superfield W_α as the supersymmetric generalization of the electromagnetic field strength:

$$W_\alpha = (\bar{\mathcal{D}}\bar{\mathcal{D}})\mathcal{D}_\alpha V\,, \tag{2.68}$$

where $\mathcal{D}_\alpha$ and $\bar{\mathcal{D}}_{\dot\alpha}$ are given in Eqs. (2.23), (2.25). For the expansion in components one finds:

$$W_\alpha(x, \theta) = 4i\lambda_\alpha - 4\theta_\alpha D + 4i\theta^\beta\sigma_{\nu\alpha\dot\beta}\sigma^{\dot\beta}_{\mu\beta}(\partial^\mu V^\nu - \partial^\nu V^\mu) - 4\theta^2\sigma_{\mu\alpha\dot\beta}\partial^\mu\bar\lambda^{\dot\beta}\,. \tag{2.69}$$

The Lagrangian density for a pure Abelian *super Yang-Mills* theory is obtained from the F-component of the chiral superfield $W^\alpha W_\alpha$ that is invariant under supersymmetry and gauge transformations, in components it reads

$$\frac{1}{32}\int \mathrm{d}^2\theta W^\alpha W_\alpha = -\frac{1}{4}V_{\mu\nu}V^{\mu\nu} - \frac{i}{2}\lambda^\alpha\sigma_{\mu\alpha\dot\gamma}\partial^\mu\bar\lambda^{\dot\gamma} - \frac{i}{2}\sigma^\alpha_{\mu\dot\beta}(\partial^\mu\bar\lambda^{\dot\beta})\lambda_\alpha + \frac{1}{2}D^2\,, \tag{2.70}$$

where D is an auxiliary field and can be eliminated through the Euler-Lagrange equations, for a pure gauge theory $\partial\mathcal{L}/\partial D = 0 \Rightarrow D = 0$. The fermionic superpartner λ of the gauge boson V^μ is usually called gaugino.

We study the coupling of the gauge bosons to matter fields with coupling constant g. This is done by replacing the Kähler potential of a chiral superfield $\left[\phi^\dagger\phi\right]_D$ by

$$\left[\phi^\dagger e^{(2gV)}\phi\right]_D = D_\mu\varphi^* D^\mu\varphi + g\varphi^*\varphi D + F^*F - \frac{i}{2}\bar{\psi}^{\dot\beta}\sigma_{\mu\alpha\dot\beta}D^\mu\psi^\alpha + ig\left[\varphi^*(\lambda\psi) - (\bar\lambda\bar\psi)\varphi\right] , \tag{2.71}$$

where $D_\mu = \partial_\mu + igV_\mu$ is the covariant derivative. In the full Lagrangian, namely considering the contributions in Eq. (2.70) and in Eq. (2.71), the scalar potential (the part of the Lagrangian that does not contain derivative or fermions) assumes the structure $\mathcal{V} = -\frac{1}{2}D^2 - g\varphi^* D\varphi$, and by making use of the Euler-Lagrange equations we find the relation $D = -g\varphi^*\varphi$. From this follows that (for zero superpotential):

$$\mathcal{V}_D = \frac{1}{2}D^2 \,. \tag{2.72}$$

If we also consider the superpotential for the chiral superfield we have:

$$\mathcal{V} = \sum_i F_i^* F_i + \frac{1}{2}D^2 \,, \tag{2.73}$$

where we have defined $\mathcal{V}_F = \sum_i F_i^* F_i$.

With minimal work these results can be generalized to non-Abelian gauge theories. This is done by introducing $V_\mu = V_\mu^a T^a$ and $\Lambda = \Lambda^a T^a$, where T^a are the generators of the non-Abelian gauge group. We define the gauge transformation for a chiral superfield:

$$\phi \to e^{-i\Lambda}\phi \,, \qquad \phi^\dagger \to \phi^\dagger e^{i\Lambda^\dagger} \,. \tag{2.74}$$

Inspired by Eq. (2.64) and Eq. (2.74), the natural generalization of the gauge transformation to the non-Abelian gauge superfield V is given by

$$e^{gV} \to e^{-ig\Lambda^\dagger} e^{gV} e^{ig\Lambda} \,. \tag{2.75}$$

To probe the validity of this formula, we derive the infinitesimal transformation properties of the vector field V, using the Baker-Campbell-Hausdorff formula:

$$\exp(gV) \to \exp\left(g(V + i(\Lambda - \Lambda^\dagger) - \frac{ig}{2}\left[\Lambda^\dagger, V\right] + \frac{ig}{2}\left[V, \Lambda\right] + \dots\right) \tag{2.76}$$

therefore we finally get

$$V \to V + i(\Lambda - \Lambda^\dagger) - \frac{ig}{2}\left[\Lambda + \Lambda^\dagger, V\right] \,, \tag{2.77}$$

where we recover the same result as in Eq. (2.64) for the Abelian case. Expanding in components we read the infinitesimal gauge transformation for the gauge field V^μ:

$$V_\mu \to V_\mu - \partial_\mu(\varphi_\Lambda + \varphi_\Lambda^\dagger) - \frac{ig}{2}\left[\varphi_\Lambda + \varphi_\Lambda^\dagger, V_\mu\right] \,, \tag{2.78}$$

where V_μ is in the adjoint representation of the gauge group.

One constructs the spinor chiral superfield for non-Abelian groups in analogy with Eq. (2.68):

$$W_\alpha = \bar{\mathcal{D}}\bar{\mathcal{D}}\left(e^{-gV}\mathcal{D}_\alpha e^{gV}\right) \,, \tag{2.79}$$

that transforms under gauge transformations as:

$$W_\alpha \to e^{-ig\Lambda} W_\alpha e^{ig\Lambda} \,. \tag{2.80}$$

The quantity $\mathrm{Tr}\,[W^\alpha W_\alpha]$ is therefore gauge invariant and its F-component provides a Lagrangian density for a pure supersymmetric Yang-Mills theory:

$$\begin{aligned}\int \frac{\mathrm{d}^2\theta}{32g^2}\mathrm{Tr}\,[W^\alpha W_\alpha] &= \mathrm{Tr}\left[-\frac{1}{4}G_{\mu\nu}G^{\mu\nu} + \frac{1}{2}D^2\right] \\ &\quad -\frac{i}{2}\mathrm{Tr}\left[\lambda^\alpha \sigma_{\mu\alpha\dot{\beta}}\left(\partial^\mu \bar{\lambda}^{\dot{\beta}} + ig[V^\mu, \bar{\lambda}^{\dot{\beta}}]\right)\right] \\ &\quad +\frac{i}{2}\mathrm{Tr}\left[\left(\partial^\mu \bar{\lambda}^{\dot{\beta}} + ig[V^\mu, \bar{\lambda}^{\dot{\beta}}]\right)\sigma_{\mu\alpha\dot{\beta}}\lambda^\alpha\right] \,, \end{aligned} \tag{2.81}$$

where $G_{\mu\nu} = \partial_\mu V_\nu - \partial_\nu V_\mu + ig[V_\mu, V_\nu]$ and $\lambda = \lambda^a T^a$ is in the adjoint representation of the gauge group. The coupling to matter is given as before from the D-term contribution $\left[\phi^\dagger e^{2gV}\phi\right]_D$. The superpotential for the chiral superfield has to be invariant under gauge transformations in Eq. (2.74). In the non-Abelian case, the scalar potential assumes the form

$$\mathcal{V} = \mathcal{V}_F + \mathcal{V}_D = \sum_i F_i^\dagger F_i + \frac{1}{2}D^a D^a \,, \tag{2.82}$$

where $D^a = -g\varphi^\dagger T^a \varphi$ from the Euler-Lagrange equations.

2.3. The Minimal Supersymmetric Standard Model

In this section we briefly summarize the ingredients needed to construct a Minimal Supersymmetric extension of the Standard Model (MSSM).

In order to extend the SM we need to include in the supersymmetry formalism all the known SM particles. Therefore each of the known fundamental particles has to reside either in a chiral or in a gauge supermultiplet together with the respective superpartner. The fundamental particle and its superpartner differ by a 1/2 unit of spin. The names for the scalar partners of the fermions are built by prepending an "s", which stand for "scalar", in front of the name of the particle, i.e. "squarks" for the quarks partners or "sleptons" for the leptons partners. The scalar superpartners are denoted with the same symbol as for the SM particle plus a "$\sim$" on top. The left-handed and the right-handed fermions transform differently under gauge transformations, therefore they will reside in two different chiral superfields each of them with a different superpartner. For example the superpartner of a left-handed/right-handed electron will be called left-handed/right-handed selectron, identified by the symbol $\widetilde{e}_L/\widetilde{e}_R$. Since the selectrons are scalar particles, the subscript L, R identifies the chirality of their fermionic partners. The smuons and staus are denoted by $\widetilde{\mu}_L$, $\widetilde{\mu}_R$, $\widetilde{\tau}_L$, $\widetilde{\tau}_R$, and the squarks by $\widetilde{q}_L$, $\widetilde{q}_R$ where $q = u, d, s, c, b, t$. If we neglect their small masses, the SM neutrinos are always left-handed, therefore we can drop the L subscript and denote the sneutrinos by the their lepton flavor $\widetilde{\nu}_e$, $\widetilde{\nu}_\mu$, $\widetilde{\nu}_\tau$. The Higgs boson will be part of a chiral superfield, since it has spin 0. But it can be shown that just one chiral superfield is not enough, indeed a second Higgs multiplet is needed. One reason for this is that a second chiral multiplet is needed for the cancellation of the electroweak gauge anomaly. The two Higgs supermultiplet have opposite hypercharges, $Y = \pm 1/2$, in order to have the cancellation of the total contribution to the gauge anomaly, $\mathrm{Tr}\,[Y^3] = 0$. The second reason is that in supersymmetric theories only a $Y = 1/2$ Higgs chiral superfield can give mass to the up-type quarks, and only a Higgs with $Y = -1/2$ can give masses to down-type quarks and to the charged leptons. This is due to the fact that a general superpotential contains only one type of chiral superfields, by convention it contains only left handed chiral superfields. The two Higgs doublets, the one with $Y = 1/2$ and the one with $Y = -1/2$ are called H_u, H_d respectively. H_u has weak isospin $T_3 = (1/2, -1/2)$ and electric charge $Q = (1, 0)$, it is identified by $H_u = (H_u^+, H_u^0)$. Similary the two components of H_d are denoted by $H_d = (H_d^0, H_d^-)$. The fermionic superpartners of the Higgs fields are called Higgsinos and denoted by $\widetilde{H}_u = (\widetilde{H}_u^+, \widetilde{H}_u^0)$, $\widetilde{H}_d = (\widetilde{H}_d^0, \widetilde{H}_d^-)$. The two Higgs doublets just introduced will develop two different VEVs:

$$v_u = \langle H_u^0 \rangle \,, \qquad v_d = \langle H_d^0 \rangle \,, \tag{2.83}$$

and it is convenient to parametrize their ratio as:

$$\tan\beta \equiv v_u / v_d \,. \tag{2.84}$$

Moreover they are related to the Z boson mass via

$$v_{\mathrm{SM}} = v_u^2 + v_d^2 = \frac{2 m_Z^2}{g'^2 + g^2} \,. \tag{2.85}$$

Names		spin 0	spin 1/2	$SU(3)_C$, $SU(2)_L$, $U(1)_Y$
squarks, quarks	U_i	$(\widetilde{u}_{Li}\ \ \widetilde{d}_{Li})$	$(u_{Li}\ \ d_{Li})$	$(\,\mathbf{3},\ \mathbf{2}\,,\ \frac{1}{6})$
(×3 families) i=1,2,3	$\overline{u}_i$	$\widetilde{u}^*_{Ri}$	$u^\dagger_{Ri}$	$(\,\overline{\mathbf{3}},\ \mathbf{1},\ -\frac{2}{3})$
	$\overline{d}_i$	$\widetilde{d}^*_{Ri}$	$d^\dagger_{Ri}$	$(\,\overline{\mathbf{3}},\ \mathbf{1},\ \frac{1}{3})$
sleptons, leptons	L_i	$(\widetilde{\nu}_i\ \ \widetilde{e}_{Li})$	$(\nu_i\ \ e_{Li})$	$(\,\mathbf{1},\ \mathbf{2}\,,\ -\frac{1}{2})$
(×3 families) i=1,2,3	$\overline{e}_i$	$\widetilde{e}^*_{Ri}$	$e^\dagger_{Ri}$	$(\,\mathbf{1},\ \mathbf{1},\ 1)$
Higgs, higgsinos	H_u	$(H^+_u\ \ H^0_u)$	$(\widetilde{H}^+_u\ \ \widetilde{H}^0_u)$	$(\,\mathbf{1},\ \mathbf{2}\,,\ +\frac{1}{2})$
	H_d	$(H^0_d\ \ H^-_d)$	$(\widetilde{H}^0_d\ \ \widetilde{H}^-_d)$	$(\,\mathbf{1},\ \mathbf{2}\,,\ -\frac{1}{2})$

Table 2.1.: List of the chiral superfields in the MSSM. The fermionic components of the chiral superfields are left-handed Weyl spinors. Table taken from [21].

Names	spin 1/2	spin 1	$SU(3)_C$, $SU(2)_L$, $U(1)_Y$
gluino, gluon	$\widetilde{g}$	g	$(\,\mathbf{8},\ \mathbf{1}\,,\ 0)$
winos, W bosons	$\widetilde{W}^\pm\ \ \widetilde{W}^0$	$W^\pm\ \ W^0$	$(\,\mathbf{1},\ \mathbf{3}\,,\ 0)$
bino, B boson	$\widetilde{B}^0$	B^0	$(\,\mathbf{1},\ \mathbf{1}\,,\ 0)$

Table 2.2.: List of the vector superfields in the MSSM. Table taken from [21].

Since the gauge bosons of the SM are spin 1 particles, they need to be part of vector supermultiplets. Their fermionic superpartners are generically called gauginos. The W^+, W^0, W^- and B^0 are the gauge bosons of the elecroweak sector of the SM. Their spin 1/2 superpartners are denoted respectively by $\widetilde{W}^+$, $\widetilde{W}^0$, $\widetilde{W}^-$ called *winos* and $\widetilde{B}^0$ called *bino*. The interaction of the elecroweak gauge bosons with the Higgs field gives rise, after elecroweak symmetry breaking, to a non diagonal mass matrix for the gauge bosons. After diagonalization one finds the physical mass eigenstates: the Z boson and the photon, γ. They are a combination of the gauge eigenstates W^0 and B^0. We have the same mixing in the gaugino sector, the fermionic superpartners of Z and γ are respectively the *zino*, $\widetilde{Z}$, and the *photino*, $\widetilde{\gamma}$. The strong interactions in the SM ($SU(3)_C$) are mediated by the gluon, g, which is a color-octet spin 1 particle. Its fermionic color-octet superpartner is called gluino and it is indentified by $\widetilde{g}$.

We have just given a complete list of all the chiral and gauge superfields needed to construct a minimal supersymmetric extension of the SM, we summarize them respectively in Tables 2.1, 2.2.

2.3.1. Interactions in the MSSM

In Section 2.3 we already described the MSSM particle spectrum, and in Subsections 2.2.3 and 2.2.4 we discussed how to write down gauge interactions terms, Eq. (2.81), and the coupling to matter via, e.g.

$$\left[U^{a\dagger}e^{2\sum_i(g_iV^iT^i_{ab})}U^b\right]_D\,.$$

To have a complete description of the model we still need to discuss the Yukawa couplings and the Higgs potential.

The generalization of the SM Yukawa interactions are contained in the MSSM superpotential which reads:

$$\mathcal{W}_{\rm MSSM} = -y^d_{ij}U^a_i H_{d\,a}\bar{d}_j + y^u_{ij}U^a_i\epsilon_{ab}H^b_u\bar{u}_j - y^e_{ij}L^a_i H_{d\,a}\bar{e}_j + \mu H^a_u\epsilon_{ab}H^b_d\,, \tag{2.86}$$

where H_u, H_d, U, L, $\bar{u}$, $\bar{d}$, $\bar{e}$ are the chiral superfields reported in Tab. (2.1). The Yukawa couplings y^u, y^d, y^e are 3x3 matrices in the family space with indices $i,j=1,2,3$. The $SU(2)_L$ weak isospin indices $a,b=1,2$ are explicitly written (ϵ_{ab} is the total antisymmetric tensor in two dimensions). The color indices are suppressed. The last term in Eq. (2.86) is called the *μ-term* and it is the supersymmetric version of the Higgs mass term in the SM scalar potential before electroweak symmetry breaking. We would like to make just a short comment about the necessity of a second Higgs superfield. Since the superpotential must be holomorphic in the chiral superfields we are not allowed to write down terms like $UH^*_d\bar{u}$, therefore we are obliged to introduce a new Higgs doublet H_u with the right hypercharge quantum number, $Y=+1/2$. One can make the exercise of separating the several weak isospin components in Eq. (2.86), and, just for simplicity, we consider the third generation of chiral superfields. By explicitly writing the $SU(2)_L$ doublets as

$$U_3=(t\,b)\,,\; L_3=(\nu_\tau\,\tau)\,,\; H_u=(H^+_u\,H^0_u)\,,\; H_d=(H^0_d\,H^-_d)\,,\; \bar{u}_3=\bar{t}\,,\; \bar{d}_3=\bar{b}\,,\quad \bar{e}_3=\bar{\tau}\,, \tag{2.87}$$

one finds that the superpotential reads:

$$\begin{aligned}\mathcal{W}_{\rm MSSM} \;=\;& y^t(tH^0_u\bar{t}-bH^+_u\bar{t}) - y^b(tH^-_d\bar{b}-bH^0_d\bar{b}) - y^\tau(\nu_\tau H^-_d\bar{\tau}-\tau H^0_d\bar{\tau})\\ &+\mu(H^+_uH^-_d - H^0_uH^0_d)\,.\end{aligned} \tag{2.88}$$

The expression for the superpotential in Eq. (2.86) is minimal in the sense it preserves both baryon number (B) and lepton number (L). In the SM these two global symmetries are not assumed by default in the construction of the Lagrangian, but they are a rather accidental consequence of renormalizability. In the MSSM, by simply requiring gauge invariance and renormalizability, but without assuming B and L invariance, we have that some other terms are allowed in the superpotential:

$$\Delta\mathcal{W}_{\rm MSSM} \sim \lambda_{ijk}U^a_iL_{aj}\bar{d}_k + \lambda'_{ijk}L^a_iL_{aj}\bar{e}_k + \mu'^i H^a_u\epsilon_{ab}L^b_i + \lambda''_{ijk}\bar{u}\bar{d}\bar{d}\,, \tag{2.89}$$

where $i,j,k=1,2,3$ are family indices. These interactions produce dangerous consequences, the first three terms in Eq. (2.89) violate lepton number by one unit, $\Delta L=1$, and the last term violate baryon number by one unit, $\Delta B=1$. These contributions, in particular the terms with λ and λ'' couplings, could combine and lead to proton decay with a rate which is several orders of magnitude larger than current experimental limits. These terms should therefore be absent from the superpotential. In order to achieve this we could directly postulate B and L conservation as global symmetries of nature, but there is another viable way in supersymmetry. One can introduce a new discrete symmetry called "R-parity" which forbids the problematic terms in Eq. 2.89 and allows the terms in Eq. (2.86).

R-parity for a single particle is defined as

$$P_R = (-1)^{3B+L+2S}\,, \tag{2.90}$$

where S is the spin of the particle. From Eq. (2.90) follows that superpartners don't have the same R-parity, due to the different spin. Thus R-parity doesn't commute with supersymmetry. It turns out that all of the SM particles and the Higgs bosons have R-parity, $P_R = 1$, while all of the newly introduced particles have R-parity, $P_R = -1$. R-parity conservation implies that every interaction vertex must contain an even number of supersymmetric particles (namely R-parity odd particles). This means that supersymmetric particles can only be produced in pair and that the lightest supersymmetric particle (LSP) is stable. Moreover, if the LSP is neutral it provides a good dark matter candidate.

2.3.2. Soft supersymmetry breaking

We have already mentioned in the introduction that supersymmetry must be broken at some energy scale in order that the supersymmetric partners are not mass degenerate with the SM particles. Therefore we introduce in the Lagrangian extra soft terms (of positive mass dimension) that explicitly break supersymmetry such that quadratic divergences are absent. Soft supersymmetry breaking at low energies should be tought as the effect of a spontaneous supersymmetry breaking of more fundamental theory at higher energy scales. Soft supersymmetry terms have to respect gauge symmetries and R-parity. The possible soft terms which can be introduced in the Lagrangian of a general theory exhibit the general structure:

$$\mathcal{L}_{\text{soft}} = -m^2_{0\,ij}\phi^*_i\phi_j - \left[\frac{1}{2}m_{1/2\,j}\lambda_j\lambda_j + \frac{1}{6}A_{ijk}\phi_i\phi_j\phi_k + \frac{1}{2}b_{ij}\phi_i\phi_j + \text{c.c.}\right]\,, \tag{2.91}$$

where $m^2_{0\,ij}$, b_{ij} are squared mass terms, $m_{1/2\,j}$ are the gaugino mass terms for each gauge group and A_{ijk} are the trilinear couplings also called A-terms.

Following the general recipe in Eq. (2.91) we are able to specify the soft supersymmetry breaking terms for the MSSM. These are explicitly given in [21]:

$$\begin{aligned}
\mathcal{L}^{\text{MSSM}}_{\text{soft}} \;&=\; -\frac{1}{2}\left[m_{\widetilde{g}}\widetilde{g}\widetilde{g} + m_{\widetilde{W}}\widetilde{W}\widetilde{W} + m_{\widetilde{B}}\widetilde{B}\widetilde{B} + \text{c.c.}\right] \\
&\quad - \left[A^u_{ij}\widetilde{U}_i H_{u\,j}\widetilde{\overline{u}} - A^d_{ij}\widetilde{U}_i H_{d\,j}\widetilde{\overline{d}} - A^e_{ij}\widetilde{L}_i H_{d\,j}\widetilde{\overline{e}} + \text{c.c.}\right]
\end{aligned}$$

$$
\begin{aligned}
& -m^2_{U\,ij}\,\widetilde{U}_i^*\widetilde{U}_j - m^2_{L\,ij}\,\widetilde{L}_i^*\widetilde{L}_j - m^2_{\overline{u}\,ij}\,\widetilde{\overline{u}}_i^*\widetilde{\overline{u}}_j - m^2_{\overline{d}\,ij}\,\widetilde{\overline{d}}_i^*\widetilde{\overline{d}}_j - m^2_{\overline{e}\,ij}\,\widetilde{\overline{e}}_i^*\widetilde{\overline{e}}_j \\
& - m^2_{H_u} H_u^* H_u - m^2_{H_d} H_d^* H_d - (b\,H_u H_d + \text{c.c.})\ , \qquad (2.92)
\end{aligned}
$$

where we have suppressed all the gauge indices. In Eq. (2.92), $m_{\widetilde{g}}$, $m_{\widetilde{W}}$, $m_{\widetilde{B}}$ are respectively the gluino, wino and bino mass terms. The A-terms in the second line of Eq. (2.92) have the same structure as the Yukawa couplings in the superpotential in Eq. (2.86), in particular A^u, A^d, A^e are 3x3 matrices in the family space. In the third line of Eq. (2.92) we have the squared mass terms for squarks and sleptons. The last line of Eq. (2.92) contains squared mass terms for the Higgs fields, H_u and H_d and the mixed b-term contribution to the Higgs potential. We will discuss the Higgs potential more extensively in the next subsection.

Compared to the supersymmetry-preserving part of the MSSM Lagrangian, the soft supersymmetry breaking Lagrangian, $\mathcal{L}^{\text{MSSM}}_{\text{soft}}$, in Eq. (2.92), introduce a huge number of new parameters which were not present in the SM. It is possible to count up tp 105 independent parameters: masses, phases and mixing angles which cannot be rotated away. Fortunately there are many experimental constraints which require that many of these parameters are small, therefore the soft supersymmetry breaking parameters cannot be chosen randomly. In the past years, several different models were developed in order to explain the origin of supersymmetry breaking and, consequently, of soft terms in the MSSM Lagrangian. They usually predict masses and mixing angles for the MSSM particles in terms of a small set of parameters which are typically given at a certain high energy scale. By evolving the RG equations for the soft terms "down“ to the electroweak scale, it is possible to obtain a pattern for the mass spectrum of the undiscovered supersymmetric particles. The most popular models for supersymmetry breaking are the supergravity inspired MSSM (MSUGRA) scenarios and the gauge-mediated scenarios (GMSB). We are not going to discuss these models for supersymmetry breaking in the present introduction to supersymmetry, therefore if one is interested in an extensive analysis and related literature we refer to [21].

2.3.3. Higgs potential in the MSSM

The scalar potential for the Higgs fields $H_u = (H_u^+, H_u^0)$, $H_d = (H_d^0, H_d^-)$ receive contributions from different terms in the MSSM Lagrangian. As specified by the general formula in Eq. (2.82) we find F-term contributions coming from the μ-term in Eq. (2.86), and D-terms contributions coming from the gauge couplings in the Kähler potential. The F-term contribution reads:

$$
\begin{aligned}
\mathcal{V}_F &= \Big|\frac{\partial \mathcal{W}_{\text{MSSM}}}{\partial H_u^0}\Big|^2 + \Big|\frac{\partial \mathcal{W}_{\text{MSSM}}}{\partial H_d^0}\Big|^2 + \Big|\frac{\partial \mathcal{W}_{\text{MSSM}}}{\partial H_u^+}\Big|^2 + \Big|\frac{\partial \mathcal{W}_{\text{MSSM}}}{\partial H_d^-}\Big|^2 , \\
&= |\mu|^2 (|H_d^0|^2 + |H_u^0|^2 + |H_d^-|^2 + |H_u^+|^2)\,. \qquad (2.93)
\end{aligned}
$$

The D-term contribution has the following expression:

$$\mathcal{V}_D = \frac{g'^2}{2}\left[\sum_{\varphi}\varphi^* Y \varphi\right]^2 + \frac{g^2}{2}\sum_{a=1}^{3}\left[\sum_{i=1}^{2}(\varphi^*\,,\varphi^*)_i\, T^a \begin{pmatrix}\varphi\\ \varphi\end{pmatrix}_i\right]^2 , \tag{2.94}$$

$$= \frac{1}{8}(g'^2+g^2)\left(|H_u^0|^2+|H_u^+|-|H_d^0|^2-|H_d^-|^2\right)^2+\frac{1}{2}g^2|H_u^+H_d^{0*}+H_u^0H_d^{-*}|^2 , \tag{2.95}$$

where g' and g are the $U(1)_Y$ and $SU(2)$ gauge couplings, Y and $T^a = \sigma^a/2$ are the hypercharge and $SU(2)$ generators and $\varphi \in \{H_d^0, H_d^-, H_u^+, H_u^0\}$, $(\varphi,\varphi)_1 = (H_d^0, H_d^-)$, $(\varphi,\varphi)_2 = (H_u^+, H_u^0)$. Finally we have to include the terms coming from the soft breaking Lagrangian $\mathcal{L}_{\text{soft}}$, namely the contributions in the last line of Eq. (2.92). In total we find for the Higgs scalar potential:

$$\mathcal{V} = \mathcal{V}_F + \mathcal{V}_D + \mathcal{V}_{\text{soft}} \tag{2.96}$$

$$\begin{aligned} &= (|\mu|^2 + m_{H_u}^2)(|H_u^0|^2 + |H_u^+|^2) + (|\mu|^2 + m_{H_d}^2)(|H_d^0|^2 + |H_d^-|^2) \\ &\quad + \left[b(H_u^+H_d^- - H_u^0H_d^0) + \text{c.c.}\right] \\ &\quad + \frac{1}{8}(g'^2+g^2)\left(|H_u^0|^2+|H_u^+|-|H_u^+|^2-|H_d^-|^2\right)^2+\frac{1}{2}g^2|H_u^+H_d^{0*}+H_u^0H_d^{-*}|^2 . \end{aligned} \tag{2.97}$$

The above expression for the Higgs potential can be simplified around the minimum. One can use the $SU(2)_L$ invariance to rotate away a possible VEV at the minimum of the potential, we can therefore set $H_u^+ = 0$. Moreover the minimum condition $\partial\mathcal{V}/\partial H_u^+ = 0$ implies that $H_d^- = 0$. We are therefore left with the expression:

$$\begin{aligned} \mathcal{V} &= (|\mu|^2 + m_{H_u}^2)(|H_u^0|^2) + (|\mu|^2 + m_{H_d}^2)(|H_d^0|^2) - \left[b\, H_u^0H_d^0 + \text{c.c.}\right] \\ &\quad + \frac{1}{8}(g'^2+g^2)\left(|H_u^0|^2 - |H_d^0|^2\right)^2 , \end{aligned} \tag{2.98}$$

where b can be taken real and positive after a phase redefinition of H_u^0 and H_d^0. We have to make sure that the Higgs potential fulfills some important conditions in order to have the correct pattern for elecroweak symmetry breaking. The potential should be bounded from below for arbitrary large values of the scalar fields, in order for $\mathcal{V}$ to have a minimum. The quartic interactions will stabilize the potential for almost every value of H_u^0, H_d^0 except for the special D-flat directions, $|H_u^0| = |H_d^0|$. In this case the quartic contribution to $\mathcal{V}$ vanishes. Thus we have to demand that the quadratic coupling is positive along the D-flat directions. We get the condition:

$$2b < 2|\mu|^2 + m_{H_u}^2 + m_{H_d}^2 . \tag{2.99}$$

The second condition requires that $\mathcal{V}$ doesn't have a local minimum near $H_u^0 = H_d^0 = 0$. This is done by imposing a negative determinant to the squared mass matrix for H_u^0, H_d^0. From this follows the inequality:

$$b^2 > (|\mu|^2 + m_{H_u}^2)(|\mu|^2 + m_{H_d}^2) . \tag{2.100}$$

The two $SU(2)_L$ Higgs doublets in the MSSM correspond to eight real scalar degrees of freedom. After elecroweak symmetry breaking, three of the eight degrees of freedom, namely the would-be Nambu-Goldstone bosons G^0, $G^{\pm}$, become the longitudinal modes of the three massive gauge bosons Z and $W^{\pm}$ respectively. By diagonalizing the mass matrix one finds that the remaining five physical scalar Higgs fields correspond to one CP-odd neutral pseudoscalar called A^0, two CP-even neutral scalars h^0 and H^0, two charged scalars $H^{\pm}$. We assume h^0 to be lighter than H^0. One finds that the mass eigenvalues of the physical Higgs scalars are:

$$m_{A^0}^2 = \frac{2b}{\sin(2\beta)}\,, \tag{2.101}$$

$$m_{h^0,H^0}^2 = \frac{1}{2}\left(m_{A^0}^2 + m_Z^2 \mp \sqrt{m_{A^0}^4 + m_Z^4 - 2m_{A^0}^2 m_Z^2 \cos(4\beta)}\right)\,, \tag{2.102}$$

$$m_{H^{\pm}}^2 = m_{A^0}^2 + m_W^2\,. \tag{2.103}$$

From Eqs. (2.101), (2.102), (2.103) follows that m_{A^0}, m_{H^0}, $m_{H^{\pm}}$ can be arbitrarily large since they grow like $b/\sin(2\beta)$. On the contrary m_{h^0} is bounded from above; this is shown in [26], [27] and it is a consequence of Eq. (2.102) for m_{h^0}. At tree level one finds that the mass of the lighter MSSM Higgs boson cannot be heavier that the Z mass:

$$m_{h^0} < m_Z|\cos(2\beta)|\,. \tag{2.104}$$

However, the inequality in Eq. (2.104) gets important quantum corrections due to top and stops loops. By including one-loop and two-loop radiative corrections one can get the following upper bound in MSSM:

$$m_{h^0} \lesssim 135\,\mathrm{GeV}\,, \tag{2.105}$$

where it was assumed that all the supersymmetric particles contributing to $m_{h^0}^2$ in the loops have masses lower or equal to 1 TeV.

2.3.4. Squarks and Sleptons Mixings

If we assume completely arbitrary soft terms for the MSSM in Eq. (2.92), the mass eigenstates of squarks and sleptons are obtained by diagonalizing three 6×6 squared mass matrices for up type squarks $(\widetilde{u}_L, \widetilde{c}_L, \widetilde{t}_L, \widetilde{u}_R, \widetilde{c}_R, \widetilde{t}_R)$, down type squarks $(\widetilde{d}_L, \widetilde{s}_L, \widetilde{b}_L, \widetilde{d}_R, \widetilde{s}_R, \widetilde{b}_R)$, charged sleptons $(\widetilde{e}_L, \widetilde{\mu}_L, \widetilde{\tau}_L, \widetilde{e}_R, \widetilde{\mu}_R, \widetilde{\tau}_R)$ and one 3×3 matrix for sneutrinos $(\widetilde{\nu}_e, \widetilde{\nu}_\mu, \widetilde{\nu}_\tau)$. Fortunately, there are experimental indications which tell us that most of these mixing angles are very small. The RG equations for the running masses of the third family squarks and sleptons are sensitive to the effects of large Yukawa couplings. Therefore stops, sbottoms and staus can have very different masses respect to the first two families of sfermions. Moreover, they can have a significant mixing in pairs $(\widetilde{t}_L, \widetilde{t}_R)$, $(\widetilde{b}_L, \widetilde{b}_R)$, $(\widetilde{\tau}_L, \widetilde{\tau}_R)$. On the contrary, the first and the second family sfermions have negligible Yukawa couplings, and this produces 7 nearly degenerate unmixed states $(\widetilde{e}_R, \widetilde{\mu}_R)$, $(\widetilde{\nu}_e, \widetilde{\nu}_\mu)$, $(\widetilde{e}_L, \widetilde{\mu}_L)$, $(\widetilde{u}_R, \widetilde{c}_R)$, $(\widetilde{d}_R, \widetilde{s}_R)$, $(\widetilde{u}_L, \widetilde{c}_L)$, $(\widetilde{d}_L, \widetilde{s}_L)$.

Now we are going to consider the squared mass matrix for top-squarks. There are several important contributions: squared mass terms from soft terms and D-term scalar quartic interactions when the neutral Higgs scalars get VEVs, F-terms proportional to m_t^2 when we substitute the Higgs VEVs and finally trilinear scalar contributions from F-terms and soft term after electroweak symmetry breaking. Putting all these different contributions together we find that the stop squared mass matrix, in the gauge eigenstate basis $(\widetilde{t}_L,\ \widetilde{t}_R)$, has the following expression:

$$\mathbf{m}^{\mathbf{2}}_{\widetilde{\mathbf{t}}} = \begin{pmatrix} m^2_{U_{33}} + m_t^2 + \left(\frac{1}{2} - \frac{2}{3} s^2_{\theta_W}\right) m_Z^2 \cos(2\beta) & v_{\mathrm{SM}} \left(A^t \sin(\beta) - \mu y^t \cos(\beta)\right) \\ v_{\mathrm{SM}} \left(A^t \sin(\beta) - \mu y^t \cos(\beta)\right) & m^2_{\bar{u}_{33}} + m_t^2 + \frac{2}{3} s^2_{\theta_W} m_Z^2 \cos(2\beta) \end{pmatrix}, \tag{2.106}$$

where θ_W is the Weinberg angle. The squared mass matrix can be diagonalized by a rotation matrix which gives the two stop mass eigenstates:

$$\begin{pmatrix} \widetilde{t}_1 \\ \widetilde{t}_2 \end{pmatrix} = \begin{pmatrix} \cos(\alpha) & \sin(\alpha) \\ -\sin(\alpha) & \cos(\alpha) \end{pmatrix} \begin{pmatrix} \widetilde{t}_L \\ \widetilde{t}_R \end{pmatrix}, \tag{2.107}$$

where $\widetilde{t}_1$ is defined to be lighter between the two stops: $m^2_{\widetilde{t}_1} < m^2_{\widetilde{t}_2}$. The non-negligible diagonal entries will produce an important mixing which increases the splitting between the two mass eigenstates.

One can also compute the squared mass matrices for bottom squarks and staus in their gauge eigenstates basis, which respectively read

$$\mathbf{m}^{\mathbf{2}}_{\widetilde{\mathbf{b}}} = \begin{pmatrix} m^2_{U_{33}} + \left(-\frac{1}{2} + \frac{1}{3} s^2_{\theta_W}\right) m_Z^2 \cos(2\beta) & v_{\mathrm{SM}} \left(A^b \sin(\beta) - \mu y^b \cos(\beta)\right) \\ v_{\mathrm{SM}} \left(A^b \sin(\beta) - \mu y^b \cos(\beta)\right) & m^2_{\bar{d}_{33}} - \frac{1}{3} s^2_{\theta_W} m_Z^2 \cos(2\beta) \end{pmatrix}, \tag{2.108}$$

$$\mathbf{m}^{\mathbf{2}}_{\widetilde{\tau}} = \begin{pmatrix} m^2_{L_{33}} + \left(-\frac{1}{2} + s^2_{\theta_W}\right) m_Z^2 \cos(2\beta) & v_{\mathrm{SM}} \left(A^\tau \sin(\beta) - \mu y^\tau \cos(\beta)\right) \\ v_{\mathrm{SM}} \left(A^\tau \sin(\beta) - \mu y^\tau \cos(\beta)\right) & m^2_{\bar{e}_{33}} - s^2_{\theta_W} m_Z^2 \cos(2\beta) \end{pmatrix}. \tag{2.109}$$

Since y^b, $y^\tau \ll y^t$, the impact of mixing in sbottom and stau sectors depends on the value of $\tan(\beta)$. If $\tan(\beta)$ is chosen to be small, $\tan(\beta) < 10$, the mixing is small and the mass eigenstates are nearly the same as the gauge eigenstates. On the contrary, if $\tan(\beta)$ is larger, it is possible to obtain a significant mixing.

In our analysis of slepton-pair production in Chapter 5 and stop-pair production in Chapter 6, we assume for simplicity that we have mixing only in the stau and stop sector. As we will discuss later, this choice is motivated by the fact that the dependence of virtual corrections from SUSY parameters is very mild.

3. Soft-Collinear Effective Theory

3.1. Introduction

SCET is an effective field theory (EFT) of QCD which offers a natural framework to describe high-energy processes at hadron colliders. SCET has been developed over the last ten years originally with a focus on B-physics and its foundations were posed in a series of papers [28–34]. By now it has been applied in a large variety of processes, from B-meson decay to collider physics processes.

Effective field theories are used, in quantum field theory (QFT), whenever one encounters problems with two different scales, a high-energy scale Λ_h and a lower scale Λ_l. EFTs allow one to expand physical quantities in the small ratios of scales and to separate the low-energy contributions from the high-energy part. Performing the expansion usually greatly simplifies the problem and is often necessary in order to attack a field theory problem at all. In QCD, the low energy part is usually non-perturbative, while the high-energy contribution can be computed perturbatively. Using an EFT one is able to separate the two pieces and compute them with appropriate techniques. For hadron collider observables, the leading non-perturbative low-energy part is typically encoded in the PDFs. However, even in those cases where all scales in a given problem are in the perturbative domain, it is necessary to separate the contributions associated with different scales. If this is not done, higher-order corrections are enhanced by large logarithms of the scale ratios. For processes described in SCET, like the Sudakov problem, the leading logarithmic terms at n-th order in perturbation theory have the form $\alpha_s^n \ln^{2n}(\Lambda_h/\Lambda_l)$, where α_s is the strong coupling constant. These large logarithms can be resummed to all orders in SCET.

In the next chapter we will give an introduction to SCET, based on [35,36]. We will start from the expansion of Feynman diagrams in different momentum regions and construct an effective Lagrangian, which produces the different terms, which contribute to the expanded diagrams. The technique we use for the expansion is called the strategy of regions and is based on dimensional regularization. There are two different low energy regions contributing in processes with energetic particles: the soft and the collinear regions. They are respectively related to the possibility for the particles to split into collinear particles and to emit soft particles. Therefore, as its name suggests, SCET includes different low energy fields, which describes the collinear and the soft emissions. As a consequence of this, the same QCD field is represented in the low-energy theory by different fields. We will analyze the Sudakov problem in ϕ^3 scalar theory, check that we reproduce the full theory result at one-loop order. After this, we extend the construction to QCD.

To see the methods at work we study soft-gluon resummation for the inclusive Drell-Yan cross section $pp \to \gamma^*/Z + X \to \ell^+\ell^- + X$ in Chapter 4 of this thesis. This is one of the basic processes at hadron-colliders, and one of the first for which resummation was performed in SCET [5].

During the last few years SCET has been used to perform higher-logarithm resummation for many processes, up to now only for inclusive final states such as e^+e^- event shapes [37], vector boson production [38], Higgs production [6,7,39] and top-pair production at hadron colliders [9,10,40,41].

3.2. The Strategy of Regions

The strategy of regions [42] is a technique which allows one to carry out asymptotic expansions of loop integrals, in dimensional regularization, around various limits [43]. The expansion is obtained by splitting the integration into different regions and appropriately expanding the integrand in each case. In the effective theory, the different regions will be represented by different effective fields. The expanded integrals, obtained by means of the strategy of regions technique, are in one-to-one correspondence to the Feynman diagrams of the effective theory, regularized in dimensional regularization.

If one is simply interested in expanding some pertubative result in a small parameter, one can work directly with the strategy of regions technique, without constructing an effective Lagrangian. However, the use of an effective field theory offers important advantages when one is interested in deriving all-order statements. In particular, one can use the effective Lagrangian

- to derive factorization theorems,
- to resum logarithmically enhanced contributions at all orders in the coupling constant using RG techniques.

In addition, in the effective field theory, gauge invariance is manifest at the Lagrangian level, which is not the case for individual Feynman diagrams.

3.2.1. A Simple Example

In order to illustrate the main idea of the strategy of regions we start by considering a simple integral, which we will expand using different methods, first using a cutoff to separate two different regions and then with dimensional regularization. The integral we will consider is

$$I = \int_0^\infty dk \frac{k}{(k^2+m^2)(k^2+M^2)} = \frac{\ln \frac{M}{m}}{M^2-m^2}\,. \tag{3.1}$$

This corresponds to a self-energy one-loop integral with two different particle masses at zero external momentum, evaluated in $d = 2$. We will assume a large hierarchy between the masses, for example $m^2 \ll M^2$, and will discuss the expansion of the integral around the limit of small m. Since we know the full result, we can obtain the expansion simply by expanding the denominator on the right-hand side of (3.1)

$$I = \frac{\ln \frac{M}{m}}{M^2} \left(1 + \frac{m^2}{M^2} + \frac{m^4}{M^4} + \cdots \right) . \tag{3.2}$$

Note that the integral is not analytic in the expansion parameter m/M because of the presence of the logarithm. Our goal in the following is to obtain the expansion in Eq. (3.2) by expanding the integrand in Eq. (3.1) before carrying out the integral. This is important in cases where the full result is not available. It will also tell us what kind of degrees of freedom the effective theory will contain.

A naive expansion of the integrand leads to trouble, because it gives rise to infrared (IR) divergent integrals. In fact

$$\frac{k}{(k^2 + m^2)(k^2 + M^2)} = \frac{k}{k^2(k^2 + M^2)} \left(1 - \frac{m^2}{k^2} + \frac{m^4}{k^4} + \cdots \right) , \tag{3.3}$$

cannot be used in place of the integrand of Eq. (3.1):

$$I \neq \int_0^\infty \frac{k}{k^2(k^2 + M^2)} \left(1 - \frac{m^2}{k^2} + \frac{m^4}{k^4} + \cdots \right) . \tag{3.4}$$

This was to be expected since, if the expansion and integration commute, the result would be analytic in m/M and we stressed above that this is not the case. So just from the form of the result (3.2), it is clear the expansion and integration do not commute. The reason for this is simply that the series expansion in Eq. (3.3) is valid only for $k \gg m^2$, while the integration domain in Eq. (3.1) includes a region in which $k^2 \sim m^2$, which contributes to the integral. To account for this fact, we should split the integration into two regions. We can do this by introducing a new scale Λ, such that $m \ll \Lambda \ll M$. We will call the scale Λ a cut-off, even though the name is misleading. The role of Λ is to separate the two momentum regions. We then obtain

$$I = \underbrace{\int_0^\Lambda dk \frac{k}{(k^2 + m^2)(k^2 + M^2)}}_{I_{(I)}} + \underbrace{\int_\Lambda^\infty dk \frac{k}{(k^2 + m^2)(k^2 + M^2)}}_{I_{(II)}} . \tag{3.5}$$

We call the region $[0, \Lambda]$ the *low-energy* region. In this region $k \sim m \ll M$, therefore one can expand the integrand in the integral $I_{(I)}$ as follows

$$I_{(I)} = \int_0^\Lambda dk \frac{k}{(k^2 + m^2)(k^2 + M^2)} = \int_0^\Lambda dk \frac{k}{(k^2 + m^2)M^2} \left(1 - \frac{k^2}{M^2} + \frac{k^4}{M^4} + \cdots \right) . \tag{3.6}$$

The scale Λ acts as an ultraviolet cut-off for the integrals on the right-hand-side (r.h.s.) of the Eq. (3.6).

The region $[\Lambda, \infty]$ is referred to as the *high-energy* region; in that region $m \ll k \sim M$, and one can expand the integrand according to

$$I_{(II)} = \int_{\Lambda}^{\infty} dk \frac{k}{(k^2+m^2)(k^2+M^2)} = \int_{\Lambda}^{\infty} dk \frac{k}{k^2(k^2+M^2)} \left(1 - \frac{m^2}{k^2} + \frac{m^4}{k^4} + \cdots \right) . \tag{3.7}$$

In the equation above, Λ acts as an infrared cut-off.

By integrating the first two terms on the r.h.s. of Eq. (3.6) one finds

$$I_{(I)} \approx \frac{M^2+m^2}{2M^4} \ln\left(1 + \frac{\Lambda^2}{m^2}\right) - \frac{\Lambda^2}{2M^4} = -\frac{1}{M^2} \ln\left(\frac{m}{\Lambda}\right) - \frac{\Lambda^2}{2M^4} + \ldots , \tag{3.8}$$

since it was assumed above that $\Lambda \gg m$. Similarly, by integrating the first term on the r.h.s. of Eq. (3.7) one obtains

$$I_{(II)} \approx \frac{1}{2M^2} \ln\left(1 + \frac{M^2}{\Lambda^2}\right) = -\frac{1}{M^2} \ln\left(\frac{\Lambda}{M}\right) + \frac{\Lambda^2}{2M^4} + \ldots . \tag{3.9}$$

Adding up the Eq. (3.8) and (3.9) one finally obtains

$$I = I_{(I)} + I_{(II)} = -\frac{1}{M^2} \ln\left(\frac{m}{M}\right) + \ldots , \tag{3.10}$$

which is the expected result (see Eq. (3.2)). When summing the results for the low-energy and high-energy regions, the terms which depend on the cut off Λ cancel out; this is also expected, since Λ is not present in the original integral but it was introduced in order to split the original integral in the sum of two different terms. Since the final result cannot depend on Λ, there should be a way to obtain the expansion without introducing this additional scale. Our ultimate goal is to similarly expand Feynman loop integrals. It is well known that the use of hard cut-offs is impractical in loop calculations; fortunately it is possible to repeat the procedure by separating the low- and high-energy regions using dimensional regularization. Let us rewrite the original integral as follows

$$I = \int_0^{\infty} dk\, k^{-\varepsilon} \frac{k}{(k^2+m^2)(k^2+M^2)} , \tag{3.11}$$

where we will send $\varepsilon \to 0$ at the end of the calculation. (For simplicity, we did not introduce the d-dimensional angular integration so this is not exactly dimensional regularization).

The integral in the low-energy region $k \sim m \ll M$ is

$$I_{(I)} = \int_0^{\infty} dk\, k^{-\varepsilon} \frac{k}{(k^2+m^2)M^2} \left(1 - \frac{k^2}{M^2} + \frac{k^4}{M^4} + \cdots \right) . \tag{3.12}$$

Due to the fact that the integral in Eq. (3.12) is infrared safe in the region in which $k \to 0$, it is natural to take ε to be a positive real number since this renders the integral ultraviolet finite as well. The integral in the high energy region is

$$I_{(II)} = \int_0^{\infty} dk\, k^{-\varepsilon} \frac{k}{k^2(k^2+M^2)} \left(1 - \frac{m^2}{k^2} + \frac{m^4}{k^4} + \cdots \right) . \tag{3.13}$$

The integral is ultraviolet safe, and we consider $\varepsilon < 0$, so that the integrand does not give rise to an infrared singularity in the region where $k \to 0$. By integrating the first term on the r.h.s. of Eq. (3.12) one finds, at leading power in the expansion around m/M,

$$I_{(I)} \approx \frac{m^{-\varepsilon}}{2M^2}\Gamma\left(1-\frac{\varepsilon}{2}\right)\Gamma(\frac{\varepsilon}{2}) = \frac{1}{M^2}\left(\frac{1}{\varepsilon} - \ln m + \mathcal{O}(\varepsilon)\right) . \tag{3.14}$$

The integral of the first term on the r.h.s. of Eq. (3.13) is

$$I_{(II)} \approx \frac{M^{-\varepsilon}}{2M^2}\Gamma\left(1+\frac{\varepsilon}{2}\right)\Gamma(-\frac{\varepsilon}{2}) = \frac{1}{M^2}\left(-\frac{1}{\varepsilon} + \ln M + \mathcal{O}(\varepsilon)\right) . \tag{3.15}$$

The poles in ε cancel in the sum of Eqs. (3.14) and (3.15), and the final result is again the one obtained by means of the cut-off method in Eq. (3.10). One might be worried that we choose $\varepsilon > 0$ in the low-energy region and $\varepsilon < 0$ in the high-energy region and then combine the two. It is important to remember that the integrals in dimensional regularization are defined for arbitrary ε: we only choose $\varepsilon > 0$ to be able to evaluate $I_{(I)}$ as a standard integral, but by analytic continuation the resulting function on the right hand side is uniquely defined for any complex-valued ε and can be combined with $I_{(II)}$.

The fact that, in both Eq. (3.12) and Eq. (3.13), the integration domain coincides with the full integration domain of the original integral might be also surprising. However, one should note that the two integrals scale differently; the low-energy integral $I_{(I)}$ contains an overall factor of $m^{-\varepsilon}$, whereas the high-energy integral $I_{(II)}$ contains an overall factor of $M^{-\varepsilon}$. When one keeps the complete dependence on m and M, the result is

$$I = \frac{1}{2}\Gamma\left(1-\frac{\varepsilon}{2}\right)\Gamma\left(\frac{\varepsilon}{2}\right)\frac{m^{-\varepsilon} - M^{-\varepsilon}}{M^2 - m^2} . \tag{3.16}$$

This form of the result clearly displays the low-energy and the high-energy part. Expanding in one region, one ignores the region complementary to it and the full integral is recovered only after adding the two contributions. Even though we integrate twice, over the full integration domain, there is no double counting, since the two pieces scale differently. In other words, the low energy integrals can never produce a factor of $M^{-\varepsilon}$ and the high energy integrals can never produce a factor of $m^{-\varepsilon}$.

To convince ourselves that there is indeed no double counting, let us now see what happens if we insist in restricting the integration domains of the low- and high-energy integrals, when using dimensional regularization. The integral in the low-energy region would become in this case

$$\begin{aligned} I_{(I)} &= \int_0^\Lambda dk\, k^{-\varepsilon}\frac{k}{(k^2+m^2)M^2}\left(1-\frac{k^2}{M^2}+\frac{k^4}{M^4}+\cdots\right) , \\ &= \left[\int_0^\infty dk - \int_\Lambda^\infty dk\right] k^{-\varepsilon}\frac{k}{(k^2+m^2)M^2}\left(1-\frac{k^2}{M^2}+\frac{k^4}{M^4}+\cdots\right) . \end{aligned} \tag{3.17}$$

The first integral in the second line of the equation above is the same as the one in Eq. (3.12). In the second integrand, which depends on the cutoff Λ, one can use the fact that $k \geq \Lambda \gg m^2$ to expand the integrand in the small m limit

$$\int_\Lambda^\infty dk k^{-\varepsilon} \frac{k}{(k^2+m^2)M^2}\left(1-\frac{k^2}{M^2}+\cdots\right) = \int_\Lambda^\infty dk k^{-\varepsilon}\frac{k}{k^2M^2}\left(1-\frac{m^2}{k^2}-\frac{k^2}{M^2}+\cdots\right). \tag{3.18}$$

At this point it is sufficient to observe that for dimensional reasons the integrals in the equation above must behave as follows

$$\int_\Lambda^\infty dk\, k^{n-\varepsilon} \sim \Lambda^{n+1-\varepsilon}\,. \tag{3.19}$$

So the cutoff pieces scale as fractional powers of the cutoff. Since the Λ dependent terms must cancel out completely in the calculation of I, one can also drop the Λ dependent integrals from the start. Therefore, when regulating divergences by means of dimensional regularization, one can integrate over the complete integration domain, in this case $k \in [0,\infty]$.

3.2.2. The Sudakov Problem

The example, considered in the previous section, was intended to bring to the attention of the reader some general features that one encounters when dealing with the expansion of Feynman diagrams occurring in physical processes. The general strategy to obtain the expansion of a given Feynman integral in a given kinematic limit is the following [43]:

i) identify all regions of the integrand which lead to singularities in the limit under consideration,

ii) expand the integrand in each region and integrate each expansion over the full phase space,

iii) add the result of the integrations over the different regions to obtain the expansion of the original full integral.

In order for the procedure to work, it is necessary to make sure that all of the expanded integrals are properly regularized. We also stress that so far there is no general proof that the above procedure always produces the correct result. Recent work towards such a proof can be found in [44].

We now wish to consider the simplest possible example, a one-loop vertex correction where we neglect the complications related to the spin of the particles; the momentum regions that one finds in the calculation of the tensor integrals are the same as the regions that one finds in the calculation of the scalar integral considered below. The vertex correction, depicted in Figure 3.1, requires the evaluation of the following Feynman integral:

$$\mathcal{I} = i\pi^{-d/2}\mu^{4-d}\int d^dk \frac{1}{(k^2+i0^+)\left[(k+l)^2+i0^+\right]\left[(k+p)^2+i0^+\right]}\,, \tag{3.20}$$

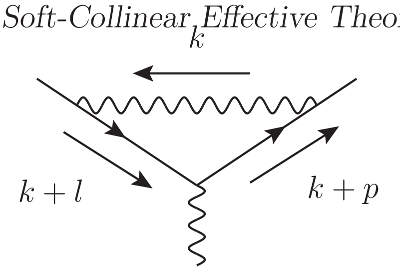

Figure 3.1.: One-loop vertex corrections. The Feynman diagram is shown here in terms of fermions and photons. However, for simplicity, the spin structure of the diagram is neglected in this section.

where $d = 4 - 2\varepsilon$ is the dimensional regulator and μ is the 't Hooft scale. We introduce the following notation:

$$L^2 \equiv -l^2 - i0^+ \,, \qquad P^2 \equiv -p^2 - i0^+ \,, \qquad Q^2 \equiv -(l-p)^2 - i0^+ \,. \tag{3.21}$$

The goal is to calculate the integral in Eq. (3.20) in the limit in which $L^2 \sim P^2 \ll Q^2$ that is, in the case in which the external legs carrying momenta l and p have large energies but small invariant masses.

Before going any further, we now need to introduce some basic notation used in SCET. We introduce two light-like reference vectors in the direction of the momenta p and l in the frame in which $\vec{Q} = 0$:

$$n_\mu = (1,0,0,1) \quad \text{and} \quad \bar{n}_\mu = (1,0,0,-1) \,. \tag{3.22}$$

It is straightforward to verify that

$$n^2 = \bar{n}^2 = 0 \,, \quad \text{and} \quad n \cdot \bar{n} = 2 \,. \tag{3.23}$$

Any vector can be then decomposed in a component proportional to n, a part proportional to $\bar{n}$, and a component perpendicular to both

$$p^\mu = (n \cdot p)\frac{\bar{n}^\mu}{2} + (\bar{n} \cdot p)\frac{n^\mu}{2} + p_\perp^\mu \equiv p_+^\mu + p_-^\mu + p_\perp^\mu \,. \tag{3.24}$$

Splitting the vectors into their light-cone components turns out to be a useful way to organize the expansion, since the different components scale differently. For the square of the vector p one then finds

$$p^2 = (n \cdot p)(\bar{n} \cdot p) + p_\perp^2 \,, \tag{3.25}$$

while the scalar product between two vectors p and q becomes

$$p \cdot q = p_+ \cdot q_- + p_- \cdot q_+ + p_\perp \cdot q_\perp \,. \tag{3.26}$$

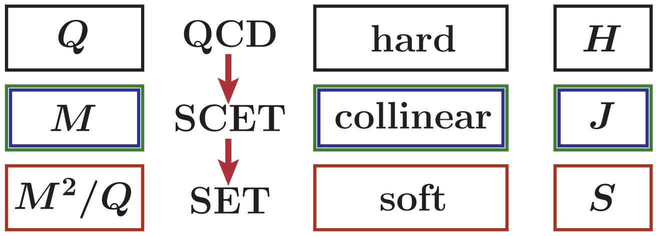

Figure 3.2.: Chart of the regions and scales involved in the calculation. Q is the hard scale, M the scale characterizing collinear physics, and M^2/Q the soft scale. SET stands for Soft Effective Theory.

In the following we will often identify a vector by means of its components in the n, $\bar{n}$, and $\perp$ basis, with the notation

$$p^\mu = (\underbrace{n \cdot p}_{\text{"+ comp."}}, \underbrace{\bar{n} \cdot p}_{\text{"− comp."}}, p_\perp^\mu) \,. \tag{3.27}$$

We now introduce an expansion parameter λ which vanishes in the limit in which we are interested:

$$\lambda^2 \sim \frac{P^2}{Q^2} \sim \frac{L^2}{Q^2} \,, \qquad \text{and} \qquad p^2 \sim l^2 \sim \lambda^2 Q^2 \,. \tag{3.28}$$

By choosing n^μ such that $p^\mu \approx Q n^\mu/2$ one finds that the components of p and l scale as follows

$$p^\mu \sim \left(\lambda^2, 1, \lambda\right) Q \,, \qquad \text{and} \qquad l^\mu \sim \left(1, \lambda^2, \lambda\right) Q \,. \tag{3.29}$$

At this stage it is necessary to distinguish the various regions of the integration momentum which contribute to the integral. These regions are

- **Hard Region** (denoted by h in the following) where the components of the integration momentum scale as $k^\mu \sim (1,1,1)Q$,
- **Region Collinear to $\boldsymbol{p}$** (denoted by c) where k scales as $k^\mu \sim (\lambda^2, 1, \lambda)Q$,
- **Region Collinear to $\boldsymbol{l}$** (denoted by $\bar{c}$) where k scales as $k^\mu \sim (1, \lambda^2, \lambda)Q$,
- **Soft Region** (denoted by s) where k scales as $k^\mu \sim (\lambda^2, \lambda^2, \lambda^2)Q$.

In SCET, each region listed above is represented by a different field; the situation is schematically illustrated in Figure 3.2.

It is interesting to observe that in the soft region the square of a four momentum is proportional to λ^4:

$$p_s^2 \sim \lambda^4 Q^2 \sim \frac{L^2 P^2}{Q^2} \,. \tag{3.30}$$

The squared momenta scaling as λ^4 are also often called *ultra soft* in the literature. The interesting part about the presence of this contribution, is that it implies that the loop diagrams involve a scale which is smaller than the invariants which can be formed by the external momenta.

In order to determine what integral to evaluate, when the integration momentum is considered hard, we consider the way in which the terms in the propagators in Eq. (3.20) scale. Clearly $k^2 \sim \lambda^0 Q^2$; for the other two propagators one finds

$$(k+l)^2 = \overbrace{k^2}^{\mathcal{O}(1)} + 2(\overbrace{k_+ \cdot l_-}^{\mathcal{O}(\lambda^2)} + \overbrace{k_- \cdot l_+}^{\mathcal{O}(1)} + \overbrace{k_\perp \cdot l_\perp}^{\mathcal{O}(\lambda)}) + \overbrace{l^2}^{\mathcal{O}(\lambda^2)} = k^2 + 2k_- \cdot l_+ + \mathcal{O}(\lambda)\,, \qquad (3.31)$$

and, similarly

$$(k+p)^2 = k^2 + 2k_+ \cdot p_- + \mathcal{O}(\lambda)\,. \qquad (3.32)$$

The contribution of the **hard region** to the integral $\mathcal{I}$ is therefore given by

$$\mathcal{I}_h = i\pi^{-d/2}\mu^{4-d} \int d^dk \frac{1}{(k^2+i0^+)\,(k^2+2k_-\cdot l_+ + i0^+)\,(k^2+2k_+\cdot p_- + i0^+)}\,; \qquad (3.33)$$

it coincides with the form factor integral with on shell external legs (i. e. calculated by setting $p^2 = l^2 = 0$ from the start). The integral evaluates to

$$\begin{aligned} \mathcal{I}_h &= \frac{\Gamma(1+\varepsilon)}{2l_+\cdot p_-}\frac{\Gamma^2(-\varepsilon)}{\Gamma(1-2\varepsilon)}\left(\frac{\mu^2}{2l_+\cdot p_-}\right)^{\varepsilon}\,, \\ &= \frac{\Gamma(1+\varepsilon)}{Q^2}\left(\frac{1}{\varepsilon^2} + \frac{1}{\varepsilon}\ln\frac{\mu^2}{Q^2} + \frac{1}{2}\ln^2\frac{\mu^2}{Q^2} - \frac{\pi^2}{6}\right) + \mathcal{O}(\varepsilon)\,. \end{aligned} \qquad (3.34)$$

The poles in ε are of infrared origin. More details on the calculation of $\mathcal{I}_h$ can be found in Appendix A.1.1.

In the region collinear to p the integration momentum scales as $k^\mu \sim (\lambda^2, 1, \lambda)Q$. In this region $k^2 \sim \lambda^2 Q^2$, which implies that

$$(k+l)^2 = 2k_-\cdot l_+ + \mathcal{O}(\lambda^2)\,, \qquad (k+p)^2 = \mathcal{O}(\lambda^2)\,. \qquad (3.35)$$

The **collinear region** integral is obtained by keeping only the leading term in each propagator

$$\begin{aligned} \mathcal{I}_c &= i\pi^{-d/2}\mu^{4-d}\int d^dk \frac{1}{(k^2+i0^+)\,(2k_-\cdot l_+ + i0^+)\,[(k+p)^2+i0^+]}\,, \\ &= -\frac{\Gamma(1+\varepsilon)}{2l_+\cdot p_-}\frac{\Gamma^2(-\varepsilon)}{\Gamma(1-2\varepsilon)}\left(\frac{\mu^2}{P^2}\right)^{\varepsilon}, \\ &= \frac{\Gamma(1+\varepsilon)}{Q^2}\left(-\frac{1}{\varepsilon^2} - \frac{1}{\varepsilon}\ln\frac{\mu^2}{P^2} - \frac{1}{2}\ln^2\frac{\mu^2}{P^2} + \frac{\pi^2}{6}\right) + \mathcal{O}(\varepsilon)\,. \end{aligned} \qquad (3.36)$$

Some details on the calculation leading to the above result are collected in Appendix A.1.2. We observe that the integral scales as $P^{-2\varepsilon}$. The calculation of the integral in the region collinear to l is identical to the calculation presented in this section, except that one needs to replace P^2 everywhere with L^2 in the final result.

In the soft region all of the components of the integration momentum are proportional to λ^2. Therefore

$$k^2 = \mathcal{O}(\lambda^4)\,, \quad (k+l)^2 = 2k_-\cdot l_+ + l^2 + \mathcal{O}(\lambda^3)\,, \text{ and } \quad (k+p)^2 = 2k_+\cdot p_- + p^2 + \mathcal{O}(\lambda^3)\,. \tag{3.37}$$

It follows that the integral in the **soft region** is simply

$$\begin{aligned}
\mathcal{I}_s &= i\pi^{-d/2}\mu^{4-d}\int d^dk \frac{1}{(k^2+i0^+)\left(2k_-\cdot l_+ + l^2 + i0^+\right)\left(2k_+\cdot p_- + p^2 + i0^+\right)}\,,\\
&= -\frac{\Gamma\left(1+\varepsilon\right)}{2l_+\cdot p_-}\Gamma(\varepsilon)\Gamma\left(-\varepsilon\right)\left(\frac{2\mu^2 l_+\cdot p_-}{L^2P^2}\right)^{\varepsilon}\,,\\
&= \frac{\Gamma(1+\varepsilon)}{Q^2}\left(\frac{1}{\varepsilon^2}+\frac{1}{\varepsilon}\ln\frac{\mu^2Q^2}{L^2P^2}+\frac{1}{2}\ln^2\frac{\mu^2Q^2}{L^2P^2}+\frac{\pi^2}{6}\right)+\mathcal{O}\left(\varepsilon\right).
\end{aligned}\tag{3.38}$$

The poles in the last line of Eq. (3.38) are of ultraviolet origin. As expected, the result depends on the "new" soft scale $\Lambda_{\text{soft}} \sim P^2L^2/Q^2$. Further details on the calculation of $\mathcal{I}_s$ can be found in Appendix A.1.3.

One can now sum the results, obtained in the different regions, to obtain what was the original goal of the calculation: an analytic expression for the integral in Eq. (3.20) in the limit in which $L^2 \sim P^2 \ll Q^2$. One finds

$$\begin{aligned}
\mathcal{I}_h &= \frac{\Gamma\left(1+\varepsilon\right)}{Q^2}\left(\frac{1}{\varepsilon^2}+\frac{1}{\varepsilon}\ln\frac{\mu^2}{Q^2}+\frac{1}{2}\ln^2\frac{\mu^2}{Q^2}-\frac{\pi^2}{6}\right)\\
\mathcal{I}_c &= \frac{\Gamma\left(1+\varepsilon\right)}{Q^2}\left(-\frac{1}{\varepsilon^2}-\frac{1}{\varepsilon}\ln\frac{\mu^2}{P^2}-\frac{1}{2}\ln^2\frac{\mu^2}{P^2}+\frac{\pi^2}{6}\right)\\
\mathcal{I}_{\bar{c}} &= \frac{\Gamma\left(1+\varepsilon\right)}{Q^2}\left(-\frac{1}{\varepsilon^2}-\frac{1}{\varepsilon}\ln\frac{\mu^2}{L^2}-\frac{1}{2}\ln^2\frac{\mu^2}{L^2}+\frac{\pi^2}{6}\right)\\
\mathcal{I}_s &= \frac{\Gamma\left(1+\varepsilon\right)}{Q^2}\left(\frac{1}{\varepsilon^2}+\frac{1}{\varepsilon}\ln\frac{\mu^2Q^2}{L^2P^2}+\frac{1}{2}\ln^2\frac{\mu^2Q^2}{L^2P^2}+\frac{\pi^2}{6}\right)\\
\hline
\mathcal{I}\equiv\mathcal{I}_h+\mathcal{I}_c+\mathcal{I}_{\bar{c}}+\mathcal{I}_s &= \frac{1}{Q^2}\left(\ln\frac{Q^2}{L^2}\ln\frac{Q^2}{P^2}+\frac{\pi^2}{3}+\mathcal{O}(\lambda)\right).
\end{aligned}\tag{3.39}$$

The final result does not depend on the dimensional regulator ε and it coincides with the one that would be obtained by evaluating directly the integral in Eq. (3.20) and then expanding the result in the $\lambda \to 0$ limit. We stress the fact that the infrared divergences found in the hard region cancel out against the ultraviolet divergences found in the soft and collinear region. This feature is general and requires a non trivial interplay of the logarithms found in the various integrals:

$$-\frac{1}{\varepsilon}\ln\frac{\mu^2}{P^2}-\frac{1}{\varepsilon}\ln\frac{\mu^2}{L^2}+\frac{1}{\varepsilon}\ln\frac{\mu^2 Q^2}{L^2 P^2}=-\frac{1}{\varepsilon}\ln\frac{\mu^2}{Q^2}\,. \tag{3.40}$$

The requirement that infrared divergences of the hard region should cancel against the ultraviolet divergences of the soft and collinear regions leads to constraints that must be satisfied by the infrared pole structure of a generic amplitude.

3.3. Scalar SCET

We now construct an effective field theory whose Feynman rules directly give the hard, collinear, and soft integrals for the Sudakov form factor that we just considered in Section 3.2. Initially we restrict our derivation to the case of a scalar ϕ^3 theory. The procedure outlined in the following will be applied to QCD in section 3.4. However, since the different components of the quark and gluon fields scale differently, the effective Lagrangian derived from QCD will be more complicated than the one that we derive here for a scalar theory.

3.3.1. The Scalar SCET Lagrangian

The starting point of our discussion is the Lagrangian

$$\mathcal{L}\left(\phi\right)=\frac{1}{2}\partial_\mu\phi(x)\partial^\mu\phi(x)-\frac{g}{3!}\phi^3(x)\,, \tag{3.41}$$

where ϕ is the scalar field and g the coupling constant of the theory. In order to derive the SCET effective Lagrangian needed for the calculation of the Sudakov form factor in this theory, one needs to split the scalar field into a sum of a field collinear to p, a field collinear to l, and a soft field:

$$\phi(x)\to\phi_c(x)+\phi_{\bar{c}}(x)+\phi_s(x)\,. \tag{3.42}$$

It was not necessary to introduce, in the sum above, a field for the hard region, since these contributions are absorbed into the *Wilson coefficients*, which are the "coupling constants" of the effective theory. When constructing the effective Lagrangian, we assume that the momenta of the different fields scale in the proper way.

By splitting each one of the fields according to Eq. (3.42), the original Lagrangian can be written as the sum of four terms:

$$\mathcal{L}(\phi)=\underbrace{\mathcal{L}\left(\phi_c\right)}_{\equiv\mathcal{L}_c}+\underbrace{\mathcal{L}\left(\phi_{\bar{c}}\right)}_{\equiv\mathcal{L}_{\bar{c}}}+\underbrace{\mathcal{L}\left(\phi_s\right)}_{\equiv\mathcal{L}_s}+\mathcal{L}_{c+s}\left(\phi_c,\phi_{\bar{c}},\phi_s\right)\,. \tag{3.43}$$

The first three terms on the r.h.s. of the equation above are simply copies of the original

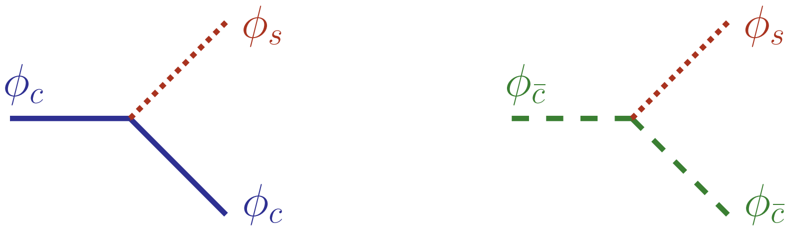

Figure 3.3.: Interaction vertices generated from the Lagrangian $\mathcal{L}_{c+s}$

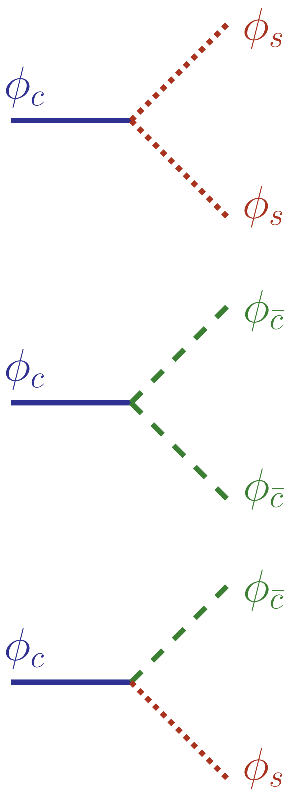

$\phi_c(x)\phi_s^2(x)$ — An energetic particle cannot decay into two soft particles

$\phi_c(x)\phi_{\bar{c}}^2(x)$ — A particle moving along the $+z$ direction cannot decay into two particle moving along the $-z$ direction

$\phi_c(x)\phi_{\bar{c}}(x)\phi_s(x)$ — The "+ component" of the c field is of order λ^2, it cannot give rise to a field with a "+ component" of order 1, such as $\bar{c}$

Figure 3.4.: Interaction forbidden by momentum conservation.

Lagrangian where all the fields are either collinear to p, collinear to l, or soft. The fourth term in Eq. (3.42) describes the interaction of collinear and soft fields

$$\mathcal{L}_{c+s}(\phi_c, \phi_{\bar{c}}, \phi_s) = -\frac{g}{2}{\phi_c}^2\phi_s - \frac{g}{2}{\phi_{\bar{c}}}^2\phi_s\,, \tag{3.44}$$

which give origin to the interaction vertices shown in Fig. 3.3. At first sight, it looks like there should be many additional interaction terms, but the interactions between the fields which do not appear in Eq. (3.43) are forbidden by momentum conservation, as is shown in Fig. 3.4.

As a last step, one needs to expand each interaction term in its small momentum components. This procedure is called derivative (or multipole) expansion [33]. Consider the

Fourier transform of the fields in a given interaction term;

$$\int d^d x \phi_c^2(x)\phi_s(x) = \int d^d x \int \frac{d^d p_1}{(2\pi)^d} \int \frac{d^d p_2}{(2\pi)^d} \int \frac{d^d p_s}{(2\pi)^d} \tilde{\phi}_c(p_1)\tilde{\phi}_c(p_2)\tilde{\phi}_s(p_s) e^{-i(p_1+p_2+p_s)\cdot x} \,, \quad (3.45)$$

where the tilde indicates the transformed fields. If, as we assumed, the momenta p_1 and p_2 are collinear to p, while p_s is soft, then the sum of the three momenta scales as

$$p_1^\mu + p_2^\mu + p_s^\mu \sim \left(\lambda^2, 1, \lambda\right) Q \,. \quad (3.46)$$

Consequently the components of x must scale as

$$x^\mu \sim \left(1, \frac{1}{\lambda^2}, \frac{1}{\lambda}\right) \frac{1}{Q} \,. \quad (3.47)$$

If one now considers the fact that all of the components of the soft momentum scale as λ^2, one finds that

$$p_s \cdot x = \underbrace{(p_s)_+ \cdot x_-}_{\mathcal{O}(1)} + \underbrace{(p_s)_- \cdot x_+}_{\mathcal{O}(\lambda^2)} + \underbrace{(p_s)_\perp \cdot x_\perp}_{\mathcal{O}(\lambda)} \,. \quad (3.48)$$

Since the derivatives of the soft field scale as the components of the soft momentum, the Taylor expansion of the soft field around the point $x_-^\mu = (x \cdot \bar{n}) n^\mu / 2$ is

$$\phi_s(x) = \phi_s(x_-) + \underbrace{x_\perp \cdot \partial_\perp \phi_s(x_-)}_{\mathcal{O}(\lambda)} + \underbrace{x_+ \cdot \partial_- \phi_s(x_-)}_{\mathcal{O}(\lambda^2)} + \frac{1}{2}\Big(\underbrace{x_{\mu\perp} x_{\nu\perp} \partial^\mu \partial^\nu \phi_s(x_-)}_{\mathcal{O}(\lambda^2)}\Big) + \mathcal{O}(\lambda^3) \,. \quad (3.49)$$

Consequently, up to first order in λ, the interaction term between the collinear and soft field can be rewritten as

$$\int d^d x \, \phi_c^2(x)\phi_s(x) = \int d^d x \, \phi_c^2(x)\phi_s(x_-) + \mathcal{O}(\lambda) \,. \quad (3.50)$$

The leading power scalar SCET Lagrangian has then the following form:

$$\begin{aligned} \mathcal{L}_{\text{eff}} \;&=\; \frac{1}{2}\partial_\mu \phi_c(x) \partial^\mu \phi_c(x) - \frac{g}{3!}\phi_c^3(x) + \frac{1}{2}\partial_\mu \phi_{\bar{c}}(x) \partial^\mu \phi_{\bar{c}}(x) - \frac{g}{3!}\phi_{\bar{c}}^3(x) \\ &+\; \frac{1}{2}\partial_\mu \phi_s(x) \partial^\mu \phi_s(x) - \frac{g}{3!}\phi_s^3(x) - \frac{g}{2}\phi_c^2(x)\phi_s(x_-) - \frac{g}{2}\phi_{\bar{c}}^2(x)\phi_s(x_+) \,. \end{aligned} \quad (3.51)$$

3.3.2. Matching Procedure and Current Operator

In an effective theory, the hard contributions lead to matching corrections. The procedure which allows the hard corrections to be taken into account is the following:

1) write down the most general form of the Lagrangian, including all the operators which are compatible with the symmetry of the theory, each one of which will be multiplied by arbitrary coefficients (the *Wilson coefficients*);

ii) calculate a given interaction process both in the full theory and in the effective theory,

iii) fix the values of the Wilson coefficients in such a way that the results obtained in the full and in the effective theory coincide.

In general, such matching corrections modify the effective Lagrangian. However, for the case of SCET, it turns out that only the operators which involve collinear fields in different directions get matching corrections. To describe the Sudakov form factor, we introduce an external current coupling to two scalar fields

$J = \phi^2 =$ 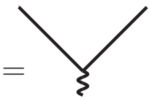 (3.52)

and will consider the current at large momentum transfer. In the following, we first explain why the matching corrections are absent for the Lagrangian derived in the last section and then compute them for the current operator, which will involve collinear fields in both directions.

To allow for the presence of matching corrections in the Lagrangian, we introduce Wilson coefficients which multiply the interaction terms in Eq. (3.51); in particular the term involving three collinear c fields will become

$$-\frac{g}{3!}\phi_c^3(x) \to -\frac{g}{3!}C\phi_c^3(x) \equiv -\frac{g}{3!}\left(1 + g^2C^{(1)} + g^4C^{(2)} + \cdots\right)\phi_c^3(x)\,. \tag{3.53}$$

In order to fix the coefficient $C^{(1)}$ one requires that the corrections of order g^2 to the interaction of three scalar fields are the same in the full theory and in the effective theory. In the full theory these corrections coincide with the one-loop corrections to the ϕ^3 vertex, while in the effective theory one finds contributions originating from one-loop graphs and contributions proportional to $C^{(1)}$. One obtains the following diagrammatic equation

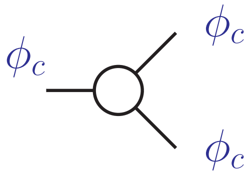

$=$ 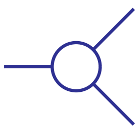 $+$ 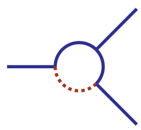 $+\cdots+g^2C^{(1)}$ 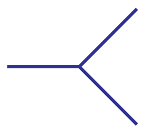 , (3.54)

where all the external legs have momenta collinear to p, blue lines indicate collinear fields in the effective theory, while red lines indicates the soft ϕ field in the effective theory. The dots in Eq. (3.54) indicate two additional diagrams which can be obtained from the second diagram by moving the internal soft line in the other two possible positions. All of the loop integrals in Eq. (3.54) are scaleless, since they do not have internal masses and all of the scalar products, that can be generated with the external legs momenta, will be proportional to the square of the momentum p, which vanishes in the $\lambda \to 0$ limit. Since in dimensional regularization scaleless integrals evaluate to zero, we can conclude that the one-loop matching condition is $C^{(1)} = 0$. The same kind of reasoning applies if one considers a larger number of loops; we can conclude that $C = 1$ to all orders in perturbation theory. The same kind of reasoning can be applied to all of the interaction terms appearing in Eq. (3.51).

While the terms appearing in the Lagrangian in Eq. (3.51) do not receive matching corrections, the terms originating from the current operator J do. The most general form that the current operator can have in the effective theory is the following:

$$J \to J_2 + J_3 + \cdots = C_2 \phi_c \phi_{\bar{c}} + \frac{C_3}{2!}\left(\phi_c^2 \phi_{\bar{c}} + \phi_c \phi_{\bar{c}}^2\right) + \cdots , \tag{3.55}$$

where the subscript in J_i and C_i indicates the number of fields involved in the corresponding operator. Moreover, one should consider the scaling of the derivative of collinear fields; as was shown above, the projection of the derivative of the collinear field in a given direction scales as the corresponding component of the momentum, therefore

$$n \cdot \partial \phi_c(x) \sim \lambda^2 \phi_c(x)\,, \quad \partial_\perp^\mu \phi_c(x) \sim \lambda \phi_c(x)\,, \quad \bar{n} \cdot \partial \phi_c(x) \sim \lambda^0 \phi_c(x)\,, \tag{3.56}$$

and similarly

$$\bar{n} \cdot \partial \phi_{\bar{c}}(x) \sim \lambda^2 \phi_{\bar{c}}(x)\,, \quad \partial_\perp^\mu \phi_{\bar{c}}(x) \sim \lambda \phi_{\bar{c}}(x)\,, \quad n \cdot \partial \phi_{\bar{c}}(x) \sim \lambda^0 \phi_{\bar{c}}(x)\,. \tag{3.57}$$

The derivatives $\bar{n} \cdot \partial \phi_c$ and $n \cdot \partial \phi_{\bar{c}}$ are not power suppressed, because the collinear fields carry large energies in these directions. Even at leading power in λ, one needs to allow the current operators in the EFT to contain an arbitrary number of terms of this kind. The expansion of a collinear field along the collinear direction can be written as an infinite sum over the non-power suppressed derivatives

$$\phi(x + tn) = \sum_{i=0}^{\infty} \frac{t^i}{i!} n \cdot \partial^i \phi(x)\,. \tag{3.58}$$

Therefore, to include terms with arbitrarily high derivatives is equivalent to allowing for non-locality of the collinear fields along the collinear directions. For example, the operator J_2 in Eq. (3.55) can be written as

$$J_2(x) = \int ds dt\, C_2(s,t,\mu)\, \phi_c\,(x + s\bar{n}) \phi_{\bar{c}}\,(x + tn)\,. \tag{3.59}$$

The SCET operators are thus non-local along the light-cone directions. The non-locality of the operators in position space is reflected in the dependence of the Wilson coefficients on the large energies scales present in the problem. In fact, the Fourier transform of the coefficient $C_2(s,t)$ will be

$$\tilde{C}_2\,(\bar{n} \cdot p\,, n \cdot l, \mu) = \int ds dt\, e^{is\bar{n}\cdot p} e^{-itn\cdot l} C_2(s,t,\mu)\,. \tag{3.60}$$

To be precise, we have indicated that the Wilson coefficient $C_2(s,t,\mu)$ will depend on the renormalization scale μ. This dependence is governed by a RG equation and, as we will show later, can be used to perform resummation. The function $\tilde{C}_2$ must be expanded in powers of the coupling constant g as follows

$$\tilde{C}_2 = \tilde{C}_2^{(0)} + g^2 \tilde{C}_2^{(1)} + g^4 \tilde{C}_2^{(2)} + \cdots\,. \tag{3.61}$$

One can immediately see that the simple matching condition at order g^0 leads to the relation $\tilde{C}_2^{(0)} = 1$. At this stage it is possible to write the matching equation which allows one to fix of the value of $\tilde{C}_2$ at order g^2

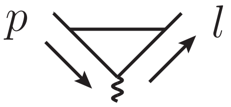

$$= \quad \tilde{C}_2^{(1)}(\underbrace{\bar{n}\cdot p\, n\cdot l}_{=Q^2})$$

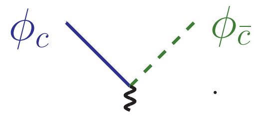

$$. \tag{3.62}$$

The momenta p and l are both on-shell, and the diagram on the left-hand-side (l.h.s.) of the equation above coincides with the hard region integral introduced in Section 3.2. On the r.h.s. of the matching equation, one should also include the contribution of the one-loop diagram with an internal soft leg multiplied by $\tilde{C}_2^{(0)}$. However, that integral corresponds to the soft region integral calculated in the previous section, but with on-shell external legs. The latter vanishes in dimensional regularization if one sets $p^2 = l^2 = 0$ from the start, as it is shown in Appendix A.1.3. One should also add on the r.h.s. the two one-loop diagrams with the collinear leg corrections multiplied by $\tilde{C}_3^{(0)}$, but they also vanish because they are scaleless (p and l on-shell).

We now want to match the Feynman diagrams involving a current operator, two collinear fields of type $\bar{c}$, and one collinear field of type c onto the effective theory at lowest order in the coupling constant. The relevant diagrammatic equation is

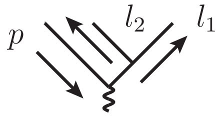

$$+$$

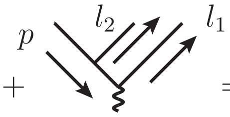

$$= \tilde{C}_2^{(0)}$$

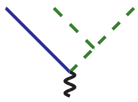

$$+ \tilde{C}_3^{(0)}$$

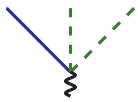

$$. \tag{3.63}$$

The diagrams on the l.h.s. of the Eq. (3.63) are easily evaluated, since they involve only single propagators carrying momenta

$$(p - l_2)^2 = -2p\cdot l_2 + \mathcal{O}\left(\lambda^2\right) = -\left(n\cdot l_2\right)\left(\bar{n}\cdot p\right) + \mathcal{O}\left(\lambda^2\right) \tag{3.64}$$

and $(l_1 + l_2)^2$. Since $\tilde{C}_2^{(0)} = 1$ the first diagram on the l.h.s. and the first diagram on the r.h.s. of Eq. (3.63) give identical contributions and drop out of the equation. The value of the coefficient $\tilde{C}_3^{(0)}$ is therefore determined by the second diagram on the l.h.s. of Eq. (3.63):

$$\tilde{C}_3^{(0)}\left(n\cdot l_1, n\cdot l_2, \bar{n}\cdot p, \mu\right) = \frac{-g}{-\left(n\cdot l_2\right)\left(\bar{n}\cdot p\right) + i0^+}\,. \tag{3.65}$$

At this point, we would like to go back to the effective Lagrangian and extract the form of the Wilson coefficients C_2^0 and C_3^0 in position space. The correspondence $p^\mu \leftrightarrow i\partial^\mu$ indicates that the Wilson coefficient C_3^0 comes from an effective Lagrangian involving inverse derivatives:

$$\frac{-g}{-\left(n\cdot l_2\right)\left(\bar{n}\cdot p\right) + i0^+} \longleftrightarrow g\left(\frac{1}{\bar{n}\cdot\partial}\phi_c\right)\left(\frac{1}{n\cdot\partial}\phi_{\bar{c}}\right)\phi_{\bar{c}}\,. \tag{3.66}$$

The two derivatives scale both like $\lambda^0 Q$ and therefore the current operator J_3 is suppressed by a factor $1/Q^2$. The presence of an inverse derivative is at first sight disturbing, but it is again an effect of the non-locality mentioned above. Observe that the inverse derivative of a field can be written as an integral

$$\frac{i}{in\cdot\partial + i0^+}\,\phi(x) = \int_{-\infty}^{0} ds\,\phi(x+sn)\,; \tag{3.67}$$

in fact the relation above can be checked by applying the derivative to the r.h.s.

$$n^\mu \int_{-\infty}^{0} ds\,\partial_\mu\phi(x+sn) = n^\mu \int_{-\infty}^{0} ds\,\frac{1}{n^\mu}\frac{\partial}{\partial s}\phi(x+sn) = \phi(x+sn)|_{\infty}^{0} = \phi(x)\,. \tag{3.68}$$

It is a characteristic feature of SCET that the operators are non-local along the directions of large light-cone momentum. In general, in order to write down the most general SCET operators, one smears the fields along the light cone. Therefore the current operator in the full theory, which is quadratic in the fields, will be replaced as follows

$$J = \phi^2(x) \to J_2(x) + J_3(x) + \cdots\,, \tag{3.69}$$

where the operator $J_2(x)$ has the form shown in Eq. (3.59), while

$$J_3(x) = \int_{-\infty}^{+\infty} ds \int_{-\infty}^{+\infty} dt_1 \int_{-\infty}^{+\infty} dt_2\, C_3(s,t_1,t_2,\mu)\phi_c(x+s\bar{n})\phi_{\bar{c}}(x+t_1 n)\phi_{\bar{c}}(x+t_2 n) + (c \leftrightarrow \bar{c})\,. \tag{3.70}$$

According to the discussion in this section, one finds that

$$\begin{aligned} C_2(s,t,\mu) &= \delta(s)\delta(t) + \mathcal{O}(g^2)\,, \\ C_3(s,t_1,t_2,\mu) &= g\theta(-s)\delta(t_1)\theta(-t_2) + \mathcal{O}(g^3)\,. \end{aligned} \tag{3.71}$$

In fact

$$\begin{aligned} \tilde{C}_2^{(0)} &= \int_{-\infty}^{+\infty} ds \int_{-\infty}^{+\infty} dt e^{is\bar{n}\cdot p} e^{-itn\cdot l}\,\delta(s)\delta(t) = 1\,, \\ \tilde{C}_3^{(0)} &= g\int_{-\infty}^{+\infty} ds \int_{-\infty}^{+\infty} dt_1 \int_{-\infty}^{+\infty} dt_2 e^{is\bar{n}\cdot p} e^{-it_1 n\cdot l_1} e^{-it_2 n\cdot l_2}\theta(-s)\theta(-t_2)\delta(t_1)\,, \\ &= g\int_{-\infty}^{0} ds \int_{-\infty}^{0} dt_2 e^{is\bar{n}\cdot p} e^{-it_2 n\cdot l_2} = \frac{g}{(\bar{n}\cdot p)\,(n\cdot l_2)}\,. \end{aligned} \tag{3.72}$$

The dependence of the functions C_i on s,t is equivalent to the dependence of the coefficients $\tilde{C}_i$ on the large energy scale in momentum space; the correspondence between the two notations is given by

$$\delta(s) \leftrightarrow 1\,, \qquad \theta(-s) \leftrightarrow \frac{1}{Q}\,. \tag{3.73}$$

3.3.3. Sudakov Form Factor in SCET

At this point, all of the pieces of the one-loop correction to the current operator of ϕ^3 theory in the limit $\lambda \to 0$ are available. By employing the Feynman rules derived from the SCET Lagrangian one finds

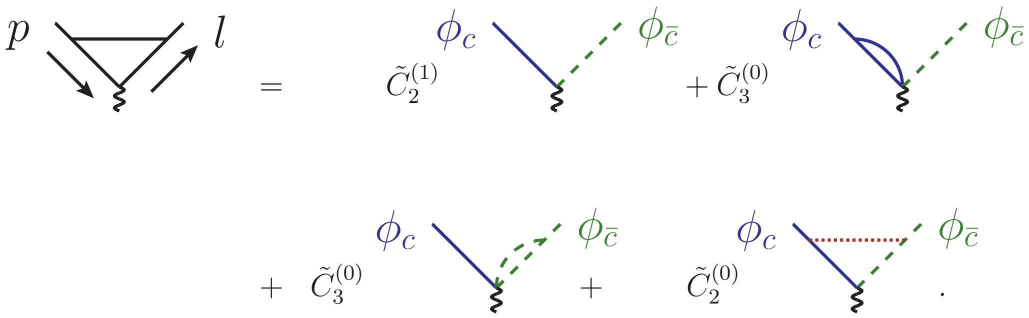

. (3.74)

It is perhaps useful to repeat that, in the relation above, the external squared momenta p^2 and l^2 are small but not exactly equal to zero from the start as in the matching calculation. By employing the expressions of the Wilson coefficients provided in the previous sections one can check that the four diagrams on the r.h.s. of Eq. (3.74) are the hard-region integral, the two collinear region integrals, and the soft-region integral which were found using the strategy of regions. For example, let us consider the third diagram in the r.h.s. of Eq. (3.74); one finds that

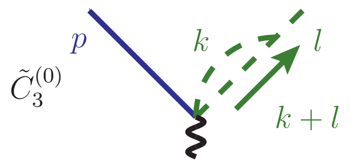

$$\sim g \int d^d k \frac{1}{(k^2 + i0^+)\left[(k+l)^2 + i0^+\right]} \underbrace{\frac{1}{2k_+ \cdot p_- + i0^+}}_{=\tilde{C}_3^{(0)}} \, . \tag{3.75}$$

Similarly, one can prove that the fourth integral on the r.h.s. of Eq. (3.74) gives rise to the integral in Eq. (3.38), simply by observing that the momentum in the soft internal line scales like $k^2 \sim \lambda^4$ and therefore one must neglect k^2 in the two collinear propagators.

For order-by-order calculations, the direct application of the strategy of regions is more efficient. However, SCET allows to study all-order properties of scattering amplitudes, such as factorization theorems. As an example we discuss a factorization theorem for the Sudakov form factor in Appendix A.2.

3.4. Generalization to QCD

The method which allowed us to write down the SCET Lagrangian for the scalar ϕ^3 theory in the previous section is analogous to the method that one employs to construct an effective theory for QCD. In particular, the same momentum regions appear, since only the numerators of the diagrams differ between the ϕ^3 theory case and the QCD case.

However, in the QCD[1] case three complications arise:

i) different components of the quark field $q(x)$ and of the gluon field $A_\mu(x)$ scale differently,

ii) the effective theory must simultaneously be gauge invariant and respect the power counting,

iii) the non-local operators must involve Wilson lines to preserve gauge invariance.

To make things as simple as possible let us start by considering only one type of collinear field, with a momentum which scales as

$$p^\mu \sim \left(\lambda^2, 1, \lambda\right) Q\,. \tag{3.76}$$

One then splits the gluon and quark fields into a collinear and a soft part

$$A^\mu(x) \to A_c^\mu(x) + A_s^\mu(x)\,, \qquad \psi(x) \to \psi_c(x) + \psi_s(x)\,. \tag{3.77}$$

We now consider the collinear part of the fermion field and we further split it into two components as follows

$$\psi_c(x) \equiv \xi(x) + \eta(x)\,, \tag{3.78}$$

where

$$\xi = P_+\,\psi_c \equiv \frac{\not{n}\not{\bar{n}}}{4}\psi_c\,, \qquad \eta = P_-\,\psi_c \equiv \frac{\not{\bar{n}}\not{n}}{4}\psi_c\,. \tag{3.79}$$

As a consequence of the definition of the operators $P_\pm$ and of the fact that $n^2 = \bar{n}^2 = 0$ one finds that

$$\not{n}\,\xi(x) = 0\,, \quad \text{and} \quad \not{\bar{n}}\,\eta(x) = 0\,. \tag{3.80}$$

It is easy to check that $P_\pm$ are projection operators:

$$P_+ + P_- \;=\; \frac{\not{n}\not{\bar{n}}}{4} + \frac{\not{\bar{n}}\not{n}}{4} = \frac{2\bar{n}\cdot n}{4} = 1\,, \tag{3.81}$$

and one can also immediately verify that $P_+^2 = P_+$ and $P_-^2 = P_-$.

3.4.1. Power Counting

As a first step, we want to determine the powers of λ which characterize the scaling of the components of the fermionic collinear field. This information can be obtained by looking at appropriate two points correlators. We start from the ξ component[2]

$$\langle 0|T\left\{\xi(x)\bar{\xi}(0)\right\}|0\rangle \;=\; \frac{\not{n}\not{\bar{n}}}{4}\langle 0|T\left\{\psi_c(x)\bar{\psi}_c(0)\right\}|0\rangle\frac{\not{\bar{n}}\not{n}}{4}\,,$$

[1]The derivation of the SCET Lagrangian for supersymmetric QCD is exactly the same as in QCD since the soft and collinear modes of the two theories are the same. The difference arise at the level of the matching with current operators. In that case, the hard modes introduced by supersymmetry will enter the Wilson coefficients of those operators.

[2]Observe that $\overline{(\not{n}\not{\bar{n}}\psi_c)} = \psi_c^\dagger \not{\bar{n}}^\dagger \not{n}^\dagger \gamma_0 = \bar{\psi}_c \not{\bar{n}}\not{n}$, which follows after inserting $\left(\gamma^0\right)^2 = 1$ between the Dirac matrices and using $\gamma^0\gamma^{\mu\dagger}\gamma^0 = \gamma^\mu$.

$$= \int \frac{d^4p}{(2\pi)^4} \frac{i}{p^2 + i0} e^{-ip\cdot x} \frac{\not{n}\not{\bar{n}}}{4} \not{p} \frac{\not{\bar{n}}\not{n}}{4} \sim \lambda^4 \frac{1}{\lambda^2} = \lambda^2 \,, \tag{3.82}$$

where we employed the identity

$$\frac{\not{n}\not{\bar{n}}}{4} \not{p} \frac{\not{\bar{n}}\not{n}}{4} = \frac{\not{n}\not{\bar{n}}}{4} \left[\bar{n} \cdot p \frac{\not{n}}{2} + n \cdot p \frac{\not{\bar{n}}}{2} + \not{p}_\perp \right] \frac{\not{\bar{n}}\not{n}}{4} = \bar{n} \cdot p \frac{\not{n}}{2} \sim \lambda^0 \,. \tag{3.83}$$

Therefore $\xi(x) \sim \lambda$. The correlator for the η component is

$$\langle 0 | T \left\{ \eta(x) \bar{\eta}(0) \right\} | 0 \rangle = \frac{\not{\bar{n}}\not{n}}{4} \langle 0 | T \left\{ \psi_c(x) \bar{\psi}_c(0) \right\} | 0 \rangle \frac{\not{n}\not{\bar{n}}}{4} \,, \tag{3.84}$$

$$= \int \frac{d^4p}{(2\pi)^4} \frac{i}{p^2 + i0} e^{-ip\cdot x} \underbrace{\frac{\not{\bar{n}}\not{n}}{4} \not{p} \frac{\not{n}\not{\bar{n}}}{4}}_{= n\cdot p \frac{\not{\bar{n}}}{2}} \sim \lambda^4 \lambda^2 \frac{1}{\lambda^2} = \lambda^4 \,; \tag{3.85}$$

the scaling of this component $\eta(x) \sim \lambda^2$. Finally for the soft field one finds

$$\langle 0 | T \left\{ \psi_s(x) \bar{\psi}_s(0) \right\} | 0 \rangle = \int \frac{d^4p}{(2\pi)^4} \frac{i\not{p}}{p^2 + i0} e^{-ip\cdot x} \sim (\lambda^2)^4 \lambda^2 \frac{1}{\lambda^4} = \lambda^6 \,, \tag{3.86}$$

so that $\psi_s \sim \lambda^3$.

The two-point correlator for the gluon field is

$$\langle 0 | T \left\{ A^\mu(x) A^\nu(0) \right\} | 0 \rangle = \int \frac{d^4p}{(2\pi)^4} \frac{i}{p^2 + i0} e^{-ip\cdot x} \left[-g^{\mu\nu} + (1-\alpha) \frac{p^\mu p^\nu}{p^2} \right] \,; \tag{3.87}$$

A glance to the second term in the square bracket shows that the gluon field scales like its momentum, therefore $A_s^\mu(x) \sim p_s^\mu$ and $A_c^\mu(x) \sim p_c^\mu$, or equivalently

$$\bar{n} \cdot A_c \sim \lambda^0 \,, \quad n \cdot A_c \sim \lambda^2 \,, \quad A_{c\perp} \sim \lambda \,; \quad A_s^\mu \sim \lambda^2 \,. \tag{3.88}$$

The $\bar{n} \cdot A_s$ and $A_{s\perp}$ components of the soft gluon field are power suppressed relative to the corresponding components of the collinear gluon field. The $n \cdot A_s$ component of the soft gluon field scales the same way as the corresponding component of the collinear gluon field.

3.4.2. Effective Lagrangian

The collinear fermion Lagrangian has a special form since the η components are of higher order in λ than the ξ components and can therefore be integrated out. The covariant derivative is as usual defined as

$$iD_\mu \equiv i\partial_\mu + gA_\mu = i\partial_\mu + g(A_{c\mu}^{\,a} + A_{s\mu}^{\,a})\, t^a \,, \tag{3.89}$$

where the matrices t^a are the usual generators of $SU(3)$, in the fundamental representation. For the moment, we will keep both the soft and collinear componets of the gluon field even though $A_{s\perp}$ and A_{s+} are power suppressed relative to the collinear gluon field. We will come back to this point when discussing the soft-collinear interactions. By using the relations $\not{n}\xi = \bar{\xi}\not{n} = 0$ and $\not{\bar{n}}\eta = \bar{\eta}\not{\bar{n}} = 0$, $\bar{\xi}\not{D}_\perp\xi = 0$ and $\bar{\eta}\not{D}_\perp\eta = 0$ one obtains [3]

$$\begin{aligned}
\mathcal{L}_c &= \bar{\psi}_c i\not{D}\psi_c\,, \\
&= \left(\bar{\xi}+\bar{\eta}\right)\left[\frac{\not{n}}{2}i\bar{n}\cdot D + \frac{\not{\bar{n}}}{2}in\cdot D + i\not{D}_\perp\right]\left(\xi+\eta\right)\,, \\
&= \bar{\xi}\frac{\not{\bar{n}}}{2}in\cdot D\xi + \bar{\xi}i\not{D}_\perp\eta + \bar{\eta}i\not{D}_\perp\xi + \bar{\eta}\frac{\not{n}}{2}i\bar{n}\cdot D\eta\,.
\end{aligned} \tag{3.90}$$

Since the action is quadratic, one can integrate out η exactly. An easy way to obtain the Lagrangian that one arrives once the field η is integrated out makes use of the equations of motion derived from the Lagrangian in Eq. (3.90). The equations of motion for $\bar{\xi}$ are

$$\partial_\mu\frac{\partial\mathcal{L}_c}{\partial(\partial_\mu\bar{\xi})} - \frac{\partial\mathcal{L}_c}{\partial\bar{\xi}} = -\frac{\partial\mathcal{L}_c}{\partial\bar{\xi}} = -\frac{\not{\bar{n}}}{2}in\cdot D\xi - i\not{D}_\perp\eta = 0\,, \tag{3.91}$$

or equivalently

$$\frac{\not{\bar{n}}}{2}n\cdot D\xi = -\not{D}_\perp\eta\,. \tag{3.92}$$

Similarly for $\bar{\eta}$ one finds

$$\not{D}_\perp\xi = -\frac{\not{n}}{2}\bar{n}\cdot D\eta\,. \tag{3.93}$$

From the latter one obtains

$$\frac{\not{\bar{n}}}{2}\not{D}_\perp\xi = -\frac{\not{\bar{n}}\not{n}}{4}\bar{n}\cdot D\eta = -\bar{n}\cdot D\eta\,. \tag{3.94}$$

Solving for η one finds

$$\eta = -\frac{\not{\bar{n}}}{2\bar{n}\cdot D}\not{D}_\perp\xi\,, \quad \text{and} \quad \bar{\eta} = -\bar{\xi}\overleftarrow{\not{D}}_\perp\frac{\not{\bar{n}}}{2\bar{n}\cdot\overleftarrow{D}}\,, \tag{3.95}$$

where the arrow indicates that the covariant derivative is acting to the left. At this stage one can insert Eqs. (3.95) in the collinear Lagrangian in order to eliminate η:

$$\begin{aligned}
\mathcal{L}_c &= \bar{\xi}\frac{\not{\bar{n}}}{2}in\cdot D\xi + \bar{\xi}i\not{D}_\perp\frac{1}{i\bar{n}\cdot D}i\not{D}_\perp\frac{\not{\bar{n}}}{2}\xi + \bar{\xi}i\overleftarrow{\not{D}}_\perp\frac{1}{i\bar{n}\cdot\overleftarrow{D}}i\not{D}_\perp\frac{\not{\bar{n}}}{2}\xi \\
&+ \bar{\xi}i\overleftarrow{\not{D}}_\perp\frac{\not{\bar{n}}}{2i\bar{n}\cdot\overleftarrow{D}}\underbrace{\frac{\not{n}}{2}i\bar{n}\cdot D\frac{\not{\bar{n}}}{2i\bar{n}\cdot D}}_{\frac{\not{n}\not{\bar{n}}}{4}=P_+}i\not{D}_\perp\xi\,,
\end{aligned}$$

[3] Note that $\bar{\xi}\not{D}_\perp\xi = \bar{\xi}P_-\not{D}_\perp P_+\xi = \bar{\xi}\not{D}_\perp P_-P_+\xi = 0$, where we have used $\{\not{n},\not{D}_\perp\} = \{\not{\bar{n}},\not{D}_\perp\} = 0$.

$$= \quad \bar{\xi}\frac{\bar{\not{n}}}{2} in\cdot D\xi + \bar{\xi} i\not{D}_\perp \frac{1}{i\bar{n}\cdot D} i\not{D}_\perp \frac{\bar{\not{n}}}{2}\xi\,. \tag{3.96}$$

In deriving the equation above we repeatedly used the fact that $\{\bar{\not{n}}, \not{D}_\perp\} = 0$ and in the last line we used the fact that

$$P_+\not{D}_\perp\xi = \not{D}_\perp P_+\xi \quad = \quad \not{D}_\perp\xi\,. \tag{3.97}$$

In the path integral, the integration over the fermionic fields η and $\bar{\eta}$ gives (see for example [45], page 110)

$$\int \mathcal{D}[\eta]\mathcal{D}[\bar{\eta}] \exp\left\{ i\int d^4x\, \bar{\eta}\frac{\not{n}}{2} i\bar{n}\cdot D\eta\right\} \sim \det\left(\frac{\not{n}}{2} i\bar{n}\cdot D\right)\,. \tag{3.98}$$

We will now show that this overall determinant is irrelevant. Observe that the determinant is gauge invariant. In fact, if we indicate with V a SU(N) matrix, such that a quark field transforms according to $\psi \to V\psi$ under gauge transformations, the determinant's covariant derivative will transform as $D \to VDV^\dagger$. Therefore

$$\begin{aligned} \det\left(\frac{\not{n}}{2} i\bar{n}\cdot D\right) \to \det\left(\frac{\not{n}}{2} V i\bar{n}\cdot DV^\dagger\right) \quad &= \quad \underbrace{\det(V)}_{=1} \det\left(\frac{\not{n}}{2} i\bar{n}\cdot D\right) \underbrace{\det\left(V^\dagger\right)}_{=1}\,, \\ &= \quad \det\left(\frac{\not{n}}{2} i\bar{n}\cdot D\right)\,. \end{aligned} \tag{3.99}$$

In the light cone gauge, where $\bar{n}\cdot A = 0$, the determinant is trivially independent from the gluon field; since the determinant was just proven to be gauge independent, it does not depend on the gluon field in any gauge, and is therefore an irrelevant factor multiplying the path integral.

While the collinear quark Lagrangian has a somewhat complicated structure, the collinear gluon Lagrangian is simply a copy of the QCD Lagrangian in which the gluon field A^μ is replaced by the collinear gluon field A_c^μ. The same is true for the kinetic terms of the Lagrangian for the soft fields,

$$\mathcal{L}_s = \bar{\psi}_s i\not{D}_s\psi_s - \frac{1}{4}(F_s^a)_{\mu\nu}(F_s^a)^{\mu\nu}\,, \tag{3.100}$$

where the covariant derivative and field strength tensor are defined as

$$\begin{aligned} iD_s^\mu \quad &= \quad i\partial^\mu + gA_s^\mu = i\partial^\mu + g(A_s^a)^\mu t^a\,, \\ ig(F_s^a)^{\mu\nu}t^a \quad &= \quad [iD_s^\mu, iD_s^\nu] = ig\left\{\partial^\mu A_s^\nu - \partial^\nu A_s^\mu - ig\left[A_s^\mu, A_s^\nu\right]\right\}\,, \\ &= \quad ig\left\{\partial^\mu (A_s^a)^\nu - \partial^\nu (A_s^a)^\mu + gf^{abc}(A_s^b)^\mu (A_s^c)^\nu\right\} t^a\,. \end{aligned} \tag{3.101}$$

Therefore, the kinetic terms of the SCET QCD Lagrangian are given by Eqs. (3.90), (3.100) and by a standard kinetic term for the collinear gluons. We now need to consider the terms describing the interactions between soft and collinear fields.

3.4.3. Soft Collinear Interactions

The general construction of the soft-collinear interaction terms is somewhat involved and beyond the scope of this thesis, it can be found in [33]. For collider physics applications, it is usually sufficient to consider soft-collinear interactions at leading power. To obtain the interactions at leading order in λ, let us remind ourselves of the scaling of the different fields

$$\begin{aligned} (n\cdot A_c, \bar{n}\cdot A_c, A_{c\perp}) &\sim \left(\lambda^2, 1, \lambda\right) , \\ (n\cdot A_s, \bar{n}\cdot A_s, A_{s\perp}) &\sim \left(\lambda^2, \lambda^2, \lambda^2\right) , \\ \xi\sim\lambda\,, &\qquad \psi_s\sim\lambda^3\,. \end{aligned} \tag{3.102}$$

In the case of the ϕ^3 theory the soft-collinear interactions were obtained by replacing once the fields in the interaction term with a soft field

$$-\frac{g}{3!}\int d^4x\,\phi^3(x)\longrightarrow -\frac{g}{2!}\int d^4x\,\phi_c^2(x)\phi_s(x_-)\,. \tag{3.103}$$

In the SCET Lagrangian for QCD, soft-collinear interactions involving soft quarks do not appear at leading order, since ψ_s is power suppressed with respect to ξ. Furthermore, only the $n\cdot A_s$ component of the soft gluon field is not power suppressed with respect to the corresponding component of the collinear gluon field, so only this component enters the leading soft-collinear interactions. Therefore one can replace

$$A^\mu(x)\longrightarrow \left(n\cdot A_c(x)+n\cdot A_s(x_-)\right)\frac{\bar{n}^\mu}{2}+\bar{n}\cdot A_c(x)\frac{n^\mu}{2}+A^\mu_{c\perp}(x)\,. \tag{3.104}$$

in the collinear Lagrangian. To summarize the SCET Lagrangian for QCD can be written in a compact form as follows

$$\mathcal{L}_{\text{SCET}}=\bar{\psi}_s i\not{D}_s\psi_s+\bar{\xi}\frac{\not{\bar{n}}}{2}\left[in\cdot D+i\not{D}_{c\perp}\frac{1}{i\bar{n}\cdot D_c}i\not{D}_{c\perp}\right]\xi-\frac{1}{4}\left(F^{s,a}_{\mu\nu}\right)^2-\frac{1}{4}\left(F^{c,a}_{\mu\nu}\right)^2\,. \tag{3.105}$$

The various covariant derivatives which appear in Eq. (3.105) are given by

$$\begin{aligned} iD_s &= i\partial+gA_s=i\partial+gA^a_s t^a\,, \\ iD_c &= i\partial+gA_c=i\partial+gA^a_c t^a\,, \\ in\cdot D &= in\cdot\partial+g\,n\cdot A_c(x)+g\,n\cdot A_s(x_-)\,, \end{aligned} \tag{3.106}$$

where we suppressed the Lorentz index. The field strengths are

$$\begin{aligned} igF^{s,a}_{\mu\nu}t^a &= \left[iD^s_\mu, iD^s_\nu\right]\,, \\ igF^{c,a}_{\mu\nu}t^a &= \left[iD_\mu, iD_\nu\right]\,, \end{aligned} \tag{3.107}$$

where the covariant derivative appearing in the commutator in the last line of Eq. (3.107) is

$$D^\mu = n\cdot D\frac{\bar{n}^\mu}{2} + \bar{n}\cdot D_c\frac{n^\mu}{2} + D_{c\perp}\,. \tag{3.108}$$

The Lagrangian in Eq. (3.105) includes only one collinear sector, but in many applications one needs two or more collinear sectors. As in the case of the scalar ϕ^3 theory, we will in the following consider two collinear momenta $p \sim (\lambda^2, 1, \lambda)$ and $l \sim (1, \lambda^2, \lambda)$. The second collinear sector in the Lagrangian can be obtained by replacing $n^\mu \leftrightarrow \bar{n}^\mu$ (i. e. $x_+ \leftrightarrow x_-$) in the first collinear sector.

3.4.4. Gauge Trasformations

In the same way in which we expanded the Lagrangian, it is necessary to expand the gauge transformations, and one must make sure that the gauge transformations respect the scaling of the fields. For example, we will see that transforming a soft field by means of a gauge transformation with gauge parameter $\alpha(x)$ will turn the soft field into a collinear field if $\alpha(x)$ has collinear scaling.

We will consider two types of gauge transformations; the soft gauge transformation

$$V_s(x) = \exp\left[i\alpha_s^a(x)t^a\right], \tag{3.109}$$

and the collinear gauge transformation

$$V_c(x) = \exp\left[i\alpha_c^a(x)t^a\right]. \tag{3.110}$$

The functions $\alpha_s^a(x)$ have soft scaling (i. e. $\partial\alpha_s^a(x) \sim \lambda^2\alpha_s^a(x)$), and $\alpha_c^a(x)$ have collinear scaling. We analyze the soft transformations first. Under a **soft gauge transformation** the soft fields transform in the standard way

$$\begin{aligned}
\psi_s(x) &\to V_s(x)\psi_s(x)\,,\\
A_s^\mu(x) &\to V_s(x)A_s^\mu(x)V_s^\dagger(x) + \frac{i}{g}V_s(x)\left[\partial^\mu, V_s^\dagger(x)\right]\,.
\end{aligned} \tag{3.111}$$

The collinear fields transform instead as follows

$$\begin{aligned}
\xi(x) &\to V_s(x_-)\xi(x)\,,\\
A_c^\mu(x) &\to V_s(x_-)A_c^\mu(x)V_s^\dagger(x_-)\,.
\end{aligned} \tag{3.112}$$

The gauge transformation matrices in Eq. (3.112) depend only on x_- since, when transforming the collinear fields, one needs to expand the soft fields around x_- in order to avoid inducing higher power corrections. In fact the expansion of the full soft gauge transformation follows the same pattern already encountered in Eq. (3.49)

$$V_s(x) = V_s(x_-) + \underbrace{x_\perp\cdot\partial V_s(x_-)}_{\mathcal{O}(\lambda)} + \mathcal{O}(\lambda^2)\,. \tag{3.113}$$

A detailed discussion of the gauge transformation properties of the non-abelian gauge Lagrangian is provided in [33].

The transformation of the collinear gluon field differs from the standard one because it is missing the term $V_s[\partial^\mu, V_s^\dagger] \sim \lambda^2$. This term is a higher power correction for the $A_{c\perp}$ and $\bar{n}\cdot A_c$ components of the collinear gluon field. The component $n\cdot A_c \sim \lambda^2$ only appears implicitly in the term $n\cdot D$ (last line of Eq. (3.106)); this term $n\cdot D$ transforms as expected

$$\begin{aligned} n\cdot A_c(x) + n\cdot A_s(x_-) &\rightarrow V_s(x_-)\left[n\cdot A_c(x) + n\cdot A_s(x_-)\right]V_s^\dagger(x_-) \\ &+ \frac{i}{g}V_s(x_-)\left[n\cdot\partial, V_s^\dagger(x_-)\right] , \end{aligned} \tag{3.114}$$

$$in\cdot D \rightarrow V_s(x_-)\, in\cdot D\, V_s^\dagger(x_-) . \tag{3.115}$$

Since the **collinear gauge transformations** involve a field with large energy, the soft fields cannot transform under them:

$$\psi_s(x) \rightarrow \psi_s(x) , \qquad A_s^\mu(x) \rightarrow A_s^\mu(x) . \tag{3.116}$$

The collinear fields instead transform as follows

$$\begin{aligned} \xi(x) &\rightarrow V_c(x)\xi(x) , \\ A_c^\mu(x) &\rightarrow V_c(x)A_c^\mu(x)V_c^\dagger(x) + \frac{1}{g}V_c(x)\left[i\partial^\mu + \frac{\bar{n}^\mu}{2}n\cdot A_s(x_-), V_c^\dagger(x)\right] , \end{aligned} \tag{3.117}$$

which implies

$$\begin{aligned} A_{c\perp}^\mu &\rightarrow V_c A_{c\perp}^\mu V_c^\dagger + \frac{i}{g}V_c\left[\partial_\perp^\mu, V_c^\dagger\right] , \\ \bar{n}\cdot A_c &\rightarrow V_c\bar{n}\cdot A_c V_c^\dagger + \frac{i}{g}V_c\left[\bar{n}\cdot\partial, V_c^\dagger\right] , \\ n\cdot A_c &\rightarrow V_c n\cdot A_c V_c^\dagger + \frac{i}{g}V_c\left[n\cdot D_s(x_-), V_c^\dagger\right] . \end{aligned} \tag{3.118}$$

The last transformation law in the equation above ensures that

$$in\cdot D \rightarrow V_c\, in\cdot D\, V_c^\dagger . \tag{3.119}$$

It is easy to check that the Lagrangian in Eq. (3.105) is separately invariant under soft and collinear gauge transformations. The various covariant derivatives all transform according to

$$D_\mu \rightarrow V_i D_\mu V_i^\dagger ,$$

where $i \in \{s, c\}$, and the fermions transform according to

$$\psi \rightarrow V_i\psi ,$$

with the replacement $x \rightarrow x_-$ in the appropriate places. A complete discussion of the gauge transformations and of the construction of the higher power terms can be found in [33].

3.4.5. Wilson Lines

While discussing the scalar ϕ^3 theory, we encountered non-local operators (see Subsection 3.3.2 in particular Eq. (3.59)). In a gauge theory, a product of fields at different space time points is gauge invariant only if the fields are connected by *Wilson lines*, defined as

$$[x + s\bar{n}, x] \equiv \mathbf{P} \exp \left[ig \int_0^s ds' \, \bar{n} \cdot A(x + s'\bar{n}) \right] . \tag{3.120}$$

The operator $\mathbf{P}$ indicates the path ordering of the color matrices, such that

$$\mathbf{P}[A(x)A(x + s\bar{n})] = A(x + s\bar{n})A(x) \, , \qquad \text{for } \; s > 0. \tag{3.121}$$

The conjugate Wilson line is defined with the opposite ordering prescription. Under gauge transformations the Wilson lines transform as follows (see Appendix A.3)

$$[x + s\bar{n}, x] \longrightarrow V(x + s\bar{n}) \, [x + s\bar{n}, x] \, V^\dagger(x) \, , \tag{3.122}$$

therefore products of the form

$$\bar{\psi}(x + s\bar{n}) \, [x + s\bar{n}, x] \, \psi(x) \, ,$$

are gauge invariant.

In SCET it is customary to work with Wilson lines which go to infinity[4]:

$$W(x) \equiv [x, -\infty\bar{n}] = \mathbf{P} \exp \left[ig \int_{-\infty}^0 ds \bar{n} \cdot A(x + s\bar{n}) \right] . \tag{3.123}$$

The Wilson line along a finite segment can be written as a product of two Wilson lines extending to infinity:

$$\begin{aligned} [x + s\bar{n}, x] &= W\,(x + s\bar{n}) \, W^\dagger(x) \, , \\ &= \mathbf{P} \exp \left[ig \int_{-\infty}^0 dt \, \bar{n} \cdot A(x + s\bar{n} + t\bar{n}) \right] \mathbf{P} \exp \left[-ig \int_{-\infty}^0 dt \, \bar{n} \cdot A(x + t\bar{n}) \right] , \end{aligned}$$

[4]To see that $W(x)$ corresponds to $[x, -\infty\bar{n}]$ let us start from the definition in Eq. (3.120); by setting $x = x' - s\bar{n}$ one obtains

$$[x', x' - s\bar{n}] \equiv \mathbf{P} \exp \left[ig \int_0^s ds' \, \bar{n} \cdot A(x' - s\bar{n} + s'\bar{n}) \right] .$$

One can then shift the integration variable according to $s' = t + s$ to obtain

$$[x', x' - s\bar{n}] \equiv \mathbf{P} \exp \left[ig \int_{-s}^0 dt \, \bar{n} \cdot A(x' + t\bar{n}) \right] .$$

Finally, one can send $s \to \infty$ and rename $x' \to x$ to obtain Eq. (3.123).

$$= \mathbf{P}\exp\left[ig\int_0^s dt\,\bar{n}\cdot A(x+t\bar{n})\right]. \tag{3.124}$$

The Wilson lines extending to infinity transform as follows under gauge transformations

$$W(x) \to V(x)W(x)V^\dagger(-\infty\bar{n}). \tag{3.125}$$

If one considers gauge functions vanishing at infinity, such that $V(-\infty\bar{n}) = 1$, the combinations

$$\chi(x) \equiv W^\dagger(x)\psi(x), \qquad \text{and} \quad \bar{\chi}(x) \equiv \bar{\psi}(x)W(x), \tag{3.126}$$

are gauge invariant and can be used as building blocks to construct non-local operators.

In Appendix A.3 it is shown that the covariant derivative of the Wilson lines along the integration path in the exponent of the line vanishes; in our case in particular this implies that

$$\bar{n}\cdot DW(x) = 0. \tag{3.127}$$

Since there are two kinds of gauge fields in the SCET Lagrangian, collinear gauge fields and soft ones, it is possible to use two different types of Wilson lines,

$$\begin{aligned} W_c(x) &= \mathbf{P}\exp\left[ig\int_{-\infty}^0 ds\,\bar{n}\cdot A_c(x+s\bar{n})\right] \qquad (\text{ collinear}) \\ &\text{and} \\ S_n(x) &= \mathbf{P}\exp\left[ig\int_{-\infty}^0 ds\,n\cdot A_s(x+sn)\right] \qquad (\text{ soft}). \end{aligned} \tag{3.128}$$

As we will see in the following, the collinear Wilson lines are useful to construct operators, while the soft Wilson lines are useful because of the structure of the soft interaction.

3.4.6. Decoupling Transformation

As seen In Subsection 3.4.3, the interaction between collinear quarks and soft gluons in the SCET Lagrangian takes the form

$$\mathcal{L}_{c+s} = \bar{\xi}\frac{\bar{\not{n}}}{2}in\cdot D\xi, \tag{3.129}$$

where the specific form of the covariant derivative in this case is given in Eq. (3.106). We now redefine the fields ξ and $A_c^\mu(x)$ employing the soft Wilson line defined in Eq. (3.128)

$$\begin{aligned} \xi(x) &\to S_n(x_-)\xi^{(0)}(x), \\ A_c^\mu(x) &\to S_n(x_-)A_c^{(0)\mu}(x)S_n^\dagger(x_-). \end{aligned} \tag{3.130}$$

As a consequence of this one finds that

$$in\cdot D\xi(x) \to in\cdot D' S_n(x_-)\xi^{(0)}(x),$$

$$
\begin{aligned}
&= \left(in\cdot\partial + gn_\mu S_n(x_-)A_c^{(0)\mu}(x)S_n^\dagger(x_-) + gn\cdot A_s(x_-)\right)S_n(x_-)\xi^{(0)}(x)\,,\\
&= \Big(in\cdot\partial_- S_n(x_-) + S_n(x_-)in\cdot\partial + S_n(x_-)\,gn\cdot A_c^{(0)\mu}(x)\\
&\quad + gn\cdot A_s(x_-)S_n(x_-)\Big)\xi^{(0)}(x)\,,\\
&= \Big[\underbrace{(in\cdot D_{s\,-}S_n(x_-))}_{=0} + S_n(x_-)in\cdot\partial + S_n(x_-)gn\cdot A_c^{(0)\mu}(x)\Big]\xi^{(0)}(x)\;,\\
&= S_n(x_-)\left(in\cdot\partial + gn\cdot A_c^{(0)\mu}(x)\right)\xi^{(0)}(x) \equiv S_n(x_-)in\cdot D_c^{(0)}\xi^{(0)}(x)\,,
\end{aligned}
\tag{3.131}
$$

where we made use of the fact that the covariant derivative along the Wilson line is zero, and of the fact that

$$
n^\alpha\frac{\partial}{\partial x^\alpha}S_n(x_-) = n^\alpha\frac{\partial x_-^\beta}{\partial x^\alpha}\frac{\partial}{\partial x_-^\beta}S_n(x_-) = \frac{n^\alpha\bar{n}_\alpha}{2}n^\beta\frac{\partial}{\partial x_-^\beta}S_n(x_-) \equiv n\cdot\partial_- S_n(x_-)\,. \tag{3.132}
$$

(Remember that $x_-^\mu = \bar{n}\cdot x\, n^\mu/2$.) In conclusion, under the field transformations in Eq. (3.130), the Lagrangian in Eq. (3.129) changes as follows

$$
\mathcal{L}_{c+s} \to \xi^{(0)}\frac{\not{\bar{n}}}{2}in\cdot D_c^{(0)}\xi^{(0)}(x)\,; \tag{3.133}
$$

the soft gluon field no longer appears in the collinear Lagrangian (the subscript and superscript in the covariant derivative indicate that it depends on $A_c^{(0)}$ only). This kind of transformation is called a *decoupling transformation*, since it decouples the soft gluons from the leading power collinear Lagrangian. However, it is important to stress that at subleading powers soft-collinear interactions are still present in the Lagrangian.

The decoupling transformation plays an important role in the proofs of factorization theorems, but does not imply that everything factorizes at leading power. For example, to analyze the Sudakov problem, one needs to match the vector current operator onto an effective theory operator; while the soft fields decouple from the Lagrangian, they are still present in the current operator. To deal with the Sudakov problem we need to introduce two collinear directions, as we did when considering the analogous problem in the ϕ^3 theory.

For example, the QED current operator

$$
J^\mu(x) = \bar{\psi}(x)\gamma^\mu\psi(x)\,, \tag{3.134}
$$

corresponds to the SCET non-local operator

$$
J^\mu(x) \to \int ds\int dt C_V(s,t)\bar{\chi}_c\,(x+s\bar{n})\gamma_\perp^\mu\chi_{\bar{c}}(x+tn)\,, \tag{3.135}
$$

where the fields χ_c and $\chi_{\bar{c}}$ are defined according to Eq. (3.126):

$$
\chi_c = W_c^\dagger\xi_c\,, \qquad \not{n}\chi_c = 0\,,
$$

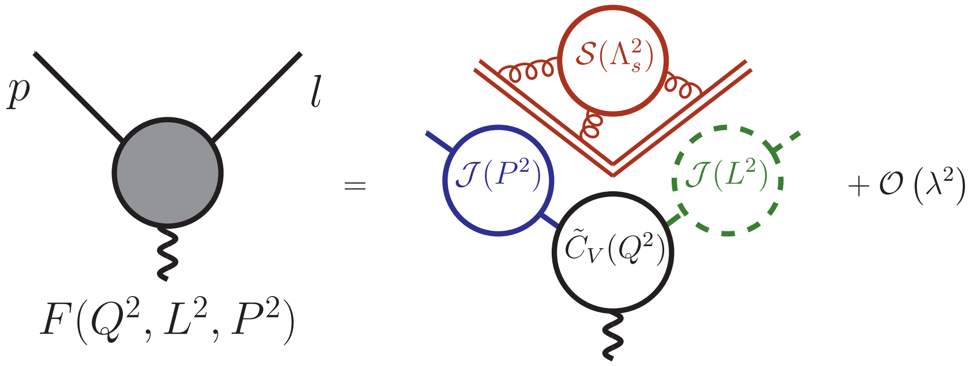

Figure 3.5.: Diagrammatic representation of the Sudakov form factor in QCD; the diagrams illustrate the separation of the various scales present in the problem. The soft scale is $\Lambda_s^2 = L^2P^2/Q^2$.

$$\chi_{\bar{c}} = W_{\bar{c}}^{\dagger}\xi_{\bar{c}}\,, \qquad \not{\bar{n}}\chi_{\bar{c}} = 0\,. \tag{3.136}$$

Since

$$\gamma^\mu = \not{n}\frac{\bar{n}^\mu}{2} + \not{\bar{n}}\frac{n^\mu}{2} + \gamma_\perp^\mu\,, \tag{3.137}$$

the only component surviving in Eq. (3.135) is $\gamma_\perp^\mu$. When applying the decoupling transformations

$$\begin{aligned} \chi_c(x) &\rightarrow S_n\,(x_-)\chi_c^{(0)}(x)\,, \\ \chi_{\bar{c}}(x) &\rightarrow S_{\bar{n}}\,(x_+)\chi_{\bar{c}}^{(0)}(x)\,, \end{aligned} \tag{3.138}$$

the source term becomes

$$J^\mu(x) = \int ds \int dt C_V(s,t)\bar{\chi}_c^{(0)}\,(x+s\bar{n})S_n^\dagger\,(x_-)\,S_{\bar{n}}\,(x_+)\gamma_\perp^\mu\chi_{\bar{c}}^{(0)}(x+tn)\,. \tag{3.139}$$

Therefore the soft interactions do not cancel, and the Sudakov form factor receives low energy contributions which describe a long range interaction between the fast moving incoming and outgoing quarks. The situation is summarized in diagrammatic form in Fig. 3.5, where the double lines represent the Wilson lines S.

Do the soft corrections factorize? It depends on the precise meaning that one attributes to the word factorization. Unfortunately, there are two different definitions of the word factorization which are employed in this context:

i) factorization = *scale separation*. In the source term in Eq. (3.139) the pieces associated to different scales are separated, so according to this definition the form factor is factorized,

ii) factorization = *no low energy interactions*. The two collinear sectors in Eq. (3.139) interact through soft interactions. So the form factor is not factorized in this sense.

3.4.7. Gauge Invariant Building Blocks

In Eq. (3.126) of Subsection 3.4.5, we introduced the notation

$$\chi(x) \equiv W^\dagger(x)\xi(x) = W^\dagger(x)\frac{\not{n}\not{\bar{n}}}{4}\psi(x)\,. \tag{3.140}$$

It is convenient to work with the field $\chi(x)$ instead of the $\psi(x)$ because $\chi(x)$ is invariant under collinear gauge transformations and this makes it easy to construct gauge invariant operators. Similarly, one introduces gauge invariant building blocks for the collinear gluon fields. We start by defining the block $\mathcal{A}$ as follows:

$$\mathcal{A}^\mu = W^\dagger(x)\Big(iD_c{}^\mu W(x)\Big) \tag{3.141}$$

From the definition above, it is possible to see that $\bar{n}\cdot\mathcal{A} = 0$, since $\bar{n}\cdot DW = 0$, as shown in Appendix A.3 . The component $n\cdot\mathcal{A}$ will instead have the expression

$$n\cdot\mathcal{A} = W^\dagger(x)\Big(in\cdot D_c W(x)\Big)\,. \tag{3.142}$$

Finally, the perpendicular component of the block $\mathcal{A}$ is

$$\mathcal{A}^\mu_\perp = W^\dagger(x)\Big(iD_{c\perp}^{\ \mu} W(x)\Big)\,. \tag{3.143}$$

The notation above indicates that the covariant derivative acts only on the Wilson line. In the literature the fields $\mathcal{A}_\perp$ are sometimes also defined as

$$\mathcal{A}^\mu_\perp = W^\dagger(x)\Big[iD_{c\perp}^{\ \mu}, W(x)\Big]\,. \tag{3.144}$$

The two definitions are equivalent, as it can be seen by multiplying the commutator by a test function f:

$$\Big[D^\mu, W(x)\Big]f(x) = D^\mu\Big(W(x)f(x)\Big) - W(x)\Big(D^\mu f(x)\Big) = \Big(D^\mu W(x)\Big)f(x)\,. \tag{3.145}$$

For leading-power operators, it suffices to consider the perpendicular components of the field $\mathcal{A}$. In fact, $\bar{n}\cdot\mathcal{A} = 0$ and $n\cdot\mathcal{A}$ is power suppressed, since it involves the smallest component of the momentum and gluon field.

The gauge invariance of the fields χ and $\mathcal{A}$ follows immediately from the behavior of the fields ξ, the Wilson lines W, and the covariant derivatives under collinear gauge transformations.

It is possible to rewrite the collinear Lagrangian $\mathcal{L}_c$ as a function of gauge invariant fields [34]. To do this, one needs to make use of the relation

$$W^\dagger iD_c^\mu W = W^\dagger\Big(iD_c^\mu W\Big) + W^\dagger W i\partial^\mu = \mathcal{A}^\mu + i\partial^\mu \equiv i\mathfrak{D}_\mu\,, \tag{3.146}$$

Moreover, the relation

$$W^\dagger i\bar{n}\cdot D_c W = W^\dagger \Big(\underbrace{i\bar{n}\cdot D_c W}_{=0}\Big) + i\bar{n}\cdot\partial = i\bar{n}\cdot\partial \tag{3.147}$$

leads to the identity

$$\frac{1}{i\bar{n}\cdot D_c} = WW^\dagger \left(i\bar{n}\cdot D_c\right)^{-1} WW^\dagger = W\left(W^\dagger i\bar{n}\cdot D_c W\right)^{-1} W^\dagger = W\frac{1}{i\bar{n}\cdot\partial}W^\dagger\,. \tag{3.148}$$

By inserting repeatedly $W^\dagger W = \mathbf{1}$ between the fields, the collinear Lagrangian in Eq. (3.96) can then be rewritten as

$$\mathcal{L}_c = \bar{\chi}\frac{\bar{\not{n}}}{2}\left(in\cdot\mathfrak{D}\right)\chi + \bar{\chi}i\not{\mathfrak{D}}_\perp\frac{1}{i\bar{n}\cdot\partial}i\not{\mathfrak{D}}_\perp\frac{\bar{\not{n}}}{2}\chi\,. \tag{3.149}$$

In order to rewrite the collinear gluon Lagrangian in terms of the $\mathcal{A}$ fields we observe that

$$W^\dagger F_{\mu\nu}W \equiv W^\dagger F^a_{\mu\nu}t^a W = \frac{1}{ig}W^\dagger\left[iD_{c,\mu}, iD_{c,\nu}\right]W = \frac{1}{g}\left(\partial_\mu\mathcal{A}_\nu - \partial_\nu\mathcal{A}_\nu - i\left[\mathcal{A}_\mu,\mathcal{A}_\nu\right]\right) \tag{3.150}$$

Therefore, by defining

$$\mathcal{F}_{\mu\nu} \equiv \partial_\mu\mathcal{A}_\nu - \partial_\nu\mathcal{A}_\nu - i\left[\mathcal{A}_\mu,\mathcal{A}_\nu\right]\,, \tag{3.151}$$

one finds that the kinetic term for the collinear gluons can be written as

$$-\frac{1}{4}F^a_{\mu\nu}F^{a,\mu\nu} = -\frac{1}{2}\mathrm{Tr}\left[F_{\mu\nu}F^{\mu\nu}\right] = -\frac{1}{2}\mathrm{Tr}\left[W^\dagger F_{\mu\nu}F^{\mu\nu}W\right] = -\frac{1}{2g^2}\mathrm{Tr}\left[\mathcal{F}_{\mu\nu}\mathcal{F}^{\mu\nu}\right]\,. \tag{3.152}$$

The leading soft-collinear interaction terms can be obtained by the replacement in Eq. (3.104). At the level of invariant building blocks, this corresponds to the replacement

$$\mathcal{A}^\mu(x) \to \mathcal{A}^\mu(x) + \frac{\bar{n}^\mu}{2}W^\dagger(x)gn\cdot A_s(x_-)W(x)\,. \tag{3.153}$$

3.5. Resummation by RG Evolution

In this section we will discuss the renormalization and the RG evolution of the Sudakov form factor in the effective theory. The relevant factorization theorem (in the sense of scale separation) was obtained in Subsection 3.4.6. This simple example illustrates the salient features which one also encounters in the analysis of physical processes; the RG equations are regulated by anomalous dimensions involving a logarithmic and a non-logarithmic part, and they can be solved by means of the same methods which are also employed in more complicated situations.

In the following, the Fourier transform of the matching coefficient of the current operator $C(s,t)$ in Eq. (3.139) will be indicated by $\widetilde{C}_V^{\mathrm{bare}}(Q^2)$. The value of this Wilson coefficient is determined in a way analogous to that discussed in the ϕ^3-theory case, by matching it

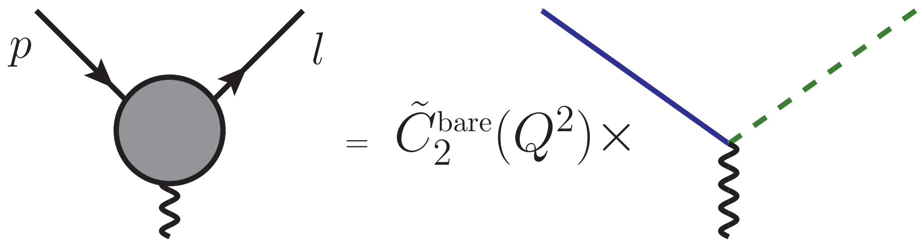

Figure 3.6.: Matching condition which allows to obtain $\tilde{C}_V^{\text{bare}}(Q^2)$. In the calculation of the form factor one should set from the start $p^2 = l^2 = 0$.

to the calculation of the on-shell form factor, as shown diagrammatically in Fig. 3.6. The matching procedure leads to the following result

$$\tilde{C}_V^{\text{bare}}(Q^2,\mu) = 1 + \frac{\alpha_s^{\text{bare}}}{4\pi} C_F \left(-\frac{2}{\varepsilon^2} - \frac{3}{\varepsilon} - 8 + \frac{\pi^2}{6} + \mathcal{O}(\varepsilon)\right)\left(\frac{Q^2}{\mu^2}\right)^{-\varepsilon} + \mathcal{O}\left(\alpha_s^2\right). \tag{3.154}$$

(The form factor is known to three-loop [46, 47].)

We can now define a renormalized Wilson coefficient by absorbing the divergences in a Z factor as follows

$$\tilde{C}_V(Q^2,\mu) = \lim_{\varepsilon\to 0} Z^{-1}\left(Q^2,\mu\right)\tilde{C}_V^{\text{bare}}(Q^2,\mu), \tag{3.155}$$

where[5] $\alpha_s^{\text{bare}} = Z_\alpha \mu^{2\varepsilon}\alpha_s(\mu)$ and

$$Z\left(Q^2,\mu\right) = 1 + \frac{\alpha_s(\mu)}{4\pi} C_F \left(-\frac{2}{\varepsilon^2} + \frac{2}{\varepsilon}\ln\frac{Q^2}{\mu^2} - \frac{3}{\varepsilon}\right). \tag{3.156}$$

Consequently, the renormalized Wilson coefficient $\tilde{C}_V$ at order α_s is

$$\tilde{C}_V(Q^2,\mu) = 1 + \frac{\alpha_s(\mu)}{4\pi} C_F \left(-\ln^2\frac{Q^2}{\mu^2} + 3\ln\frac{Q^2}{\mu^2} + \frac{\pi^2}{6} - 8\right) + \mathcal{O}(\alpha_s^2). \tag{3.157}$$

It is easy to verify explicitly that the expression in Eq. (3.157) satisfies the following differential equation:

$$\frac{d}{d\ln\mu}\tilde{C}_V(Q^2,\mu) = \left[C_F\gamma_{\text{cusp}}(\alpha_s)\ln\frac{Q^2}{\mu^2} + \gamma^V(\alpha_s)\right]\tilde{C}_V(Q^2,\mu), \tag{3.158}$$

where the functions γ_{cusp} and γ^V are, up to order α_s,

$$\gamma_{\text{cusp}}(\alpha_s) = 4\frac{\alpha_s(\mu)}{4\pi}, \qquad \text{and} \qquad \gamma^V(\alpha_s) = -6C_F\frac{\alpha_s(\mu)}{4\pi}. \tag{3.159}$$

[5] Z_α is the coupling constant renormalization factor; since its expansion is $Z_\alpha = 1 + \mathcal{O}(\alpha_s)$, it does not affect the functional form of Eq. (3.156).

(We remind the reader that $d\alpha_s/d\ln\mu \propto \alpha_s^2$.) Eq. (3.158) is the RG equation satisfied by the Wilson coefficient $\tilde{C}_V$ and the function γ_{cusp} is the *Cusp Anomalous Dimension*. Currently the on-shell form factor is known up to three loops, therefore it is possible to extract the anomalous dimensions γ_{cusp} and γ^V up to order α_s^3. The RG equation in Eq. (3.158) contains an explicit logarithmic dependence on the scale μ, this feature is a characteristic of problems involving Sudakov double logarithms.

The solution of the RG equation in Eq. (3.158) sums the logarithmic terms to all orders in α_s, in fact one obtains the solution:

$$\tilde{C}_V(Q^2,\mu) = \exp\left\{\int_{\mu_h}^{\mu}\left[C_F\gamma_{\text{cusp}}(\alpha_s)\ln\frac{Q^2}{\mu'^2} + \gamma^V(\alpha_s)\right]d\ln\mu'\right\}\tilde{C}_V(Q^2,\mu_h)\,, \tag{3.160}$$

where the logarithm appears in the exponential. It is convenient to write the solution as the product of the Wilson coefficient calculated at a high scale μ_h and an evolution matrix U which "runs down" the scale from μ_h to μ:

$$\tilde{C}_V(Q^2,\mu) = U\left(\mu_h,\mu\right)\tilde{C}_V(Q^2,\mu_h)\,. \tag{3.161}$$

In Eq. (3.160) we can rewrite the integration over the scale as an integration over the coupling by changing the integration variable from μ' to $\alpha_s(\mu')$ using

$$\frac{d\alpha_s(\mu')}{d\ln\mu'} = \beta\left(\alpha_s(\mu')\right)\,. \tag{3.162}$$

One can also rewrite the logarithm in the exponent (3.160) by employing the relation

$$\ln\frac{\nu}{\mu'} = \int_{\alpha_s(\mu')}^{\alpha_s(\nu)}\frac{d\alpha}{\beta(\alpha)}\,. \tag{3.163}$$

Finally the evolution matrix can be written in the form

$$U\left(\mu_h,\mu\right) = \exp\left[2C_F S(\mu_h,\mu) - A_{\gamma^V}(\mu_h,\mu)\right]\left(\frac{Q^2}{\mu_h^2}\right)^{-C_F A_{\gamma_{\text{cusp}}}(\mu_h,\mu)}\,, \tag{3.164}$$

where the quantities S and A_γ are defined as

$$\begin{aligned} S\left(\nu,\mu\right) &= -\int_{\alpha_s(\nu)}^{\alpha_s(\mu)}d\alpha\frac{\gamma_{\text{cusp}}(\alpha)}{\beta(\alpha)}\int_{\alpha_s(\nu)}^{\alpha}\frac{d\alpha'}{\beta(\alpha')}\,, \\ A_{\gamma_i}(\nu,\mu) &= -\int_{\alpha_s(\nu)}^{\alpha_s(\mu)}d\alpha\frac{\gamma_i(\alpha)}{\beta(\alpha)}\,; \end{aligned} \tag{3.165}$$

with $i \in \{V, \text{cusp}\}$. It is straightforward to check that Eq. (3.161) with Eq. (3.164) indeed solves the RG equation Eq. (3.158) by observing that

$$\frac{d}{d\ln\mu}S\left(\nu,\mu\right) = -\gamma_{\text{cusp}}\left(\alpha_s(\mu)\right)\int_{\alpha_s(\nu)}^{\alpha_s(\mu)}\frac{d\alpha'}{\beta(\alpha')}\,,$$

$$\frac{d}{d\ln\mu}A_i(\nu,\mu) = -\gamma_i(\alpha_s(\mu)) \,. \tag{3.166}$$

Since $d\alpha_s/\beta = d\ln\mu$, one can conclude from Eqs. (3.165) that the functions A_i are responsible for the resummation of the single logarithms and the function S for the resummation of the double logarithms. Explicit expressions for of these functions can be obtained by inserting the perturbative expansion of the beta and γ functions into Eqs. (3.165). By parameterizing the expansions of the beta function and anomalous dimensions γ_i as follows

$$\begin{aligned}
\beta(\alpha_s) &= -2\alpha_s\left[\beta_0\left(\frac{\alpha_s}{4\pi}\right)+\beta_1\left(\frac{\alpha_s}{4\pi}\right)^2+\mathcal{O}(\alpha_s^3)\right], \\
\gamma_{\rm cusp}(\alpha_s) &= \gamma_0^{\rm cusp}\left(\frac{\alpha_s}{4\pi}\right)+\gamma_1^{\rm cusp}\left(\frac{\alpha_s}{4\pi}\right)^2+\mathcal{O}(\alpha_s^3), \\
\gamma^V(\alpha_s) &= \gamma_0^V\left(\frac{\alpha_s}{4\pi}\right)+\gamma_1^V\left(\frac{\alpha_s}{4\pi}\right)^2+\mathcal{O}(\alpha_s^3),
\end{aligned} \tag{3.167}$$

and by inserting these expansions into the integrands of Eqs. (3.165), one obtains

$$\begin{aligned}
A_{\gamma^V}(\nu,\mu) &= \frac{\gamma_0^V}{2\beta_0}\ln\frac{\alpha_s(\mu)}{\alpha_s(\nu)}+\mathcal{O}(\alpha_s), \\
A_{\gamma_{\rm cusp}}(\nu,\mu) &= \frac{\gamma_0^{\rm cusp}}{2\beta_0}\ln\frac{\alpha_s(\mu)}{\alpha_s(\nu)}+\mathcal{O}(\alpha_s), \\
S(\nu,\mu) &= \frac{\gamma_0^{\rm cusp}}{4\beta_0^2}\left[\frac{4\pi}{\alpha_s(\nu)}\left(\frac{r-1}{r}-\ln r\right)+\left(\frac{\gamma_1^{\rm cusp}}{\gamma_0^{\rm cusp}}-\frac{\beta_1}{\beta_0}\right)(1-r+\ln r)\right. \\
&\quad \left.+\frac{\beta_1}{2\beta_0}\ln^2 r\right]+\mathcal{O}(\alpha_s),
\end{aligned} \tag{3.168}$$

where $r=\alpha_s(\mu)/\alpha_s(\nu)$. Note that $S(\nu,\mu)$ contains a term proportional to $1/\alpha_s$. By expanding $S(\nu,\mu)$ in terms of a single coupling $\alpha_s(\mu)$, one would find that this expansion produces terms of the form $\alpha_s^n(\mu)\ln^{2n}(\mu/\nu)$. Thus $S(\nu,\mu)$ encodes the leading logarithmic terms. The way we organize the computation, which consists of eliminating large logarithms in favor of coupling constants at different scales and then expanding in these couplings, is called *Renormalization Group Improved Perturbation Theory.* The large logarithms count as $1/\alpha_s$, as can be seen from Eq. (3.163) remembering that $\beta(\alpha_s)\sim\alpha_s^2$.

We note that the fixed-order expression for the Wilson coefficient $\tilde{C}_V$ (Eq. (3.157)), becomes meaningless when $\mu \gg Q$ or $\mu \ll Q$, since in these cases the logarithms are large and the product $\alpha_s\ln(Q^2/\mu^2)\sim 1$ cannot be used as a good expansion parameter. In contrast, if μ_h is taken to be approximately equal to the scale Q, the expression in Eq. (3.161) is valid for any value of μ for which α_s is perturbative.

4. Factorization and Resummation in SCET: Drell-Yan process

4.1. Introduction

In this chapter we review the methods, based on the effective field theory, which allows one to resum contributions coming from soft-gluon emissions. As an application we analyze the Drell-Yan cross section, namely the production of a lepton pair of momentum q, together with an arbitrary hadronic final state X at a hadron collider. By denoting the two colliding hadrons by N_1 and N_2, it follows that the reaction of interest:

$$N_1(P_1) + N_2(P_2) \to \gamma^*/Z^* + X(p_X) \to \ell^-(p_3) + \ell^+(p_4) + X(p_X)\,, \tag{4.1}$$

is mediated by a virtual photon or a Z boson. This process is a prototype for a larger class of processes that share a colorless boson as intermediate state mediator, i. e. γ, Z, W, H. These are called Drell-Yan like processes. Since the relative final state factorizes in the cross section, it will not be crucial for the following discussion. For simplicity we focus on the case of an intermediate photon propagator and a leptonic final state.

We consider a situation where we are close to the reaction threshold, and the energy of the radiation X is much smaller than the momentum transfer which is equal to the invariant mass $M^2 = q^2$ of the lepton pair, where $q = p_3 + p_4$. Even if the energy E of the radiation is large enough so that it can be computed perturbatively ($E \gg \Lambda_{\mathrm{QCD}}$), we end up with large logarithms of the energy of the soft radiation X over the invariant mass M. We will first prove the factorization theorem which separates the physics associated with the hard scale M from the soft physics, and then we will use the RG evolution to resum the associated large logarithms. This was first achieved in [1, 2] while the SCET analysis discussed below was performed in [5]. The relevant expansion parameter in the effective theory is $\lambda = E/M$. Its soft fields are scaling as $(\lambda^2, \lambda^2, \lambda^2)$ and describe the radiation into the final state together with collinear modes in the directions of the incoming hadrons.

In the center-of-mass frame, the cross section reads:

$$\frac{d\sigma}{d^4q} = \frac{1}{2s}\int \frac{d^3p_4}{(2\pi)^3 2E_4}\frac{d^3p_3}{(2\pi)^3 2E_3}\delta^{(4)}(q - p_3 - p_4)$$
$$\times \sum\!\!\!\!\!\!\int_X \; \left|\langle \ell^+\,\ell^-\,X|N_1\,N_2\rangle\right|^2 (2\pi)^{(4)}\delta^{(4)}(P_1 + P_2 - p_X - q)\,. \tag{4.2}$$

Since we are working at leading power in the electromagnetic interaction, the leptonic part thus factorizes from the hadronic part of the amplitude, which is given by:

$$\langle \ell^+ \, \ell^- \, X | N_1 \, N_2 \rangle = \frac{e^2}{q^2} \, \bar{u}(p_3) \gamma_\mu v(p_4) \, \langle X | J_\mu(0) | N_1 \, N_2 \rangle \,, \tag{4.3}$$

where $J^\mu = \sum_q e_q \bar{\psi}_q \, \gamma^\mu \, \psi_q$ is the electromagnetic-quark current. We now define the lepton tensor

$$\begin{aligned} L_{\mu\nu} &= \int \frac{d^3 p_4}{(2\pi)^3 2E_4} \frac{d^3 p_3}{(2\pi)^3 2E_3} \delta^{(4)}(q - p_3 - p_4) \sum_s \bar{u}(p_3) \gamma_\nu v(p_4) \bar{v}(p_4) \gamma_\mu u(p_3) \\ &= \int \frac{d^3 p_4}{(2\pi)^3 2E_4} \frac{d^3 p_3}{(2\pi)^3 2E_3} \delta^{(4)}(q - p_3 - p_4) \mathrm{Tr}\left[\not{p}_3 \gamma_\mu \not{p}_4 \gamma_\nu \right] \\ &= \frac{1}{(2\pi)^4} \frac{1}{6\pi} \left(q_\mu q_\nu - g_{\mu\nu} \, q^2 \right) \,. \end{aligned} \tag{4.4}$$

The tensor structure is fixed by current conservation, which implies that the tensor is transverse $q_\mu L_{\mu\nu} = q_\nu L_{\mu\nu} = 0$. The cross section is then given by the product of the lepton tensor and a hadron tensor

$$\frac{d\sigma}{d^4 q} = \frac{1}{2s} \frac{e^4}{(q^2)^2} L_{\mu\nu} W^{\mu\nu} = \frac{4\pi\alpha^2}{3sq^2} \frac{1}{(2\pi)^4} (-g_{\mu\nu}) W^{\mu\nu} \,. \tag{4.5}$$

Here we have also used that the hadron tensor is transverse. It is given by

$$\begin{aligned} W_{\mu\nu} &= \sum\!\!\!\!\!\!\int_X \; \langle N_1 N_2 | J_\mu^\dagger(0) | X \rangle \langle X | J_\nu(0) | N_1 \, N_2 \rangle (2\pi)^4 \delta^{(4)}(P_1 + P_2 - p_X - q) \\ &= \int d^4 x \, e^{-iqx} \, \langle N_1 N_2 | J_\mu^\dagger(x) J_\nu(0) | N_1 \, N_2 \rangle \,, \end{aligned} \tag{4.6}$$

where to show that the two forms are equivalent, one can insert a complete set of states between the two currents on the second line and then translate the current to zero using the momentum operator $J_\mu(x) = e^{iPx} J_\mu(0) e^{-iPx}$.

4.2. Derivation of the Factorization Formula in SCET

We are now ready to derive the factorization theorem for the hadronic tensor. Above, we have analyzed the electromagnetic current operator of a quark in the effective theory. The result was given in (3.139) and reads

$$J^\mu(x) = \int dr \int dt \, C_V(r,t) \, \bar{\chi}_{P_2} \, (x + rn) \, S_{\bar{n}}^\dagger \, (x) \, S_n \, (x) \, \gamma_\perp^\mu \chi_{P_1}(x + t\bar{n}) \,. \tag{4.7}$$

This current describes an energetic quark in the direction of N_1 and an anti-quark in the direction of N_2. There is also a second contribution, in which the directions of the quark and anti-quark are interchanged. The above result for the current operator was obtained after the decoupling transformation. The collinear and soft fields do not interact, but for simplicity we drop the label on the fields and we write χ_{P_2} instead of $\chi_{P_2}^{(0)}$.

The result for the current can now be inserted into the expression (4.6) for the hadronic tensor. Since the different fields do not interact, the hadronic tensor factorizes into a soft matrix element times collinear matrix elements. To obtain a simple form of the result, we first rearrange the collinear fields using the Fierz identity. The identity rearranges spinors as follows

$$\bar{u}_1\Gamma_1 u_2\,\bar{u}_3\Gamma_2 u_4 = \sum C_{AB}\,\bar{u}_1\Gamma_A u_4\,\bar{u}_3\Gamma_B u_2 \tag{4.8}$$

Under Fierz transformation, the combination $\Gamma_1\otimes\Gamma_2 = \gamma_\mu\otimes\gamma_\mu$ is mapped into

$$\gamma_\mu\otimes\gamma^\mu \;\to\; -\frac{1}{2}\gamma_\mu\otimes\gamma^\mu - \frac{1}{2}\gamma_\mu\gamma_5\otimes\gamma^\mu\gamma_5 + 1\otimes 1 - \gamma_5\otimes\gamma_5\,. \tag{4.9}$$

The vector currents in SCET involve the matrix $\gamma_\perp^\mu$ instead of γ^μ. The two are related by

$$\gamma^\mu = \gamma_\perp^\mu + \not{n}\frac{\bar{n}^\mu}{2} + \not{\bar{n}}\frac{n^\mu}{2}\,. \tag{4.10}$$

However, since $\not{\bar{n}}\chi_{P_2} = \not{n}\chi_{P_1} = 0$ the additional terms do not contribute and we can use the Fierz relation (4.9) for the full vector current. Using the same properties of the SCET spinors, we can then simplify the terms which appear on the right-hand side, which involve collinear spinors in the same direction,

$$\bar{\chi}_{P_1}\gamma^\mu\chi_{P_1} = n^\mu\bar{\chi}_{P_1}\frac{\not{\bar{n}}}{2}\chi_{P_1} \qquad\qquad \bar{\chi}_{P_1}\chi_{P_1} = \bar{\chi}_{P_1}\frac{\not{n}\not{\bar{n}}}{4}\chi_{P_1} = 0 \tag{4.11}$$

and analogously for the the spinor products involving γ_5. In the second relation, we have pulled out the projection operator out of the collinear fermion field and then annihilated the anti-fermion with it. The final result for the Fierz identity for the two vector currents in SCET then takes the simple form

$$\bar{\chi}_{P_1}\gamma_{\perp\mu}\chi_{P_2}\,\bar{\chi}_{P_2}\gamma_\perp^\mu\chi_{P_1} = \bar{\chi}_{P_1}\frac{\not{\bar{n}}}{2}\chi_{P_1}\,\bar{\chi}_{P_2}\frac{\not{n}}{2}\chi_{P_2} + \bar{\chi}_{P_1}\frac{\not{\bar{n}}}{2}\gamma_5\chi_{P_1}\,\bar{\chi}_{P_2}\frac{\not{n}}{2}\gamma_5\chi_{P_2}\,. \tag{4.12}$$

Note that this relation involves an extra minus sign compared to (4.9), which arises from anticommuting the fermion fields. The matrix element of the collinear fields will be the PDF. Because of parity invariance of the strong interaction, the terms involving γ_5 have vanishing matrix elements and will be dropped in the following.

Because the collinear and soft sectors do no longer interact, each matrix element must be a color singlet. When taking a collinear matrix element, we can thus average over color

$$\bar{\chi}_{P_1,\alpha}\,\frac{\not{\bar{n}}}{2}\,\chi_{P_1,\beta} \to \frac{1}{N_c}\,\delta_{\alpha\beta}\,\bar{\chi}_{P_1,\delta}\,\frac{\not{\bar{n}}}{2}\,\chi_{P_1,\delta}\,, \tag{4.13}$$

where α, β, δ are the color indices of the fields. After this averaging, the color indices of the soft Wilson lines are all contracted among themselves and the soft part of the matrix element takes the form

$$\hat{W}_{\rm DY}(x) = \frac{1}{N_c} {\rm Tr}\, \langle 0| \bar{\boldsymbol{T}} \left(S_n^\dagger\,(x)\, S_{\bar{n}}\,(x)\right) \boldsymbol{T} \left(S_{\bar{n}}^\dagger\,(0)\, S_n\,(0)\right) |0\rangle\,. \tag{4.14}$$

We have absorbed one of the factors of N_c^{-1} into the definition of the matrix element so that $\hat{W}_{\rm DY}(x) = 1 + \mathcal{O}(\alpha_s)$. We need to use anti-time ordering on the Wilson lines which arise from $J_\mu^\dagger(x)$. The reason is that we are computing an amplitude squared, see the first line of (4.6), so the propagators of the complex conjugate amplitude have the opposite $i0^+$ prescription. The soft matrix element is a vacuum matrix element since the initial state protons are composed of collinear fields and do not contain any soft partons. Soft partons cannot be part of the proton since the soft scale $E \gg \Lambda_{\rm QCD}$, but $P_1^2 \sim P_2^2 \sim \Lambda_{\rm QCD}^2$.

Next we turn to the collinear matrix elements. As a first simplification we perform the multi-pole expansion. The matrix element contains both collinear and anti-collinear fields. The position variable x^μ thus scales conjugate to the sum of the collinear momenta, as $(1, 1, \lambda^{-1})$. At leading power, we can thus set x_- and $x_\perp$ to zero in the collinear fields (and x_+ and $x_\perp$ in the anti-collinear matrix elements). After this, these matrix elements only depend on the position space variable conjugate to the large momentum and have the form

$$\langle N_1(P_1)| \bar{\chi}_{P_1}\,(x_+ + t'\bar{n})\, \frac{\bar{\not{n}}}{2} \chi_{P_1}(t\bar{n})\, |N_1(P_1)\rangle = \bar{n}\cdot P_1 \int_{-1}^{1} dx_1\, f_{q/N_1}(x_1,\mu)\, e^{i\,x_1\,(x_+ + t'\bar{n} - t\bar{n})\cdot P_1}\,. \tag{4.15}$$

The variables t and t' appear in the convolutions with the Wilson coefficients in the currents. The non-perturbative quantities $f_{q/N_1}(\xi)$ are the usual PDFs [48]. The variable x_1 is the fraction of the proton momentum carried by the quark field. Negative values correspond to the anti-quark distributions: $f_{\bar{q}/N_1}(x_1) = -f_{q/N_1}(-x_1)$. The reason that these matrix elements are exactly the same as the PDFs defined in QCD is that in the absence of soft interactions the collinear Lagrangian is completely equivalent to the standard QCD Lagrangian and the SCET collinear quark field is related to the standard quark field $\psi(x)$ simply by $\chi_{P_1}(x) = W^\dagger(x) \frac{\not{n}\bar{\not{n}}}{4} \psi(x)$. In terms of the QCD field the SCET matrix element (4.15) reads

$$\langle N_1(P_1)| \bar{\psi}\,(t''\bar{n})\, \frac{\bar{\not{n}}}{2}\, [t''\bar{n}, 0] \psi(0)\, |N_1(P_1)\rangle\,, \tag{4.16}$$

where we set $x_+ = 0$ and $t'' = t' - t$. In Eq. (4.16) we combined $W(t''\bar{n})W^\dagger(0) = [t''\bar{n}, 0]$ into a finite length Wilson line connecting the two quark fields.

We are now ready to combine all the ingredients to get the following form of the hadronic tensor

$$(-g_{\mu\nu} W^{\mu\nu}) = \frac{1}{N_c} \int_0^1 dx_1 \int_0^1 dx_2\, s |\tilde{C}_V(-\hat{s},\mu)|^2 \int d^4x\, \hat{W}_{\rm DY}(x,\mu)\, e^{i\,x\cdot(x_1\,P_{1\,-} + x_2\,P_{2\,+} - q)} \times \left[f_{q/N_1}(x_1,\mu) f_{\bar{q}/N_2}(x_2,\mu) + (q \leftrightarrow \bar{q}) \right]\,, \tag{4.17}$$

where $s = \bar{n} \cdot P_1 \, n \cdot P_2$ and $\hat{s} = x_1 x_2 s$ are the hadronic and partonic squared center of mass energy, respectively. This expression now contains the Fourier transform of the hard matching coefficient

$$\tilde{C}_V(-\hat{s}, \mu) = \int dr \int dt \, C_V(r, t, \mu) e^{-i\, x_1 \, t \bar{n} \cdot P_1} e^{-i\, x_2 \, r n \cdot P_2} \tag{4.18}$$

where the exponentials arise from the matrix element (4.15). We can thus further simplify (4.17) by replacing $\tilde{C}_V(-\hat{s}, \mu) = \tilde{C}_V(-q^2, \mu)$ since we are close to the production threshold. For the cross section, we thus obtain

$$d\sigma = \frac{d^4 q}{(2\pi)^4} \frac{4\pi\alpha^2}{3q^2 N_c} |\tilde{C}_V(-q^2, \mu)|^2 \int_0^1 dx_1 \int_0^1 dx_2 \sum_q e_q^2 \left[f_{q/N_1}(x_1, \mu) f_{\bar{q}/N_2}(x_2, \mu) + (q \leftrightarrow \bar{q}) \right]$$
$$\int d^4 x \, \hat{W}_{\mathrm{DY}}(x) \, e^{i\, x \cdot (x_1 \, P_{1\,-} + x_2 \, P_{2\,+} - q)} \tag{4.19}$$

Let us now be a bit more specific and compute the cross section differential in the boson mass $M^2 = q^2$. To compute it, we rewrite

$$\int d^4 q = \int dM^2 \int \frac{d^3 q}{2q_0} \, . \tag{4.20}$$

The electroweak boson near threshold is produced with small transverse momentum, since the transverse momentum has to be balanced by the soft radiation. We thus have $q^0 = \sqrt{\hat{s}} + \mathcal{O}(\lambda^2)$ and $|\vec{q}| \sim \lambda^2$. Since the denominator in Eq. (4.20) does not depend on $\vec{q}$ to leading power, we can then perform the $\vec{q}$ integration. This yields $\delta^{(3)}(\vec{x})$, so that we need the soft function only for $\vec{x} = 0$. In addition, the following relation holds

$$(x_1 \, P_{1\,-} + x_2 \, P_{2\,+} - q)^{(0)} = \frac{\sqrt{\hat{s}}}{2}(1 - z) + \mathcal{O}(\lambda^4) \tag{4.21}$$

where we defined

$$z \equiv \frac{M^2}{\hat{s}} \, . \tag{4.22}$$

One finds that $1 - z \sim \mathcal{O}(\lambda^2)$. In order to prove Eq. (4.21) we start by observing that the l.h.s. coincides with the energy of the additional final state partonic radiation, $p_x^{(0)}$. One can then take the square of the partonic momentum conservation to obtain

$$\hat{s} = M^2 + 2q \cdot p_x \, , \tag{4.23}$$

where the fact that in our approximation $p_x^2 \sim 0$ was used. In the partonic center of mass frame, where $x_1 l + x_2 p = 0$, one has that $\vec{q} = -\vec{p}_x$, so that $|\vec{q}| = |\vec{p}_x| = p_x^{(0)}$. Therefore Eq. (4.23) can be rewritten as

$$\hat{s} = M^2 + 2p_x^{(0)} \sqrt{M^2 + \left(p_x^{(0)}\right)^2} + \left(2p_x^{(0)}\right)^2 \, . \tag{4.24}$$

By solving the equation above with respect to $p_x^{(0)}$ one finds

$$p_x^{(0)} = \frac{M(1-z)}{2\sqrt{z}}\,, \tag{4.25}$$

which coincides with Eq. (4.21) once the relation between $\hat{s}$, M, and z is applied.

Our final result for the cross section then reads

$$\frac{d\sigma}{dM^2} = \frac{4\pi\alpha^2}{3M^2 N_c}|\tilde{C}_V(-M^2,\mu)|^2 \int_0^1 dx_1 \int_0^1 dx_2 \sum_q e_q^2 \left[f_{q/N_1}(x_1) f_{\bar{q}/N_2}(x_2) + (q \leftrightarrow \bar{q})\right] \times \\ \times \frac{1}{\sqrt{\hat{s}}} W_{\rm DY}\left(\sqrt{\hat{s}}(1-z),\mu\right) \tag{4.26}$$

where the Fourier transformed soft function is defined as

$$W_{\rm DY}(\omega,\mu) = \int \frac{dx^0}{4\pi}\, \hat{W}_{\rm DY}(x,\mu)\, e^{i\,x^0\omega/2} \tag{4.27}$$

The result now shows that the perturbative expansion involves different scales. For the hard function, the natural scale choice for the renormalization scale would is $\mu \sim M$, while the scale of the soft emissions is lower.

4.3. RG Equation for the Soft Function

In this section we derive the RG equation satisfied by the soft function $W_{\rm DY}$. For this purpose we consider the production threshold limit where the full RG invariance of the resummed cross section is ensured. We thus restrict ourselves to the collider threshold region $x_1 \sim x_2 \sim 1$ where we have

$$\sqrt{s} \simeq \sqrt{\hat{s}} \simeq M\,. \tag{4.28}$$

In this limit, the small energy of the hadronic final state is given by $E_X \simeq \sqrt{s} - M$ which is the relevant hadronic quantity near the threshold, and thus we rewrite Eq. (4.26) as follows[1]:

$$\begin{aligned} \frac{d\sigma}{dE_X} &= -2\,H(s,\mu) \sum_{i,j=\{q,\bar{q}\}} \int_0^1 dx_1 \int_0^1 dx_2 \int_0^\infty d\omega\, \delta\left(\omega - \sqrt{\hat{s}}(1-z)\right) \times \\ &\quad \times f_{i/N_1}(x_1,\mu)\, f_{j/N_2}(x_2,\mu)\, W_{\rm DY}(\omega,\mu)\,, \end{aligned} \tag{4.29}$$

where we use μ to indicate the factorization and renormalization scales and we have introduced an integration over the energy of the soft radiation.

[1]The relation between Eq. (4.26) and Eq. (4.29) can be expressed as $\frac{d\sigma}{dM^2} \simeq -\frac{1}{2\sqrt{s}}\frac{d\sigma}{dE_X}$.

In order to simplify the notation, in this section we consider the contribution of a single quark flavor q. By comparing with Eq. (4.26), one can see that

$$H\left(M^2,\mu\right) \equiv \frac{4\pi\alpha^2}{3M^2N_c}|\tilde{C}_V(-M^2,\mu)|^2 e_q^2 \,. \tag{4.30}$$

For our discussion it will be convenient to Laplace transform the cross section and its various ingredients. We now first consider the renormalization of the PDFs in the limit $x \to 1$ and then we will analyze the cross section itself.

For $x \to 1$, the PDFs satisfy the simplified Altarelli-Parisi equation

$$\frac{df_{q/N}(y,\mu)}{d\ln\mu} = \int_y^1 \frac{dx}{x} P(x) f_{q/N}(y/x,\mu)\,, \tag{4.31}$$

where the splitting function $P(x)$ is given by

$$P(x) = 2C_F\gamma_{\rm cusp}(\alpha_s)\left[\frac{1}{\bar{x}}\right]_+ + 2\gamma^{f_q}(\alpha_s)\delta(\bar{x})\,, \tag{4.32}$$

The splitting function $P(x)$ contains the part of the full Altarelli-Parisi kernel $P_{q\leftarrow q}(x)$ which becomes singular in the threshold limit $\bar{x} \equiv 1-x \to 0$. The remainder is non-singular and can be neglected in the threshold limit. The anomalous dimension at first order in the strong coupling constant is $\gamma^{f_q} = 3C_F\alpha_s/(4\pi)$. (The expansion of γ^{f_q} to order α_s^2 can be found in Appendix A.5.)

At this stage it is convenient to introduce the Laplace transform of the PDFs

$$\begin{aligned}\tilde{f}_{q/N}(\tau,\mu) &= \int_0^1 dx \exp\left(-\frac{1-x}{\tau e^{\gamma_E}}\right) f_{q/N}(x,\mu)\,,\\ &= \int_0^\infty d\bar{x} \exp\left(-\frac{\bar{x}}{\tau e^{\gamma_E}}\right) f_{q/N}(x,\mu)\,.\end{aligned} \tag{4.33}$$

Since the quark PDF does not have support for $x<0$, the integrand in the last line of the equation above vanishes for $\bar{x}>1$. In Appendix A.4 we prove that, in terms of the Laplace transformed PDF, the RG equation for the PDFs becomes

$$\frac{d\tilde{f}_{q/N}(\tau,\mu)}{d\ln\mu} = 2\left[C_F\gamma_{\rm cusp}(\alpha_s)\ln\tau + \gamma^{f_q}(\alpha_s)\right]\tilde{f}_{q/N}(\tau,\mu)\,. \tag{4.34}$$

At this point we want to take the Laplace transform of the differential cross section, Eq. (4.29). For this purpose we observe that the energy of the partonic radiation in the final state, $p_x^{(0)}$, can be written as

$$\frac{\omega}{2} \equiv p_x^{(0)} = \underbrace{\sqrt{s}-M}_{E_X} - \left[(1-x_1)+(1-x_2)\right]\frac{\sqrt{s}}{2}\,, \tag{4.35}$$

where E_X is the energy of the complete hadronic final state, while the term within square brackets represents the energy of the proton remnant. For the Laplace transform with respect to E_X we thus obtain

$$\begin{aligned}
\tilde{\sigma}(\kappa) &= \int_0^\infty dE_X\, e^{-E_X/(\kappa e^{\gamma_E})}\,\frac{d\sigma}{dE_X}\,, \\
&= -H(s,\mu)\int_0^1 dx_1\int_0^1 dx_2\int_0^\infty d\omega e^{-\frac{1}{\kappa e^{\gamma_E}}\left[\frac{\omega}{2}+\frac{\sqrt{s}}{2}(1-x_1)+\frac{\sqrt{s}}{2}(1-x_2)\right]}\times \\
&\quad \times f_q\left(x_1,\mu\right) f_{\bar{q}}\left(x_2,\mu\right) W_{\rm DY}(\omega,\mu)\,, \\
&= -H(s,\mu)\tilde{f}_q\left(\frac{2\kappa}{\sqrt{s}},\mu\right)\tilde{f}_{\bar{q}}\left(\frac{2\kappa}{\sqrt{s}},\mu\right)\tilde{s}_{\rm DY}(2\kappa,\mu)\,,
\end{aligned} \tag{4.36}$$

where we introduced the Laplace transform of the soft function defined as

$$\widetilde{s}_{\rm DY}(\kappa,\mu) \equiv \int_0^\infty d\omega\, e^{-\omega/(\kappa e^{\gamma_E})} W_{\rm DY}(\omega,\mu)\,. \tag{4.37}$$

We point out that Eq. (4.36), the Laplace transform of the cross section, is simply given by the product of the hard, soft, and collinear functions, where the latter coincide in this case with the PDFs.

In order to derive the RG equation satisfied by the soft function, one observes that the differential cross section must be independent of the scale μ, so that one finds

$$\frac{d}{d\ln\mu}\tilde{\sigma}(\kappa) = \left[\Gamma_H + 2\Gamma_f + \Gamma_s\right]\,\tilde{\sigma}(\kappa) = 0\,, \tag{4.38}$$

where the Γ's indicate schematically the anomalous dimensions of the hard function, the PDFs, and the soft function, respectively. The hard function is given by the absolute value squared of C_V. Its RG equation was discussed in detail in Section 3.5. For the Drell-Yan process, the function $C_V(Q^2,\mu^2)$ is evaluated at $Q^2 = -M^2 - i0^+$ so that

$$\Gamma_H = \Gamma_{C_V} + \Gamma^*_{C_V} = 2{\rm Re}[\Gamma_{C_V}] = 2\left[C_F\gamma_{\rm cusp}(\alpha_s)\ln\frac{M^2}{\mu^2} + \gamma_V(\alpha_s)\right]\,. \tag{4.39}$$

Using the explicit form of the anomalous dimension of the PDF Eqs. (4.34) and solving Eq. (4.38) with respect to Γ_s one then finds

$$\begin{aligned}
\Gamma_s &= -4C_F\gamma_{\rm cusp}(\alpha_s)\ln\left(\frac{2\kappa}{\sqrt{s}}\right) - 4\gamma^{f_q}(\alpha_s) - 2C_F\gamma_{\rm cusp}(\alpha_s)\ln\left(\frac{M^2}{\mu^2}\right) - 2\gamma^V(\alpha_s)\,, \\
&\simeq -4C_F\gamma_{\rm cusp}(\alpha_s)\ln\left(\frac{2\kappa}{\mu}\right) - 2\underbrace{\left(2\gamma^{f_q}(\alpha_s) + \gamma^V(\alpha_s)\right)}_{\equiv\gamma^W}\,.
\end{aligned} \tag{4.40}$$

In the second line, we used that $M \simeq \sqrt{s}$ in the threshold region to show that the dependence on the hard scale cancels out.

The evolution equation satisfied by the Laplace transform of the soft function itself is thus

$$\frac{d\,\widetilde{s}_{\rm DY}(\kappa,\mu)}{d\ln\mu} = \left[-4C_F\gamma_{\rm cusp}(\alpha_s)\ln\left(\frac{\kappa}{\mu}\right) - 2\gamma^W(\alpha_s)\right]\widetilde{s}_{\rm DY}(\kappa,\mu)\,. \tag{4.41}$$

The differential equation above can be solved in the same way as the RG equation for the Wilson coefficient of the Sudakov form factor discussed in Section 3.5. One finds that the solution has the following expression:

$$\widetilde{s}_{\rm DY}(\kappa,\mu) = \exp\left[-4C_F S(\mu_s,\mu) + 2A_{\gamma^W}(\mu_s,\mu)\right]\widetilde{s}_{\rm DY}(\kappa,\mu_s)\left(\frac{\kappa^2}{\mu_s^2}\right)^{\eta}\,, \tag{4.42}$$

where the functions S, and $A_{\gamma_{\rm cusp}}$ are defined in Eqs. (3.165), A_{γ^W} is defined similarly to the last of Eqs. (3.165) and $\eta \equiv 2C_F A_{\gamma_{\rm cusp}}(\mu_s,\mu)$.

To compute the resummed cross section in momentum space, we need to perform the inverse Laplace transform. To do so, we observe that the κ-dependence of the solution is very simple. To any order in perturbation theory, the function $\widetilde{s}_{\rm DY}(\kappa,\mu_s)$ is a polynomial in the logarithm

$$L = \ln\frac{\kappa^2}{\mu_s^2}\,, \tag{4.43}$$

which is multiplied by a factor $(\kappa^2/\mu_s^2)^\eta$ in the solution of the evolution equation. In fact, powers of logarithms can be simply obtained as derivatives with respect to η

$$L^m\left(\frac{\kappa^2}{\mu_s^2}\right)^{\eta} = \partial_\eta^{(m)}\left(\frac{\kappa^2}{\mu_s^2}\right)^{\eta}\,. \tag{4.44}$$

Because of this relation it is convenient to write the Laplace transformed function as a function of the logarithm L and one can then replace $\widetilde{s}_{\rm DY}\left(L,\mu_s\right) \to \widetilde{s}_{\rm DY}\left(\partial_\eta,\mu_s\right)$ in Eq. (4.42). Therefore the computation of the inverse Laplace transform comes down to computing the inverse of $\kappa^{2\eta}$. By dimensional analysis, the inverse must be given by a function of η times $\omega^{2\eta-1}$. To determine the prefactor, let us compute the Laplace transform of $\omega^{2\eta-1}$:

$$\int_0^\infty d\omega\, e^{-\omega/(\kappa e^{\gamma_E})}\omega^{2\eta-1} = \Gamma(2\eta)\, e^{2\eta\gamma_E}\,\kappa^{2\eta}\,. \tag{4.45}$$

From this result and our discussion above, we conclude that if one uses L as the first argument in $\widetilde{s}_{\rm DY}$ the inverse transform can be written as [5]

$$W_{\rm DY}(\omega,\mu) = \exp\left[-4C_F S(\mu_s,\mu) + 2A_{\gamma^W}(\mu_s,\mu)\right]\widetilde{s}_{\rm DY}\left(\partial_\eta,\mu_s\right)\frac{e^{-2\gamma_E\eta}}{\Gamma(2\eta)}\frac{1}{\omega}\left(\frac{\omega}{\mu_s}\right)^{2\eta}\,. \tag{4.46}$$

This expression for $W_{\rm DY}(\omega,\mu)$ is well defined for $\eta > 0$, which is fulfilled for $\mu_s > \mu$. However, in fixed-order computations the scale μ in the PDFs is typically chosen of order the hard scale, $\mu > \mu_s$, and since the PDF fits were performed with this scale choice, we

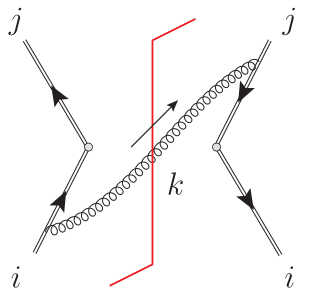

Figure 4.1.: One-loop Feynman diagram contributing to the soft function. The vertical line (the "cut") indicates that the gluon crossing is on-shell.

adopt the same choice in the effective theory. To be able to do so, we need the solution for negative η which is obtained by analytic continuation. For instance, to obtain the result for $-1/2 < \eta < 0$, it is necessary to employ the identity

$$\int_0^\Omega d\omega \frac{f(\omega)}{\omega^{1-2\eta}} = \int_0^\Omega d\omega \frac{f(\omega) - f(0)}{\omega^{1-2\eta}} + \frac{f(0)}{2\eta}\Omega^{2\eta}\,, \tag{4.47}$$

where $f(\omega)$ is a smooth test function. For the cases where $\eta < -\frac{1}{2}$ additional subtractions are needed.

4.4. Soft Matrix Element

We want now to calculate the soft function W_{DY} at order α_s. The calculation outlined below is carried out in the momentum space, however, the soft function can also be calculated in position space, see Appendix A.1.4. The function W_{DY} at two loop order can be found in [49]. In this section, we obtain the expression of the bare soft function; the poles in ε must then be renormalized in the modified minimal subtraction scheme.

The calculation of the contribution to the soft function shown in the diagram in Fig. 4.1, where a soft gluon is exchanged between the quark Wilson lines, plus the corresponding contributions in which the gluon connects the other two lines[2], requires to evaluate the following integral

[2]The latter diagram gives the same contribution of the one shown in Fig 4.1. However, due to our definition of the Fourier transform Eq. (4.27) an extra factor 1/2 multiplies the term of order g^2 in Eq. (4.48) and cancels against the factor of 2 arising from the sum of the two diagrams.

$$W_{\rm DY}(\omega,\mu) = \delta(\omega) + \mu^{4-d}\int \frac{d^dk}{(2\pi)^d} \underbrace{\left(g\frac{n_j^\mu}{n_j\cdot k}T^a\right)}_{\text{Wilson Line}} \times \underbrace{\left(-g_{\mu\nu}2\pi\delta(k^2)\theta(k_0)\right)}_{\text{Cut Gluon Propagator}} \times$$

$$\times \left(-g\frac{n_i^\mu}{n_i\cdot k}T^a\right)\delta\left(\frac{\omega}{2}-k_0\right), \tag{4.48}$$

where k is the momentum of the gluon crossing the cut in the diagram. In the Drell-Yan case, one has that the two collinear directions can be chosen back-to-back, so that

$$n_i^\mu \equiv n^\mu\,, \qquad \text{and} \qquad n_j^\mu = \bar{n}^\mu\,. \tag{4.49}$$

The integration measure can now be rewritten as follows

$$\int d^dk\,\theta\left(k_0\right) = \frac{1}{2}\int_0^\infty dk_+ \int_0^\infty dk_- \int dk_\perp^{d-2}\,, \tag{4.50}$$

where here $k_+ = k_0 + k_z = n\cdot k$ and $k_- = k_0 - k_z = \bar{n}\cdot k$. Consequently, the integral in Eq. (4.48) becomes

$$W_{\rm DY}(\omega,\mu) = \delta(\omega) + \frac{\mu^{4-d}g_s^2C_F}{(2\pi)^{d-1}}\int_0^\infty dk_+ \int_0^\infty dk_- \int dk_\perp^{d-2}\frac{1}{k_+k_-}$$

$$\times\delta\left(k_+k_- + k_\perp^2\right)\delta\left(\frac{\omega}{2}-\frac{k_++k_-}{2}\right), \tag{4.51}$$

and, after the evaluating the angular integrals one finds

$$W_{\rm DY}(\omega,\mu) = \delta(\omega) + \frac{\mu^{4-d}g_s^2C_F}{(2\pi)^{d-1}}\Omega_{d-2}\int_0^\infty dk_+ \int_0^\infty dk_- \int_0^\infty dk_T\,\frac{k_T^{d-3}}{k_+\cdot k_-} \times$$

$$\times\delta\left(k_+\cdot k_- - k_T^2\right)\delta\left(\frac{\omega}{2}-\frac{k_++k_-}{2}\right), \tag{4.52}$$

where the magnitude of the transverse spatial momentum is indicated by

$$k_T \equiv \sqrt{-k_\perp^2}\,, \tag{4.53}$$

and the d-dimensional solid angle is $\Omega_d = 2\pi^{d/2}/\Gamma(d/2)$.

After integrating over k_T and k_-, and after defining $d = 4-2\varepsilon$, the integral in Eq. (4.52) can be rewritten as

$$W_{\rm DY}(\omega,\mu) = \delta(\omega) + \frac{\alpha_s(4\pi\mu^2)^\varepsilon C_F}{\pi\Gamma(1-\varepsilon)}\int_0^\omega dk_+\frac{1}{\left(k_+(\omega-k_+)\right)^{1+\varepsilon}}\,, \tag{4.54}$$

where the upper limit of integration is determined by the fact that the last delta function in Eq. (4.52) fixes $k_- = \omega - k_+$ where both k_+ and ω are positive. Therefore one is left with the integral

$$\begin{aligned} W_{\rm DY}(\omega,\mu) &= \delta(\omega) + \frac{\alpha_s(4\pi\mu^2)^\varepsilon C_F}{\pi\Gamma(1-\varepsilon)}\frac{1}{\omega^{1+2\varepsilon}}\int_0^1 dt \frac{1}{(t(1-t))^{1+\varepsilon}} \\ &= \delta(\omega) + \frac{\alpha_s(4\pi\mu^2)^\varepsilon C_F}{\pi\Gamma(1-\varepsilon)}\frac{1}{\omega^{1+2\varepsilon}}\frac{\Gamma^2(-\varepsilon)}{\Gamma(-2\varepsilon)} \\ &= \delta(\omega) + \frac{\alpha_s(4\pi\mu^2)^\varepsilon C_F}{\pi}\frac{1}{\omega^{1+2\varepsilon}}\frac{\Gamma(1-\varepsilon)}{\varepsilon^2\Gamma(-2\varepsilon)}\,. \end{aligned} \tag{4.55}$$

This expression can be rewritten in terms of

$$\mu_{\overline{\rm MS}}^{2\varepsilon} \equiv e^{-\varepsilon\gamma_E}\mu^{2\varepsilon}(4\pi)^\varepsilon\,, \tag{4.56}$$

and as a result we find:

$$W_{\rm DY}(\omega,\mu) = \delta(\omega) + \frac{\alpha_s}{\pi}C_F e^{-\varepsilon\gamma_E}(\mu_{\overline{\rm MS}}^2 e^{2\gamma_E})^\varepsilon \frac{1}{\omega^{1+2\varepsilon}}\frac{\Gamma(1-\varepsilon)}{\varepsilon^2\Gamma(-2\varepsilon)}\,. \tag{4.57}$$

In order to calculate the bare Laplace transform of the soft function $\widetilde{s}_{\rm DY}$, one needs to insert the result above in Eq. (4.37), where we identify $\kappa = \mu_{\overline{\rm MS}}e^{L/2}$. By taking the Laplace transform of the equation above and expanding for $\varepsilon \to 0$ we obtain the unrenormalized $\widetilde{s}_{\rm DY}$ at order α_s, which reads

$$\widetilde{s}_{\rm DY}(L,\mu) = 1 + \frac{\alpha_s}{4\pi}C_F\left[\frac{4}{\varepsilon^2} - \frac{4L}{\varepsilon} + 2L^2 + \frac{\pi^2}{3}\right] + \mathcal{O}(\alpha_s^2)\,. \tag{4.58}$$

Finally one can take the inverse Fourier transform with respect to omega of Eq. (4.57) to get the expression in position space for $\hat{W}_{\rm DY}(x_0,\mu)$:

$$\hat{W}_{\rm DY}(x_0,\mu) = 1 + \frac{\alpha_s(-\pi\mu^2 x_0^2)^\varepsilon C_F}{\pi}\frac{\Gamma(1-\varepsilon)}{\varepsilon^2}\,, \tag{4.59}$$

which agrees with the result Eq. (A.34) in Appendix A.1.4. After introducing $\mu_{\overline{\rm MS}}$ and expanding in $\varepsilon \to 0$ one finds

$$\hat{W}_{\rm DY}(x_0,\mu) = 1 + \frac{\alpha_s}{4\pi}C_F\left[\frac{4}{\varepsilon^2} + \frac{4L_0}{\varepsilon} + 2L_0^2 + \frac{\pi^2}{3}\right] + \mathcal{O}(\alpha_s^2)\,, \tag{4.60}$$

where

$$L_0 = \ln\left(-\frac{1}{4}\mu_{\overline{\rm MS}}^2 x_0^2 e^{2\gamma_E}\right)\,. \tag{4.61}$$

It is easy to show, by applying the Laplace transform in Eq. (4.37) to Eq. (4.27), that the soft function in position space $\hat{W}_{\rm DY}(x_0,\mu)$ has the same functional form of the soft function in Laplace space $\widetilde{s}_{\rm DY}(L,\mu)$. Indeed, it is possible to obtain one from the other by replacing the argument in the following way:

$$\widetilde{s}_{\rm DY}(L,\mu) = \hat{W}_{\rm DY}\left(x_0 = \frac{-2i}{e^{\gamma_E}\mu_{\overline{\rm MS}}e^{L/2}}, \mu\right) , \tag{4.62}$$

which is equivalent to replace L_0 with $-L$ in Eq. (4.60). In the following we drop the subscript $\overline{\rm MS}$ for the scale μ.

4.5. Resummation of Large Logarithms

As shown in Eq. (4.26) the partonic Drell Yan cross section factors into the product of the squared Wilson coefficient and the soft function. The product of these two terms describes the hard scattering interactions at the parton level. Being more precise one can define the hard-scattering kernel as

$$C(z, M, \mu_f) \equiv \left|\tilde{C}_V(-M^2, \mu_f)\right|^2 \sqrt{\hat{s}} W_{\rm DY}\left(\sqrt{\hat{s}}(1-z), \mu_f\right) , \tag{4.63}$$

following the notation employed in [5].

The hadronic cross section is obtained by integrating the product of the hard-scattering kernel and the PDFs over the appropriate domain. In Section 3.5 we solved the RG equation satisfied by the Wilson coefficient $\tilde{C}_V$, cf. Eqs. (3.161), (3.164), while the solution of the RG equation satisfied by the soft function is presented in Eq. (4.46). By combining these two elements it is possible obtain a resummed formula for the hard scattering kernel.

The solution of the RG equation for $\tilde{C}_V$ that was derived in Eq. (3.164) is valid for space-like momenta. Therefore the solution for time-like momenta needed in Drell-Yan scattering, can be obtained from the one valid for space-like momenta by analytic continuation. The sign of the imaginary part extracted from the logarithm in the RG equation can be determined by writing explicitly the infinitesimal imaginary part of M^2. The RG equation becomes [5]

$$\frac{d}{d\ln\mu}\tilde{C}_V(-M^2 - i0^+, \mu) = \left[C_F\gamma_{\rm cusp}(\alpha_s)\left(\ln\frac{M^2}{\mu^2} - i\pi\right) + \gamma^V(\alpha_s)\right]\tilde{C}_V(-M^2 - i0^+, \mu) , \tag{4.64}$$

and its solution is

$$\begin{aligned}\tilde{C}_V(-M^2 - i0^+, \mu_f) &= \exp\left[2C_F S(\mu_h, \mu_f) - A_{\gamma^V}(\mu_h, \mu_f) + i\pi C_F A_{\gamma_{\rm cusp}}(\mu_h, \mu_f)\right] \times \\ &\quad \times \left(\frac{M^2}{\mu_h^2}\right)^{-C_F A_{\gamma_{\rm cusp}}(\mu_h,\mu_f)} \tilde{C}_V(-M^2, \mu_h) .\end{aligned} \tag{4.65}$$

The functions S and A_{γ^i} are defined in Eqs. (3.165).

In order to obtain the resummed result, we simply insert the solutions of RG equations of the soft function, Eq. (4.46), and the hard function, Eq. (4.65), into Eq. (4.63). The result can be simplified by making use of the following relations:

$$\begin{aligned} A_{\gamma^i}\left(\mu_h,\mu_f\right) &= A_{\gamma^i}\left(\mu_h,\mu_s\right)+A_{\gamma^i}\left(\mu_s,\mu_f\right)\,, \\ S\left(\mu_h,\mu_f\right)-S\left(\mu_s,\mu_f\right) &= S\left(\mu_h,\mu_s\right)-A_{\gamma_{\rm cusp}}\left(\mu_s,\mu_f\right)\ln\frac{\mu_h}{\mu_s}\,, \end{aligned} \tag{4.66}$$

as well as $\gamma^W = 2\gamma^{f_q}+\gamma^V$. In this way one finds

$$C(z,M,\mu_f) = \left|\tilde{C}_V(-M^2,\mu_h)\right|^2 U(M,\mu_h,\mu_f,\mu_s)\frac{\sqrt{\hat{s}}}{\omega}\left(\frac{M}{\mu_s}\right)^{-2\eta}\widetilde{s}_{\rm DY}\left(\partial_\eta,\mu_s\right)\left(\frac{\mu_s}{\omega}\right)^{-2\eta}\frac{e^{-2\gamma_E\eta}}{\Gamma(2\eta)}\,, \tag{4.67}$$

where the evolution function U is defined as

$$\begin{aligned} U(M,\mu_h,\mu_f,\mu_s) = \exp\left[4C_F S\left(\mu_h,\mu_s\right)+4A_{\gamma^{f_q}}\left(\mu_s,\mu_f\right)-2A_{\gamma^V}\left(\mu_h,\mu_s\right)\right]\times \\ \times\left(\frac{M^2}{\mu_h^2}\right)^{-2C_F A_{\gamma_{\rm cusp}}(\mu_h,\mu_s)}\,. \end{aligned} \tag{4.68}$$

The factor $(\mu_s/\omega)^{-2\eta}$ in Eq. (4.67) can be moved to the left of the soft function $\widetilde{s}_{\rm DY}$ to get

$$C(z,M,\mu_f) = \left|\tilde{C}_V(-M^2,\mu_h)\right|^2 U(M,\mu_h,\mu_f,\mu_s)\frac{\sqrt{\hat{s}}}{\omega}\left(\frac{M}{\omega}\right)^{-2\eta}\widetilde{s}_{\rm DY}\left(\ln\frac{\omega^2}{\mu_s^2}+\partial_\eta,\mu_s\right)\frac{e^{-2\gamma_E\eta}}{\Gamma(2\eta)}\,. \tag{4.69}$$

The explicit z dependence of the hard-scattering kernel can be obtained by inserting the relation $\omega = M(1-z)/\sqrt{z}$. Finally, for the resummed result of the hard-scattering kernel, one finds:

$$\begin{aligned} C(z,M,\mu_f) &= \left|\tilde{C}_V(-M^2,\mu_h)\right|^2 U(M,\mu_h,\mu_f,\mu_s)\,\frac{z^{-\eta}}{(1-z)^{1-2\eta}}\times \\ &\quad\times\widetilde{s}_{\rm DY}\left(\ln\frac{M^2(1-z)^2}{\mu_s^2 z}+\partial_\eta,\mu_s\right)\frac{e^{-2\gamma_E\eta}}{\Gamma(2\eta)}\,. \end{aligned} \tag{4.70}$$

As it was observed after Eq. (4.46), the formula above is well defined for $\eta > 0$, which corresponds to the case $\mu_s > \mu_f$. In the physically more relevant case in which $\mu_s < \mu_f$, $\eta < 0$; consequently the integrals of $\ln(1-z)/(1-z)^{1-2\eta}$ with test functions $f(z)$ must be defined using a subtraction at $z = 1$ and analytic continuation in η. This procedure gives rise to plus distributions in the variable $1-z$.

The resummed formula for the hard-scattering kernel, Eq. (4.70), is formally independent from the hard scale μ_h and the soft scale μ_s. Since $\mu_h \sim M$ and $\mu_s \sim \omega$, the Wilson coefficient $\tilde{C}_V$ and the soft function $\widetilde{s}_{\rm DY}$ in Eq. (4.70) are free of large logarithms and can be evaluated in perturbation theory. (We remind the reader that $\mu_s \gg \Lambda_{\rm QCD}$.) A residual

Table 4.1.: Different approximation schemes for the evaluation of the resummed cross-section formulae. Table taken from [5].

RG-impr. PT	Log. approx.	Accuracy $\sim \alpha_s^n L^k$	$\gamma_{\rm cusp}$	γ^V, γ^{f_q}	C_V, $\widetilde{s}_{\rm DY}$
—	LL	$k = 2n$	1-loop	tree-level	tree-level
LO	NLL	$2n-1 \le k \le 2n$	2-loop	1-loop	tree-level
NLO	NNLL	$2n-3 \le k \le 2n$	3-loop	2-loop	1-loop
NNLO	NNNLL	$2n-5 \le k \le 2n$	4-loop	3-loop	2-loop

dependence on μ_s and μ_h in the hard-scattering kernel arises precisely form the fact that the matching coefficients and the anomalous dimensions are evaluated up to a given order in perturbation theory. The residual scale dependence can be employed to give an estimate of the perturbative uncertainty. Similarly, the dependence on the factorization scale μ_f cancels formally in the convolution of the hard-scattering kernel with the PDFs.

The fixed-order expression for the hard scattering kernel in perturbative QCD includes terms which are singular in the $z \to 1$ limit (plus distributions and Dirac delta functions). These singular terms can be obtained by setting $\mu_s = \mu_f = \mu_h$ in Eq. (4.70) and by expanding the formula in powers of α_s. In particular this implies that after taking the derivatives with respect to η, one should take the limit $\eta = 0$.

The resummed expression for the hard-scattering kernel can be evaluated at any desired order in resummed perturbation theory. Different levels of accuracy require the evaluation of the matching coefficients and anomalous dimensions at different orders in perturbation theory; Table 4.1 summarizes the situation. There are two different ways to label the level of accuracy at which a resummed formula is evaluated. In the counting scheme of RG-improved perturbation theory, the LO approximation includes all terms of $\mathcal{O}(1)$, the NLO approximation includes all of the terms of $\mathcal{O}(\alpha_s)$, and so on. However, in this counting one should consider the fact that the large logarithms $\ln(\mu_h/\mu_s)$ are numerically $\sim 1/\alpha_s$. In the literature the alternative "leading logarithm" counting is often employed. N^{n}LO accuracy corresponds to N^{n+1}LL accuracy in the leading logarithm counting. A full analysis of the Drell-Yan resummed cross section at NNNLL (matched to NNLO fixed-order calculations) is carried out in [5].

5. Soft-gluon resummation for slepton-pair production

5.1. Introduction

In this chapter we will apply the soft-gluon resummation techniques discussed in Section 4 to improve the theoretical prediction for slepton-pair production at hadron colliders [50–53]. We will analyze this purely supersymmetric process and, as a byproduct, we will also study the impact of SUSY virtual corrections for Drell-Yan process in the context of soft-gluon resummation. These two processes can be considered together because they arise from the same hard-scattering interaction: the annihilation of a quark-antiquark pair into a virtual photon or Z boson, which then decays, respectively, into a slepton or a lepton pair. The effect of strongly-interacting SUSY particles enters in the hard-scattering interaction of both processes only at the one-loop level through the virtual exchange of squarks and gluinos. Both processes are interesting and play an important role: Drell-Yan production can be considered as a prototype for other collider processes and, among other things, its cross section as a function of the invariant mass of the lepton pair can be used to search for new heavy resonances. Sleptons are expected to be among the lightest SUSY particles, which means that in many scenarios they decay directly into the corresponding SM partners and the LSP, giving rise to simple signatures such as a pair of energetic leptons plus missing energy.

Both processes have been studied extensively in the past. The calculation of the cross section and rapidity distribution at NLO in α_s for the Drell-Yan process in the SM has been accomplished long ago [54], while the corresponding results at NNLO were obtained more recently [55–60]. A study of Supersymmetric Quantum Chromodynamics (SUSY-QCD) and electroweak corrections at NLO was performed in [61]. Results for the total cross section for slepton-pair production at NLO in α_s were obtained in [14–16]. The main uncertainties in the theoretical predictions arise from the imperfect knowledge of the PDFs and from the truncation of the perturbative expansion, which introduces a dependence on the unphysical factorization and renormalization scales. The two sources of errors are of comparable size. In particular, the uncertainty due to scale variations is smaller than in similar production processes involving colored particles in the final states, like top-quark-pair production or stop-pair production. This is because, at the partonic tree level, (s)lepton-pair production is a purely electroweak process, and therefore at leading order the uncertainty arise only from the variation of the factorization scale of the PDFs. The uncertainty from the renormalization scale starts at order α_s and is therefore suppressed.

A reduction of the scale uncertainties is nevertheless desirable, because having a small error on the cross section and the differential distributions allows one to extract interesting information, such as the slepton masses, with better precision.

Resummation was first achieved at next-to-leading-logarithmic (NLL) order for the Drell-Yan invariant-mass distribution in [1, 2], based on a method involving the solution of certain evolution equations in Mellin moment space. It was later extended to the rapidity distribution [62], and to N^{3}LL order in [63, 64]. In the case of slepton-pair production, the resummation was performed at NLL level for the invariant-mass distribution and total cross section [17].

In this chapter we extend the previous analyses in various directions. First, we extend the results of [5] for the Drell-Yan production of lepton pairs by including the contribution from a virtual Z boson as well as SUSY-QCD corrections at order α_s. In the case of slepton-pair production, we extend the results of [17] by performing the threshold resummation at N^{3}LL order. While this has a minor effect on the total correction to the differential distributions and cross section, it may be relevant for the theoretical uncertainty estimate. We present results for the differential and total cross sections for the Tevatron and the LHC with a center of mass energy of 7 and 14 TeV following the analysis done by the author in [65].

In Section 5.2 we recall the basic formulas for the differential distributions and define the kinematics of the threshold region. Section 5.3 is devoted to a comprehensive phenomenological analysis. We estimate the relevance of SUSY-QCD corrections and the impact of soft-gluon resummation on the invariant-mass distribution and the total cross section for slepton-pair production. We also discuss the uncertainties due to scale variations and the errors on the PDFs.

5.2. Kinematics and factorization at threshold

We consider the production of a (s)lepton pair with invariant mass M in hadron-hadron collisions, at center of mass energy $\sqrt{s}$. The process involves the reaction

$$N_1(P_1) + N_2(P_2) \to \gamma^*/Z^{0*} + X\,, \tag{5.1}$$

where X represents an inclusive hadronic final state, followed by $\gamma^*/Z^{0*} \to \tilde{l}^-(p_3) + \tilde{l}^+(p_4)$ or $l^-(p_3) + l^+(p_4)$. We start by focusing on the double-differential cross section in the invariant mass $M^2 = q^2$ and rapidity $Y = \frac{1}{2}\ln\frac{q^0+q^3}{q^0-q^3}$ of the (s)lepton pair in the center of mass frame, where $q = p_3 + p_4$. This cross section can be calculated in perturbative QCD and expressed in terms of convolutions of short-distance partonic cross sections with PDFs:

$$\frac{d^2\sigma}{dM^2dY} = \sigma_0 \sum_{ij} \int dx_1 dx_2\, \widetilde{C}_{ij}(x_1, x_2, s, M, \mu_f)\, f_{i/N_1}(x_1, \mu_f)\, f_{j/N_2}(x_2, \mu_f)\,, \tag{5.2}$$

where μ_f is the factorization scale, $f_{i/N}(x, \mu_f)$ gives the probability of finding a parton i with longitudinal momentum fraction x inside the hadron N, and

$$\sigma_0 = \frac{4\pi\alpha_{em}^2}{3N_c M^2 s} \quad \text{for } l^- l^+ \,, \qquad \sigma_0 = \frac{\pi\alpha_{em}^2 \beta_{\tilde{l}}^3}{3N_c M^2 s} \quad \text{for } \tilde{l}^- \tilde{l}^+ \,, \tag{5.3}$$

with $\beta_{\tilde{l}} = \sqrt{1 - 4m_{\tilde{l}}^2/M^2}$ denoting the 3-velocity of the slepton in the $\tilde{l}^- \tilde{l}^+$ rest frame. The hard-scattering kernels $\widetilde{C}_{ij}$ are related to the partonic cross sections and can be calculated as power series in α_s. At leading order ($\sim \alpha_s^0$) the sum involves only the channels $(ij) = (q\bar{q}), (\bar{q}q)$, with $p_1 = x_1 P_1$, $p_2 = x_2 P_2$. At NLO ($\sim \alpha_s$) one has to take into account $(ij) = (q\bar{q}), (\bar{q}q), (qg), (gq), (\bar{q}g), (g\bar{q})$. Here we are interested in the evaluation of higher-order radiative corrections near threshold, for which it is useful to define the quantity

$$\tau \equiv \frac{M^2}{s} \,, \tag{5.4}$$

and from this follows that the variable $z = M^2/\hat{s}$, defined in Eq. (4.22), can be rewritten as

$$z = \frac{M^2}{\hat{s}} = \frac{\tau}{x_1 x_2} \,, \tag{5.5}$$

where $\hat{s} = x_1 x_2 s$ is the partonic center of mass energy squared. The partonic threshold region is defined by the limit $z \to 1$, in which the dynamics of the process is greatly simplified. Since the partonic center of mass energy is just sufficient to create the (s)lepton pair, there is no phase space available for the emission of additional energetic partons. The cross section is dominated by the terms which are singular in the $z \to 1$ limit, which correspond to the virtual corrections and the real emission of soft gluons. Such terms only arise for the $(q\bar{q})$ and $(\bar{q}q)$ channels.

We define the couplings of the (s)fermions to a gauge boson $i = \gamma, Z$ following the notation of [66]. The relevant chiral currents

$$\begin{aligned} J^\mu_{f,i} &= \sum_f \left(g_L^{f,i} \bar{f} \gamma^\mu P_L f + g_R^{f,i} \bar{f} \gamma^\mu P_R f \right) , \\ J^\mu_{\tilde{f},i} &= \sum_{\tilde{f}} \left(g_L^{\tilde{f},i} \tilde{f}_L^* \overleftrightarrow{\partial}^\mu \tilde{f}_L + g_R^{\tilde{f},i} \tilde{f}_R^* \overleftrightarrow{\partial}^\mu \tilde{f}_R \right) , \end{aligned} \tag{5.6}$$

with $P_{L/R} = \frac{1}{2}(1 \mp \gamma_5)$, involve the couplings

$$\begin{aligned} & g_L^{q,\gamma} = g_L^{\tilde{q},\gamma} = e_q \,, && g_R^{q,\gamma} = g_R^{\tilde{q},\gamma} = e_q \,, \\ & g_L^{q,Z} = g_L^{\tilde{q},Z} = \tfrac{-1+\frac{4}{3}s_{\theta_W}^2}{2s_{\theta_W}c_{\theta_W}} \,, && g_R^{q,Z} = g_R^{\tilde{q},Z} = \tfrac{\frac{4}{3}s_{\theta_W}^2}{2s_{\theta_W}c_{\theta_W}} \,, \\ & g_L^{l,\gamma} = g_L^{\tilde{l},\gamma} = 1 \,, && g_R^{l,\gamma} = g_R^{\tilde{l},\gamma} = 1 \,, \\ & g_L^{l,Z} = g_L^{\tilde{l},Z} = \tfrac{1-2s_{\theta_W}^2}{2s_{\theta_W}c_{\theta_W}} \,, && g_R^{l,Z} = g_R^{\tilde{l},Z} = \tfrac{-2s_{\theta_W}^2}{2s_{\theta_W}c_{\theta_W}} \,, \\ & g^{\tilde{\tau}_1,Z} = \tfrac{\cos\theta_{\tilde{\tau}} - 2s_{\theta_W}^2}{2s_{\theta_W}c_{\theta_W}} \,, && g^{\tilde{\tau}_2,Z} = \tfrac{\sin\theta_{\tilde{\tau}} - 2s_{\theta_W}^2}{2s_{\theta_W}c_{\theta_W}} \,. \end{aligned} \tag{5.7}$$

Here $s_{\theta_W} = \sin\theta_W$, $c_{\theta_W} = \cos\theta_W$, where θ_W is the electroweak mixing angle. We consider the possibility of mixing between the third-generation sleptons, introducing the mass eigenstates $\tilde\tau_1$, $\tilde\tau_2$ and the corresponding mixing angle $\theta_{\tilde\tau}$.

The leading contributions to the double-differential cross section arising near the partonic threshold $z \to 1$ can be written as [5]

$$\frac{d^2\sigma^{\rm thresh}}{dM^2 dY} = \sigma_0 \sum_q h_q^{(l,\tilde l)} \int \frac{dz}{z} C(z, M, m_{\tilde q}, m_{\tilde g}, \mu_f) \tag{5.8}$$
$$\times \left[\frac{f_{q/N_1}(\sqrt{\tau} e^Y, \mu_f)\, f_{\bar q/N_2}(\frac{\sqrt{\tau}}{z} e^{-Y}, \mu_f) + f_{q/N_1}(\frac{\sqrt{\tau}}{z} e^Y, \mu_f)\, f_{\bar q/N_2}(\sqrt{\tau} e^{-Y}, \mu_f)}{2} + (q \leftrightarrow \bar q) \right].$$

The coefficients $h_q^{(l,\tilde l)}$ take into account the photon, Z boson, and γ-Z interference contributions. For lepton-pair production they read

$$h_q^{(l)} = \left[e_q^2 - \frac{1}{2} \frac{e_q (g_L^{q,Z} + g_R^{q,Z})(g_L^{l,Z} + g_R^{l,Z})}{1 - m_Z^2/M^2} + \frac{1}{4} \frac{(g_L^{q,Z^2} + g_R^{q,Z^2})(g_L^{l,Z^2} + g_R^{l,Z^2})}{(1 - m_Z^2/M^2)^2} \right], \tag{5.9}$$

while for the production of a slepton pair of type $\tilde l$

$$h_q^{(\tilde l)} = \left[e_q^2 - \frac{e_q (g_L^q + g_R^q) g^{\tilde l,Z}}{1 - m_Z^2/M^2} + \frac{1}{2} \frac{(g_L^{q\,2} + g_R^{q\,2}) g^{\tilde l,Z^2}}{(1 - m_Z^2/M^2)^2} \right]. \tag{5.10}$$

The hard-scattering kernel $C(z, M, m_{\tilde q}, m_{\tilde g}, \mu_f)$ in (5.8) contains both SM and SUSY-QCD corrections. The SM QCD corrections are known to two-loop order [57]. The SUSY corrections arising at NLO are given by a vertex diagram with a gluino-squark-squark loop plus external-leg corrections. They have been calculated in [15, 17, 61, 67]. We recomputed these contributions and find agreement with results in the literature. Integrating over the rapidity, one obtains from (5.8) the single-differential cross section

$$\frac{d\sigma^{\rm thresh}}{dM^2} = \sigma_0 \sum_q h_q^{(l,\tilde l)} \int_\tau^1 \frac{dz}{z} C(z, M, m_{\tilde q}, m_{\tilde g}, \mu_f)\, ff(\tau/z, \mu_f), \tag{5.11}$$

where

$$ff(y, \mu_f) = \int_y^1 \frac{dx}{x} \left[f_{q/N_1}(x, \mu_f)\, f_{\bar q/N_2}(y/x, \mu_f) + (q \leftrightarrow \bar q) \right] \tag{5.12}$$

defines the parton luminosity function.

The hard-scattering kernel $C(z, M, m_{\tilde q}, m_{\tilde g}, \mu_f)$ depends on the invariant mass M and on the masses of squarks and gluinos, $m_{\tilde q}$ and $m_{\tilde g}$. We will assume in our analysis that these scales are of similar order. For $z \to 1$ one can then distinguish two well separated mass scales, the "hard" scale $\mu_h \sim M$ and the "soft" scale $\mu_s \sim M(1-z)/\sqrt{z} = \sqrt{\hat s}(1-z)$, which correspond to the energy of the emitted soft gluons. As shown in Eq. (4.63), the presence of these two scales is reflected in the factorization of the coefficient $C(z, M, m_{\tilde{q}}, m_{\tilde{g}}, \mu_f)$ into a hard and a soft function,

$$C(z, M, m_{\tilde{q}}, m_{\tilde{g}}, \mu_f) = H(M, m_{\tilde{q}}, m_{\tilde{g}}, \mu_f)\, S(\sqrt{\hat{s}}(1-z), \mu_f)\,, \tag{5.13}$$

where

$$H(M, m_{\tilde{q}}, m_{\tilde{g}}, \mu_h) = \left|C_V(-M^2 - i0^+, m_{\tilde{q}}, m_{\tilde{g}}, \mu_h)\right|^2. \tag{5.14}$$

Choosing the factorization scale μ_f in (5.8) close to μ_h or μ_s unavoidably causes the appearance of large logarithms in one of the two factors. Threshold resummation addresses the problem of resumming these large logarithms to all orders in perturbation theory. The proof of the factorization of the SUSY hard-scattering kernel in Eq. (5.13) follows closely the derivation discussed for the Drell-Yan case in Chapter 4. However one should be careful when considering the contribution of the Z boson as an intermediate mediator. In the process of matching the current operator onto SCET operators one should distinguish between left and right chiral fields and their different couplings to the Z boson, in particular the current $J^\mu_{q,Z}$ is matched onto

$$J^\mu_{q,Z} \to C_V(-M^2 - i0^+, m_{\tilde{q}}, m_{\tilde{g}}, \mu) \sum_q \left(g_L^{q,Z} \bar{\chi}_{P_2} S^\dagger_{\bar{n}} \gamma^\mu P_L S_n \chi_{P_1} + g_R^{q,Z} \bar{\chi}_{P_2} S^\dagger_{\bar{n}} \gamma^\mu P_R S_n \chi_{P_1} \right), \tag{5.15}$$

where the effective fields $\chi_{P_1} = W^\dagger_{P_1} \xi_{P_1}$ and $\chi_{P_2} = W^\dagger_{P_2} \xi_{P_2}$ are the gauge-invariant combinations of collinear quark fields and collinear Wilson lines in SCET. The matching coefficient C_V depends on the time-like, hard momentum transfer M^2. It is given by the on-shell massless quark form factor [4], which in the present case must be calculated including SUSY-QCD corrections. On the other hand, the soft function in Eq. (5.13) is insensitive to short-distance physics, therefore its analytic expression is the same as for Drell-Yan. Its expression up to order α_s^2 can be found in [5] and, as an example, it has been explicitly computed at order α_s in Eq. (4.57).

The resummation of threshold logarithms can be achieved directly in momentum space by solving the RG equations for the hard and soft functions. In this way, one obtains for the resummed hard-scattering kernel the compact expression in Eq. (4.70).

In the SM, the expression for C_V has recently been derived up to three-loop order [68,69]. Including the additional virtual corrections of SUSY particles, the perturbative expansion up to order $\mathcal{O}(\alpha_s^2)$ can be written as

$$\begin{aligned} C_V(-M^2, m_{\tilde{q}}, m_{\tilde{g}}, \mu_h) \;&=\; 1 + \frac{\alpha_s}{4\pi}\left[c_V^{(1)}(-M^2, \mu_h) + c_{V,\text{SUSY}}^{(1)}(-M^2, m_{\tilde{q}}^2, m_{\tilde{g}}^2)\right] \\ &\quad + \left(\frac{\alpha_s}{4\pi}\right)^2 \left[c_V^{(2)}(-M^2, \mu_h) + c_{V,\text{SUSY}}^{(2)}(-M^2, m_{\tilde{q}}^2, m_{\tilde{g}}^2, \mu_h)\right], \end{aligned} \tag{5.16}$$

where $c_V^{(1)}$ and $c_V^{(2)}$ include the one- and two-loop QCD corrections present in the SM, while $c_{V,\text{SUSY}}^{(1)}$ and $c_{V,\text{SUSY}}^{(2)}$ represent the additional QCD corrections arising in its SUSY extension. In the following we will neglect the two-loop SUSY contribution, which we assume to be negligible since already $c^{(1)}_{V,\mathrm{SUSY}}$ will turn out to be very small. The explicit expressions for $c^{(1)}_V$ and $c^{(2)}_V$ can be found in [5], while

$$\begin{aligned} c^{(1)}_{V,\mathrm{SUSY}} &= C_F \Bigg\{ \frac{5}{2} - \frac{m_{\tilde g}^2}{m_{\tilde g}^2 - m_{\tilde q}^2} + \frac{2(m_{\tilde g}^2 - m_{\tilde q}^2)}{M^2} + \left[\frac{m_{\tilde g}^4}{\left(m_{\tilde g}^2 - m_{\tilde q}^2\right)^2} + \frac{2m_{\tilde g}^2}{M^2} \right] \ln \frac{m_{\tilde g}^2}{m_{\tilde q}^2} \\ &\quad - \left[1 + \frac{2(m_{\tilde g}^2 - m_{\tilde q}^2)}{M^2} \right] f_B(M^2, m_{\tilde q}^2) + 2 \left[\frac{m_{\tilde g}^2}{M^2} + \frac{\left(m_{\tilde g}^2 - m_{\tilde q}^2\right)^2}{M^4} \right] f_C(M^2, m_{\tilde q}^2, m_{\tilde g}^2) \Bigg\} . \end{aligned} \tag{5.17}$$

For simplicity we assume degenerate squark masses for $\tilde q_{L,R}$ with $q = u, d, s, c, b$. The loop functions f_B and f_C are provided in Appendix A.6. The evolution equation for C_V in (5.16) is the same as for the corresponding coefficient in the SM. As a result, $c^{(1)}_{V,\mathrm{SUSY}}$ does not depend on the renormalization scale. Note that the Wilson coefficient C_V is the same for all currents in (5.6).

5.3. Systematic studies and phenomenology

We now present a detailed numerical analysis of the invariant-mass distribution and total cross section for slepton-pair production at the Tevatron and LHC. As a byproduct, we will also study the rapidity distribution for the Drell-Yan production of lepton pairs. Our goal is to estimate the impact of soft-gluon resummation and the relevance of SUSY contributions to these observables. To this end, we will either focus on the physical cross sections directly or consider the K-factor defined as

$$\frac{d\sigma}{dM^2} = K(M^2, m_{\tilde q}^2, m_{\tilde g}^2, \tau) \left.\frac{d\sigma}{dM^2}\right|_{\mathrm{LO}} . \tag{5.18}$$

The theoretical predictions depend on various input parameters, whose numerical values are $\alpha_{em}(M_Z) = 1/128$, $\sin\theta_W = 0.23143$, $M_Z = 91.188\,\mathrm{GeV}$, and $\Gamma_Z = 2.4952\,\mathrm{GeV}$. Our assumptions for the masses of SUSY particles will be discussed in more detail below. For the systematic analyses in Sections 5.3.1 and 5.3.2 we use the PDF set MSTW2008NNLO [70, 71] and $\alpha_s(M_Z) = 0.117$ with three-loop running in the $\overline{\mathrm{MS}}$ scheme. Using a fixed set of PDFs helps to illustrate more clearly the behavior of the perturbative expansion of the hard-scattering kernel in higher orders of perturbation theory.

For appropriate choices of the hard and soft scales μ_h and μ_s, the expressions for the hard-scattering kernel given in (4.70) resums the leading singular contributions to the partonic cross sections in the limit where the partonic center of mass energy $\sqrt{\hat s}$ is close to the invariant mass M of the (s)lepton pair. In fixed-order perturbation theory, the leading terms correspond to plus distributions of the form

$$\left[\frac{1}{1-z} \ln \frac{M^2(1-z)^2}{\mu_f^2\, z} \right]_+ . \tag{5.19}$$

For Drell-Yan type processes, it is well known that, after the hard-scattering kernels are convoluted with the parton luminosities, these terms provide the dominant contributions to the perturbative series for the cross sections, typically accounting for more than 90% of the one- and two-loop corrections (see e.g. [5, 6, 9]). In realistic cases where the ratio $\tau = M^2/s$ is not very close to 1, the dominance of the region $z \lesssim 1$ in the calculation of the cross section arises dynamically, due to the strong fall-off of the parton luminosities. Below we will perform the resummation of the leading terms at different orders in RG-improved perturbation theory. As specified in Table 4.1, at NNLL order, one evaluates (5.16) using the one-loop approximations for the matching functions C_V and $\tilde{s}_{\rm DY}$ along with two-loop (three-loop) expressions for the (cusp) anomalous-dimension functions. At N^{3}LL order, one uses the two-loop approximations for the matching functions along with three-loop (four-loop) expressions for the (cusp) anomalous dimensions. The explicit expressions for all relevant anomalous dimensions can be found in Appendix A.5. Note that the two-loop virtual SUSY corrections $c_{V,\rm SUSY}^{(2)}$ in (5.17) and the four-loop cusp anomalous dimension are currently unknown, but their numerical impact on the N^{3}LL result is expected to be negligibly small. In our N^{3}LL results below, we include the known two-loop corrections to the hard and soft functions and the relevant three-loop anomalous dimensions.

Subleading terms can be added to our resummed expressions by matching them to fixed-order perturbation theory. To this end, we define

$$d\sigma^{\rm N^nLL+NLO} = d\sigma^{\rm N^nLL}|_{\mu_h,\mu_s,\mu_f} + \left(d\sigma^{\rm NLO}|_{\mu_f} - d\sigma^{\rm N^nLL}|_{\mu_h=\mu_s=\mu_f} \right)\Big|_{\mathcal{O}(\alpha_s)} . \tag{5.20}$$

The first term on the right-hand side denotes the resummed prediction for the cross section, while the second one includes those terms that are subleading in the $z \to 1$ limit. They are obtained by subtracting the fixed-order expression for the leading singular terms, derived by setting all three scales equal in expression (4.70), from the complete fixed-order result. This difference is then expanded to first order in α_s. Since the matching to fixed-order theory is somewhat cumbersome, we will sometimes restrict our analysis to the leading singular terms only. This will be mentioned explicitly below.

5.3.1. Scale setting

An appropriate choice of the matching scales μ_h and μ_s, which enter in the resummation formula (4.70), is crucial for the reduction of the remaining perturbative uncertainties in our calculation. In the spirit of effective field theory, the choice of these scales is driven by the requirement that the perturbative expansions of the matching coefficients C_V and $\tilde{s}_{\rm DY}$ should be well behaved. Since the SUSY contributions to C_V turn out to be very small (see below), these effects play no role in the scale-setting procedure, which therefore proceeds in analogy with the discussion for the Drell-Yan cross section presented in [5]. For the hard matching scale, we adopt the default choice $\mu_h^{\rm def} = M$.

The soft scale μ_s is set dynamically by minimizing the effect of the one-loop corrections to the soft function $\tilde{s}_{\rm DY}$ under the convolution integral (5.11). This scale therefore depends

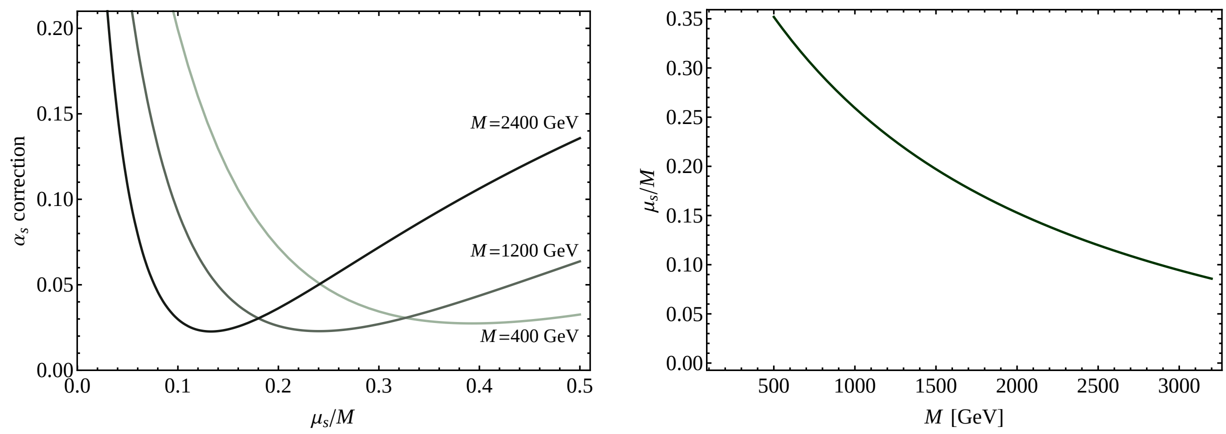

Figure 5.1.: Relative contribution of the one-loop correction to the soft function to the cross section for slepton-pair production at the LHC ($\sqrt{s} = 7\,\text{TeV}$), for different values of the pair invariant mass M (left). For each value of M we determine the soft scale by taking the point at which the correction is minimal (right).

on the value of $\tau = M^2/s$ and on the process under consideration. For the case of slepton-pair production at the LHC (with $\sqrt{s} = 7\,\text{TeV}$), the result is shown in the left plot of Figure 5.1 for different choices of the invariant mass M. Our default value for the soft scale is chosen such that, for fixed M, the contribution of the one-loop correction to the soft function to the cross section is minimized. The value of μ_s/M for which this condition is satisfied is shown in the plot on the right. We observe that for sufficiently large values of M the soft scale is indeed much smaller than the hard scale $\mu_h \sim M$, indicating the relevance of threshold resummation. The corresponding plots for the Tevatron and the LHC with $\sqrt{s} = 14\,\text{TeV}$ would look similar. For practical purposes, the values of μ_s as a function of M and s can be parametrized by means of the function

$$\mu_s^{\text{def}} = \frac{M(1-\tau)}{(a + b\,\tau^{1/2})^c}\,, \tag{5.21}$$

where $(a, b, c) = (1.1, 3.6, 1.9)$ for the Tevatron, $(1.5, 4.8, 1.7)$ for the LHC with $\sqrt{s} = 7\,\text{TeV}$, and $(1.4, 3.6, 2.0)$ for the LHC with $\sqrt{s} = 14\,\text{TeV}$.

After the matching scales have been set, our results still exhibit a residual dependence on the factorization scale μ_f, at which the PDFs are renormalized. As illustrated in Figure 5.2 for the case of the K-factor for slepton-pair production at the LHC, we find that after soft-gluon resummation this dependence is significantly weaker than in fixed-order perturbation theory, already at NLL order. For this analysis only the leading singular two-loop corrections are considered at NNLO, and this is denoted by a star (NNLO*). It follows that there is very little sensitivity to the choice of the factorization scale. Below we take $\mu_f^{\text{def}} = M$ as our default value.

In Figure 5.3, we study the K-factor for slepton-pair production at the LHC, showing results obtained at different orders of perturbation theory. Only the leading singular terms

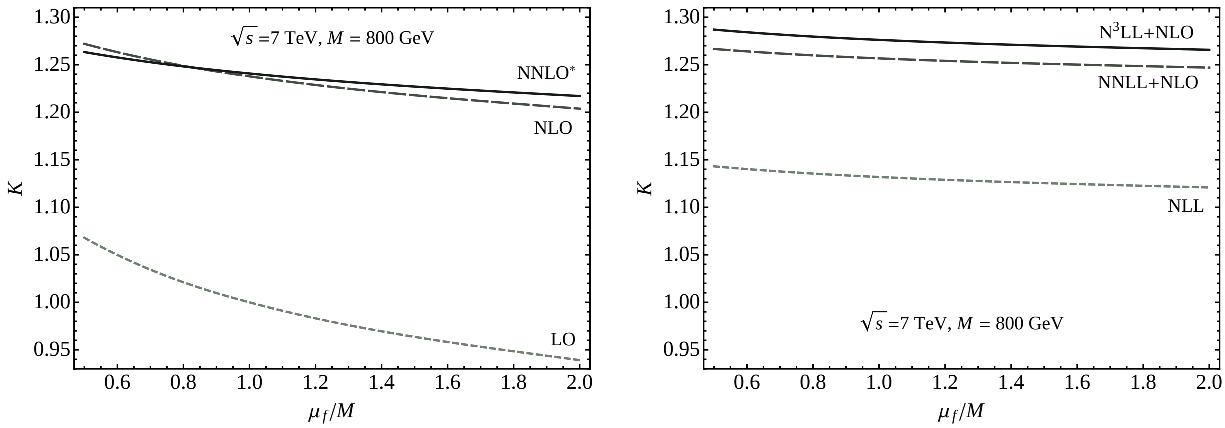

Figure 5.2.: Factorization-scale dependence of the K-factor for slepton-pair production at the LHC in fixed-order perturbation theory (left) and after soft-gluon resummation (right). The NNLO* and N^{3}LL+NLO results contain only the leading singular two-loop corrections.

are included in all cases. The widths of the various bands reflect the scale uncertainties inherent in the calculations. For the fixed-order results, they are obtained by setting the renormalization scale μ_r equal to the factorization scale μ_f, and varying the common scale between 0.5 and 2 times its default value. We performed an independent variation of the two scales as well, but the corresponding uncertainty obtained by taking an envelope of the maximum deviation from the default value does not differ appreciably from the result in Figure 5.3. This is because at leading order the cross section depends on μ_f only, while the dependence on μ_r starts at NLO and is therefore small. For the resummed results, the error bands take into account the uncertainties associated with the scales μ_h, μ_s, and μ_f. They correspond to the envelope of the predictions obtained by varying all three scales simultaneously between 0.5 and 2 times their default values. We verified that the bands obtained in this way do not differ in a significant way from those obtained by varying the three scales individually, with the other two scales held fixed, and adding then the three uncertainties in quadrature. It is evident that the convergence of the perturbative expansion and the remaining scale uncertainties are greatly improved by means of soft-gluon resummation. After resummation the three bands nicely overlap, and the scale uncertainties are reduced significantly with each order. On the contrary, the fixed-order results exhibit a slower convergence and larger scale uncertainties.

5.3.2. Impact of SUSY matching corrections

The existence of SUSY particles would affect our analysis in two ways. First, if sleptons exist and are kinematically accessible at the Tevatron or LHC, these particles can be pair produced, and via a measurement of their cross section and invariant-mass distribution

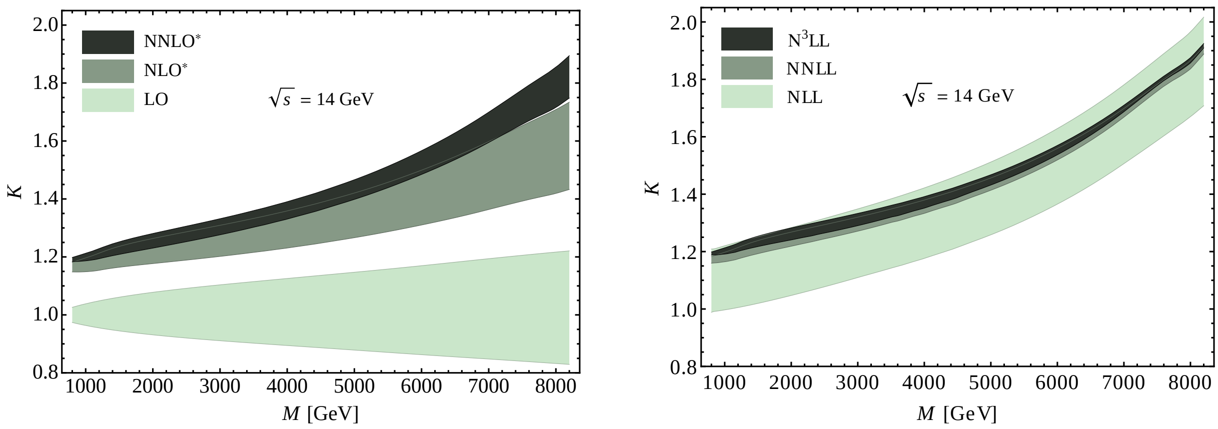

Figure 5.3.: K-factor for slepton-pair production at the LHC, at different orders in fixed-order perturbation theory (left) and including the effects of soft-gluon resummation (right). Only the leading singular terms are included.

one can address questions about the slepton masses and couplings. Secondly, strongly-interacting SUSY particles (squarks and gluinos) can affect the hard-scattering kernels for both lepton-pair and slepton-pair production at $\mathcal{O}(\alpha_s)$, via one-loop SUSY-QCD corrections to the hard matching coefficient C_V in (5.16). This second effect is obviously more subtle than the first one. We will now address if and to what extent it will be possible to probe for virtual effects of SUSY particles in high-precision measurements of the standard Drell-Yan cross section.

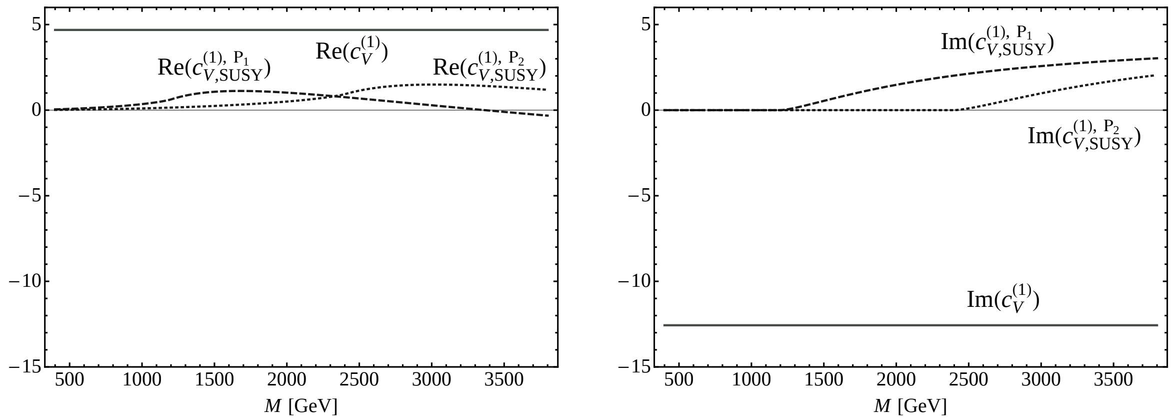

Figure 5.4.: Comparison of one-loop contributions to the hard matching coefficient C_V arising in the SM (solid lines) and in its SUSY extensions (dashed lines).

In Figure 5.4, we compare the one-loop SUSY-QCD contributions to the Wilson coefficient C_V with the corresponding QCD contributions arising in the SM, for two representa-

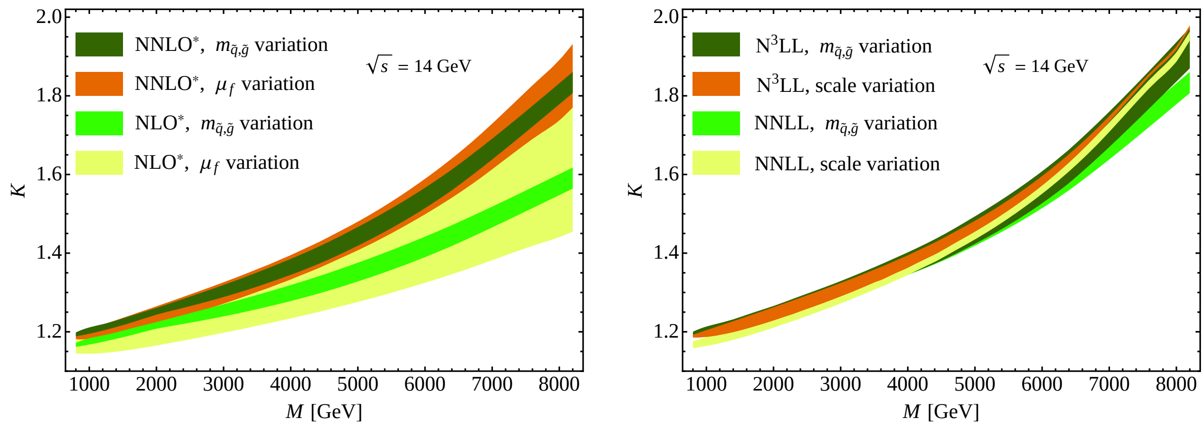

Figure 5.5.: Comparison of the scale uncertainty of the Drell-Yan K-factor for the LHC (light bands) with the maximum possible deviation due to loop effects of SUSY particles (dark bands). The left plot refers to fixed-order perturbation theory, while the right one includes the effects of soft-gluon resummation. Only the leading singular terms are included in the calculation.

tive choices of the squark and gluino masses. The first, $m_{\tilde{q}} = 600\,\text{GeV}$ and $m_{\tilde{g}} = 750\,\text{GeV}$ (parameter point $\mathcal{P}_1$), represents an average value for the squark and gluino masses close to the point SPS1a' [72]. The second, given by $m_{\tilde{q}} = 1200\,\text{GeV}$ and $m_{\tilde{g}} = 500\,\text{GeV}$ (parameter point $\mathcal{P}_2$), represents an alternative scenario with a lighter gluino and heavier squarks, inspired by scenarios like SPS2 and SPS3 [73]. We observe that for all parameter choices the SM loop corrections are at least a factor of about 3 larger in magnitude than the SUSY corrections. The real part of the SUSY contributions reaches a maximum close to the squark threshold, for $M \gtrsim 2m_{\tilde{q}}$, where the virtual contributions acquire an imaginary part. For values of M below threshold the SUSY corrections are yet much smaller. As a result, we find that the virtual SUSY effects are smaller than the residual scale uncertainties in the calculation of the cross sections. This is shown in Figure 5.5, where we compare the factorization-scale uncertainty (both at fixed-order and after resummation) of the SM-only Drell-Yan K-factor with the maximum deviation arising if we include the virtual SUSY contributions and scan the squark and gluino masses independently over the range between 400 and 2200 GeV. For each value of M we choose the points in the $(m_{\tilde{q}}, m_{\tilde{g}})$ plane which yield the largest up- and downward deviations. In the figure we consider Drell-Yan production at the LHC with $\sqrt{s} = 14\,\text{TeV}$. At lower energy or for the Tevatron the impact of virtual SUSY effects is even smaller. We observe that in fixed-order perturbation theory the maximum possible deviation due to virtual effects of SUSY particles is always much smaller than the residual scale dependence. After soft-gluon resummation the size of the effects is comparable; however, in view of the fact that additional theoretical uncertainties arise from the variation of the PDFs (not shown in the figure), we conclude that also in this case the combined theoretical error is larger than the maximum possible SUSY effect.

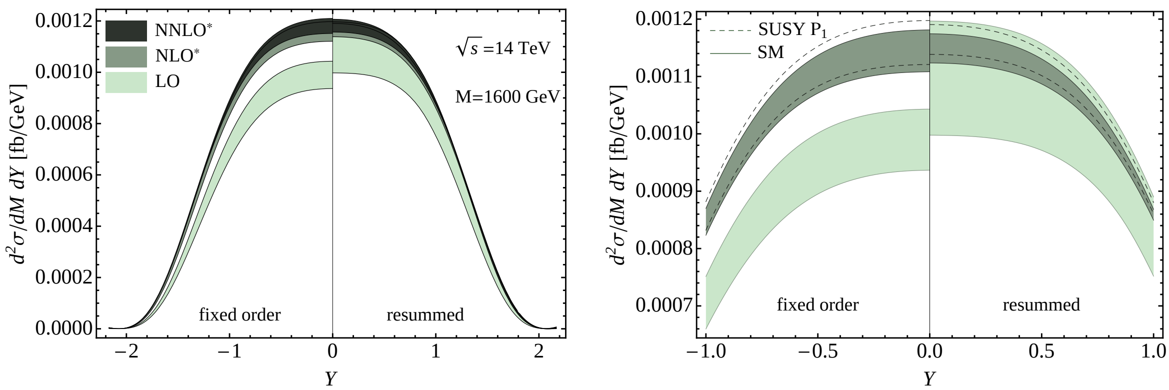

Figure 5.6.: Drell-Yan rapidity distribution at fixed $M = 1600\,\text{GeV}$ at different orders in perturbation theory. In both plots, the left half refers to fixed-order perturbation theory, while the right half includes the effects of soft-gluon resummation. The plot on the left refers to the SM, while the one on the right shows the effects of virtual squarks and gluinos by the dashed bands.

On the one hand, these findings justify an approximation at N^{3}LL order where in the two-loop corrections to the hard matching coefficient C_V in (5.16) one neglects the SUSY contribution $c_{V,\text{SUSY}}^{(2)}$ compared with the corresponding SM contribution $c_V^{(2)}$. This approximation will be adopted in our N^{3}LL predictions below. On the other hand, it appears unlikely that it will be possible to probe for SUSY effects via virtual corrections to the Drell-Yan cross section. To illustrate this latter point, we show in Figure 5.6 the result for the Drell-Yan rapidity distribution in our SUSY model $\mathcal{P}_1$ (with $m_{\tilde{q}} = 600\,\text{GeV}$ and $m_{\tilde{g}} = 750\,\text{GeV}$) at a value of the pair invariant mass for which the SUSY effects are close to maximal (cf. Figure 5.4). We consider the LHC with $\sqrt{s} = 14\,\text{TeV}$ and restrict our analysis to the leading singular terms only. In the left plot we compare the results obtained at different orders in fixed-order perturbation theory with the corresponding results obtained after soft-gluon resummation. These distributions refer to the SM without SUSY effects. We observe that resummation improves the convergence of the perturbative expansion and leads to somewhat smaller scale variations at higher orders. The right plot zooms in on the central region of the rapidity distribution and shows once again the results obtained at leading and next-to-leading order with and without resummation. The dashed lines indicate the shift of the NLO* and NNLL bands due to the presence of SUSY particles. In both cases (with and without resummation) the shift amounts to a small enhancement of the cross section, which however is only a fraction of the residual scale uncertainty indicated by the widths of the bands. Note also that the additional PDF uncertainty is not included in the plots.

5.3.3. Invariant-mass distribution for slepton-pair production

A clear signal of SUSY would come from the direct production and detection of slepton pairs. In this case, the very weak dependence on the squark and gluino masses can be seen as an advantage, since it would make it possible to use a measurement of the slepton-pair production cross section to extract the mass of the slepton produced, or alternatively to set a limit on the slepton mass from an upper limit on the production cross section. The sensitivity of the cross section (5.2) to the slepton mass $m_{\tilde{l}}$ arises from the prefactor $\beta_{\tilde{l}}^3$ in (5.3), and from the fact that the peak of the invariant mass distribution scales with $m_{\tilde{l}}$. After the determination of the matching and factorization scales in Section 5.3.1, we are now ready to analyze the impact of soft-gluon resummation on the invariant-mass distribution for slepton-pair production. For concreteness, we will consider the production of a pair of scalar leptons $\tilde{l}_L$, as this case has the largest cross section. For the SUSY masses we take $m_{\tilde{l}_L} = 180\,\mathrm{GeV}$, $m_{\tilde{q}} = 600\,\mathrm{GeV}$, and $m_{\tilde{q}} = 750\,\mathrm{GeV}$.

Our results for the slepton invariant-mass distributions are shown in Figure 5.7 for the Tevatron (top), the LHC with $\sqrt{s} = 7\,\mathrm{TeV}$ (center), and the LHC with $\sqrt{s} = 14\,\mathrm{TeV}$ (bottom). Contrary to our previous treatment, from now on we consider the PDFs and α_s at the order which is appropriate for the expansion of the corresponding hard-scattering kernels. Specifically, we use LO and NLO PDFs for the LO and NLO fixed-order results, and NLO and NNLO PDFs for the resummed results at NLL, NNLL+NLO, and N^{3}LL+NLO, since in this case the resummed terms include the bulk of the perturbative corrections appearing at one order higher in α_s. Numerically, the NNLL+NLO (not shown in the figure) and N^{3}LL+NLO results turn out to be very close to each other, but the scale dependence of the latter ones is further reduced. We thus consider the N^{3}LL+NLO approximation as our best prediction. The main effect of soft-gluon resummation is to increase the cross sections slightly and to improve the convergence of the expansion. The resummation effects become more relevant for larger invariant masses. For example, at the Tevatron the increase from NLO to N^{3}LL+NLO is 7% at 500 GeV and 13% at 1000 GeV. The corresponding increases at the LHC are around 2% for both $\sqrt{s} = 7\,\mathrm{TeV}$ and 14 TeV, indicating that at the LHC resummation effects are less important.

5.3.4. Total cross section

We obtain the total cross sections by integrating the invariant-mass distributions over M. In Table 5.1 we present results corresponding to the various approximations discussed in the previous section. In this section we provide predictions for both the NNLL+NLO and N^{3}LL+NLO total cross sections, so that the effect of including higher-order logarithmic terms can be seen. In the table the first error refers to the total scale variation, i.e. the variation of μ_f for the fixed-order cross sections and the maximum deviation from the default value obtained by varying μ_f, μ_h, and μ_s simultaneously for the resummed and matched results. The second error takes into account the uncertainty of the PDFs at the 90% confidence level, which is estimated by evaluating the cross sections with the 40 sets of PDFs provided by MSTW2008.

	Tevatron (SUSY point $\mathcal{P}_1$)	LHC (7 TeV, SUSY point $\mathcal{P}_1$)
σ_{LO}	$1.31^{+0.17\,+0.08}_{-0.14\,-0.06}$	$8.01^{+0.39\,+0.31}_{-0.36\,-0.34}$
σ_{NLL}	$1.65^{+0.27\,+0.12}_{-0.20\,-0.08}$	$9.59^{+1.25\,+0.41}_{-0.92\,-0.37}$
σ_{NLO}	$1.83^{+0.09\,+0.14}_{-0.10\,-0.10}$	$10.56^{+0.24\,+0.48}_{-0.22\,-0.43}$
$\sigma_{\text{NNLL+NLO}}$	$1.93^{+0.06\,+0.14}_{-0.07\,-0.10}$	$10.63^{+0.13\,+0.48}_{-0.17\,-0.37}$
$\sigma_{\text{N}^3\text{LL+NLO}}$	$1.96^{+0.05\,+0.14}_{-0.05\,-0.11}$	$10.81^{+0.10\,+0.48}_{-0.08\,-0.37}$
	LHC (14 TeV, SUSY point $\mathcal{P}_1$)	LHC (14 TeV, SUSY point $\mathcal{P}_2$)
σ_{LO}	$28.14^{+0.25\,+0.70}_{-0.34\,-0.94}$	$1.88^{+0.09\,+0.07}_{-0.08\,-0.08}$
σ_{NLL}	$33.36^{+4.60\,+1.10}_{-3.45\,-1.01}$	$2.24^{+0.27\,+0.09}_{-0.20\,-0.08}$
σ_{NLO}	$36.65^{+0.45\,+1.28}_{-0.35\,-1.19}$	$2.45^{+0.05\,+0.11}_{-0.05\,-0.10}$
$\sigma_{\text{NNLL+NLO}}$	$37.16^{+0.36\,+1.30}_{-0.46\,-1.03}$	$2.47^{+0.03\,+0.11}_{-0.03\,-0.08}$
$\sigma_{\text{N}^3\text{LL+NLO}}$	$37.80^{+0.25\,+1.32}_{-0.12\,-1.05}$	$2.51^{+0.02\,+0.11}_{-0.02\,-0.08}$

Table 5.1.: Total cross sections in fb. The first error refers to the perturbative uncertainties associated with scale variations, the second to PDF uncertainties.

The results shown in the first three blocks of Table 5.1 refer to the production of a slepton $\tilde{l}_L$ with mass $m_{\tilde{l}_L} = 180\,\text{GeV}$ (SUSY parameter point $\mathcal{P}_1$, with $m_{\tilde{q}} = 600\,\text{GeV}$ and $m_{\tilde{g}} = 750\,\text{GeV}$) at the Tevatron and the LHC. Note the relevance of the NLO correction, which amounts to around 40% for the Tevatron and 30% for the LHC. As expected, the resummation effects are larger at the Tevatron, where they amount to a 7% enhancement of the NNLL+NLO cross section compared with the NLO result. At the LHC the resummation gives a smaller 3% additional contribution to the total cross section. The additional contribution of the N^{3}LL+NLO result compared to the NNLL+NLO approximation is small, below 1%, but performing the resummation at N^{3}LL order helps to further reduce the scale uncertainty.

Since the effect of soft-gluon resummation becomes more important for higher invariant masses, in Table 5.1 we provide also the total cross section for a heavier slepton $\tilde{l}_L$ with mass $m_{\tilde{l}_L} = 360\,\text{GeV}$ (SUSY parameter point $\mathcal{P}_2$, with $m_{\tilde{q}} = 1200\,\text{GeV}$ and $m_{\tilde{g}} = 500\,\text{GeV}$). We only show results for the LHC with $\sqrt{s} = 14\,\text{TeV}$, because given the small cross sections it would not be possible to observe the production of such heavy sleptons at the Tevatron or during the low-energy phase of the LHC.

In Figure 5.8, we show the matched N^{3}LL+NLO total cross section as a function of the slepton mass. We now consider different types of sleptons, $\tilde{l}_{L,R}$ (with $l = e, \mu$) and $\tilde{\tau}_{1,2}$. For the staus, we assume a mixing angle $\theta_{\tilde{\tau}} = 70°$. The cross sections fall off steeply with the slepton masses. At the Tevatron it will be difficult to observe sleptons with masses exceeding about 250 GeV, while at the LHC it should be possible to observe slepton-pair production up to masses in the range 300–400 GeV. In the upper plot we show the cross sections at the Tevatron, focusing on the low mass region. The lower plots refer to the

LHC at 7 and 14 TeV of center of mass energy. At the same value of slepton mass, the slepton $\tilde{l}_L$ has the larger cross section, while the slepton $\tilde{l}_R$ has the lowest cross section. The cross sections for the production of staus lie in between. We observe that owing to the small scale uncertainty at N^{3}LL+NLO, it would be straightforward to extract the masses of the sleptons from measurements of the corresponding total cross sections.

We have compared our predictions for the LO and NLO fixed-order total cross sections for slepton production with results provided by the program `Prospino` [15], finding agreement. Despite the fact that it is difficult to compare our resummed results with those presented in [17], because contrary to these authors we do not consider squark mixing, we still find a reasonable agreement. We emphasize that the method developed here allows us to resum soft gluons up to the N^{3}LL order, so that we are able to get a smaller scale uncertainty compared with [17].

The main result of our analysis is that, using soft-gluon resummation techniques, we can reduce the theoretical uncertainty related to scale variations below the percent level, making it a subdominant source of error. This is evident from the results collected in Table 5.1, which show that the error due to uncertainties in the PDFs becomes dominant beyond NLO. At this level of precision, one may ask whether the NNLO subleading terms could also become relevant. While the full NNLO corrections have not yet been calculated for the case of slepton pair production, we can estimate their relevance by considering the case of Drell-Yan production of lepton pairs, for which the NNLO corrections are availble [57]. In this case, we find that the additional correction due to the NNLO subleading terms amounts to at most 1% of the NLO cross section. It is thus of the same order as the scale uncertainty that we find at N^{3}LL+NLO.

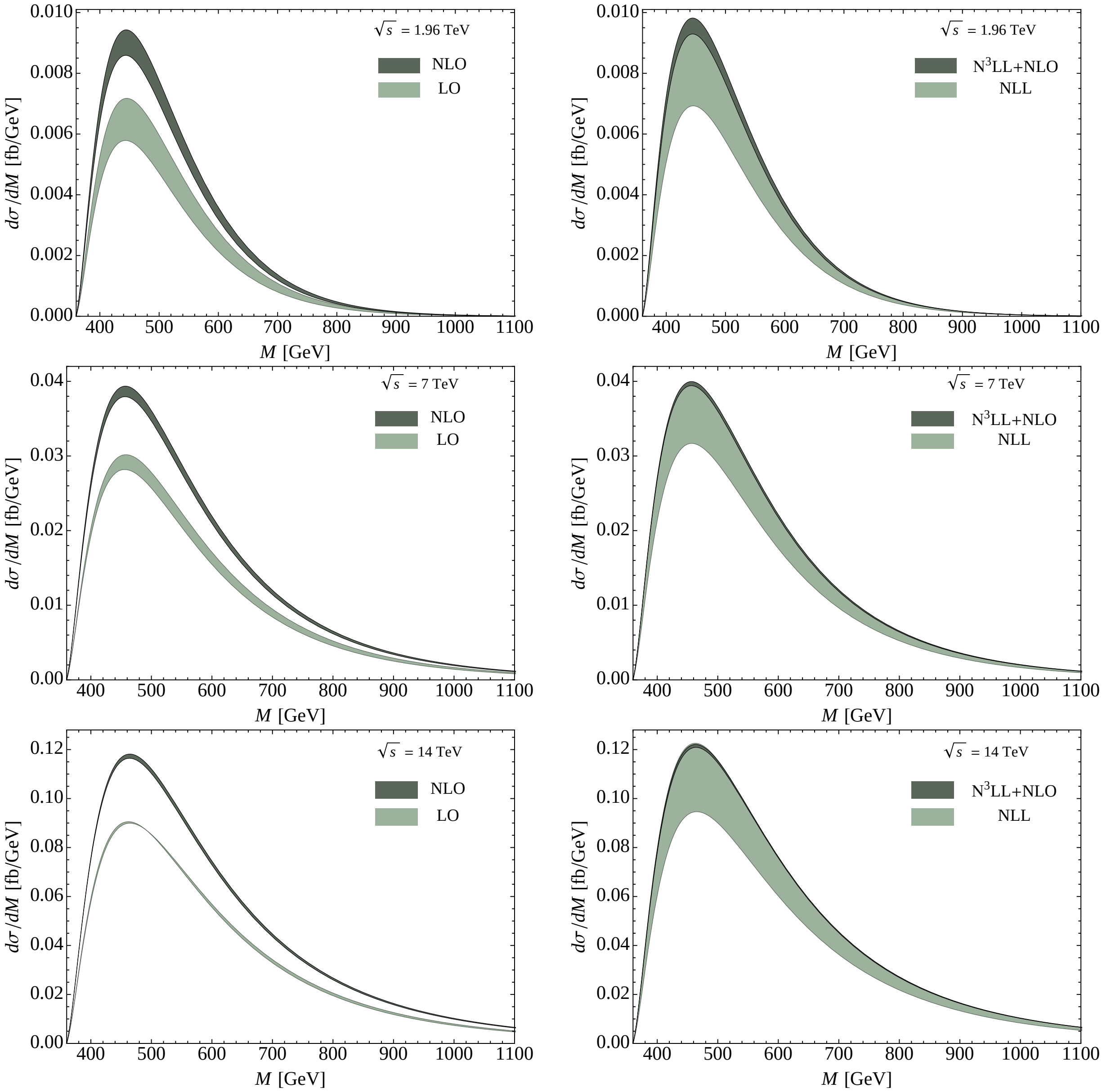

Figure 5.7.: Invariant-mass distributions for slepton-pair production at the Tevatron and LHC. The plots on the left show fixed-order results at LO and NLO, while those on the right include the effects of soft-gluon resummation at NLL and N^{3}LL+NLO. The bands indicate the uncertainty associated with scale variations.

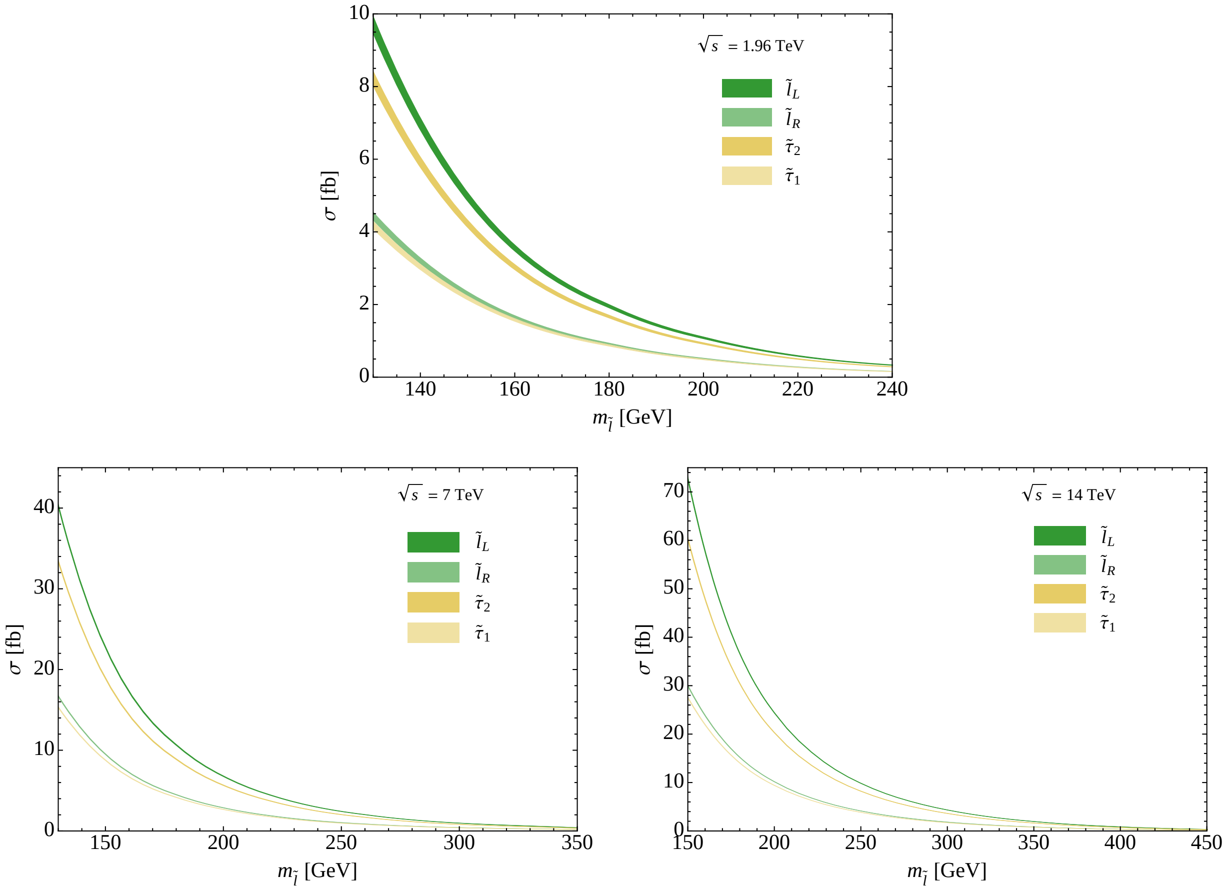

Figure 5.8.: Total cross sections for slepton-pair production as a function of the slepton masses.

6. Approximate NNLO formulas for stop-pair production

6.1. Introduction

The supersymmetric particles which are expected to be most abundantly produced at hadron colliders, are the ones which carry color charge: squarks and gluinos. Since SUSY is broken (via the soft terms), the squark and gluinos mass spectrum plays a crucial role in determining which among the colored superymmetric partners is the most accessible experimentally. Given an underlying model for the soft terms at some input scale, the scalar masses are evolved from a common high scale value down to the “low” scales accessible at the LHC, the lighter of the two supersymmetric partners of the top-quark is expected to be the lightest squark of the mass spectrum.

Precise theoretical predictions of the stop-pair production cross section are instrumental in setting a lower bound on the lightest stop mass. Moreover, if the top-squarks will be discovered, accurate predictions of the stop-pair cross section can be employed to determine the masses and other properties of these particles. For these reasons, the study of the radiative corrections to the production of stop-pairs already has a quite long history. The calculation of the NLO corrections to the stop-pair production within the context of SUSY-QCD was completed 15 years ago [18]. As expected, it was found that the NLO corrections significantly decrease the renormalization and factorization scale dependence of the prediction when compared to the leading order (LO) calculation. Furthermore, NLO SUSY-QCD corrections increase the value of the cross section if the renormalization and factorization scales are chosen close to the value of the stop mass. The NLO SUSY-QCD corrections are implemented in the computer programs `Prospino` and `Prospino2` [74]. The electroweak corrections to stop-pair production were studied in [75, 76]; while these corrections have a quite sizable effect on the tails of the invariant mass and p_T distributions, they only have a moderate impact on the total cross section. The emission of soft gluons represents a significant portion of the NLO SUSY-QCD corrections [77], which are large. For this reason, the resummation of the NLL corrections was carried out in [78], where it was found that the NLL corrections increase the cross section at the LHC by up to 10% of its NLO value, while they further decrease the scale dependence of the prediction. In these analysis, the resummation is carried out in the Mellin moment space.

Within the context of soft-gluon resummation in SCET, the production of top-squark pairs can be studied in strict analogy to the production of top-quark pairs [9,10]. It the soft limit, the partonic production cross sections for the stop and top-pair production factor into the product of hard and soft functions, which are matrices in color space. The soft functions are identical for top-squark and top-quark production, and only the hard functions, which include the full dependence on the SUSY parameters other than the lightest top-squark mass, need to be recalculated for the stop-pair production.

In this thesis, we carry out the calculation of the hard functions for the stop-pair production to NLO. By combining the NLO hard functions with the NLO soft function evaluated in [9, 10], and with the anomalous dimensions which regulate RG equations satisfied by the various terms in the factorized cross section, it is possible to resum NNLL soft gluon emission corrections. This can be done both in PIM kinematics (in analogy to what was done in [9]) and in 1PI kinematics (in analogy with [10]). Here we limit ourselves to re-expand the resummed formulas in order to obtain approximate NNLO formulas for the pair invariant mass distribution and the stop transverse momentum and rapidity distribution. By integrating those formulas over the complete phase space, we obtain predictions for the total top-squark-pair production cross section at the LHC, and we comment on the phenomenological impact of the NNLO corrections arising from soft emission.

The chapter is organized as follows: In Section 6.2 we introduce our notation and conventions, which are very similar to the ones employed in [9, 10]. Furthermore, we describe the factorization of the stop-pair production cross section in the soft limit, both in PIM and 1PI kinematics. In Section 6.3, we discuss the calculation of the soft and hard functions up to NLO. Since the expressions for the NLO hard functions are too lengthy to be typed here in analytic form, they can be provided by the author upon request. A Fortran program which evaluates the hard functions for arbitrary values of their arguments is also available. In Section 6.4, we write the RG equation satisfied by the hard and soft functions, while in Section 6.5 we present approximate NNLO formulas for the stop-pair production process. Predictions for the total top-squark-pair production cross section at the LHC can be found in Section 6.6, together with an analysis of the phenomenological impact of the approximate NNLO corrections on this observable.

6.2. Kinematics

We consider the following supersymmetric process:

$$N_1(P_1) + N_2(P_2) \to \tilde{t}_1(p_3) + \tilde{t}_1^*(p_4) + X(k)\,, \tag{6.1}$$

where N_1 and N_2 indicate the incoming protons in the case of a proton-proton collider as the LHC, while X is an inclusive hadronic final state. We treat the top-squarks as on-shell particles and neglect their decay. At the lowest order in perturbation theory, two partonic channel contribute to the process in Eq. (6.1):

$$\begin{aligned} q(p_1) + \bar{q}(p_2) &\to \tilde{t}_1(p_3) + \tilde{t}_1^*(p_4)\,, \\ g(p_1) + g(p_2) &\to \tilde{t}_1(p_3) + \tilde{t}_1^*(p_4)\,. \end{aligned} \tag{6.2}$$

where the momenta of the incoming partons are related to the momenta of the incoming hadrons by $p_i = x_i P_i$ $(i = 1, 2)$. The relevant invariants for the hadronic scattering are

$$s = (P_1 + P_2)^2 \,, \quad t_1 = (P_1 - p_3)^2 - m_{\tilde{t}_1}^2 \,, \quad u_1 = (P_2 - p_3)^2 - m_{\tilde{t}_1}^2 \,. \tag{6.3}$$

In order to describe the partonic scattering, we employ the invariants

$$\hat{s} = x_1 x_2 s = (p_1 + p_2)^2 \,, \quad \hat{t}_1 = x_1 t_1 \,, \quad \hat{u}_1 = x_2 u_1 \,,$$
$$M^2 = (p_3 + p_4)^2 \,, \quad s_4 = \hat{s} + \hat{t}_1 + \hat{u}_1 = (p_4 + k)^2 - m_{\tilde{t}_1}^2 \,. \tag{6.4}$$

In Born approximation one has that $\hat{s} + \hat{t}_1 + \hat{u}_1 = 0$ and, consequently, $M^2 = \hat{s}$ and $s_4 = 0$.

It is well known that the kinematic of the process allows to define different threshold regions. Here we consider two different cases: the PIM kinematics, in which the threshold region is defined by the limit $\hat{s} \to M^2$, and the 1PI kinematics, in which the threshold region is approached by the limit $s_4 \to 0$. Both regions were employed in the study of the top-quark-pair production cross section and differential distributions [79]. It should be emphasized that in the PIM and 1PI threshold regions the top-squarks are not forced to be nearly at rest, as it is the case in the threshold region defined by the limit $\beta = \sqrt{1 - 4m_{\tilde{t}_1}/\hat{s}} \to 0$, which is often employed in the calculation of soft gluon corrections to the total cross section [11,13,78]. We refer to the $\beta \to 0$ limit as the production threshold region.

Our goal is to employ both the PIM and 1PI kinematics to obtain approximate NNLO formulas for the total top-squark-pair production cross section. Both approaches include the numerically large contributions arising from the emission of soft gluons, but differ among them and with the production threshold calculations in the kind of power suppressed terms which are neglected.

6.2.1. PIM Kinematics

We focus first on the PIM kinematics approach. This kinematics was already introduced for slepton-pair production and it is convenient to recall here the important kinematic quantities:

$$z = \frac{M^2}{\hat{s}} \,, \qquad \tau = \frac{M^2}{s} \,, \qquad \beta_{\tilde{t}_1} = \sqrt{1 - \frac{4m_{\tilde{t}_1}^2}{M^2}} \,. \tag{6.5}$$

Consequently, the PIM threshold limit $\hat{s} \to M^2$ corresponds to the limit $z \to 1$. According to the QCD factorization theorem [80], the differential cross section in M and θ (the scattering angle of the top-squark with respect to the incoming partons beam in the partons rest frame) is given by

$$\frac{d^2\sigma}{dM\, d\cos\theta} = \frac{\pi \beta_{\tilde{t}_1}}{sM} \sum_{i,j} \int_\tau^1 \frac{dz}{z} ff_{ij}\,(\tau/z, \mu_f)\, C_{\mathrm{PIM},ij}\,(z, M, \cos\theta, \mu_f) \,, \tag{6.6}$$

where μ_f is the factorization scale, and the sum runs over the incoming partons. The parton luminosity ff was defined in Eq. (5.12) as the convolution of the PDFs for the $q\bar{q}$ case. It is trivial to extend this definition for generic incoming partons i and j:

$$\mathit{ff}_{i,j}(y,\mu_f) = \int_y^1 \frac{dx}{x} f_{i/N_1}(x,\mu_f)\, f_{j/N_2}(y/x,\mu_f) \equiv f_{i/N_1}(y) \otimes f_{j/N_2}(y)\,. \tag{6.7}$$

In the following we drop the subscript PIM (and the corresponding subscript 1PI) whenever there is no ambiguity about the kinematic scheme used. In order not to make the notation unnecessarily heavy, we do not indicate explicitly the dependence of the hard scattering kernels on the SUSY parameters and on the top-quark mass m_t. The SUSY parameters we are referring to are: the two stop masses $m_{\tilde{t}_1}$ and $m_{\tilde{t}_2}$, the mass $m_{\tilde{q}}$ of the first two families squarks and the sbottoms (which we assume to be degenerate), the gluino mass $m_{\tilde{g}}$, and the $\tilde{t}_1 - \tilde{t}_2$ mixing angle α defined in Eq. (2.107). The hard-scattering kernels C_{ij} in Eq. (6.6) are related to the partonic cross sections and can be calculated in perturbation theory. Their expansion in powers of α_s has the generic form

$$C_{ij} = \alpha_s^2 \left[C_{ij}^{(0)} + \frac{\alpha_s}{4\pi} C_{ij}^{(1)} + \left(\frac{\alpha_s}{4\pi}\right)^2 C_{ij}^{(2)} + \mathcal{O}(\alpha_s^3) \right]. \tag{6.8}$$

Only the quark annihilation and gluon fusion channels contribute to C_{ij} at lowest order in perturbation theory; in particular

$$\begin{aligned} C_{q\bar{q}}^{(0)} &= \delta(1-z) \frac{C_F}{N} \left(\frac{t_1 u_1}{M^4} - \frac{m_{\tilde{t}_1}}{M^2} \right), \\ C_{gg}^{(0)} &= \delta(1-z) \frac{1}{(N^2-1)} \left(C_F \frac{M^4}{t_1 u_1} - C_A \right) \left(\frac{t_1 u_1}{M^4} - \frac{2m_{\tilde{t}_1}^2}{M^2} + \frac{2m_{\tilde{t}_1}^4}{t_1 u_1} \right), \end{aligned} \tag{6.9}$$

where $N = 3$ and the Mandelstam invariants $\hat{t}_1$ and $\hat{u}_1$ can be written in terms of $\hat{s}$ and θ as follows:

$$\hat{t}_1 = -\frac{M^2}{2}\left(1 - \beta_{\tilde{t}_1}\cos\theta\right), \qquad \hat{u}_1 = -\frac{M^2}{2}\left(1 + \beta_{\tilde{t}_1}\cos\theta\right). \tag{6.10}$$

In order to calculate higher order corrections to $C_{q\bar{q}}$ and C_{gg} one needs to consider virtual and real emission corrections to the Born approximation. Starting at order α_s new production channels, such as $qg \to \tilde{t}_1\tilde{t}_1^* q$, open up. When working in the threshold limit $z \to 1$, the calculations are simplified by the fact that there is no phase-space available for the emission of additional (hard) partons in the final state. Consequently, both the hard gluon emission and the additional production channels are suppressed by powers of $(1-z)$ and can be neglected. By neglecting power suppressed terms in the integrand, Eq. (6.6) can be rewritten as

$$\frac{d^2\sigma}{dM\,d\cos\theta} = \frac{\pi\beta_{\tilde{t}_1}}{sM} \int_\tau^1 \frac{dz}{z} \Big[\mathit{ff}_{gg}(\tau/z,\mu_f)\, C_{gg}(z,M,\cos\theta,\mu_f)$$

$$+ ff_{q\bar{q}}\left(\tau/z,\mu_f\right) C_{q\bar{q}}\left(z,M,\cos\theta,\mu_f\right) + ff_{\bar{q}q}\left(\tau/z,\mu_f\right) C_{\bar{q}q}\left(z,M,\cos\theta,\mu_f\right)\Big] . \tag{6.11}$$

In the equation above the quark channel luminosity $ff_{q\bar{q}}$ is understood to be summed over all light quark flavors.

In the soft gluon emission limit $z \to 1$, the hard scattering kernels C_{ij} factor into a product of hard and soft functions:

$$C_{ij}\left(z,M,\cos\theta,\mu_f\right) = \mathrm{Tr}\left[\boldsymbol{H}_{ij}(M,\cos\theta,\mu_f)\boldsymbol{S}_{ij}(\sqrt{s}(1-z),\cos\theta,\mu_f)\right] + \mathcal{O}(1-z)\,, \tag{6.12}$$

where we employ boldface fonts to indicate matrices in color space, such as the hard functions $\boldsymbol{H}_{ij}$ and the soft functions $\boldsymbol{S}_{ij}$. For simplicity we drop the explicit dependence on the top mass and on the SUSY parameters from the arguments of the hard functions $\boldsymbol{H}_{ij}$. We work in the s-channel singlet-octet color bases

$$\begin{gathered}\left(c_1^{q\bar{q}}\right)_{\{a\}} = \delta_{a_1a_2}\delta_{a_3a_4}\,, \qquad \left(c_2^{q\bar{q}}\right)_{\{a\}} = t^c_{a_2a_1}t^c_{a_3a_4}\,, \\ \left(c_1^{gg}\right)_{\{a\}} = \delta^{a_1a_2}\delta_{a_3a_4}\,, \qquad \left(c_2^{gg}\right)_{\{a\}} = if^{a_1a_2c}\,t^c_{a_3a_4}\,, \qquad \left(c_3^{gg}\right)_{\{a\}} = d^{a_1a_2c}\,t^c_{a_3a_4}\,,\end{gathered} \tag{6.13}$$

where a_i represent the color index of the particle with momentum p_i. We view these structures as basis vectors $|c_I\rangle$ in the space of color-singlet amplitudes. Inner products in this space are defined through a summation over color indices as

$$\langle c_I\,|\,c_J\rangle = \sum_{\{a\}}\left(c_I\right)^*_{a_1a_2a_3a_4}\left(c_J\right)_{a_1a_2a_3a_4}\,. \tag{6.14}$$

This inner product is proportional but not equal to δ_{IJ}, so the basis vectors are orthogonal but not orthonormal.

A factorization formula for the hard scattering kernels in the threshold region was derived using SCET and Heavy-Quark Effective Theory (HQET) in [9] for the top-pair production case. The derivation is similar to the one in Chapter 4 for the Drell-Yan case, but is more involved due to the presence of additional color structures. A completely analogous procedure can be followed to derive the factorization formula in Eq. (6.12) for the hard scattering kernels of stop-pair production.

The hard functions are obtained from the virtual corrections and are ordinary functions of their arguments. The soft functions arise from the real emission of soft gluons and contain distributions which are singular in the $z \to 1$ limit. Contributions of order α_s^n to the soft functions include terms proportional to plus distributions

$$\left[\frac{\ln^m(1-z)}{1-z}\right]_+ , \quad (m = 0,\cdots,2n-1)\,, \tag{6.15}$$

as well as terms proportional to $\delta(1-z)$. The plus distributions are defined through the relation

$$\int_0^1 dz\left[\frac{\ln^m(1-z)}{1-z}\right]_+ g(z) \equiv \int_0^1 dz\frac{\ln^m(1-z)}{1-z}\left[g(z)-g(1)\right]\,, \tag{6.16}$$

and, consequently, one finds

$$\int_\tau^1 dz \left[\frac{\ln^m(1-z)}{1-z}\right]_+ g(z) = \int_\tau^1 dz \frac{\ln^m(1-z)}{1-z}\left[g(z)-g(1)\right] - g(1)\int_0^\tau dz \frac{\ln^m(1-z)}{1-z} \,. \tag{6.17}$$

In particular, for the NLO and NNLO hard scattering kernels one has (dropping the parton indices ij)

$$C_{\mathrm{PIM}} = \alpha_s^2 \left[C_{\mathrm{PIM}}^{(0)} + \frac{\alpha_s}{4\pi} C_{\mathrm{PIM}}^{(1)} + \left(\frac{\alpha_s}{4\pi}\right)^2 C_{\mathrm{PIM}}^{(2)} + \mathcal{O}(\alpha_s^3)\right] , \tag{6.18}$$

where

$$\begin{aligned}
C_{\mathrm{PIM}}^{(1)} &= D_1^{(1,\mathrm{PIM})}\left[\frac{\ln(1-z)}{1-z}\right]_+ + D_0^{(1,\mathrm{PIM})}\left[\frac{1}{1-z}\right]_+ + C_0^{(1,\mathrm{PIM})}\delta(1-z) + R^{(1,\mathrm{PIM})}(z)\,, \\
C_{\mathrm{PIM}}^{(2)} &= D_3^{(2,\mathrm{PIM})}\left[\frac{\ln^3(1-z)}{1-z}\right]_+ + D_2^{(2,\mathrm{PIM})}\left[\frac{\ln^2(1-z)}{1-z}\right]_+ + D_1^{(2,\mathrm{PIM})}\left[\frac{\ln(1-z)}{1-z}\right]_+ \\
&\quad + D_0^{(2,\mathrm{PIM})}\left[\frac{1}{1-z}\right]_+ + C_0^{(2,\mathrm{PIM})}\delta(1-z) + R^{(2,\mathrm{PIM})}(z)\,.
\end{aligned} \tag{6.19}$$

The functions $D_j^{(i)}$, $C_0^{(i)}$, and $R^{(i)}$ depend on $\cos\theta, M, \mu_f$, on the SUSY parameters and on the top mass m_t. The coefficients $D_i^{(1)}, C_0^{(1)}$ and $R^{(1)}$ can be obtained from results already present in the literature [18]. In particular the functions $R^{(i)}(z)$ are finite for $z \to 1$. One of the main results of this thesis is the calculation of the coefficients $D_j^{(2)}$ both in the quark annihilation and gluon fusion channel. In principle we could also easily get all the scale dependent terms in $C_0^{(2)}$, in both channels, but due to an ambiguity discussed later, we drop part of these terms in the numerical implementation.

6.2.2. 1PI Kinematics

The 1PI kinematics approach allows one to describe observables in which a single particle, rather than a pair, is detected. In the laboratory frame one can write the stop rapidity (y) and transverse momentum $\left(p_T = \sqrt{p_x^2+p_y^2}\right)$ distribution as

$$\frac{d^2\sigma}{dp_T dy} = \frac{2\pi p_T}{s}\sum_{ij}\int_{x_1^{\min}}^1 \frac{dx_1}{x_1}\int_{x_2^{\min}}^1 \frac{dx_2}{x_2} f_{i/N_1}(x_1,\mu_f) f_{j/N_2}(x_2,\mu_f) C_{1\mathrm{PI},ij}\left(s_4, \hat{s}, \hat{t}_1, \hat{u}_1, \mu_f\right) \,. \tag{6.20}$$

The expansion of the 1PI hard scattering kernels $C_{1\mathrm{PI}}$ in powers of α_s has the same structure shown in Eq. (6.8) for the PIM case. Obviously, also in this case only the $q\bar{q}$ channel and gg channel give a non vanishing contribution at lowest order in α_s. In the laboratory frame, the hadronic Mandelstam variables t_1 and u_1 are related to the stop rapidity and transverse momentum through the relations

$$t_1 = -\sqrt{s} m_\perp e^{-y}\,, \qquad u_1 = -\sqrt{s} m_\perp e^{y}\,, \tag{6.21}$$

where $m_\perp = \sqrt{p_T^2 + m_{\tilde{t}_1}^2}$. Therefore the kinematic variables $\hat{s}, s_4, \hat{t}_1$, and $\hat{u}_1$, which are arguments of the 1PI hard functions, can be written in terms of p_T, y, x_1, and x_2 using Eq. (6.21) and Eq. (6.4). The lower limits of integration in Eq. (6.20) are

$$x_1^{\min} = -\frac{u_1}{s+t_1}\,, \qquad x_2^{\min} = -\frac{x_1 t_1}{x_1 s + u_1}\,. \tag{6.22}$$

In order to obtain the total cross section it is necessary to integrate the double-differential distribution with respect to the stop rapidity and transverse momentum over the range

$$0 \le |y| \le \frac{1}{2}\ln\frac{1+\sqrt{1-4m_\perp^2/s}}{1-\sqrt{1-4m_\perp^2/s}}\,, \qquad 0 \le p_T \le \sqrt{\frac{s}{4} - m_{\tilde{t}_1}^2}\,. \tag{6.23}$$

As in the case of PIM kinematics, in the 1PI kinematics soft emission limit $s_4 \to 0$, the hard scattering kernels factor into the product of hard and soft functions:

$$C_{ij}\left(s_4, \hat{s}', \hat{t}_1', \hat{u}_1', \mu_f\right) = \mathrm{Tr}\left[\boldsymbol{H}_{ij}\left(\hat{s}', \hat{t}_1', \hat{u}_1', \mu_f\right)\boldsymbol{S}_{ij}\left(s_4, \hat{s}', \hat{t}_1', \hat{u}_1', \mu_f\right)\right] + \mathcal{O}(s_4)\,. \tag{6.24}$$

As explained in [10], the notation above is used to emphasize that there are ambiguities in the choice of the Mandelstam invariants $\hat{s}', \hat{t}_1'$, and $\hat{u}_1'$, which can differ from $\hat{s}, \hat{t}_1$, and $\hat{u}_1$ by power corrections that vanish at $s_4 = 0$. For example explicit results for the hard and soft functions can be rewritten employing either the relation $\hat{s}' + \hat{t}_1' + \hat{u}_1' = 0$ or $\hat{s}' + \hat{t}_1' + \hat{u}_1' = s_4$. Although the difference is due to terms suppressed by positive powers of s_4, the two choices produce different numerical results upon integration. We deal with this ambiguity in the same way as in [10].

As in the PIM case, the 1PI hard and soft function are matrices in color space originating from virtual and soft emission corrections, respectively. The hard functions are completely identical to the ones encountered in the PIM kinematics case, provided that the variables $\hat{s}, \hat{t}_1$, and $\hat{u}_1$ are written in terms of M and $\cos\theta$. The soft functions are different in the PIM and 1PI cases, but in both cases they are identical to the ones employed for top-pair production [9, 10].

The 1PI soft functions at order α_s^n depend on plus distributions of the form

$$\left[\frac{\ln^m(s_4/m_{\tilde{t}_1}^2)}{s_4}\right]_+\,, \qquad (m = 1, \cdots, 2n-1)\,. \tag{6.25}$$

The plus distributions employed in 1PI kinematics are defined as follows

$$\int_0^{m_{\tilde{t}_1}^2} ds_4 \left[\frac{\ln^m(s_4/m_{\tilde{t}_1}^2)}{s_4}\right]_+ g(s_4) \equiv \int_0^{m_{\tilde{t}_1}^2} ds_4 \frac{\ln^m(s_4/m_{\tilde{t}_1}^2)}{s_4}\left[g(s_4) - g(0)\right]\,, \tag{6.26}$$

where g is a genetic smooth test function. With this definition, the integral up to a generic upper extreme $s_4^{\max}$ is

$$\int_0^{s_4^{\max}} ds_4 \left[\frac{\ln^m(s_4/m_{\tilde{t}_1}^2)}{s_4}\right]_+ g(s_4) = \int_0^{s_4^{\max}} ds_4 \frac{\ln^m(s_4/m_{\tilde{t}_1}^2)}{s_4}\left[g(s_4) - g(0)\right] + \frac{g(0)}{m+1}\ln^{m+1}\frac{s_4^{\max}}{m_{\tilde{t}_1}^2}\,. \tag{6.27}$$

Therefore, the NLO and NNLO hard scattering kernel in 1PI kinematics have the following structure:

$$
\begin{aligned}
C_{\mathrm{1PI}} &= \alpha_s^2 \left[C_{\mathrm{1PI}}^{(0)} + \frac{\alpha_s}{4\pi} C_{\mathrm{1PI}}^{(1)} + \left(\frac{\alpha_s}{4\pi}\right)^2 C_{\mathrm{1PI}}^{(2)} + \mathcal{O}(\alpha_s^3) \right] , \\
C_{\mathrm{1PI}}^{(1)} &= D_1^{(1,\mathrm{1PI})} \left[\frac{\ln(s_4/m_{\tilde{t}_1}^2)}{s_4} \right]_+ + D_0^{(1,\mathrm{1PI})} \left[\frac{1}{s_4} \right]_+ + C_0^{(1,\mathrm{1PI})} \delta(s_4) + R^{(1,\mathrm{1PI})}(s_4) , \\
C_{\mathrm{1PI}}^{(2)} &= D_3^{(2,\mathrm{1PI})} \left[\frac{\ln^3(s_4/m_{\tilde{t}_1}^2)}{s_4} \right]_+ + D_2^{(2,\mathrm{1PI})} \left[\frac{\ln^2(s_4/m_{\tilde{t}_1}^2)}{s_4} \right]_+ + D_1^{(2,\mathrm{1PI})} \left[\frac{\ln(s_4/m_{\tilde{t}_1}^2)}{s_4} \right]_+ \\
&\quad + D_0^{(2,\mathrm{1PI})} \left[\frac{1}{s_4} \right]_+ + C_0^{(2,\mathrm{1PI})} \delta(s_4) + R^{(2,\mathrm{1PI})}(s_4) .
\end{aligned} \tag{6.28}
$$

As in the PIM case, the NLO coefficients $D_i^{(1)}, C_0^{(1)}, R^{(1)}$ can be in principle obtained from the literature. The functions $R^{(i)}(s_4)$ are finite for $s_4 \to 0$. In this work we are able to derive exact expressions for the NNLO coefficients $D_i^{(2)}$ and the scale-dependent terms in the coefficient $C_0^{(2)}$.

6.3. The Hard and Soft Functions at NLO

In this section we describe the calculation of the hard and soft matrices up to NLO in perturbation theory.

6.3.1. Hard Functions

One of the main results of this thesis is the calculation of the stop-pair production hard functions to NLO.

The hard functions are related to products of Wilson coefficients, as shown in [9,10]. To obtain the Wilson coefficients one matches renormalized Green's functions in SUSY-QCD with those in SCET. The matching can be done with any choice of external states and IR regulators. For simplicity we use on-shell partonic states for the process $(q\bar{q}, gg) \to \tilde{t}_1\tilde{t}_1^*$, and dimensional regularization in $d = 4 - 2\varepsilon$ dimensions to regularize both the ultraviolet (UV) and IR divergences. With this choice it follows that the loop graphs in SCET are scaleless and vanish, so the effective-theory matrix elements are equal to their tree-level expressions multiplied by a UV renormalization matrix $\boldsymbol{Z}$. The matrix elements in SUSY-QCD, on the other hand, are the virtual corrections to the $(q\bar{q}, gg) \to \tilde{t}_1\tilde{t}_1^*$ scattering amplitudes. The matching condition then reads [81–83]

$$
\lim_{\varepsilon \to 0} \boldsymbol{Z}^{-1}(\varepsilon, M, \cos\theta, \mu) \, |\mathcal{M}(\varepsilon, M, \cos\theta)\rangle = \sum_m \langle\!\langle O_m \rangle\!\rangle_{\mathrm{tree}} \, |C_m(M, \cos\theta, \mu)\rangle \ , \tag{6.29}
$$

where $\mathcal{M}$ is the UV-renormalized virtual SUSY-QCD amplitude expressed in terms of α_s with $n_l = 5$ active flavors and $\sum_m \langle\!\langle O_m \rangle\!\rangle_{\text{tree}}$ is the tree-level partonic matrix element in the effective theory summed over the spins m. We have moved the SCET renormalization matrix $\boldsymbol{Z}$ to act on the SUSY-QCD amplitude, so that both sides of the equation are finite in the limit $\varepsilon \to 0$. The explicit results for the matrix elements $\boldsymbol{Z}_{IJ}$ in our color basis for the $q\bar{q}$ and gg channels can be found in [83].

In practice, we are not interested in the Wilson coefficients themselves, but rather in the hard matrix H_{IJ}. To calculate this, we first define

$$|\mathcal{M}_{\text{ren}}\rangle \equiv \lim_{\varepsilon\to 0} \boldsymbol{Z}^{-1}(\varepsilon)\,|\mathcal{M}(\varepsilon)\rangle = 4\pi\alpha_s \left[\left|\mathcal{M}_{\text{ren}}^{(0)}\right\rangle + \frac{\alpha_s}{4\pi} \left|\mathcal{M}_{\text{ren}}^{(1)}\right\rangle + \dots \right], \tag{6.30}$$

where $\mathcal{M}(\varepsilon)$ and $\mathcal{M}_{\text{ren}}$ are the UV-renormalized and the IR and UV finite virtual SUSY-QCD amplitude, respectively. The renormalized amplitude is expressed in terms of α_s with $n_l = 5$ active flavors. The IR renormalization matrix $\boldsymbol{Z}$ can be easily obtained by employing the results found in [83].

The perturbative expansion of the renormalized hard functions is defined as

$$\boldsymbol{H}_{ij} = \alpha_s^2 \frac{1}{d_R} \left(\boldsymbol{H}_{ij}^{(0)} + \frac{\alpha_s}{4\pi} \boldsymbol{H}_{ij}^{(1)} + \dots \right), \tag{6.31}$$

where $d_R = N$ in the quark annihilation channel and $d_R = N^2 - 1$ in the gluon fusion channel. The matrix elements can be written in terms of the renormalized SUSY-QCD amplitudes and the color basis states c_I as follows:

$$\begin{aligned}
H_{IJ}^{(0)} &= \frac{1}{4} \frac{1}{\langle c_I | c_I \rangle \langle c_J | c_J \rangle} \left\langle c_I \,\middle|\, \mathcal{M}_{\text{ren}}^{(0)} \right\rangle \left\langle \mathcal{M}_{\text{ren}}^{(0)} \,\middle|\, c_J \right\rangle , \\
H_{IJ}^{(1)} &= \frac{1}{4} \frac{1}{\langle c_I | c_I \rangle \langle c_J | c_J \rangle} \left[\left\langle c_I \,\middle|\, \mathcal{M}_{\text{ren}}^{(0)} \right\rangle \left\langle \mathcal{M}_{\text{ren}}^{(1)} \,\middle|\, c_J \right\rangle + \left\langle c_I \,\middle|\, \mathcal{M}_{\text{ren}}^{(1)} \right\rangle \left\langle \mathcal{M}_{\text{ren}}^{(0)} \,\middle|\, c_J \right\rangle \right].
\end{aligned} \tag{6.32}$$

The leading-order result for the $q\bar{q}$ channel follows from the color decomposition of a single diagram in Fig. (6.3.1) interfered with its color-decomposed complex conjugate diagram, and it reads

$$\boldsymbol{H}_{q\bar{q}}^{(0)} = \begin{pmatrix} 0 & 0 \\ 0 & 2 \end{pmatrix} \frac{1}{\hat{t}_1 + \hat{u}_1} \left[\frac{\hat{t}_1 \hat{u}_1}{\hat{t}_1 + \hat{u}_1} + m_{\tilde{t}_1}^2 \right]. \tag{6.33}$$

For the gg channel we have to color-decompose the diagrams in Fig. (6.3.1) and interfere them with their color-decomposed complex conjugate diagrams, we find

$$\boldsymbol{H}_{gg}^{(0)} = \begin{pmatrix} \frac{1}{N^2} & \frac{1}{N}\frac{\hat{t}_1-\hat{u}_1}{M^2} & \frac{1}{N} \\ \frac{1}{N}\frac{\hat{t}_1-\hat{u}_1}{M^2} & \frac{(\hat{t}_1-\hat{u}_1)^2}{M^4} & \frac{\hat{t}_1-\hat{u}_1}{M^2} \\ \frac{1}{N} & \frac{\hat{t}_1-\hat{u}_1}{M^2} & 1 \end{pmatrix} \frac{m_{\tilde{t}_1}^4}{2\hat{t}_1\hat{u}_1} \left[-\frac{2M^2}{m_{\tilde{t}_1}^2} + \frac{\hat{t}_1\hat{u}_1}{m_{\tilde{t}_1}^4} + 4 + 2\frac{\hat{t}_1^2 + \hat{u}_1^2}{\hat{t}_1\hat{u}_1} \right], \tag{6.34}$$

where $N = 3$.

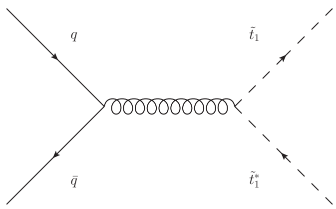

Figure 6.1.: Diagram in the $q\bar{q}$ channel contributing to the hard function matrix at LO.

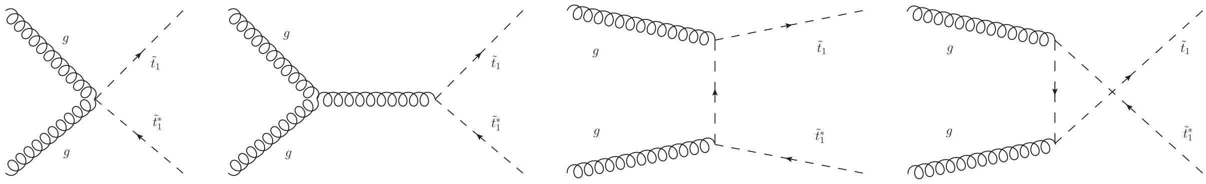

Figure 6.2.: Diagrams in the gg channel contributing to the hard function matrix at LO.

In order to calculate the NLO hard functions, one needs to evaluate the one-loop virtual corrections to the partonic scattering amplitudes, decomposed into the singlet-octet color bases. Although results for one-loop diagrams interfered with the Born-level amplitudes are known [18] and with some work it is possible to extract this information from the `Prospino` code [18], the one-loop amplitude decomposed into color bases is not available and must be calculated from scratch. We used the program `Qgraf` [84] to generate the list of diagrams for stop-pair production both in the quark-antiquark channel and in the gluon-gluon channel. By considering the first two families of squarks and the bottom squarks as mass degenerate we found 40 diagrams in the quark-antiquark channel, 152 diagrams in the gluon-gluon channel and 30 diagrams in the ghost-antighost channel. This last set of diagrams is not necessary for the computation itself but it was used as a check for the cancellation of the unphysical polarizations of the initial state gluons. Since `Qgraf` has some known problems dealing with Majorana fermions, and in particular in our case with gluinos, we had to correct some relative signs between diagrams and give the correct prescription to close the fermionic traces involving gluinos. We followed the prescriptions discussed in [85], [86].

We wrote our in-house routines in the computer language `FORM` [87] and through all the calculation we used the Pauli-Veltman metric and the conventions for the Feynman rules given in [88] adapted to the SUSY case. The calculation was carried out in the following steps both for the $q\bar{q}$ and the gg channels.

- We substituted the SUSY-QCD Feynman rules in the one-loop and in the tree level complex conjugate amplitudes.
- We color-decomposed the one-loop amplitude and we interfered it with the color-decomposed complex conjugate tree-level amplitude, then we added the hermitian

conjugate as described in Eq. (6.32).

- We computed the Dirac and color structures by means of some ad hoc routines.
- We adjusted the routing of the momenta in the single diagrams by making some translations of the loop momentum in order to match the routing of the box topologies subsectors and to use the reductions for those cases.
- We identified the diagrams with a $t_1 \leftrightarrow u_1$ or a $s \leftrightarrow u_1, t_1$ symmetry in order to use the same reduction tables for the direct and crossed diagrams.
- We generated the tensor reduction tables by using the program `Reduze` [89, 90], and we inserted the reductions to scalar integrals in our `FORM` routines.
- Then we inserted all the divergent scalar integrals analytically in order to have the full control over the UV and IR poles of our expressions,
- for simplicity we wrote the finite parts of a small set of scalar integrals depending on several different masses in terms of finite Passarino Veltman functions [91], they were later evaluated numerically by employing one of the programs presented in [92–94].
- We renormalized the UV divergences by using the renormalization constants[1] collected in Appendix A.7.
- We analytic continued our scalar integrals in the relevant physical region.
- Finally, we verified the cancellation of the IR poles by applying the IR-renormalization factor $\boldsymbol{Z}$ as described in Eq. (6.30) and we obtained a finite result for the hard function matrices at NLO.

We checked our results in several ways. The first non trivial check concerns the cancellation of IR divergences that we have just mentioned above. Second, we checked that by multiplying the one-loop hard functions by the corresponding tree-level soft functions and by subsequently taking the trace of the resulting color space matrix, we match the numerical results for the NLO virtual corrections which can be extracted from the code `Prospino` [74].

Unfortunately the outputs of our `FORM` codes are very long due to the several different scales involved. For this reason we do not type them here, but they are available upon request from the author. We also wrote a Fortran code which allows one to evaluate rapidly the hard functions in any physical kinematic configuration and for any value of the input parameters. The hard functions turned out to depend on 8 independent variables: the kinematic quantities M and $\cos\theta$, the SUSY mass parameters $m_{\tilde{t}_1}$, $m_{\tilde{t}_2}$, $m_{\tilde{q}}$, $m_{\tilde{g}}$, the $m_{\tilde{t}_1} - m_{\tilde{t}_2}$ mixing angle α defined in Eq. (2.107) and the top mass m_t.

[1] To the best of our knowledge, we didn't find in the literature the explicit expressions of all the renormalization constants needed to renormalize the stop-pair production process, therefore for convenience we provide them in Appendix A.7.

6.3.2. Soft Functions

The soft functions are vacuum expectation values of soft Wilson-loop operators. These functions are not sensitive to the spin of the particles involved, but they depend on the color structure of the process. Consequently, the soft functions needed for the calculation of the stop-pair production are precisely the same functions employed in the calculation of the top-pair production. The calculation of the PIM soft function is described in [9], while the calculation of the 1PI soft function is carried out in [10]. For convenience, the explicit results for the soft function obtained in those two paper are collected in Appendix A.8.

6.4. RG Equations for Hard and Soft Functions

By employing the Laplace transformed soft functions given in Appendix A.8, we can define the Laplace transformed hard scattering kernels as

$$\begin{aligned} \tilde{c}_{\text{PIM}}\left(\partial_\eta, M, \cos\theta, \mu\right) &= \text{Tr}[\boldsymbol{H}\left(M, \cos\theta, \mu\right) \tilde{\boldsymbol{s}}_{\text{PIM}}\left(\partial_\eta, M, \cos\theta, \mu\right)] \,, \\ \tilde{c}_{\text{1PI}}\left(\partial_\eta, \hat{s}', \hat{t}_1', \hat{u}_1', \mu\right) &= \text{Tr}[\boldsymbol{H}\left(\hat{s}', \hat{t}_1', \hat{u}_1', \mu\right) \tilde{\boldsymbol{s}}_{\text{1PI}}\left(\partial_\eta, \hat{s}', \hat{t}_1', \hat{u}_1', \mu\right)] \,, \end{aligned} \tag{6.35}$$

where ∂_η is a differential operator with respect to the auxiliary variable η. The hard scattering kernels in momentum space can be recovered through the relations

$$\begin{aligned} C_{\text{PIM}}\left(z, M, \cos\theta, \mu\right) &= \tilde{c}_{\text{PIM}}\left(\partial_\eta, M, \cos\theta, \mu\right) \left(\frac{M}{\mu}\right)^{2\eta} \frac{e^{-2\gamma_E \eta}}{\Gamma\left(2\eta\right)} \frac{z^{-\eta}}{(1-z)^{1-2\eta}} \Bigg|_{\eta=0} \,, \\ C_{\text{1PI}}\left(s_4, \hat{s}', \hat{t}_1', \hat{u}_1', \mu\right) &= \tilde{c}_{\text{1PI}}\left(\partial_\eta, \hat{s}', \hat{t}_1', \hat{u}_1', \mu\right) \frac{e^{-2\gamma_E \eta}}{\Gamma\left(2\eta\right)} \frac{1}{s_4} \left(\frac{s_4}{\sqrt{m_{\tilde{t}_1}^2 + s_4 \mu}}\right)^{2\eta} \Bigg|_{\eta=0} \,. \end{aligned} \tag{6.36}$$

In order to evaluate the above formulas one needs to take the derivatives with respect to η, and finally take the limit for $\eta \to 0$. It is possible to show that this procedure is equivalent to consider the quantities $\tilde{c}_{\text{i}}\left(L, \cdots\right)$ (i =PIM, 1PI) and operate the following replacements: in PIM kinematics

$$\begin{aligned} 1 &\to \delta(1-z) \,, \\ L &\to 2P_0'(z) + \delta(1-z) \ln\left(\frac{M^2}{\mu^2}\right) \,, \\ L^2 &\to 4P_1'(z) + \delta(1-z) \ln^2\left(\frac{M^2}{\mu^2}\right) \,, \\ L^3 &\to 6P_2'(z) - 4\pi^2 P_0'(z) + \delta(1-z) \left[\ln^3\left(\frac{M^2}{\mu^2}\right) + 4\zeta_3\right] \,, \end{aligned}$$

$$L^4 \to 8P'_3(z) - 16\pi^2 P'_1(z) + 128\zeta_3 P'_0(z) + \delta(1-z)\left[\ln^4\left(\frac{M^2}{\mu^2}\right) + 16\zeta_3 \ln\left(\frac{M^2}{\mu^2}\right)\right], \tag{6.37}$$

where the distributions $P'_n(z)$ are defined as

$$P'_n(z) = \left[\frac{1}{1-z}\ln^n\left(\frac{M^2(1-z)^2}{\mu^2 z}\right)\right]_+ , \tag{6.38}$$

and are related to the standard plus distributions

$$P_n(z) = \left[\frac{\ln^n(1-z)}{1-z}\right]_+ , \tag{6.39}$$

by the equation

$$\begin{aligned} P'_n(z) = \sum_{k=0}^{n} \binom{n}{k} \ln^{n-k}\left(\frac{M^2}{\mu^2}\right) \Bigg[& 2^k P_k(z) \\ & + \sum_{j=0}^{k-1} \binom{k}{j} 2^j (-1)^{k-j} \left(\frac{\ln^j(1-z)\ln^{k-j} z}{1-z} - \delta(1-z)\int_0^1 dx \frac{\ln^j(1-x)\ln^{k-j} x}{1-x}\right)\Bigg] . \end{aligned} \tag{6.40}$$

In 1PI kinematics instead, one needs the following set of replacements to go from $\tilde{c}_{\rm 1PI}$ to $C_{\rm 1PI}$

$$\begin{aligned} 1 &\longrightarrow \delta(s_4) , \\ L &\longrightarrow 2P_0(s_4) - \delta(s_4)\, L_m , \\ L^2 &\longrightarrow 8P_1(s_4) - 4L_m P_0(s_4) + \delta(s_4)\left(L_m^2 - \frac{2\pi^2}{3}\right) - \frac{4L_4}{s_4} , \\ L^3 &\longrightarrow 24P_2(s_4) - 24 L_m P_1(s_4) + \left(6L_m^2 - 4\pi^2\right) P_0(s_4) + \delta(s_4)\left(-L_m^3 + 2\pi^2 L_m + 16\zeta_3\right) \\ &\quad - \frac{6L_4}{s_4}\left[-L_4 + 2\ln\frac{s_4^2}{m_{\tilde{t}_1}^2\mu^2}\right] , \\ L^4 &\longrightarrow 64P_3(s_4) - 96L_m P_2(s_4) + \left(48L_m^2 - 32\pi^2\right) P_1(s_4) + \left(-8L_m^3 + 16\pi^2 L_m + 128\zeta_3\right) P_0(s_4) \\ &\quad + \delta(s_4)\left(L_m^4 - 4\pi^2 L_m^2 - 64\zeta_3 L_m + \frac{4\pi^4}{15}\right) \\ &\quad - \frac{8L_4}{s_4}\left[L_4^2 - 3L_4 \ln\frac{s_4^2}{m_{\tilde{t}_1}^2\mu^2} + 3\ln^2\frac{s_4^2}{m_{\tilde{t}_1}^2\mu^2} - 2\pi^2\right] , \end{aligned} \tag{6.41}$$

where $L_m = \ln(\mu^2/m_{\tilde{t}_1}^2)$ and $L_4 = \ln(1 + s_4/m_{\tilde{t}_1}^2)$.

Since the hard and soft functions are known up to NLO, is easy to determine the NLO coefficient in the expansion of $\tilde{c}$ in powers of α_s: suppressing the arguments and subscripts one has

$$\tilde{c} = \alpha_s^2 \left[\tilde{c}^{(0)} + \frac{\alpha_s}{4\pi} \tilde{c}^{(1)} + \left(\frac{\alpha_s}{4\pi} \right)^2 \tilde{c}^{(2)} + \mathcal{O}(\alpha_s^3) \right] , \tag{6.42}$$

where

$$\tilde{c}^{(0)} = \text{Tr} \left[\boldsymbol{H}^{(0)} \tilde{\boldsymbol{s}}^{(0)} \right] , \qquad \tilde{c}^{(1)} = \text{Tr} \left[\boldsymbol{H}^{(0)} \tilde{\boldsymbol{s}}^{(1)} \right] + \text{Tr} \left[\boldsymbol{H}^{(1)} \tilde{\boldsymbol{s}}^{(0)} \right] = \sum_{j=0}^{2} c_j^{(1)} L^j . \tag{6.43}$$

It is important to observe that the trace of the product of the LO hard functions and NLO soft functions contains the dependence of $c^{(1)}$ on L, and therefore it gives rise to the plus distributions.

In order to obtain the coefficient $\tilde{c}^{(2)}$ one needs to know the hard and soft functions at NNLO:

$$\tilde{c}^{(2)} = \text{Tr} \left[\boldsymbol{H}^{(0)} \tilde{\boldsymbol{s}}^{(2)} \right] + \text{Tr} \left[\boldsymbol{H}^{(1)} \tilde{\boldsymbol{s}}^{(1)} \right] + \text{Tr} \left[\boldsymbol{H}^{(2)} \tilde{\boldsymbol{s}}^{(0)} \right] = \sum_{j=0}^{4} c_j^{(2)} L^j . \tag{6.44}$$

The coefficients $c_i^{(2)}$ $(i = 1, \cdots, 4)$ and the scale dependent part of $c_0^{(2)}$ can be reconstructed by exploiting the information coming from the RG equations satisfied by the hard and soft functions.

The hard functions satisfy a RG equation of the form

$$\frac{d}{d \ln \mu} \boldsymbol{H} = \boldsymbol{\Gamma}_H \boldsymbol{H} + \boldsymbol{H} \boldsymbol{\Gamma}_H^\dagger . \tag{6.45}$$

In Eq. (6.45) the arguments of the function $\boldsymbol{H}$ and of the anomalous dimension matrix $\boldsymbol{\Gamma}_H$ are $M, \cos\theta$, and μ in the PIM case and $\hat{s}', \hat{t}_1', \hat{u}_1'$, and μ in the 1PI case. The matrices $\boldsymbol{\Gamma}_H$ were derived in [83], provided that one expresses the Mandelstam invariants in terms of M and $\cos\theta$ in PIM kinematics, and $\hat{s}', \hat{t}_1'$ and $\hat{u}_1'$ in 1PI kinematics. For completeness we provide the expressions up to two loop order for the anomalous dimensions matrices $\boldsymbol{\Gamma}_H$ (written in the PIM variables), both for the quark annihilation and gluon fusion channels. Their expressions can be found in [9] and they read:

$$\begin{aligned}
\boldsymbol{\Gamma}_{q\bar{q}} = & \left[C_F \, \gamma_{\text{cusp}}(\alpha_s) \left(\ln \frac{M^2}{\mu^2} - i\pi \right) + C_F \, \gamma_{\text{cusp}}(\beta_{34}, \alpha_s) + 2\gamma^q(\alpha_s) + 2\gamma^Q(\alpha_s) \right] \mathbf{1} \\
& + \frac{N}{2} \left[\gamma_{\text{cusp}}(\alpha_s) \left(\ln \frac{\hat{t}_1^2}{M^2 m_{\tilde{t}_1}^2} + i\pi \right) - \gamma_{\text{cusp}}(\beta_{34}, \alpha_s) \right] \begin{pmatrix} 0 & 0 \\ 0 & 1 \end{pmatrix} \\
& + \gamma_{\text{cusp}}(\alpha_s) \, \ln \frac{\hat{t}_1^2}{\hat{u}_1^2} \left[\begin{pmatrix} 0 & \frac{C_F}{2N} \\ 1 & -\frac{1}{N} \end{pmatrix} + \frac{\alpha_s}{4\pi} \, g(\beta_{34}) \begin{pmatrix} 0 & \frac{C_F}{2} \\ -N & 0 \end{pmatrix} \right] ,
\end{aligned} \tag{6.46}$$

and

$$
\begin{aligned}
\mathbf{\Gamma}_{gg} = & \left[N\,\gamma_{\text{cusp}}(\alpha_s) \left(\ln \frac{M^2}{\mu^2} - i\pi \right) + C_F\,\gamma_{\text{cusp}}(\beta_{34},\alpha_s) + 2\gamma^g(\alpha_s) + 2\gamma^Q(\alpha_s) \right] \mathbf{1} \\
& + \frac{N}{2} \left[\gamma_{\text{cusp}}(\alpha_s) \left(\ln \frac{\hat{t}_1^2}{M^2 m_{\tilde{t}_1}^2} + i\pi \right) - \gamma_{\text{cusp}}(\beta_{34},\alpha_s) \right] \begin{pmatrix} 0 & 0 & 0 \\ 0 & 1 & 0 \\ 0 & 0 & 1 \end{pmatrix} \\
& + \gamma_{\text{cusp}}(\alpha_s)\, \ln \frac{\hat{t}_1^2}{\hat{u}_1^2} \left[\begin{pmatrix} 0 & \frac{1}{2} & 0 \\ 1 & -\frac{N}{4} & \frac{N^2-4}{4N} \\ 0 & \frac{N}{4} & -\frac{N}{4} \end{pmatrix} + \frac{\alpha_s}{4\pi}\, g(\beta_{34}) \begin{pmatrix} 0 & \frac{N}{2} & 0 \\ -N & 0 & 0 \\ 0 & 0 & 0 \end{pmatrix} \right] ,
\end{aligned} \tag{6.47}
$$

where the various anomalous dimension functions can be found in the Appendix A.5, and the cusp angle $\beta_{34} = i\pi - \ln(1+\beta_{\tilde{t}_1})/(1-\beta_{\tilde{t}_1})$.

By employing the same notation of [9, 10], one can split the anomalous dimension up to two loop orders as follows

$$
\begin{aligned}
\mathbf{\Gamma}_H^{\text{PIM}}\left(M,\cos\theta,\alpha_s\right) &= \Gamma_{\text{cusp}}(\alpha_s) \left(\ln \frac{M^2}{\mu^2} - i\pi \right) + \boldsymbol{\gamma}^h\left(M,\cos\theta,\alpha_s\right) , \\
\mathbf{\Gamma}_H^{\text{1PI}}\left(\hat{s}',\hat{t}_1',\hat{u}'_1,\alpha_s\right) &= \Gamma_{\text{cusp}}(\alpha_s) \left(\ln \frac{\hat{s}'}{\mu^2} - i\pi \right) + \boldsymbol{\gamma}^h\left(\hat{s}',\hat{t}_1',\hat{u}_1',\alpha_s\right) ,
\end{aligned} \tag{6.48}
$$

where Γ_{cusp} is equal $C_F\gamma_{\text{cusp}}$ in the quark annihilation channel and $C_A\gamma_{\text{cusp}}$ in the gluon fusion channel; γ_{cusp} represents the universal cusp anomalous dimension. The matrices $\boldsymbol{\gamma}^h$ are defined through a direct comparison with Eq. (6.46) and Eq. (6.47).

By knowing the evolution equation of the hard functions and of the PDFs, and by employing the scale invariance of the cross section, it is possible to derive the RG equation satisfied by the soft function matrices. In PIM kinematics one finds [9]

$$
\begin{aligned}
\frac{d}{d\ln\mu} \tilde{\boldsymbol{s}}_{\text{PIM}} \left(\ln \frac{M^2}{\mu^2}, M, \cos\theta, \mu \right) = & \mathbf{\Gamma}_{s\text{PIM}}^{\dagger} \tilde{\boldsymbol{s}}_{\text{PIM}} \left(\ln \frac{M^2}{\mu^2}, M, \cos\theta, \mu \right) \\
& + \tilde{\boldsymbol{s}}_{\text{PIM}} \left(\ln \frac{M^2}{\mu^2}, M, \cos\theta, \mu \right) \mathbf{\Gamma}_{s\text{PIM}} .
\end{aligned} \tag{6.49}
$$

In the equation above the soft anomalous dimension $\mathbf{\Gamma}_{s\text{PIM}}$ is given by

$$
\tilde{\mathbf{\Gamma}}_{s\text{PIM}} = - \left[\Gamma_{\text{cusp}}(\alpha_s) \ln \frac{M^2}{\mu^2} + 2\gamma^{\phi}\left(\alpha_s\right) \right] \mathbf{1} - \boldsymbol{\gamma}^h\left(M,\cos\theta,\alpha_s\right) . \tag{6.50}
$$

In the equation above, the PDF anomalous dimension γ^{ϕ} is defined through the large x limit of the Altarelli-Parisi splitting functions

$$
P(x) = 2\Gamma_{\text{cusp}}(\alpha_s) \left[\frac{1}{1-x} \right]_+ + 2\gamma^{\phi}(\alpha_s)\delta(1-x) . \tag{6.51}
$$

$\hat{s}$	9.0×10^6 GeV^2	$m_{\tilde{t}_2}$	1319.87 GeV
$\hat{t}_1$	-2.94979×10^6 GeV^2	$m_{\tilde{q}}$	1460.3 GeV
μ	1087.17 GeV	m_t	173.3 GeV
$m_{\tilde{t}_1}$	1087.17 GeV	α	68.4°
$m_{\tilde{g}}$	1489.98 GeV		

Table 6.1.: Values of the input parameters employed to calculate the coefficients found in Eqs. (6.54), (6.55), (6.57), (6.58). The angle α is the stop mixing angle. The SUSY mass parameters and the stop mixing angle reported in this table refer to the benchmark point 40.2.5 in [95].

In 1PI kinematic, the Laplace transformed soft function matrices obey the following evolution equation [10]

$$\frac{d}{d\ln\mu}\tilde{\boldsymbol{s}}_{1\text{PI}}\left(\ln\frac{\hat{s}'}{\mu^2},\hat{s}',\hat{t}_1',\hat{u}_1',\mu\right) = \boldsymbol{\Gamma}^{\dagger}_{s1\text{PI}}\tilde{\boldsymbol{s}}_{1\text{PI}}\left(\ln\frac{\hat{s}'}{\mu^2},\hat{s}',\hat{t}_1',\hat{u}_1',\mu\right) + \tilde{\boldsymbol{s}}_{1\text{PI}}\left(\ln\frac{\hat{s}'}{\mu^2},\hat{s}',\hat{t}_1',\hat{u}_1',\mu\right)\boldsymbol{\Gamma}_{s1\text{PI}}\,, \tag{6.52}$$

where

$$\tilde{\boldsymbol{\Gamma}}_{s1\text{PI}} = -\left[\Gamma_{\text{cusp}}\ln\frac{\hat{s}'}{\mu^2} + 2\gamma^{\phi}(\alpha_s) + \Gamma_{\text{cusp}}(\alpha_s)\log\frac{\hat{s}' m_{\tilde{t}_1}^2}{\hat{t}_1'\hat{u}_1'}\right]\mathbf{1} - \boldsymbol{\gamma}^h\left(\hat{s}',\hat{t}_1',\hat{u'}_1,m_{\tilde{t}_1},\alpha_s\right). \tag{6.53}$$

If the one-loop hard and soft matrices, evolution equations, and anomalous dimensions are known, it is possible to calculate the coefficients of the positive powers of L in the expansion in Eq. (6.44) as well as in principle the scale dependent parts of the coefficient proportional to L^0.

6.5. Approximate NNLO Formulas

By employing the results described in the previous sections it is possible to obtain approximate NNLO formulas including the exact expressions of the coefficients multiplying the plus distributions up to NNLO, both in PIM and in 1PI kinematics. The values of the coefficients multiplying the various plus distributions and delta functions for arbitrary values of the input parameters can be extracted from the Fortran code mentioned above. For convenience, we include here the values of these coefficients, evaluated for the input parameters listed in Table 6.1. The SUSY spectrum appearing there correspond to the benchmark point 40.2.5 in [95], which we use in the rest of our analysis as well. By defining $\hat{C}^{(i)} = d_R C^{(i)}$ $(i = 0, 1, 2)$, in the quark annihilation channel with PIM kinematics one finds

$$\begin{aligned}
\hat{C}^{(0)}_{\text{PIM},q\bar{q}}(z) &= 0.118673\,\delta(1-z)\,, \\
\hat{C}^{(1)}_{\text{PIM},q\bar{q}}(z) &= 2.53170\left[\frac{\ln(1-z)}{1-z}\right]_+ + 1.18594\left[\frac{1}{1-z}\right]_+ + 0.834825\,\delta(1-z) + \ldots\,, \\
\hat{C}^{(2)}_{\text{PIM},q\bar{q}}(z) &= 27.0048\left[\frac{\ln^3(1-z)}{1-z}\right]_+ + 18.5403\left[\frac{\ln^2(1-z)}{1-z}\right]_+ - 56.3923\left[\frac{\ln(1-z)}{1-z}\right]_+ \\
&\quad + 62.2067\left[\frac{1}{1-z}\right]_+ - 29.5324\,\delta(1-z) + \ldots\,,
\end{aligned} \tag{6.54}$$

where the ellipses indicate terms which are subleading (and finite) in the $z \to 1$ limit. In the gluon fusion channel one finds instead

$$\begin{aligned}
\hat{C}^{(0)}_{\text{PIM},gg}(z) &= 0.348572\,\delta(1-z)\,, \\
\hat{C}^{(1)}_{\text{PIM},gg}(z) &= 16.7315\left[\frac{\ln(1-z)}{1-z}\right]_+ + 13.6194\left[\frac{1}{1-z}\right]_+ + 9.50848\,\delta(1-z) + \ldots\,, \\
\hat{C}^{(2)}_{\text{PIM},gg}(z) &= 401.555\left[\frac{\ln^3(1-z)}{1-z}\right]_+ + 852.324\left[\frac{\ln^2(1-z)}{1-z}\right]_+ - 389.724\left[\frac{\ln(1-z)}{1-z}\right]_+ \\
&\quad + 535.481\left[\frac{1}{1-z}\right]_+ + 81.9942\,\delta(1-z) + \ldots\,.
\end{aligned} \tag{6.55}$$

It is important to remark that, in order to determine completely the coefficients multiplying the plus distributions in $C^{(2)}_{ij,k}$ $(k \in \{\text{PIM}, \text{1PI}\})$, it is sufficient to know the anomalous dimension regulating the RG equations for the hard and soft matrices at NNLO and the hard and the soft function matrices at NLO. On the contrary, in order to completely determine the coefficients multiplying the Dirac delta functions in the NNLO hard scattering kernels, one would need to know the complete NNLO hard and soft matrices. Since those matrices are know only at NLO, the cofactors of the delta functions at NNLO include only the scale dependent terms. However, since the scale independent part of those coefficients is unknown, the cofactor of the delta functions at NNLO in Eq. (6.54) and in the equations below depend on an arbitrary second scale chosen to normalize the scale logarithms. In fact, for any renormalization scale μ and normalization scale μ_0 one can always rewrite

$$\ln\left(\frac{\mu_0^2}{\mu^2}\right) = \ln\left(\frac{\mu_1^2}{\mu^2}\right) + \ln\left(\frac{\mu_0^2}{\mu_1^2}\right)\,, \tag{6.56}$$

where the second term can be reabsorbed in the unknown renormalization scale independent piece. Since adding these additional μ-dependent terms one run the risk to artificially reduce the scale dependence, in Eq. (6.54) and Eq. (6.55) above, and for the 1PI kinematics as well, we drop the contribution from the two loop hard functions, in the same spirit as [10, 96].

Similarly, one finds in 1PI kinematics for the quark annihilation channel

$$
\begin{aligned}
\hat{C}^{(0)}_{1\mathrm{PI},q\bar{q}}(s_4) &= 0.118673\,\delta(s_4)\,,\\
\hat{C}^{(1)}_{1\mathrm{PI},q\bar{q}}(s_4) &= 2.53170\left[\frac{\ln(s_4/m^2_{\tilde{t}_1})}{s_4}\right]_+ - 2.03883\left[\frac{1}{s_4}\right]_+ + 1.66798\,\delta(s_4) + \dots\,,\\
\hat{C}^{(2)}_{1\mathrm{PI},q\bar{q}}(s_4) &= 27.0048\left[\frac{\ln^3(s_4/m^2_{\tilde{t}_1})}{s_4}\right]_+ - 84.6523\left[\frac{\ln^2(s_4/m^2_{\tilde{t}_1})}{s_4}\right]_+ + 34.0042\left[\frac{\ln(s_4/m^2_{\tilde{t}_1})}{s_4}\right]_+\\
&\quad + 98.7353\left[\frac{1}{s_4}\right]_+ - 166.272\,\delta(s_4) + \dots\,,
\end{aligned}
\tag{6.57}
$$

while for the gluon fusion channel one finds

$$
\begin{aligned}
\hat{C}^{(0)}_{1\mathrm{PI},gg}(s_4) &= 0.348572\,\delta(s_4)\,,\\
\hat{C}^{(1)}_{1\mathrm{PI},gg}(s_4) &= 16.7315\left[\frac{\ln(s_4/m^2_{\tilde{t}_1})}{s_4}\right]_+ - 7.69240\left[\frac{1}{s_4}\right]_+ + 7.68986\,\delta(s_4) + \dots\,,\\
\hat{C}^{(2)}_{1\mathrm{PI},gg}(s_4) &= 401.555\left[\frac{\ln^3(s_4/m^2_{\tilde{t}_1})}{s_4}\right]_+ - 682.128\left[\frac{\ln^2(s_4/m^2_{\tilde{t}_1})}{s_4}\right]_+ - 512.616\left[\frac{\ln(s_4/m^2_{\tilde{t}_1})}{s_4}\right]_+\\
&\quad + 1511.18\left[\frac{1}{s_4}\right]_+ - 1299.25\,\delta(s_4) + \dots\,.
\end{aligned}
\tag{6.58}
$$

In this context, the ellipses indicate subleading terms in the $s_4 \to 0$ limit. Also in Eqs. (6.57, 6.58), as in the PIM case, we drop the contribution of the two-loop hard functions.

6.6. Total Cross Section

In this section we present a numerical study of the stop-pair production total cross section at approximate NNLO accuracy.

To begin our analysis we describe in detail how we deal with the ambiguities due to power suppressed terms related to 1PI kinematics. As we pointed out in Subsection 6.2.2, there are power-suppressed ambiguities in the choice of the variables $\hat{s}'$, $\hat{t}'_1$ and $\hat{u}'_1$ of the hard and soft functions. In the perturbative calculation of the hard and soft functions one can set $s_4 = 0$ everywhere and use $\hat{s}' + \hat{t}'_1 + \hat{u}'_1 = 0$ to rewrite the hard-scattering kernels in several different forms. These rewritings are all formally equivalent in the limit $s_4 \to 0$, but they affect the functional dependence of the hard-scattering kernels on x_1 and x_2. Therefore the numerical integration in (6.20) gives different results for the pieces multiplying the plus-distributions in s_4. Another obvious choice is to use $\hat{s}' + \hat{t}_1' + \hat{u}_1' = s_4$ before integration, again leading to numerically different answers which are equivalent in the threshold limit $s_4 \to 0$.

We use the following procedure to fix this ambiguity. First, we set $\hat{s}' + \hat{t}_1' + \hat{u}_1' = 0$ in the hard-scattering kernels, and we use this to eliminate either $\hat{t}_1'$ or $\hat{u}_1'$ as an independent variable. We then define the two cross sections

$$\frac{d^2\sigma^t}{dp_T dy} = \frac{2\pi p_T}{s} \sum_{i,j} \int_{-u_1/(s+t_1)}^{1} \frac{dx_1}{x_1} \int_0^{x_1(s+t_1)+u_1} \frac{ds_4}{s_4 - x_1 t_1} \times f_{i/N_1}(x_1,\mu_f)\, f_{j/N_2}(x_2(s_4),\mu_f)\, C_{ij}(s_4,\hat{s}',\hat{t}_1',-\hat{s}'-\hat{t}_1',m_t,\mu_f)\,, \tag{6.59}$$

$$\frac{d^2\sigma^u}{dp_T dy} = \frac{2\pi p_T}{s} \sum_{i,j} \int_{-t_1/(s+u_1)}^{1} \frac{dx_2}{x_2} \int_0^{x_2(s+u_1)+t_1} \frac{ds_4}{s_4 - x_2 u_1} \times f_{i/N_1}(x_1(s_4),\mu_f)\, f_{j/N_2}(x_2,\mu_f)\, C_{ij}(s_4,\hat{s}',-\hat{s}'-\hat{u}_1',\hat{u}_1',m_t,\mu_f)\,. \tag{6.60}$$

We have changed variables from x_2 or x_1 to s_4 in the two equations, respectively, by using Eq. (6.4). We find

$$x_1(s_4) = \frac{s_4 - x_2 u_1}{x_2 s + t_1}\,, \quad x_2(s_4) = \frac{s_4 - x_1 t_1}{x_1 s + u_1}\,. \tag{6.61}$$

Finally, we drop all dependence on s_4 in the hard-scattering kernels by using

$$\hat{t}_1' = \hat{t}_1 = x_1 t_1\,, \quad \hat{s}' = x_1 x_2(0) s \tag{6.62}$$

in (6.59), and

$$\hat{u}_1' = \hat{u}_1 = x_2 u_1\,, \quad \hat{s}' = x_1(0) x_2 s \tag{6.63}$$

in (6.60). It is easy to see that with this choice σ^t and σ^u are not necessarily the same, although the difference is power suppressed. We take the average of the two as the final result for the differential cross section:

$$\frac{d^2\sigma}{dp_T dy} = \frac{1}{2}\left[\frac{d^2\sigma^t}{dp_T dy} + \frac{d^2\sigma^u}{dp_T dy}\right]. \tag{6.64}$$

Finally we integrate over the double-differential distribution in Eq. (6.64) to get the total cross section in 1PI kinematics.

We employ PIM_{SCET} and 1PI_{SCET} kinematic schemes described in [96]; these schemes also include, on top of contributions which are singular in the soft limit, NNLO terms which are regular in the $z \to 1$ ($\mathrm{PIM_{SCET}}$) or $s_4 \to 0$ ($\mathrm{1PI_{SCET}}$) limit and which naturally arise from the SCET formalism. Obviously, those terms do not represent the complete part of the NNLO cross section which is regular in the soft limit, since this quantity can only be obtained with a full calculation of this observable at NNLO accuracy. However, as shown in [9,10], the regular terms appearing in the $\mathrm{PIM_{SCET}}$ and $\mathrm{1PI_{SCET}}$ kinematic approach arise from the exact definition of the soft gluon emission energy and they improve the agreement between exact and approximate formulas at NLO.

We present results which are obtained by averaging the ones obtained in the two kinematic schemes that we consider. We also adopt a conservative approach and consider the difference between the predictions in the two kinematic schemes as an estimate of the theoretical uncertainty associated with the use of approximate NNLO formulas. This is justified by the fact that the two schemes neglect different power suppressed terms which are formally subleading but which can nevertheless have a noticeable numerical impact on the total cross section. To account for this uncertainty, the scale variation of the total cross section is obtained by setting the renormalization and factorization scales equal, $\mu_R = \mu_f = \mu$, and by varying this common scale, in both kinematic schemes, between $m_{\tilde{t}_1}/2 < \mu < 2m_{\tilde{t}_1}$. We then look at the difference between the largest and smallest values obtained. In summary, the central value and perturbative uncertainties for the combined results at approximate NNLO accuracy are determined by employing the following definitions

$$
\begin{aligned}
\sigma &= \frac{1}{2}\left(\sigma_{\mathrm{PIM}} + \sigma_{\mathrm{1PI}}\right) , \\
\Delta\sigma^{+} &= \max\left\{\sigma_{\mathrm{PIM}} + \Delta\sigma^{+}_{\mathrm{PIM}}, \sigma_{\mathrm{1PI}} + \Delta\sigma^{+}_{\mathrm{1PI}}\right\} - \sigma , \\
\Delta\sigma^{-} &= \min\left\{\sigma_{\mathrm{PIM}} + \Delta\sigma^{-}_{\mathrm{PIM}}, \sigma_{\mathrm{1PI}} + \Delta\sigma^{-}_{\mathrm{1PI}}\right\} - \sigma ,
\end{aligned} \tag{6.65}
$$

where the subscripts 1PI and PIM indicate that the corresponding quantities are evaluated in $\mathrm{1PI_{SCET}}$ and $\mathrm{PIM_{SCET}}$ kinematics, respectively, including the full set of NLO corrections and the contribution of the NNLO terms present in the approximate formulas for that scheme. Being more explicit, to obtain approximate NNLO results in fixed-order for both PIM and 1PI kinematics, we compute

$$
\sigma_k^{\mathrm{NNLO,\ approx}} = \sigma^{\mathrm{NLO}} + \sigma_k^{(2),\,\mathrm{approx}} \tag{6.66}
$$

where $k \in \{\mathrm{PIM}, \mathrm{1PI}\}$ and $\sigma_k^{(2),\,\mathrm{approx}}$ is the approximate NNLO correction coming from the coefficient $C^{(2)}_{\mathrm{PIM}}$ in Eq. (6.19) for PIM kinematics and from $C^{(2)}_{\mathrm{1PI}}$ in Eq. (6.28) for 1PI.

As it will been shown later, the total cross section is strongly dependent on the mass of the produced particle, $m_{\tilde{t}_1}$. Moreover, similarly to the slepton-pair production case, the dependence of the total cross section on the SUSY parameters other than the mass of the produced particles is relatively small. In order to show this behavior we fix the value of the stop mass equal to $m_{\tilde{t}_1} = 1087.17$ GeV, accordingly to the SUSY benchmark point 40.2.5 in [95], listed in Table 6.1, and we give the predictions for the total cross section for three different sets of the remaining SUSY parameters. The first set of SUSY parameters is the benchmark point 40.2.5. We refer to the second set of SUSY parameters as “double”, where we choose $m_{\tilde{t}_2} = 2639.74$ GeV, $m_{\tilde{q}} = 2920.61$ GeV, $m_{\tilde{g}} = 2979.96$ GeV, $\alpha = 136.8^\circ$ in an arbitrary way as the double of the corresponding values of the benchmark point 40.2.5, the remaining parameters are set equal to the ones in Table 6.1. We refer to the third SUSY set of parameters as “half” where we choose $m_{\tilde{t}_2} = 659.93$ GeV, $m_{\tilde{q}} = 730.15$ GeV, $m_{\tilde{g}} = 744.99$ GeV, $\alpha = 34.2^\circ$. In Table 6.6 we report the values of the total cross sections, with the relative scale uncertainty, for the three different sets of SUSY parameters discussed above. We observe that the numerical values are considerably close to each other nonetheless the input parameters were chosen at the boundaries of very broad intervals.

LHC 14 TeV	MSTW2008	
SUSY point	$m_{\tilde{t}_1}$ [GeV]	1087.17
40.2.5	$(\sigma \pm \Delta\sigma_\mu)_{\mathrm{NLO}}$ [pb]	$44.2^{+4.9}_{-6.0} \times 10^{-4}$
“double”	$(\sigma \pm \Delta\sigma_\mu)_{\mathrm{NLO}}$ [pb]	$44.5^{+5.1}_{-6.1} \times 10^{-4}$
“half”	$(\sigma \pm \Delta\sigma_\mu)_{\mathrm{NLO}}$ [pb]	$42.4^{+4.0}_{-5.4} \times 10^{-4}$
40.2.5	$(\sigma \pm \Delta\sigma_\mu)_{\mathrm{approx.NNLO}}$ [pb]	$44.3^{+1.3}_{-2.2} \times 10^{-4}$
“double”	$(\sigma \pm \Delta\sigma_\mu)_{\mathrm{approx.NNLO}}$ [pb]	$44.7^{+1.3}_{-2.3} \times 10^{-4}$
“half”	$(\sigma \pm \Delta\sigma_\mu)_{\mathrm{approx.NNLO}}$ [pb]	$42.3^{+0.6}_{-1.8} \times 10^{-4}$

Table 6.2.: Stop-pair production cross sections at the LHC 14 TeV for three different sets of the SUSY parameters described in the text. The stop mass is fixed to $m_{\tilde{t}_1} = 1087.17$ GeV. The numbers are obtained by using MSTW2008 PDFs.

From now on in all of the plots and tables we fix the SUSY parameters to the values corresponding to the benchmark point 40.2.5 in Table 6.1. The mass of the lightest stop follows this rule, except in the figures in which we plot the cross section as a function of the stop mass or when a different choice of the stop mass is explicitly indicated.

All of the numbers and plots are obtained by means of an in-house Fortran code in which the approximate NNLO formulas are implemented. The NLO calculations, which are one of the elements needed to obtain predictions at approximate NNLO accuracy, are carried out by modifying the public version of `Prospino` [74].

As a first step, we compare the full NLO cross section with the approximate NLO cross section given by the leading singular terms. In the approximate NLO results we keep all of the terms proportional to $\delta(1-z)$ (PIM$_{\text{SCET}}$) and $\delta(s_4)$ (1PI$_{\text{SCET}}$) which arise from the NLO hard and soft functions. The purpose of this comparison is to establish to what extent the leading terms in the threshold approximation reproduce the full cross section, or, in other words, if the dynamical threshold enhancement of the soft emission region takes place. This comparison is shown in Fig. 6.3, for the case of a hadronic center of mass energy of 8 TeV. The two lines in the figure refer to two different choices of the PDF set. NLO PDFs are employed in all of the four panels. One observes that the average

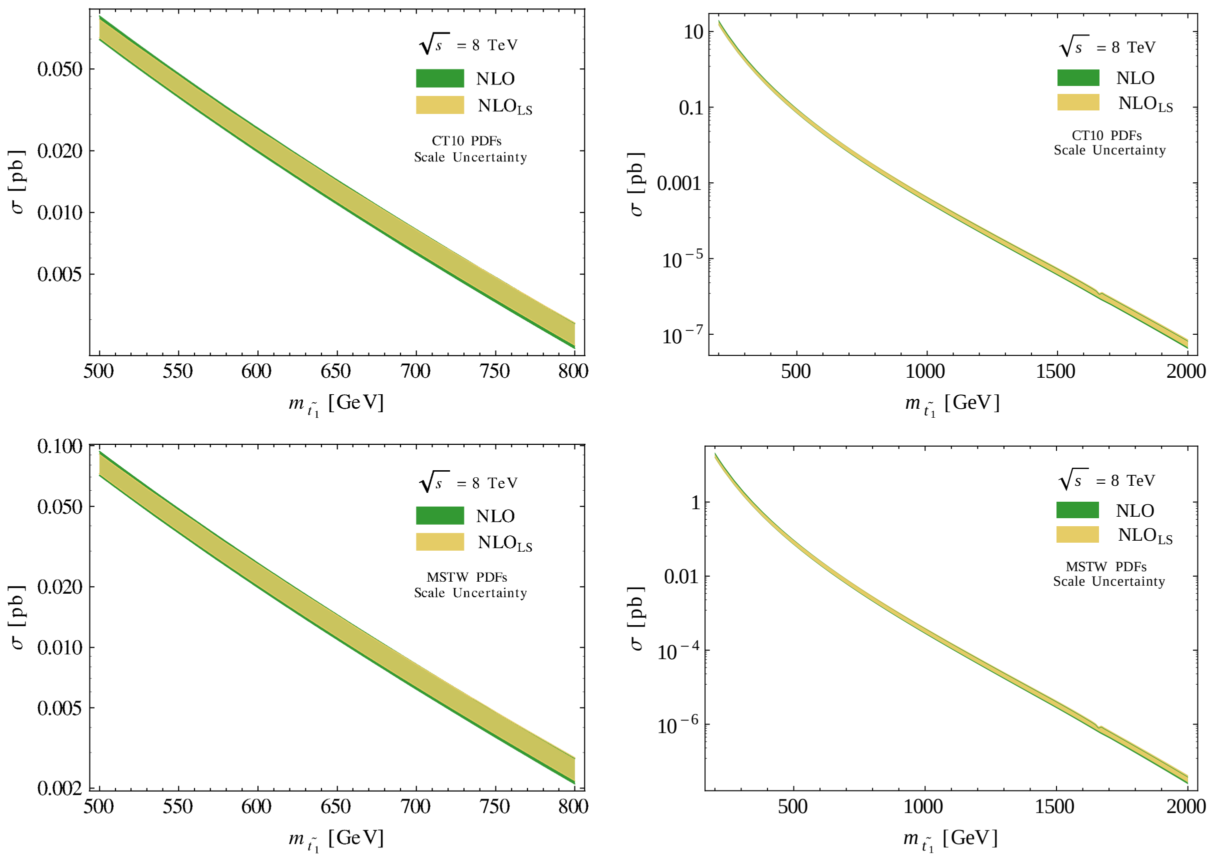

Figure 6.3.: Comparison of the full NLO cross section with the approximate NLO one. All panels refer to the LHC with a hadronic center of mass energy of 8 TeV. The first and second row employ CT10 and MSTW2008 NLO PDFs, respectively. The left and right columns show different ranges in the stop mass.

of the approximate PIM and 1PI NLO formulas reproduces very well the band obtained by varying the factorization scale, put equal to the renormalization scale, in the full NLO result. Similarly, it is reasonable to expect that the approximate NNLO formulas reproduce to a good extent the unknown full NNLO corrections.

We now turn to the discussion of the approximate NNLO results. Before commenting on the approximate NNLO predictions, we recall that the approximate NNLO formulas do not include the terms proportional to the Dirac delta functions with arguments $1-z$ (PIM_{SCET}) or s_4 (1PI_{SCET}) arising from the NNLO hard functions, since the scale independent parts of the NNLO hard functions are unknown.

As expected, the approximate NNLO predictions for the pair production cross section show a smaller scale dependence than the NLO calculations of the same quantity. This is illustrated in Fig. 6.4, where two different LHC center of mass energies (8 TeV and 14 TeV) and two different stop quark masses ($m_{\tilde{t}_1} = 500$ GeV and $m_{\tilde{t}_1} = 1087.17$ GeV)

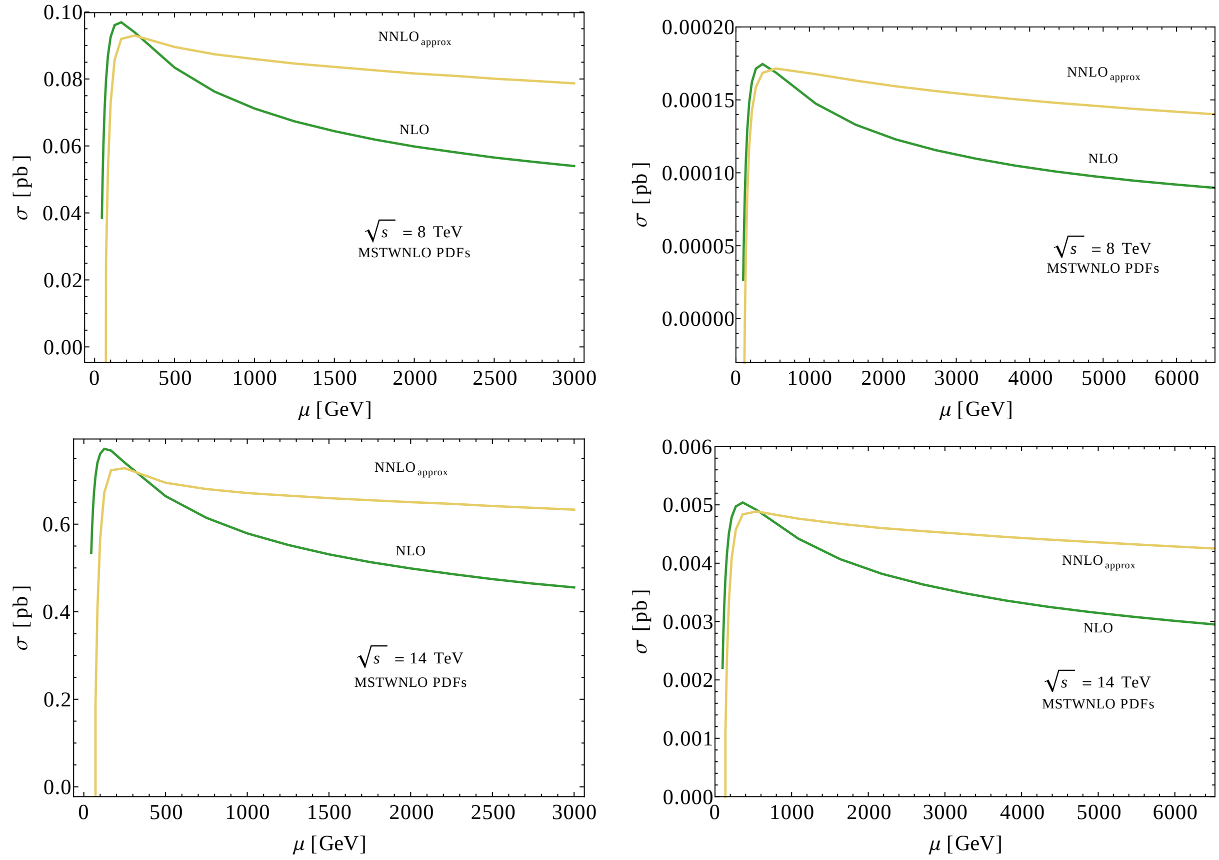

Figure 6.4.: Scale dependence of the NLO and approximate NNLO cross sections. The left panels refer to the production of a top-squark of mass $m_{\tilde{t}_1} = 500$ GeV, the right panels refer to the case $m_{\tilde{t}_1} = 1087.17$ GeV. The two figures in the first row are obtained for LHC at $\sqrt{s} = 8$ TeV, the ones in the second row refer to the case $\sqrt{s} = 14$ TeV. All of the SUSY parameters other than $m_{\tilde{t}_1}$ are fixed at the values of the benchmark point 40.2.5 [95].

are considered. In order to show the effect of the approximate NNLO corrections on the scale dependence, both the NLO and approximate NNLO curves are plotted by using MSTW2008 NLO PDFs. It is important to stress that what is here referred to as approximate NNLO scale uncertainty reflects in reality also a kinematic scheme uncertainty, which is associated to the different sets of non-singular terms which are neglected in $1\mathrm{PI}_{\mathrm{SCET}}$ and $\mathrm{PIM}_{\mathrm{SCET}}$ kinematics.

A more precise assessment of the impact of the approximate NNLO corrections on the central value of the cross section and on the associated perturbative uncertainty can be

LHC 7 TeV	MSTW2008	
$m_{\tilde{t}_1}$ [GeV]	500	1087.17
$(\sigma \pm \Delta\sigma_\mu \pm \Delta_{\rm pdf})_{\rm LO}$ [pb]	$34.4^{+15.8+3.8}_{-10.0-3.6} \times 10^{-3}$	$38.8^{+19.7+10.4}_{-12.1-8.2} \times 10^{-6}$
$(\sigma \pm \Delta\sigma_\mu \pm \Delta_{\rm pdf+\alpha_s})_{\rm NLO}$ [pb]	$46.2^{+6.1+6.6}_{-7.0-5.3} \times 10^{-3}$	$49.6^{+8.0+15.2}_{-8.7-10.5} \times 10^{-6}$
$(\sigma \pm \Delta\sigma_\mu \pm \Delta_{\rm pdf+\alpha_s})_{\rm approx.NNLO}$ [pb]	$46.2^{+1.7+8.0}_{-2.9-5.9} \times 10^{-3}$	$52.8^{+1.4+25.8}_{-3.6-12.1} \times 10^{-6}$
$K_{\rm NLO}$	1.34	1.28
$K_{\rm approx.NNLO}$	1.34	1.36

Table 6.3.: Stop-pair production cross section for two different values of $m_{\tilde{t}_1}$ at LHC 7 TeV. The numbers are obtained by using MSTW2008 PDFs. Here and in the following tables, all of the SUSY parameters (with the exception of $m_{\tilde{t}_1}$) are fixed at the values prescribed by the benchmark point 40.2.5 [95].

LHC 7 TeV	CT10	
$m_{\tilde{t}_1}$ [GeV]	500	1087.17
$(\sigma \pm \Delta\sigma_\mu \pm \Delta_{\rm pdf+\alpha_s})_{\rm LO}$ [pb]	$30.1^{+12.2+7.1}_{-8.1-5.1} \times 10^{-3}$	$36.7^{+17.9+30.7}_{-11.3-13.4} \times 10^{-6}$
$(\sigma \pm \Delta\sigma_\mu \pm \Delta_{\rm pdf+\alpha_s})_{\rm NLO}$ [pb]	$45.3^{+5.8+11.0}_{-6.6-8.1} \times 10^{-3}$	$58.4^{+9.3+49.9}_{-10.2-22.4} \times 10^{-6}$
$(\sigma \pm \Delta\sigma_\mu \pm \Delta_{\rm pdf+\alpha_s})_{\rm approx.NNLO}$ [pb]	$46.7^{+1.7+11.6}_{-2.9-8.3} \times 10^{-3}$	$51.7^{+1.1+34.1}_{-3.6-18.6} \times 10^{-6}$
$K_{\rm NLO}$	1.50	1.59
$K_{\rm approx.NNLO}$	1.55	1.41

Table 6.4.: Stop-pair production cross section for two different values of $m_{\tilde{t}_1}$ at LHC 7 TeV. The numbers are obtained by using CT10 PDFs.

obtained by comparing predictions for fixed values of the stop mass. This analysis is presented in Tables 6.3 and 6.4, which refer to the LHC at a center of mass energy of 7 TeV, in Tables 6.5 and 6.6, which refer to the LHC with a center of mass energy of 8 TeV, and in Tables 6.7 and 6.8, which refer to the LHC with a center of mass energy of 14 TeV. In all tables we consider two different values of the lightest top-squark mass: *i)* the value associated to the benchmark point 40.2.5, $m_{\tilde{t}_1} = 1087.17$ GeV, and *ii)* a stop mass close to the current lower bounds for this particle, $m_{\tilde{t}_1} = 500$ GeV, as determined by searches at the LHC. In all tables, the first uncertainty refers to the scale variation as explained above, while the second uncertainty is obtained by scanning over the 90 % CL PDF sets of the corresponding PDFs and by taking into account the error on $\alpha_s(m_Z)$. The numbers for the cross section have been obtained by employing PDFs fitted at the corresponding order: LO predictions are obtained by employing LO PDFs, NLO predictions employ NLO PDFs, and approximate NNLO predictions employ NNLO PDFs.

In all cases listed in the tables, the inclusion of the approximate NNLO corrections reduces the perturbative uncertainty, when expressed as a percentage of the central value,

LHC 8 TeV	MSTW2008	
$m_{\tilde{t}_1}$ [GeV]	500	1087.17
$(\sigma \pm \Delta\sigma_\mu \pm \Delta_{\rm pdf})_{\rm LO}$ [pb]	$61.7^{+27.3+6.1}_{-17.5-6.0} \times 10^{-3}$	$11.5^{+5.6+2.5}_{-3.5-2.1} \times 10^{-5}$
$(\sigma \pm \Delta\sigma_\mu \pm \Delta_{\rm pdf+\alpha_s})_{\rm NLO}$ [pb]	$83.4^{+10.5+10.6}_{-12.2-8.8} \times 10^{-3}$	$14.7^{+2.1+3.7}_{-2.5-2.8} \times 10^{-5}$
$(\sigma \pm \Delta\sigma_\mu \pm \Delta_{\rm pdf+\alpha_s})_{\rm approx.NNLO}$ [pb]	$83.2^{+3.3+12.6}_{-4.9-9.9} \times 10^{-3}$	$15.3^{+0.3+5.8}_{-1.0-3.0} \times 10^{-5}$
$K_{\rm NLO}$	1.35	1.29
$K_{\rm approx.NNLO}$	1.35	1.34

Table 6.5.: Stop-pair production cross section for two different values of $m_{\tilde{t}_1}$ at LHC 8 TeV. The numbers are obtained by using MSTW2008 PDFs.

LHC 8 TeV	CT10	
$m_{\tilde{t}_1}$ [GeV]	500	1087.17
$(\sigma \pm \Delta\sigma_\mu \pm \Delta_{\rm pdf+\alpha_s})_{\rm LO}$ [pb]	$54.0^{+21.2+11.0}_{-14.2-8.3} \times 10^{-3}$	$10.6^{+4.8+6.6}_{-3.1-3.2} \times 10^{-5}$
$(\sigma \pm \Delta\sigma_\mu \pm \Delta_{\rm pdf+\alpha_s})_{\rm NLO}$ [pb]	$80.9^{+9.8+16.6}_{-11.4-13.1} \times 10^{-3}$	$16.5^{+2.3+10.4}_{-2.7-5.3} \times 10^{-5}$
$(\sigma \pm \Delta\sigma_\mu \pm \Delta_{\rm pdf+\alpha_s})_{\rm approx.NNLO}$ [pb]	$83.6^{+3.6+19.0}_{-4.8-12.3} \times 10^{-3}$	$15.2^{+0.3+8.1}_{-1.0-4.7} \times 10^{-5}$
$K_{\rm NLO}$	1.50	1.56
$K_{\rm approx.NNLO}$	1.55	1.44

Table 6.6.: Stop-pair production cross section for two different values of $m_{\tilde{t}_1}$ at LHC 8 TeV. The numbers are obtained by using CT10 PDFs.

by more than a factor of 2 with respect to the corresponding NLO prediction. We can summarize the content of the tables as follows: the scale variation in the range $m_{\tilde{t}_1}/2 \leq \mu \leq 2m_{\tilde{t}_1}$ can increase the NLO central value up to $+[11, 16]\%$ or lower it up to $-[13, 18]\%$. At approximate NNLO, the scale variation can increase the cross section central value up to $+[2, 5]\%$ or decrease it up to $-[5, 7]\%$. These considerations are valid both when one employs CT10 PDFs or MSTW2008 PDFs.

In almost all cases illustrated in the tables, the PDF and α_s uncertainty grows marginally in the approximate NNLO predictions with respect to the NLO predictions. Another way to look at the PDF and α_s uncertainty in shown in Fig. 6.5, where this uncertainty band is plotted as function of the top-squark mass in the range $m_{\tilde{t}_1} \in [200, 2000]$ GeV at the LHC with center of mass energy of 8 TeV. The left panel refers to the case in which CT10 PDFs are employed, while the right panel refers to the case in which the PDFs employed are MSTW2008. One sees that both bands become larger for large stop masses. The approximate NNLO band in the left panel is almost everywhere inside the NLO band, while in the right panel the approximate NNLO band is larger than the NLO band. However, the bands obtained by using CT10 PDFs remain larger than the ones obtained when using MSTW2008 PDFs.

LHC 14 TeV	MSTW2008	
$m_{\tilde{t}_1}$ [GeV]	500	1087.17
$(\sigma \pm \Delta\sigma_\mu \pm \Delta_{\rm pdf})_{\rm LO}$ [pb]	$48.3^{+18.4+3.3}_{-12.4-3.4} \times 10^{-2}$	$33.5^{+13.8+3.7}_{-9.1-3.6} \times 10^{-4}$
$(\sigma \pm \Delta\sigma_\mu \pm \Delta_{\rm pdf+\alpha_s})_{\rm NLO}$ [pb]	$66.4^{+7.7+6.2}_{-8.5-5.2} \times 10^{-2}$	$44.2^{+4.9+6.4}_{-6.0-5.1} \times 10^{-4}$
$(\sigma \pm \Delta\sigma_\mu \pm \Delta_{\rm pdf+\alpha_s})_{\rm approx.NNLO}$ [pb]	$65.7^{+3.3+6.5}_{-3.4-6.2} \times 10^{-2}$	$44.3^{+1.3+7.8}_{-2.2-5.4} \times 10^{-4}$
$K_{\rm NLO}$	1.38	1.32
$K_{\rm approx.NNLO}$	1.36	1.32

Table 6.7.: Stop-pair production cross section for two different values of $m_{\tilde{t}_1}$ at LHC 14 TeV. The numbers are obtained by using MSTW2008 PDFs.

LHC 14 TeV	CT10	
$m_{\tilde{t}_1}$ [GeV]	500	1087.17
$(\sigma \pm \Delta\sigma_\mu \pm \Delta_{\rm pdf+\alpha_s})_{\rm LO}$ [pb]	$42.6^{+14.4+5.0}_{-10.1-4.3} \times 10^{-2}$	$30.1^{+11.3+7.8}_{-7.7-5.2} \times 10^{-4}$
$(\sigma \pm \Delta\sigma_\mu \pm \Delta_{\rm pdf+\alpha_s})_{\rm NLO}$ [pb]	$63.2^{+7.0+7.6}_{-7.8-6.6} \times 10^{-2}$	$44.11^{+4.8+11.7}_{-5.8-8.1} \times 10^{-4}$
$(\sigma \pm \Delta\sigma_\mu \pm \Delta_{\rm pdf+\alpha_s})_{\rm approx.NNLO}$ [pb]	$65.9^{+3.4+8.2}_{-3.4-6.6} \times 10^{-2}$	$44.6^{+1.3+12.1}_{-2.1-7.8} \times 10^{-4}$
$K_{\rm NLO}$	1.48	1.47
$K_{\rm approx.NNLO}$	1.55	1.48

Table 6.8.: Stop-pair production cross section for two different values of $m_{\tilde{t}_1}$ at LHC 14 TeV. The numbers are obtained by using CT10 PDFs.

The tables also include the values for the NLO and approximate NNLO K factors, which are both normalized to the LO cross section:

$$K_{\rm NLO} = \frac{\sigma_{\rm NLO}}{\sigma_{\rm LO}}\,, \qquad K_{\rm approx.NNLO} = \frac{\sigma_{\rm approx.NNLO}}{\sigma_{\rm LO}}\,. \tag{6.67}$$

The NLO K factors tend to be slightly larger when CT10 PDFs rather than MSTW2008 PDFs are employed (roughly 1.5 vs 1.3), but they are not very sensitive to the collider center of mass energy or to the mass of the top-squark. The ratio $K_{\rm approx.NNLO}/K_{\rm NLO}$ ranges from 0.88 to 1.06, therefore the approximate NNLO corrections have only a moderate impact on the central value of the NLO cross section.[2] For top-squark masses smaller than ~ 1 TeV, the central value for the approximate NNLO cross section falls well within the NLO scale uncertainty band.

Finally, Figs. 6.7 and 6.6 show the cross section as a function of the top-squark mass up to $m_{\tilde{t}_1} = 2$ TeV for the LHC at 7, 8 and 14 TeV center of mass energy. In all cases, the bands represent the residual perturbative scale uncertainties, obtained as explained above.

[2] In this numerical analysis we use NNLO PDFs together with our approximate NNLO results for the hard scattering kernels. One could also make a different choice and use NLO PDFs with the approximate NNLO formulas, in that case the impact on the central value of our predictions would be bigger.

In Fig. 6.7 we employ CT10 PDFs; one sees that, for large values of the stop mass, the approximate NNLO band is below the NLO band at 7 and 8 TeV center of mass energy, while, for the LHC at 14 TeV, the approximate NNLO band overlaps with the lower part of the NLO band. As a comparison, just for the LHC 8 TeV, in Fig. 6.6 MSTW2008 PDFs are employed. In this case, for large stop masses, the approximate NNLO scale uncertainty bands tend to be slightly above the NLO bands.

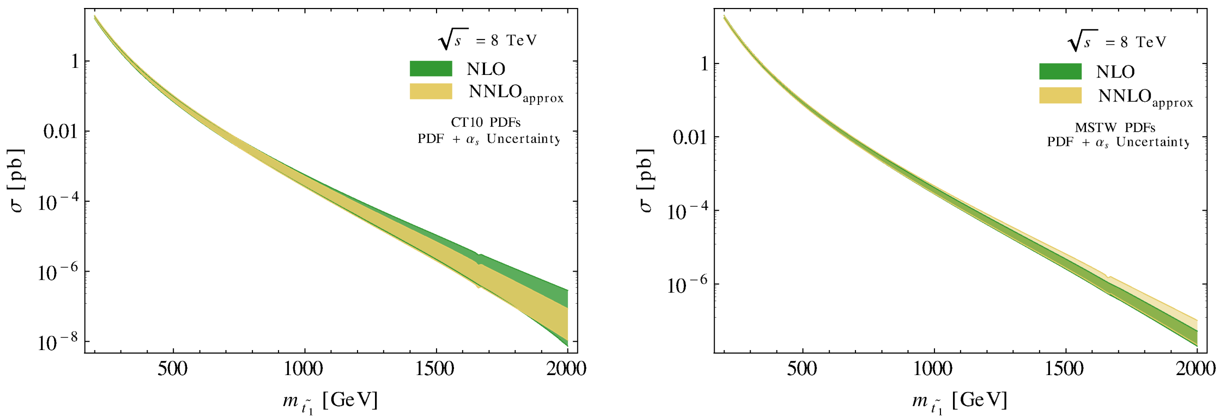

Figure 6.5.: PDF+α_s uncertainty on the total stop production cross section at the LHC with center of mass energy of 8 TeV.

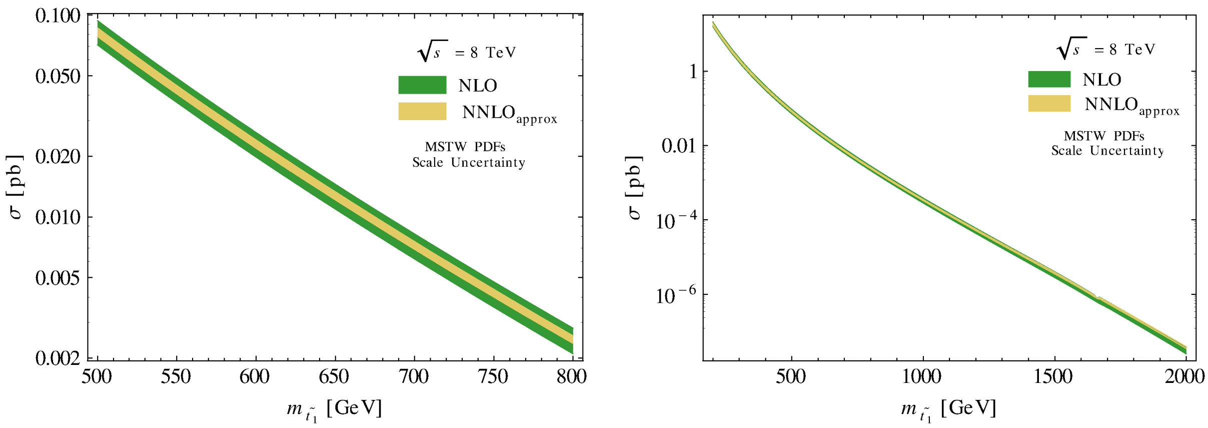

Figure 6.6.: Mass scans with MSTW2008 PDFs for the LHC at 8 TeV center of mass energy. The bands represent the perturbative scale uncertainty at NLO and NNLO.

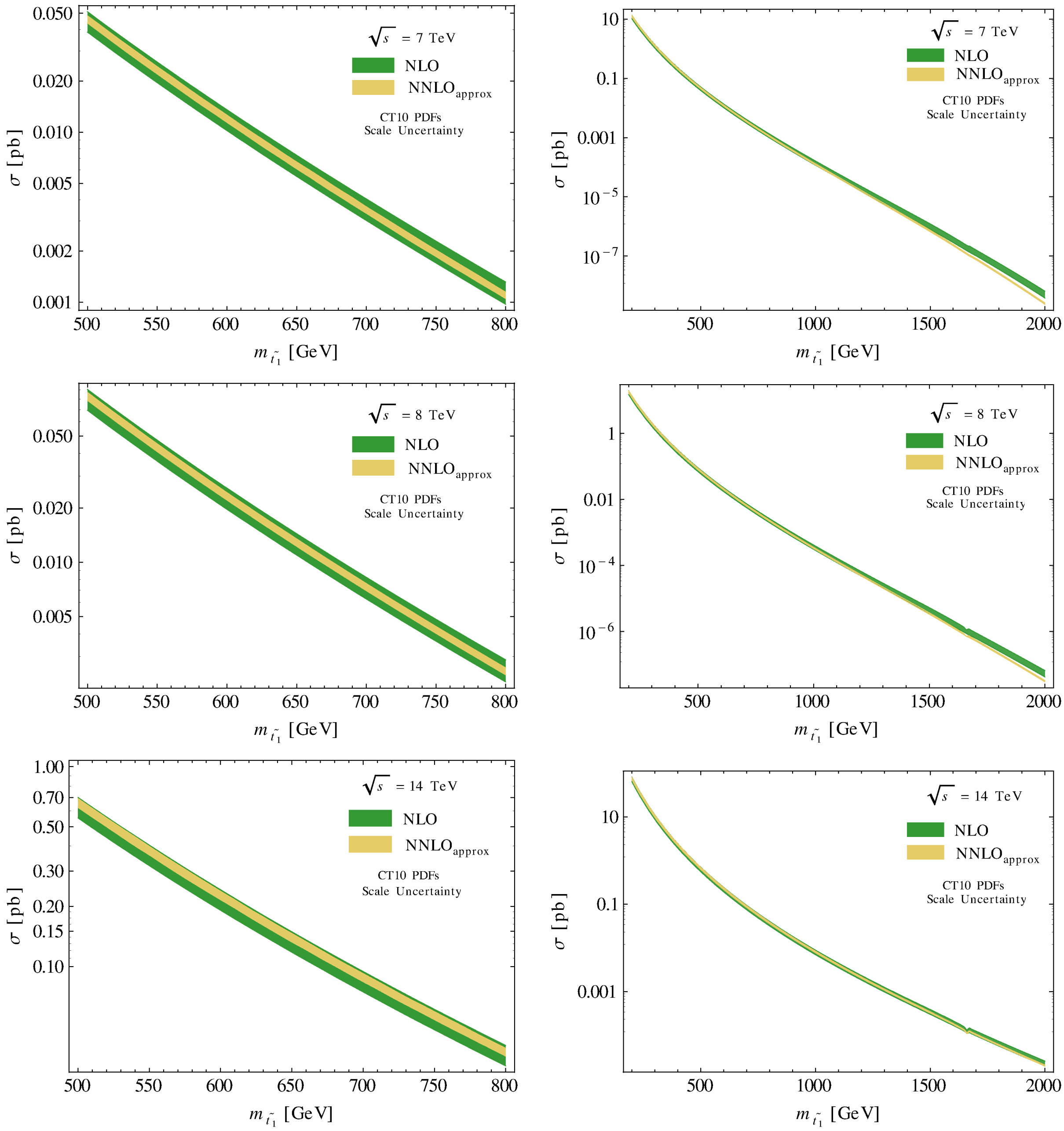

Figure 6.7.: Mass scans with CT10 PDFs for the LHC at 7, 8, and 14 TeV center of mass energies. The bands represent the perturbative scale uncertainty at NLO and NNLO.

7. Conclusions

Supersymmetry is certainly one of the best motivated scenarios for physics beyond the SM. If supersymmetry is broken just above the electroweak scale, the supersymmetric partners of the known SM particles are expected to have masses of the order of 1 TeV, and they could soon be observed at the LHC. For these reasons it is important to have precise theoretical predictions for the production cross sections of supersymmetric particles at hadron colliders. In this thesis we have used effective field theory techniques to improve upon existing calculations for slepton-pair production and stop-pair production by studying higher-order perturbative corrections. Both of these processes are interesting and have a number of positive discovery features. Sleptons are expected to be among the lightest supersymmetric particles and, for a wide range of SUSY scenarios, they have a very simple decay signature, consisting of a pair of energetic leptons plus missing energy. Top-squarks are expected to be the lightest colored supersymmetric particles, and, for this reason, they are likely to be abundantly produced at the LHC. Therefore, top-squarks might be the most accessible supersymmetric particles in the near future.

We have given an introduction to supersymmetry. We discussed the basic formalism and the construction of generic supersymmetric Lagrangians for chiral and vector superfields. We also discussed the particle content and interactions of the MSSM. We have also given a detailed introduction to SCET, first studying the scalar case and then generalizing the construction to QCD. We also reviewed the main ingredients of factorization and resummation in the effective theory by analyzing the relevant theorems for the Drell-Yan process. With the aim of obtaining accurate predictions by taking into account the effects of soft-gluon resummation, we have analyzed the slepton-pair production cross sections at the Tevatron and LHC, together with the related cross section for the Drell-Yan production of a lepton pair. This was done using methods of effective field theory, which allow us to perform the resummation directly in momentum space. The factorized cross sections in the partonic threshold region are expressed in terms of Wilson coefficiens of SCET operators. Solving the RG equations obeyed by these operators allowed us to resum the large logarithms arising due to soft gluon emissions to all orders in the strong coupling constant.

We have extended the results available in literature in various directions. For the Drell-Yan process, we have calculated the effect of virtual SUSY QCD corrections at one-loop order. In the case of slepton-pair production, we have extended previous results by performing the resummation up to the N^{3}LL level. Moreover, given the fact that we perform the resummation not in Mellin moment space but directly in momentum space, our results constitute an independent estimation of soft-gluon effects. We have provided a detailed phenomenological analysis, presenting results valid for the Tevatron and for the LHC. We find that the SUSY QCD corrections due to the exchange of squark and gluinos are very small in comparison to the associated SM QCD corrections, and also in comparison to the uncertainties in the perturbative calculations. It would therefore be challenging if not impossible to observe the effects of virtual SUSY particles in the Drell-Yan rapidity and invariant mass distributions. We have found that soft-gluon resummation has a small effect on the total cross sections for slepton-pair production, ranging from 7% at the Tevatron to 3% at the LHC for a slepton mass of 180 GeV. This is a consequence of the fact that resummation effects are important only for large values of the invariant mass, corresponding to a region where the invariant-mass distribution is very small and gives a tiny contribution to the total cross section. Resummation is therefore more important for colliders where $\tau = M^2/s$ is larger, i.e. the Tevatron, or for higher slepton masses. On the other hand, it still proves useful for the reduction of the theoretical uncertainty due to scale variations. We find that the scale uncertainty is reduced by about a factor of two when going from the fixed-order NLO calculation to the N^{3}LL+NLO result. The dominant uncertainties then arise from other sources, such as the imperfect knowledge of the PDFs, the parameters of the SUSY spectrum and the Monte-Carlo modeling of the experimental acceptances for these SUSY final states.

We have studied the total stop-pair production cross section at the LHC, including higher order perturbative corrections, in two different kinematic schemes, PIM and 1PI. We carried out the calculation of the hard function matrices for stop-pair production up to NLO. By combining the NLO hard and soft functions together with the relative anomalous dimensions, we were able to resum soft gluon emissions to NNLL order. In particular by re-expanding the resummed formula, it was possible to obtain expressions for the cross section which are valid up to $\mathcal{O}(\alpha_s^4)$ in fixed-order perturbation theory. These results allowed us to obtain analytic expressions for all of the coefficients multiplying the singular plus distributions in the variables $(1-z)$ and s_4 up to NNLO order in the hard-scattering kernels, depending on the kinematic scheme. In order to obtain better predictions and better control over the subleading terms in the total cross section, we have presented results obtained by averaging the ones in PIM and 1PI kinematics. We finally matched our results in the threshold regions with the exact fixed-order NLO results. As in the slepton case, it was shown that the total cross section depends strongly on the mass of the produced particles. On the contrary, the dependence on the SUSY virtual parameters is relatively weak. We have found that the inclusion of the approximate NNLO corrections for the pair production cross section reduces the perturbative uncertainty, due to scale dependence, by more than a factor two relative to the fixed-order NLO results. We recall that, in our approach, the scale uncertainty also reflects a kinematic scheme uncertainty. It turned out that, in our analysis, the ratio $K_{\text{approx.NNLO}}/K_{\text{NLO}}$ ranged from 0.88 to 1.06, which implies that the NNLO corrections have only a moderate impact on the central value of the total NLO cross section. Moreover, for top-squark masses smaller than ~ 1 TeV, the central value for the approximate NNLO cross section falls well within the NLO scale uncertainty band. We conclude by noting that the main theoretical uncertainties for stop-pair production, after the inclusion of the approximate NNLO corrections, come from the large uncertainties on the PDFs, especially when larger values of the stop mass are considered.

A. Appendix

A.1. One-Loop Integrals

In this Appendix we collect some details concerning the explicit calculation of the loop integrals discussed in sections 3.2 and 4.

A.1.1. Integral $\mathcal{I}_h$

In order to obtain the result in Eq. (3.34) for the integral $\mathcal{I}_h$, we start by applying the Feynman parameterization

$$\frac{1}{abc} = 2\int_0^1 dx \int_0^x dy \frac{1}{\left[ay + b(x-y) + c(1-x)\right]^3}\,, \tag{A.1}$$

to the integral in Eq. (3.33). We then obtain

$$\begin{aligned}\mathcal{I}_h &= i\pi^{-d/2}\mu^{4-d}\int d^dk \frac{1}{k^2\,(k^2+2k_-\cdot l_+)\,(k^2+2k_+\cdot p_-)}\,,\\ &= i\pi^{-d/2}\mu^{4-d}\int_0^1 dx\int_0^x dy\int d^dk \frac{2}{\chi^3(x,y,k)}\,,\end{aligned} \tag{A.2}$$

where

$$\begin{aligned}\chi^3(x,y,k) &= (k^2+2k_+\cdot p_-)y + k^2(x-y) + (k^2+2k_-\cdot l_+)(1-x)\,,\\ &= k^2 + 2k\cdot\left[py + l(1-x)\right] + \mathcal{O}(\lambda)\,.\end{aligned} \tag{A.3}$$

The integral over the virtual momentum can be evaluated by employing the formula

$$\int d^dk \frac{1}{(k^2+2k\cdot Q - M^2)^\alpha} = (-1)^\alpha \frac{i\pi^{\frac{d}{2}}}{(M^2+Q^2)^{\alpha-\frac{d}{2}}}\frac{\Gamma\left(\alpha-\frac{d}{2}\right)}{\Gamma\left(\alpha\right)}\,. \tag{A.4}$$

In this one finds

$$\int d^dk \frac{1}{\chi^3(x,y,k)} = -\frac{i\pi^{\frac{d}{2}}}{2}\Gamma\left(3-\frac{d}{2}\right)V^{\frac{d}{2}-3}\left(x,y\right)\,, \tag{A.5}$$

with

$$V(x,y) = p^2 y + l^2(1-x) + 2p\cdot l y(1-x) = 2l_+\cdot p_- y(1-x) + \mathcal{O}(\lambda^2)\,. \tag{A.6}$$

Therefore, after rewriting the spacetime dimension as $d = 4 - 2\varepsilon$, the integral $\mathcal{I}_h$ becomes

$$\mathcal{I}_h = \frac{\Gamma(1+\varepsilon)}{2l_+ \cdot p_-} \left(\frac{\mu^2}{2l_+ \cdot p_-} \right)^{\varepsilon} \int_0^1 dx \int_0^x dy \frac{1}{[y(1-x)]^{1+\varepsilon}} \,. \tag{A.7}$$

The integral over the Feynman parameters x and y gives

$$\begin{aligned} \int_0^1 dx \int_0^x dy \frac{1}{[y(1-x)]^{1+\varepsilon}} &= -\frac{1}{\varepsilon} \int_0^1 dx x^{-\varepsilon} (1-x)^{-1-\varepsilon} \,, \\ &= -\frac{1}{\varepsilon} \frac{\Gamma(1-\varepsilon)\Gamma(-\varepsilon)}{\Gamma(1-2\varepsilon)} = \frac{\Gamma^2(-\varepsilon)}{\Gamma(1-2\varepsilon)} \,. \end{aligned} \tag{A.8}$$

By inserting the equation above in Eq.(A.7) one obtains Eq. (3.34).

A.1.2. Integral $\mathcal{I}_c$

In this appendix we evaluate the soft region integral in Eq. (3.36). We employ the following parametrization of the integrand

$$\frac{1}{abc} = \int_0^\infty dx_1 \int_0^\infty dx_2 \, \frac{2}{(a + bx_1 + cx_2)^3} \,, \tag{A.9}$$

where we identify the denominators as follows: $a = k^2$, $c = 2l_+ \cdot k$, and $b = (k+p)^2$. In this way one finds that

$$\mathcal{I}_c = i\pi^{-\frac{d}{2}} \mu^{4-d} \int_0^\infty dx_1 \int_0^\infty dx_2 \int d^d k \, \frac{2}{[(1+x_1)(k^2 + 2k \cdot V - M^2)]^3} \,, \tag{A.10}$$

with

$$V^\mu = \frac{x_1 p^\mu + x_2 l_+^\mu}{(1+x_1)} \,, \qquad M^2 = \frac{-x_1 p^2}{(1+x_1)} \,. \tag{A.11}$$

At this stage it is possible to evaluate the integral over the virtual momentum by employing the master formula Eq. (A.4); in this way one finds

$$\begin{aligned} \mathcal{I}_c &= \mu^{2\varepsilon} \Gamma(1+\varepsilon) \int_0^\infty dx_1 \frac{1}{(1+x_1)^3} \int_0^\infty dx_2 \left(\frac{P^2 x_1 + 2l_+ \cdot p_- x_1 x_2}{(1+x_1)^2} \right)^{-1-\varepsilon} \\ &= \mu^{2\varepsilon} \Gamma(1+\varepsilon) \int_0^\infty dx_1 \frac{x_1^{-1-\varepsilon}}{(1+x_1)^{1-2\varepsilon}} \int_0^\infty dx_2 \left(P^2 + 2l_+ \cdot p_- x_2 \right)^{-1-\varepsilon} \,, \end{aligned} \tag{A.12}$$

where $p^2 = -P^2$. The integrals over x_1 and x_2 factor and one finds

$$\mathcal{I}_c = \mu^{2\varepsilon} \Gamma(1+\varepsilon) P^{-2-2\varepsilon} \frac{\Gamma(1-\varepsilon)\Gamma(-\varepsilon)}{\Gamma(1-2\varepsilon)} \int_0^\infty dx_2 \, (1 + rx_2)^{-1-\varepsilon} \,, \tag{A.13}$$

with $r = 2l_+ \cdot p_-/P^2$. By replacing $x_2 \to x_2'/r$ one finds

$$\begin{aligned}
\mathcal{I}_c &= \left(\frac{\mu^2}{P^2}\right)^{\varepsilon} \frac{\Gamma(1+\varepsilon)}{2l_+ \cdot p_-} \frac{\Gamma(1-\varepsilon)\Gamma(-\varepsilon)}{\Gamma(1-2\varepsilon)} \int_0^\infty dx_2' \left(1+x_2'\right)^{-1-\varepsilon} \\
&= \left(\frac{\mu^2}{P^2}\right)^{\varepsilon} \frac{\Gamma(1+\varepsilon)}{2l_+ \cdot p_-} \frac{\Gamma(1-\varepsilon)\Gamma(-\varepsilon)}{\varepsilon\Gamma(1-2\varepsilon)} \\
&= -\frac{\Gamma(1+\varepsilon)}{2l_+ \cdot p_-} \frac{\Gamma^2(-\varepsilon)}{\Gamma(1-2\varepsilon)} \left(\frac{\mu^2}{P^2}\right)^{\varepsilon}, \qquad \text{(A.14)}
\end{aligned}$$

which is the result found in Eq. (3.36).

A.1.3. Integral $\mathcal{I}_s$

In this appendix we evaluate the soft region integral in Eq. (3.38). As a first step we apply the Feynman parametrization in Eq. (A.9). By choosing $a = k^2$, $b = 2l_+ \cdot k + l^2$, and $c = 2p_- \cdot k + p^2$, the denominator of the integrand of Eq. (A.9) becomes

$$a + bx_1 + cx_2 = k^2 + 2k \cdot (p_- x_1 + l_+ x_2) + p^2 x_1 + l^2 x_2 \,. \qquad \text{(A.15)}$$

It is now possible to integrate over the virtual momentum by employing the master formula in Eq. (A.4) so that one finds

$$\mathcal{I}_s = \mu^{4-d}\Gamma\left(3 - \frac{d}{2}\right) \int_0^\infty dx_1 \int_0^\infty dx_2 \left(x_1 P^2 + x_2 L^2 + 2l_+ \cdot p_- x_1 x_2\right)^{\frac{d}{2}-\alpha}, \qquad \text{(A.16)}$$

where $P^2 = -p^2$ and $L^2 = -l^2$. To complete the evaluation of the integral we need to resort to a series of changes of variables. One starts by replacing $x_1 \to x_1'/P^2$ and $x_2 \to x_2'/L^2$; in this way the integral becomes (neglecting the prime superscript)

$$\mathcal{I}_s = \mu^{2\varepsilon} \frac{\Gamma(1+\varepsilon)}{P^2 L^2} \int_0^\infty dx_1 \int_0^\infty dx_2 \left(x_1 + x_2 + a x_1 x_2\right)^{-1-\varepsilon}, \qquad \text{(A.17)}$$

with $a = 2l_+ \cdot p_-/(P^2 L^2)$. It is now convenient to separate the integration variables; we send $x_2 \to x_1 x_2'$ to obtain

$$\mathcal{I}_s = \mu^{2\varepsilon} \frac{\Gamma(1+\varepsilon)}{P^2 L^2} \int_0^\infty dx_1 \int_0^\infty dx_2 x_1^{-\varepsilon} \left(1 + x_2 + a x_1 x_2\right)^{-1-\varepsilon}. \qquad \text{(A.18)}$$

Then, we replace $x_2 \to x_2'/(1 + a x_1)$; in this way one finds

$$\mathcal{I}_s = \mu^{2\varepsilon} \frac{\Gamma(1+\varepsilon)}{P^2 L^2} \int_0^\infty dx_1 \frac{x_1^{-\varepsilon}}{1 + a x_1} \int_0^\infty dx_2 \left(1 + x_2\right)^{-1-\varepsilon}; \qquad \text{(A.19)}$$

the two integrals are now factored. To complete the calculation we replace $x_1 \to x_1'/a$ to obtain

$$\mathcal{I}_s = \mu^{2\varepsilon}\frac{\Gamma(1+\varepsilon)}{P^2L^2}a^{-1+\varepsilon}\underbrace{\int_0^\infty dx_1\frac{x_1^{-\varepsilon}}{1+x_1}}_{=\Gamma(1-\varepsilon)\Gamma(\varepsilon)}\underbrace{\int_0^\infty dx_2\,(1+x_2)^{-1-\varepsilon}}_{=\frac{1}{\varepsilon}}\,. \tag{A.20}$$

Finally, one finds

$$\mathcal{I}_s = \frac{\Gamma(1+\varepsilon)}{P^2L^2}\left(\frac{P^2L^2}{2l_+\cdot p_-}\right)\left(\frac{2l_+\cdot p_-\mu^2}{P^2L^2}\right)^{\varepsilon}\frac{(-\varepsilon)\Gamma(\varepsilon)\Gamma(-\varepsilon)}{\varepsilon} \tag{A.21}$$

$$= -\frac{\Gamma(1+\varepsilon)}{2l_+\cdot p_-}\Gamma(\varepsilon)\Gamma(-\varepsilon)\left(\frac{2l_+\cdot p_-\mu^2}{P^2L^2}\right)^{\varepsilon}, \tag{A.22}$$

which is the result in Eq. (3.38).

If the external legs are set on-shell at the beginning of the calculation ($p^2 = l^2 = 0$) the integral vanishes, even if $p\cdot l \neq 0$. This can be readily proved by setting $p^2 = l^2 = 0$ in Eq. (A.16). By doing this one obtains

$$\mathcal{I}_s\left(p^2=0,l^2=0\right) = \mu^{2\varepsilon}\Gamma(1+\varepsilon)\int_0^\infty dx_1\int_0^\infty dx_2\,(2l_+\cdot p_-)^{-1-\varepsilon}(x_1x_2)^{-1-\varepsilon}\,, \tag{A.23}$$

where the two integrals in x_1 and x_2 factorize. It is now sufficient to prove that one of the two integrals vanishes. Let us consider the x_1 integration:

$$\int_0^\infty dx_1\frac{1}{x^{1+\varepsilon}}\,, \tag{A.24}$$

it develops an ultraviolet divergence for $\varepsilon < 0$ and an infrared divergence for $\varepsilon > 0$. In order to give a mathematical meaning to this integral we split the integration region into two parts using a regulator Λ: the infrared region for $x_1 < \Lambda$ and the ultraviolet region for $x_1 > \Lambda$:

$$\int_0^\infty dx_1\frac{1}{x^{1+\varepsilon}} = \int_0^\Lambda dx_1\frac{1}{x^{1+\varepsilon}} + \int_\Lambda^\infty dx_1\frac{1}{x^{1+\varepsilon}}\,. \tag{A.25}$$

On the r.h.s. the first integral is convergent for $\varepsilon < 0$, while the second one is convergent for $\varepsilon > 0$. To distinguish the nature of the two divergencies we can use two different regulators in the two different regions, by working out the integration for $\varepsilon_{\mathrm{I}} < 0$ and for $\varepsilon_{\mathrm{U}} > 0$ we find

$$\int_0^\infty dx_1\frac{1}{x^{1+\varepsilon}} = -\frac{\Lambda^{-\varepsilon_{\mathrm{I}}}}{\varepsilon_{\mathrm{I}}} + \frac{\Lambda^{-\varepsilon_{\mathrm{U}}}}{\varepsilon_{\mathrm{U}}}\,, \tag{A.26}$$

where both integrals develop poles for $\varepsilon_{\mathrm{I}} = \varepsilon_{\mathrm{U}} = 0$. The r.h.s. can be analytically continued for arbitrary values of ε_{I} and ε_{U} without any constraint, therefore we are free to identify ε_{I} and ε_{U}. As a consequence of this, the integral in Eq. (A.26) vanishes. Another interesting way of proving that

$$\int d^dk\frac{1}{k^2(k\cdot p_1)(k\cdot p_2)} = 0\,, \tag{A.27}$$

for any p_1, p_2 involves integration by parts identities. One starts from the fact that in dimensional regularization

$$\int d^d k \, \frac{\partial}{\partial k^\mu} \frac{v^\mu}{k^2 (k \cdot p_1)(k \cdot p_2)} = 0 \,, \tag{A.28}$$

for any v^μ. By choosing $v^\mu = k^\mu$ applying the derivative to the integrand one obtains

$$0 \;=\; \int d^d k \left[\frac{d-4}{(k^2)(k \cdot p_1)(k \cdot p_2)} \right] . \tag{A.29}$$

Since in dimensional regularization one works in $d \neq 4$ (and then one takes the limit $\varepsilon \to 0$) the relation above implies Eq. (A.27).

A.1.4. Soft Function in Position Space

In this appendix we descibe the calculation of the Drell-Yan soft function $\hat{W}_{\mathrm{DY}}(x, \mu_f)$ directly in position space. $\hat{W}_{\mathrm{DY}}(x, \mu_f)$ can be expressed as a closed Wilson loop[1] by the product of the soft Wilson lines in the two currents:

$$\begin{aligned} \hat{W}_{\mathrm{DY}}(x, \mu_f) &= \frac{1}{N_c} \mathrm{Tr} \, \langle 0 | \bar{\boldsymbol{T}} \left(S_n^\dagger (x) \, S_{\bar{n}} (x) \right) \boldsymbol{T} \left(S_{\bar{n}}^\dagger (0) \, S_n (0) \right) | 0 \rangle \,, \\ &= \langle 0 | \mathbf{P} \exp \left(ig \int_{C_{\mathrm{DY}}} dy_\mu \, A^\mu(y) \right) | 0 \rangle \,, \end{aligned} \tag{A.30}$$

where the trace is over color indices and $\mathbf{T}$, $\overline{\mathbf{T}}$ are the time and anti-time ordering operators. We then expand the $\mathbf{P}$ ordered exponential in Eq. (A.30) as

$$\hat{W}_{\mathrm{DY}}(x, \mu_f) \;=\; 1 + \frac{1}{2} (ig)^2 C_F \int_{C_{\mathrm{DY}}} dx_1^\mu \int_{C_{\mathrm{DY}}} dx_2^\nu \, D_{\mu\nu}(x_1 - x_2) \,, \tag{A.31}$$

where $D_{\mu\nu}(x_1 - x_2)$ is the cut gluon propagator. At order α_s, the Wilson loop $\hat{W}_{\mathrm{DY}}(y, \mu_f)$ require the evaluation of the one-loop diagram shown in Fig. (4.1), plus the corresponding diagram in which the gluon is attached to the other two lines. Using the Feynman rule for the cut gluon propagator in position space[2], we evaluate the contribution of the two

[1] This can be easily seen using the definition of the soft Wilson line

$$S_n(x) \;=\; \langle 0 | \mathbf{P} \exp \left[i \int_{-\infty}^{0} ds \, n \cdot A_s(x + sn) \right] | 0 \rangle \,,$$

where $\mathbf{P}$ indicates the path ordering of the color matrices.

[2] The cut propagator $D^{\mu\nu}(x) = -g^{\mu\nu} D(x)$ is definded in position space as

$$D(x) \;=\; \int \frac{d^d k}{(2\pi)^d} \, e^{-ikx} 2\pi \theta(k_0) \delta(k^2) \;=\; \frac{\Gamma(d/2 - 1)}{4\pi^{d/2}} \, \left[-2(x_+ - i0)(x_- - i0) \right]^{1-d/2}$$

diagrams and we find

$$\hat{W}_{\rm DY}(x,\mu_f) \;=\; 1+4g^2\mu^{2\varepsilon}\,C_F\int_{-\infty}^{0}dt_1\int_{0}^{\infty}dt_2\,\frac{\Gamma(1-\varepsilon)}{4\pi^{2-\varepsilon}}(x-nt_1-\bar{n}t_2)^{2\varepsilon-2}\,, \tag{A.32}$$

Assuming that $x=(x_0,0,0,0)$ we obtain the factorization of the two integrals

$$\hat{W}_{\rm DY}(x,\mu_f)=1+4g^2\mu^{2\varepsilon}\,C_F\frac{\Gamma(1-\varepsilon)}{4\pi^{2-\varepsilon}}\int_{-\infty}^{0}dt_1(2t_1-x_0)^{\varepsilon-1}\int_{0}^{\infty}dt_2\,(x_0-2t_2)^{\varepsilon-1}\,. \tag{A.33}$$

By replacing $t_1\to x_0t_1/2$, $t_2\to -x_0t_2/2$ we find

$$\begin{aligned}\hat{W}_{\rm DY}(x,\mu_f) \;&=\; 1-g^2\mu^{2\varepsilon}\,C_F\frac{\Gamma(1-\varepsilon)}{4\pi^{2-\varepsilon}}\int_{-\infty}^{0}dt_1\,x_0^{\varepsilon}(t_1-1)^{\varepsilon-1}\\ &\quad\times\int_{0}^{\infty}dt_2\,x_0^{\varepsilon}(t_2+1)^{\varepsilon-1}\,,\\ &=\; 1-g^2\mu^{2\varepsilon}C_F\frac{\Gamma(1-\varepsilon)}{4\pi^{2-\varepsilon}}x_0^{2\varepsilon}\int_{-\infty}^{-1}dt_1\,(t_1)^{\varepsilon-1}\int_{1}^{\infty}dt_2\,(t_2)^{\varepsilon-1}\,,\\ &=\; 1+C_F\frac{\alpha_s}{\pi}\frac{\Gamma(1-\varepsilon)}{\varepsilon^2}\left(-\mu^2x_0^2\pi\right)^{\varepsilon}\,.\end{aligned} \tag{A.34}$$

If we define $\mu^{2\varepsilon}_{\overline{\rm MS}}\;\equiv\;e^{-\varepsilon\gamma_E}\mu_f^{2\varepsilon}(4\pi)^{\varepsilon}$ it is possible to rewrite $\hat{W}_{\rm DY}(x,\mu_f)$ in the following way:

$$\hat{W}_{\rm DY}(x,\mu_{\overline{\rm MS}})=1+C_F\frac{\alpha_s}{\pi}\frac{\Gamma(1-\varepsilon)}{\varepsilon^2}e^{-\varepsilon\gamma_E}\left(-\frac{1}{4}\mu^2_{\overline{\rm MS}}x_0^2e^{2\gamma_E}\right)^{\varepsilon}\,. \tag{A.35}$$

A.2. Factorization of the Sudakov Form Factor in $d=6$

In this Appendix we want to employ the SCET Lagrangian derived from the ϕ^3 theory in Section 3.3 to prove a factorization theorem for the Sudakov form factor. In four dimensions, the analysis is complicated by the fact that the coupling constant g is not dimensionless. To avoid this problem, we will consider the theory in six dimensions. By writing the action of the theory in d-dimensions

$$S=\int d^dx\left[\frac{1}{2}\partial_\mu\phi(x)\,\partial^\mu\phi(x)-\frac{g}{3!}\phi^3(x)+J(x)\right]\,, \tag{A.36}$$

which is dimensionless when setting $\hbar=1$, and by looking at the kinetic term, one can see that the mass dimension of the field is

$$[\phi]=\frac{d-2}{2}\,;\qquad [\phi]=1\quad\text{in}\quad d=4\,,\qquad [\phi]=2\quad\text{in}\quad d=6\,.$$

Similarly, by looking at the interaction term one can determine the mass dimension of the coupling

$$[g] = \frac{6-d}{2}\,; \qquad [g] = 1 \quad \text{in} \quad d = 4\,, \qquad [g] = 0 \quad \text{in} \quad d = 6\,. \tag{A.37}$$

At this stage, we want to study how the various fields in the effective theory scale in terms of powers of λ in $d = 6$. We consider now the two-point correlator for collinear fields[3]

$$\langle \phi_c(x)\phi_c(0)\rangle \sim \int \underbrace{d^6p}_{\lambda^6}\, \underbrace{e^{-ip\cdot x}}_{\lambda^0}\, \underbrace{\frac{i}{p^2}}_{\lambda^{-2}} \sim \lambda^4\,, \tag{A.38}$$

and conclude that the collinear fields scale as $\phi_c \sim \lambda^2$. One can carry out the same analysis by considering the correlator of two soft fields (in this case all of the components of the soft momentum scale as λ^2)

$$\langle \phi_s(x)\phi_s(0)\rangle \sim \int \underbrace{d^6p}_{\lambda^{12}}\, \underbrace{e^{-ip\cdot x}}_{\lambda^0}\, \underbrace{\frac{i}{p^2}}_{\lambda^{-4}} \sim \lambda^8\,, \tag{A.39}$$

so that $\phi_s \sim \lambda^4$.

Next, we determine the scaling of each of the terms which appear in the effective Lagrangian. Keeping in mind that the scaling of the integration measure is given by the components of x which are conjugate to p, one finds

$$\begin{array}{lclcll}
\int d^6x\, \frac{1}{2}\partial_\mu\phi_c(x)\, \partial^\mu\phi_c(x) & \sim & \frac{1}{\lambda^6}\left(\lambda\lambda^2\right)^2 & = & \lambda^0\,, & \\
\int d^6x\, \frac{1}{2}\partial_\mu\phi_s(x)\, \partial^\mu\phi_s(x) & \sim & \frac{1}{\lambda^{12}}\left(\lambda^2\lambda^4\right)^2 & = & \lambda^0\,, & \\
-\frac{g}{3!}\int d^6x\, \phi_c^3(x) & \sim & \frac{1}{\lambda^6}\left(\lambda^2\right)^3 & = & \lambda^0\,, & \\
-\frac{g}{3!}\int d^6x\, \phi_s^3(x) & \sim & \frac{1}{\lambda^{12}}\left(\lambda^4\right)^3 & = & \lambda^0\,, & \\
-\frac{g}{2}\int d^6x\, \phi_c^2(x)\, \phi_s(x_-) & \sim & \frac{1}{\lambda^6}\left(\lambda^2\right)^2\lambda^4 & = & \lambda^2 & \Longrightarrow \quad \text{Suppressed}\,.
\end{array} \tag{A.40}$$

The terms originating from the current operator $J = \phi^2$ scale instead as follows

$$\int d^6x\, J_2(x) \propto \int d^6x\, \phi_c(x)\, \phi_{\bar{c}}(x) \sim \frac{1}{\lambda^4}\lambda^2\lambda^2 = \lambda^0\,, \tag{A.41}$$

[3] We remind the reader that in Eq. (A.38) p is a collinear momentum in six dimension, where the component in the collinear direction scales as λ^0, the component anti-parallel to the collinear direction scales as λ^2 (as in the four dimensional case), and the four transverse directions scale proportionally to λ.

Combinations involving more fields are powers suppressed, as it can be seen below:

$$\int d^6x\, \phi_c^2(x)\, \phi_{\bar{c}}(x) \sim \frac{1}{\lambda^4}\left(\lambda^2\right)^2 \lambda^2 = \lambda^2 \quad \Longrightarrow \quad \text{Suppressed}\,,$$

$$\int d^6x\, \phi_c(x)\, \phi_{\bar{c}}(x)\, \phi_s(x) \sim \frac{1}{\lambda^4}\left(\lambda^2\right)^2 \lambda^4 = \lambda^4 \quad \Longrightarrow \quad \text{Suppressed}\,. \tag{A.42}$$

Observe that the integration measure in Eqs. (A.42) scales as $1/\lambda^4$ because both the plus and minus components of x^μ are of λ^0, since they are conjugate to a momentum which is a sum of l-collinear and p-collinear momenta. Therefore $d^6x \sim (p_\perp)^{-4} \sim \lambda^{-4}$.

In summary we conclude that

$$\int d^6x\, \mathcal{L}_{\text{SCET}} = \int d^6x\, \left[\mathcal{L}_c + \mathcal{L}_{\bar{c}} + \mathcal{L}_s\right] + \mathcal{O}\left(\lambda^2\right)\,, \tag{A.43}$$

while for the current operator one finds

$$\int d^6x\, J(x) \to \int d^6x \int ds \int dt\, C(s,t,\mu)\, \phi_c\left(x+s\bar{n}\right) \phi_{\bar{c}}\left(x+tn\right) + \mathcal{O}\left(\lambda^2\right)\,. \tag{A.44}$$

Since soft-collinear interactions are power suppressed, it is possible to obtain a factorization theorem.

Let us consider the following correlator

$$\begin{aligned} G(p,l,\mu) &= \int d^6x_1 \int d^6x_2\, e^{-ip\cdot x_1 + il\cdot x_2} \langle 0|T\left\{\phi_c(x_1) J(0) \phi_{\bar{c}}(x_2)\right\}|0\rangle\,, \\ &= \int d^6x_1 \int d^6x_2\, e^{-ip\cdot x_1 + il\cdot x_2} \int ds \int dt\, C(s,t,\mu) \times \\ &\times \ \langle 0|T\left\{\phi_c(x_1)\phi_c(s\bar{n})\right\}|0\rangle \langle 0|T\left\{\phi_{\bar{c}}(tn)\phi_{\bar{c}}(x_2)\right\}|0\rangle\,, \end{aligned} \tag{A.45}$$

Since the soft-collinear interactions are power suppressed, the fields ϕ_c and $\phi_{\bar{c}}$ do not interact whith each other. Up to power suppressed terms, we now deal with two separate theories and the matrix element in the first line reduces to a collinear matrix element of the ϕ_c fields times a matrix element of the $\phi_{\bar{c}}$ fields.

Translation invariance implies that

$$\langle 0|T\left\{\phi_c(x_1)\phi_c(s\bar{n})\right\}|0\rangle = \langle 0|T\left\{\phi_c(x_1 - s\bar{n})\phi_c(0)\right\}|0\rangle\,, \tag{A.46}$$

and a similar relation for the other time ordered product. One can then carry out the following changes of variables in Eq. (A.45):

$$x_1 \to x_1 + s\bar{n}\,, \qquad \text{and} \qquad x_2 \to x_2 + tn\,, \tag{A.47}$$

to obtain

$$G(p,l,\mu) = \int ds \int dt\, C\left(s,t,\mu\right) e^{-isp\cdot\bar{n} + itl\cdot n} \mathcal{J}\left(p^2\right) \mathcal{J}\left(l^2\right)\,, \tag{A.48}$$

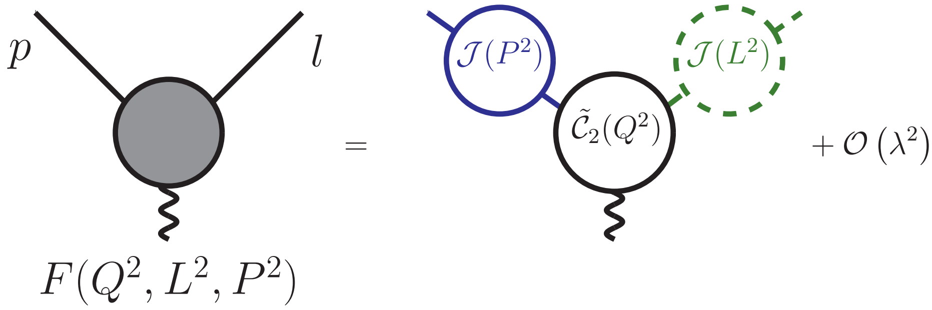

Figure A.1.: Diagrammatic representation of the factorization theorem for the ϕ^3 theory in $d = 6$.

with

$$\begin{aligned} \mathcal{J}\left(p^2,\mu\right) &\equiv \int d^6x_1\, e^{-ip\cdot x_1}\langle 0|T\left\{\phi_c(x_1)\phi_c(0)\right\}|0\rangle\,, \\ \mathcal{J}\left(l^2,\mu\right) &\equiv \int d^6x_2\, e^{il\cdot x_2}\langle 0|T\left\{\phi_{\bar{c}}(0)\phi_{\bar{c}}(x_2)\right\}|0\rangle\,. \end{aligned} \tag{A.49}$$

The functions $\mathcal{J}$ do not depend on s and t, and therefore the integral in Eq. (A.48) factors out. By introducing the notation

$$\tilde{\mathcal{C}}_2\left(\bar{n}\cdot p, n\cdot l,\mu\right) \equiv \int ds \int dt\, C\left(s,t,\mu\right) e^{-isp\cdot\bar{n}+itl\cdot n}\,, \tag{A.50}$$

one can rewrite the three-point correlator in Eq. (A.48) as the product of three functions

$$G(p,l,\mu) = \tilde{\mathcal{C}}_2\left(\bar{n}\cdot p, n\cdot l,\mu\right)\mathcal{J}\left(p^2,\mu\right)\mathcal{J}\left(l^2,\mu\right)\,. \tag{A.51}$$

We have factorized the Green function G into a product of a *hard function* $\tilde{\mathcal{C}}$ and two *jet functions* $\mathcal{J}$. The jet function can be calculated within the full theory since the collinear Lagrangian is identical to the complete ϕ^3 Lagrangian. The content of the factorization theorem is summarized in diagrammatic form in Fig. A.1. The nontrivial part of the factorization theorem is that the hard function can be calculated at $p^2 = l^2 = 0$, so that we have managed to factor a function of three variables into a product of three functions of a single variable. The full Sudakov form factor is split into an high-energy contribution (the hard function), and two low-energy contributions (the jet functions).

It would be interesting to use the factorization theorem to resum Sudakov logarithms to all orders in the coupling constant; this can be done by employing RG tools within the effective theory. The Sudakov logarithms have the form

$$\left(g^2\right)^n \ln^n\left(\frac{p^2l^2}{Q^4}\right)\,,$$

so there is only a single logarithm at each order in perturbation theory. This is due to the absence of a soft contribution to the Sudakov form factor (A.51): the double logarithms arise in the interplay of soft and collinear contributions and will be present in the QCD case.

A.3. Wilson Lines and Gauge Transformations

In this appendix, we derive a few fundamental properties of Wilson lines. We start by considering a generic Wilson line connecting two space-time points y and z, for an Abelian theory such as QED. In the Abelian case, no path ordering is needed, and we will indicate a Wilson line as

$$[z,y]_A \equiv \exp\left[-ie\int_P dx^\mu A_\mu(x)\right] , \tag{A.52}$$

where P is a path which connects y with z, and where $e=-g$ is the Abelian coupling constant. In most cases, we drop the subscript indicating the gauge field; however, in the following discussion we need to carry out gauge transformations, and it is therefore convenient to indicate explicitly which gauge field appears in the Wilson line. The Wilson line can be rewritten as

$$[z,y]_A = \exp\left[-ie\int_{s_y}^{s_z} ds\frac{dx^\mu}{ds}A_\mu\big(x(s)\big)\right] ; \tag{A.53}$$

where s is a variable parameterizing the path and s_y, s_z are such that

$$y \equiv x(s_y)\,, \qquad z \equiv x(s_z)\,. \tag{A.54}$$

The Wilson lines employed in the rest of this appendix involve paths which are straight segments, so that

$$x(s) = x_0 + s\bar{n}\,, \quad \text{and} \quad \frac{dx^\mu}{ds} = \bar{n}^\mu\,. \tag{A.55}$$

Moreover we typically choose $s_y = 0$ and rewrite $s_z \to s$ and $x_0 \to 0$. In this appendix however we will consider the more general case of Wilson lines along arbitrary paths.

Under a gauge transformation $V(x) = e^{i\alpha(x)}$, the field $A_\mu(x)$ transforms as

$$A_\mu(x) \to A'_\mu(x) = A_\mu(x) + \frac{1}{g}\partial_\mu\alpha(x)\,, \tag{A.56}$$

and the Wilson line changes to

$$\begin{aligned}
[z,y]_A \;&\to\; [z,y]_{A'}\,, \\
&= \exp\left[-ie\int_{s_y}^{s_z} ds\frac{dx^\mu}{ds}A_\mu\big(x(s)\big) + i\int_{s_y}^{s_z} ds\frac{dx^\mu}{ds}\partial_\mu\alpha\left(x(s)\right)\right] ,
\end{aligned}$$

$$
\begin{aligned}
&= \exp\left[-ie\int_{s_y}^{s_z} ds\frac{dx^\mu}{ds}A_\mu\big(x(s)\big) + i\int_{s_y}^{s_z} ds\frac{d}{ds}\alpha\left(x(s)\right)\right] , \\
&= \exp\left[-ie\int_{s_y}^{s_z} ds\frac{dx^\mu}{ds}A_\mu\big(x(s)\big) + i\alpha\left(z\right) - i\alpha\left(y\right)\right] , \\
&= V(z)\left[z,y\right]_A V^\dagger(y) . \qquad\qquad (A.57)
\end{aligned}
$$

From the last line above it is easy to see that if $y = z$ (closed path) the Wilson loop is gauge invariant.

Next, we will to prove that the covariant derivative of the Wilson line along the integration path is zero. To this end, we consider an intermediate point $x^\mu \equiv x^\mu(s)$ and compute

$$
\begin{aligned}
\frac{dx^\mu}{ds}D_\mu\left[x,y\right]_A &= \frac{dx^\mu}{ds}\left(\partial_\mu + ieA_\mu(x)\right)\left[x,y\right]_A , \\
&= ie\frac{dx^\mu}{ds}\left[\left(-\frac{d}{dx^\mu}\int_{s_y}^{s} dt\frac{dx^\nu}{dt}A_\nu(x)\right) + A_\mu(x)\right]\left[x,y\right]_A , \\
&= ie\left[\left(-\frac{d}{ds}\int_{s_y}^{s} dt\frac{dx^\nu}{dt}A_\nu(x)\right) + \frac{dx^\mu}{ds}A_\mu(x)\right]\left[x,y\right]_A , \\
&= ie\left[-\frac{dx^\nu}{ds}A_\nu(x(s)) + \frac{dx^\mu}{ds}A_\mu(x)\right]\left[x,y\right]_A , \\
&= 0 . \qquad\qquad (A.58)
\end{aligned}
$$

The properties shown in Eqs. (A.57), (A.58) are valid also in the non-Abelian case; as we show below. For the Wilson lines, the only difference in the non-Abelian case is that the exponent is matrix-valued and we therefore need to specify an ordering prescription. The proper prescription is to define

$$
\left[z,y\right]_A = \mathbf{P}\exp\left[ig\int_{s_y}^{s_z}\frac{dx^\mu}{ds}A_\mu^b\left(x(s)\right)t^b\right] , \qquad (A.59)
$$

where $\mathbf{P}$ indicates the path ordering of the integrands in such a way that an integrand evaluated at a given value of s appears to the right of integrands evaluated at larger values of the parameter s, while it appears to the left of integrands evaluated at smaller values of the parameter s. In the adjoint Wilson line $[z,y]_A^\dagger$ the symbols $\mathbf{P}$ indicates the opposite ordering prescription with respect to the one just described. In the following, in order to keep the notation compact, we introduce a symbol for the argument of the integrand in Eq. (A.59):

$$
\boldsymbol{F}(s) \equiv \frac{dx^\mu}{ds}A_\mu^b\left(x(s)\right)t^b . \qquad (A.60)
$$

We use boldface fonts for $\boldsymbol{F}$ to indicate that these objects are matrices. By employing the usual series representation of the exponential

$$e^x = \sum_{n=0}^{\infty} \frac{x^n}{n!}\,, \tag{A.61}$$

one can rewrite the Wilson line as

$$[z,y]_A = \sum_{n=0}^{\infty} \frac{(ig)^n}{n!} \int_{s_y}^{s_z} ds_1 \int_{s_y}^{s_z} ds_2 \cdots \int_{s_y}^{s_z} ds_n \mathbf{P}\left\{\boldsymbol{F}(s_1)\boldsymbol{F}(s_2)\cdots\boldsymbol{F}(s_n)\right\}\,. \tag{A.62}$$

The path ordering prescribes that the non-commuting functions F should be ordered considering the decreasing order of the arguments. Therefore, if $s_1 > s_2 > \cdots > s_n$, the product of F's in the integrand should be $F(s_1)F(s_2)\cdots F(s_n)$. The integration region in Eq. (A.62) is a n-dimensional hypercube. It is possible to subdivide the integration region in $n!$ subregions, which correspond to the $n!$ possible ordering of the elements in the set $\{s_1, s_2, \cdots, s_n\}$. The $n!$ integration regions are simplexes, as it is easy to see by considering the simple case in which $n = 2$, $s_y = 0$, and $s_z = 1$; in this case

$$\begin{aligned}
\int_0^1 ds_1 \int_0^1 ds_2 \mathbf{P}\left\{\boldsymbol{F}(s_1)\boldsymbol{F}(s_2)\right\} &= \int_0^1 ds_1 \int_0^{s_1} ds_2 \boldsymbol{F}(s_1)\boldsymbol{F}(s_2) + \int_0^1 ds_2 \int_0^{s_2} ds_2 \boldsymbol{F}(s_2)\boldsymbol{F}(s_1)\,, \\
&= 2\int_0^1 ds_1 \int_0^{s_1} ds_2 \boldsymbol{F}(s_1)\boldsymbol{F}(s_2)\,.
\end{aligned} \tag{A.63}$$

This procedure can be generalized to the n-dimensional case, each of the integration regions give the same contribution so that one can eliminate the path ordering and multiply by $n!$ each term[4] in Eq. (A.62):

$$[z,y]_A = \sum_{n=0}^{\infty} (ig)^n \int_{s_y}^{s_z} ds_1 \int_{s_y}^{s_1} ds_2 \cdots \int_{s_y}^{s_{n-1}} ds_n \boldsymbol{F}(s_1)\boldsymbol{F}(s_2)\cdots\boldsymbol{F}(s_n)\,. \tag{A.65}$$

We then redefine $s_y \equiv s_0$ and $s_z \equiv s$ and we calculate the derivative of the Wilson line with respect to s

$$\frac{d}{ds}\left[x(s), x(s_0)\right]_A = \frac{d}{ds}\left(\mathbf{1} + ig\int_{s_0}^{s} ds_1 \boldsymbol{F}(s_1) + (ig)^2 \int_{s_0}^{s} ds_1 \int_{s_0}^{s_1} ds_2 \boldsymbol{F}(s_1)\boldsymbol{F}(s_2) + \cdots\right)\,. \tag{A.66}$$

[4] Following the same procedure, but taking into account the opposite path ordering prescription, the adjunct Wilson line can be written as

$$[z,y]_A^\dagger = \sum_{n=0}^{\infty} (-ig)^n \int_{s_y}^{s_z} ds_1 \int_{s_1}^{s_z} ds_2 \cdots \int_{s_{n-1}}^{s_z} ds_n \boldsymbol{F}(s_1)\boldsymbol{F}(s_2)\cdots\boldsymbol{F}(s_n)\,. \tag{A.64}$$

It is easy to take the derivative in each term in the r.h.s. of the equation above by observing that for a generic function $g(s)$

$$\frac{d}{ds}\int_{s_0}^{s} dt g(t) = g(s)\,. \tag{A.67}$$

Eq. (A.66) becomes

$$\begin{aligned}
\frac{d}{ds}\left[x(s),x(s_0)\right]_A &= (ig)\boldsymbol{F}(s) + (ig)^2\boldsymbol{F}(s)\int_{s_0}^{s} ds_2 \boldsymbol{F}(s_2) \\
&\quad + (ig)^3\boldsymbol{F}(s)\int_{s_0}^{s} ds_2 \boldsymbol{F}(s_2)\int_{s_0}^{s_2} ds_3 \boldsymbol{F}(s_3) + \cdots\,, \\
&= (ig)\boldsymbol{F}(s)\left[x(s),x(s_0)\right]_A\,, \\
&= (ig)\frac{dx^\mu}{ds}A^b_\mu\left(x(s)\right)t^b\left[x(s),x(s_0)\right]_A\,.
\end{aligned} \tag{A.68}$$

It is now trivial to see that

$$\frac{dx^\mu}{ds}\left(\frac{\partial}{\partial x^\mu} - igA^b_\mu\left(x(s)\right)t^b\right)\left[x(s),x(s_0)\right]_A = \frac{dx^\mu}{ds}D_\mu\left[x(s),x(s_0)\right]_A = 0\,, \tag{A.69}$$

and therefore the covariant derivative of the Wilson line along the path is zero also in the non-Abelian case. Once an initial condition is specified, this first order differential equation determines the Wilson line. The initial condition is simply that the Wilson line of zero length is the identity matrix $[x(s_y),y]_A = [y,y]_A = \mathbf{1}$. The Wilson lines along the path P from y to z is the unique solution of the differential equation in Eq. (A.69) which satisfies the initial condition $[y,y]_A = \mathbf{1}$.

Finally, we are ready to prove that also in the non-Abelian case the Wilson line transforms according to Eq. (A.57) under gauge transformations. Let us define the quantity

$$[x,y]_{A'} = V(x)[x,y]_A V^\dagger(y)\,, \tag{A.70}$$

And prove that it satisfies the differential equation (A.69) when the covariant derivative depends on the field A', which is the gauge transformation of the field A. In fact

$$\begin{aligned}
\frac{dx^\mu}{ds}D_\mu(A')[x,y]_{A'} &= \frac{dx^\mu}{ds}D_\mu(A')V(x)[x,y]_A V^\dagger(y)\,, \\
&= \frac{dx^\mu}{ds}V(x)D_\mu(A)V^\dagger(x)V(x)[x,y]_A V^\dagger(y)\,, \\
&= V(x)\frac{dx^\mu}{ds}D_\mu(A)[x,y]_{A'}V^\dagger(y) = 0\,,
\end{aligned} \tag{A.71}$$

where the last equality follows from the fact that $[x,y]_A$ is the solution of Eq. (A.69). Our proof is completed by checking that $[x,y]_{A'}$ also satisfies the correct initial condition

$$[y,y]_{A'} = V(y)\underbrace{[y,y]_A}_{=1}V^\dagger(y) = 1\,. \tag{A.72}$$

Therefore the non-Abelian Wilson lines transform according to Eq. (A.70) under gauge transformations.

A.4. Evolution equation for the PDFs in Laplace space

In this Appendix we derive the expression in terms of the Laplace transform for the simplified Altarelli-Parisi evolution equation in Eq. (4.31). The Laplace transform of the PDFs was defined in Eq. (4.33). One starts by rewriting Eq. (4.31) as

$$\frac{df_{q/N}(y,\mu)}{d\ln\mu} = \int_0^{\bar{y}} d\bar{x}\ \left[P(x) f_{q/N}(y+\bar{x},\mu) + \mathcal{O}(\bar{x})\right] , \tag{A.73}$$

where $\bar{x} \equiv 1-x$ and $\bar{y} \equiv 1-y$. We are working in the limit in which $\bar{y} \to 0$, therefore the subleading terms in $\bar{x}$ in the integrand can be neglected. By taking the Laplace transform of Eq. (A.73) with respect to y one finds

$$\frac{d\tilde{f}(\tau,\mu)}{d\ln\mu} = \int_0^{\infty} d\bar{y} \exp\left(-\frac{\bar{y}}{\tau e^{\gamma_E}}\right) \int_0^{\infty} d\bar{x} P(x) f_{q/N}(y+\bar{x},\mu)\theta\left(\bar{y}-\bar{x}\right) . \tag{A.74}$$

The Laplace transform of a convolution of two function is the product of the Laplace transforms of the two functions; in fact, by introducing the variable $z = y + \bar{x}$, the integral in Eq. (A.74) factors as follows

$$\begin{aligned}\frac{d\tilde{f}_{q/N}(\tau,\mu)}{d\ln\mu} &= \left(\int_0^{\infty} d\bar{x} \exp\left(-\frac{\bar{x}}{\tau e^{\gamma_E}}\right) P(x)\right)\left(\int_0^{\infty} d\bar{z} \exp\left(-\frac{\bar{z}}{\tau e^{\gamma_E}}\right) f_{q/N}(z,\mu)\right) \\ &= \tilde{P}(\tau)\tilde{f}_{q/N}(\tau,\mu) .\end{aligned} \tag{A.75}$$

Finally, one needs to calculate the Laplace transform of Eq. (4.32). A convenient way of obtaining the Laplace transform of a plus distribution is the following: one evaluates the integral

$$\int_0^{\infty} d\bar{x} \exp\left(-\frac{\bar{x}}{\tau e^{\gamma_E}}\right) \frac{1}{\bar{x}^{1-\lambda}} = e^{\gamma_E \lambda}\Gamma(\lambda)\,\tau^{\lambda} . \tag{A.76}$$

It is then possible to expand both the integrand and the r.h.s. of the equation above in the limit of vanishing λ :

$$\begin{aligned}\frac{1}{\bar{x}^{1-\lambda}} &= \frac{1}{\lambda}\delta(\bar{x}) + \left[\frac{1}{\bar{x}}\right]_+ + \lambda\left[\frac{\ln\bar{x}}{\bar{x}}\right]_+ + \dots . \\ e^{\gamma_E\lambda}\Gamma(\lambda)\,\tau^{\lambda} &= \frac{1}{\lambda} + \ln\tau + \frac{1}{2}\left(\frac{\pi^2}{6} + \ln^2\tau\right)\lambda + \dots .\end{aligned} \tag{A.77}$$

It is then straightforward to conclude that

$$\tilde{P}(\tau) = 2C_F\gamma_{\text{cusp}}(\alpha_s)\ln\tau + 2\gamma^{f_q}(\alpha_s) . \tag{A.78}$$

This proves that Eq. (4.34) is satisfied.

A.5. Anomalous Dimensions

For the conveninence of the reader, we collect here the explicit expressions of the coefficients of the anomalous dimensions and the QCD β-function needed for slepton-pair production and stop-pair production.

We first define the expansion coefficients of the anomalous dimensions and QCD β-function as

$$\begin{aligned}\Gamma_{\text{cusp}}(\alpha_s) &= \Gamma_0 \frac{\alpha_s}{4\pi} + \Gamma_1 \left(\frac{\alpha_s}{4\pi}\right)^2 + \Gamma_2 \left(\frac{\alpha_s}{4\pi}\right)^3 + \dots\,, \\ \beta(\alpha_s) &= -2\alpha_s \left[\beta_0 \frac{\alpha_s}{4\pi} + \beta_1 \left(\frac{\alpha_s}{4\pi}\right)^2 + \beta_2 \left(\frac{\alpha_s}{4\pi}\right)^3 + \dots\right], \end{aligned} \tag{A.79}$$

and similarly for the other anomalous dimensions (recall that $\Gamma_{\text{cusp}} = C_F \gamma_{\text{cusp}}$ for the $q\bar{q}$ channel, and $\Gamma_{\text{cusp}} = C_A \gamma_{\text{cusp}}$ for the gg channel). In terms of these quantities, the function a_Γ is given by [3, 97]

$$\begin{aligned} a_\Gamma(\nu,\mu) &= \frac{\Gamma_0}{2\beta_0} \Bigg\{ \ln \frac{\alpha_s(\mu)}{\alpha_s(\nu)} + \left(\frac{\Gamma_1}{\Gamma_0} - \frac{\beta_1}{\beta_0}\right) \frac{\alpha_s(\mu) - \alpha_s(\nu)}{4\pi} \\ &\quad + \left[\frac{\Gamma_2}{\Gamma_0} - \frac{\beta_2}{\beta_0} - \frac{\beta_1}{\beta_0}\left(\frac{\Gamma_1}{\Gamma_0} - \frac{\beta_1}{\beta_0}\right)\right] \frac{\alpha_s^2(\mu) - \alpha_s^2(\nu)}{32\pi^2} + \dots \Bigg\}, \end{aligned} \tag{A.80}$$

and the result for the Sudakov factor S reads

$$\begin{aligned} S(\nu,\mu) &= \frac{\Gamma_0}{4\beta_0^2} \Bigg\{ \frac{4\pi}{\alpha_s(\nu)} \left(1 - \frac{1}{r} - \ln r\right) + \left(\frac{\Gamma_1}{\Gamma_0} - \frac{\beta_1}{\beta_0}\right)(1 - r + \ln r) + \frac{\beta_1}{2\beta_0} \ln^2 r \\ &\quad + \frac{\alpha_s(\nu)}{4\pi} \Bigg[\left(\frac{\beta_1 \Gamma_1}{\beta_0 \Gamma_0} - \frac{\beta_2}{\beta_0}\right)(1 - r + r\ln r) + \left(\frac{\beta_1^2}{\beta_0^2} - \frac{\beta_2}{\beta_0}\right)(1 - r)\ln r \\ &\quad - \left(\frac{\beta_1^2}{\beta_0^2} - \frac{\beta_2}{\beta_0} - \frac{\beta_1 \Gamma_1}{\beta_0 \Gamma_0} + \frac{\Gamma_2}{\Gamma_0}\right) \frac{(1-r)^2}{2} \Bigg] \\ &\quad + \left(\frac{\alpha_s(\nu)}{4\pi}\right)^2 \Bigg[\left(\frac{\beta_1 \beta_2}{\beta_0^2} - \frac{\beta_1^3}{2\beta_0^3} - \frac{\beta_3}{2\beta_0} + \frac{\beta_1}{\beta_0}\left(\frac{\Gamma_2}{\Gamma_0} - \frac{\beta_2}{\beta_0} + \frac{\beta_1^2}{\beta_0^2} - \frac{\beta_1 \Gamma_1}{\beta_0 \Gamma_0}\right) \frac{r^2}{2} \right) \ln r \\ &\quad + \left(\frac{\Gamma_3}{\Gamma_0} - \frac{\beta_3}{\beta_0} + \frac{2\beta_1\beta_2}{\beta_0^2} + \frac{\beta_1^2}{\beta_0^2}\left(\frac{\Gamma_1}{\Gamma_0} - \frac{\beta_1}{\beta_0}\right) - \frac{\beta_2 \Gamma_1}{\beta_0 \Gamma_0} - \frac{\beta_1 \Gamma_2}{\beta_0 \Gamma_0}\right) \frac{(1-r)^3}{3} \\ &\quad + \left(\frac{3\beta_3}{4\beta_0} - \frac{\Gamma_3}{2\Gamma_0} + \frac{\beta_1^3}{\beta_0^3} - \frac{3\beta_1^2 \Gamma_1}{4\beta_0^2 \Gamma_0} + \frac{\beta_2 \Gamma_1}{\beta_0 \Gamma_0} + \frac{\beta_1 \Gamma_2}{4\beta_0 \Gamma_0} - \frac{7\beta_1 \beta_2}{4\beta_0^2}\right)(1-r)^2 \end{aligned}$$

$$+\left(\frac{\beta_1\beta_2}{\beta_0^2}-\frac{\beta_3}{\beta_0}-\frac{\beta_1^2\Gamma_1}{\beta_0^2\Gamma_0}+\frac{\beta_1\Gamma_2}{\beta_0\Gamma_0}\right)\frac{1-r}{2}\Bigg]+\dots\Bigg\}, \tag{A.81}$$

where $r=\alpha_s(\mu)/\alpha_s(\nu)$.

The QCD beta function up to four loops is given by

$$\begin{aligned}
\beta_0 &= \frac{11}{3}\,C_A-\frac{4}{3}\,T_F n_f\,,\\
\beta_1 &= \frac{34}{3}\,C_A^2-\frac{20}{3}\,C_A T_F n_f-4C_F T_F n_f\,, \qquad\qquad (A.82)\\
\beta_2 &= \frac{2857}{54}\,C_A^3+\left(2C_F^2-\frac{205}{9}\,C_F C_A-\frac{1415}{27}\,C_A^2\right)T_F n_f+\left(\frac{44}{9}\,C_F+\frac{158}{27}\,C_A\right)T_F^2 n_f^2\,,\\
\beta_3 &= \frac{149753}{6}+3564\zeta_3-\left(\frac{1078361}{162}+\frac{6508}{27}\,\zeta_3\right)n_f+\left(\frac{50065}{162}+\frac{6472}{81}\,\zeta_3\right)n_f^2+\frac{1093}{729}\,n_f^3\,.
\end{aligned}$$

where $T_F=1/2$ and n_f is the number of active quark flavors.

The coefficients for the cusp anomalous dimension are [98]

$$\begin{aligned}
\gamma_0^{\rm cusp} &= 4\,,\\
\gamma_1^{\rm cusp} &= \left(\frac{268}{9}-\frac{4\pi^2}{3}\right)C_A-\frac{80}{9}\,T_F n_f\,,\\
\gamma_2^{\rm cusp} &= C_A^2\left(\frac{490}{3}-\frac{536\pi^2}{27}+\frac{44\pi^4}{45}+\frac{88}{3}\,\zeta_3\right)+C_A T_F n_f\left(-\frac{1672}{27}+\frac{160\pi^2}{27}-\frac{224}{3}\,\zeta_3\right)\\
&\quad +C_F T_F n_f\left(-\frac{220}{3}+64\zeta_3\right)-\frac{64}{27}\,T_F^2 n_f^2\,. \qquad\qquad (A.83)
\end{aligned}$$

For the four-loop coefficient $\gamma_3^{\rm cusp}$ we use the Padé approximant $\gamma_3^{\rm cusp}=\gamma_2^{\rm cusp\,2}/\gamma_1^{\rm cusp}$.

The anomalous dimension $\gamma^q=\gamma^{\bar q}$ can be determined from the three-loop expression for the divergent part of the on-shell quark form factor in QCD [99]. The result was extracted in [3]. In the notation of this thesis $2\gamma^q=\gamma^V$. One obtains

$$\begin{aligned}
\gamma_0^q &= -3C_F\,,\\
\gamma_1^q &= C_F^2\left(-\frac{3}{2}+2\pi^2-24\zeta_3\right)+C_F C_A\left(-\frac{961}{54}-\frac{11\pi^2}{6}+26\zeta_3\right)+C_F T_F n_f\left(\frac{130}{27}+\frac{2\pi^2}{3}\right),\\
\gamma_2^q &= C_F^3\left(-\frac{29}{2}-3\pi^2-\frac{8\pi^4}{5}-68\zeta_3+\frac{16\pi^2}{3}\,\zeta_3+240\zeta_5\right)\\
&\quad +C_F^2 C_A\left(-\frac{151}{4}+\frac{205\pi^2}{9}+\frac{247\pi^4}{135}-\frac{844}{3}\,\zeta_3-\frac{8\pi^2}{3}\,\zeta_3-120\zeta_5\right)
\end{aligned}$$

$$
\begin{aligned}
&+ C_F C_A^2 \left(-\frac{139345}{2916} - \frac{7163\pi^2}{486} - \frac{83\pi^4}{90} + \frac{3526}{9}\,\zeta_3 - \frac{44\pi^2}{9}\,\zeta_3 - 136\zeta_5 \right) \\
&+ C_F^2 T_F n_f \left(\frac{2953}{27} - \frac{26\pi^2}{9} - \frac{28\pi^4}{27} + \frac{512}{9}\,\zeta_3 \right) \\
&+ C_F C_A T_F n_f \left(-\frac{17318}{729} + \frac{2594\pi^2}{243} + \frac{22\pi^4}{45} - \frac{1928}{27}\,\zeta_3 \right) \\
&+ C_F T_F^2 n_f^2 \left(\frac{9668}{729} - \frac{40\pi^2}{27} - \frac{32}{27}\,\zeta_3 \right) . \qquad \text{(A.84)}
\end{aligned}
$$

Similarly, the expression for the gluon anomalous dimension can be extracted from the divergent part of the gluon form factor obtained in [99]. One finds

$$
\begin{aligned}
\gamma_0^g &= -\beta_0 = -\frac{11}{3}\,C_A + \frac{4}{3}\,T_F n_f \,, \\
\gamma_1^g &= C_A^2 \left(-\frac{692}{27} + \frac{11\pi^2}{18} + 2\zeta_3 \right) + C_A T_F n_f \left(\frac{256}{27} - \frac{2\pi^2}{9} \right) + 4 C_F T_F n_f \,, \\
\gamma_2^g &= C_A^3 \left(-\frac{97186}{729} + \frac{6109\pi^2}{486} - \frac{319\pi^4}{270} + \frac{122}{3}\,\zeta_3 - \frac{20\pi^2}{9}\,\zeta_3 - 16\zeta_5 \right) \\
&\quad + C_A^2 T_F n_f \left(\frac{30715}{729} - \frac{1198\pi^2}{243} + \frac{82\pi^4}{135} + \frac{712}{27}\,\zeta_3 \right) \\
&\quad + C_A C_F T_F n_f \left(\frac{2434}{27} - \frac{2\pi^2}{3} - \frac{8\pi^4}{45} - \frac{304}{9}\,\zeta_3 \right) - 2 C_F^2 T_F n_f \\
&\quad + C_A T_F^2 n_f^2 \left(-\frac{538}{729} + \frac{40\pi^2}{81} - \frac{224}{27}\,\zeta_3 \right) - \frac{44}{9}\,C_F T_F^2 n_f^2 \,. \qquad \text{(A.85)}
\end{aligned}
$$

These results for γ^q and γ^g are valid in conventional dimensional regularization, where polarization vectors and spinors of all particles are treated as d-dimensional objects (so that gluons have $(2-2\varepsilon)$ helicity states).

The first two coefficients of the anomalous dimension for massive quarks are [82].

$$
\begin{aligned}
\gamma_0^Q &= -2C_F \,, \\
\gamma_1^Q &= C_F C_A \left(-\frac{98}{9} + \frac{2\pi^2}{3} - 4\zeta_3 \right) + \frac{40}{9} C_F T_F n_f \,. \qquad \text{(A.86)}
\end{aligned}
$$

The cusp anomalous dimension for massive partons which depends on hyperbolic angles β_{IJ} are given by [82, 100–102]

$$
\gamma_0^{\text{cusp}}(\beta) = \gamma_0^{\text{cusp}} \beta \coth \beta \,,
$$

$$\begin{aligned}\gamma_1^{\rm cusp}(\beta) &= \gamma_1^{\rm cusp}\beta\coth\beta + 8C_A\Bigg\{\frac{\pi^2}{6}+\zeta_3+\beta^2 \\ &\quad + \coth^2\beta\left[\mathrm{Li}_3(e^{-2\beta})+\beta\mathrm{Li}_2(e^{-2\beta})-\zeta_3+\frac{\pi^2}{6}\beta+\frac{\beta^3}{3}\right] \\ &\quad + \coth\beta\left[\mathrm{Li}_2(e^{-2\beta})-2\beta\ln(1-e^{-2\beta})-\frac{\pi^2}{6}(1+\beta)-\beta^2-\frac{\beta^3}{3}\right]\Bigg\} \quad \text{(A.87)}\end{aligned}$$

$$\text{(A.88)}$$

$$\begin{aligned} g_0(\beta) &= 0, \\ g_1(\beta) &= \coth\beta\left[\beta^2+2\beta\ln(1-e^{-2\beta})-\mathrm{Li}_2(e^{-2\beta})+\frac{\pi^2}{6}\right]-\beta^2-\frac{\pi^2}{6}. \quad \text{(A.89)}\end{aligned}$$

The anomalous dimension describing the evolution of the quark PDFs near $x=1$ is [8]

$$\begin{aligned}\gamma_0^{f_q} &= 3C_F\,, \\ \gamma_1^{f_q} &= C_F^2\left(\frac{3}{2}-2\pi^2+24\zeta(3)\right)+C_FC_A\left(\frac{17}{6}+\frac{22\pi^2}{9}-12\zeta_3\right)-C_FT_Fn_f\left(\frac{2}{3}+\frac{8\pi^2}{9}\right) \quad \text{(A.90)}\end{aligned}$$

Similarly, for the gluon case, one finds

$$\begin{aligned}\gamma_0^{f_g} &= \beta_0\,, \\ \gamma_1^{f_g} &= C_A^2\left(\frac{32}{3}+12\zeta_3\right)-\frac{16}{3}C_AT_Fn_f-4C_FT_Fn_f\,. \quad \text{(A.91)}\end{aligned}$$

A.6. Loop Integrals for SUSY corrections in slepton-pair production

Here we provide explicit expressions for the loop functions f_B and f_C appearing in (5.17), distinguishing two kinematical regimes. Below the squark production threshold, i.e. for $M^2 \le 4m_{\tilde q}^2$, the two functions are real, while above threshold they develop an imaginary part. We first give results for the function f_B. Denoting $x = 4m_{\tilde q}^2/M^2$, we obtain

$$\begin{aligned} f_B(M^2,m_{\tilde q}^2) &= 2\sqrt{x-1}\,\arctan\frac{1}{\sqrt{x-1}}\,; \quad x\ge 1\,, \\ f_B(M^2,m_{\tilde q}^2) &= \sqrt{1-x}\left(\ln\frac{1+\sqrt{1-x}}{1-\sqrt{1-x}}-i\pi\right); \quad x<1\,. \quad \text{(A.92)}\end{aligned}$$

To express the function f_C in a compact form, it is convenient to define

$$y_0 = \frac{m_{\tilde{q}}^2 - m_{\tilde{g}}^2}{M^2}\,, \qquad y_1 = \frac{m_{\tilde{g}}^2}{m_{\tilde{g}}^2 - m_{\tilde{q}}^2}\,, \qquad y_\pm = \frac{1 \pm \sqrt{1-x}}{2}\,. \tag{A.93}$$

For $M^2 \le 4m_{\tilde{q}}^2$ we then obtain

$$\begin{aligned} f_C(M^2, m_{\tilde{q}}^2, m_{\tilde{g}}^2) \;&=\; \mathrm{Li}_2\!\left(\frac{y_0-1}{y_0-y_1}\right) - \mathrm{Li}_2\!\left(\frac{y_0}{y_0-y_1}\right) + \mathrm{Li}_2\!\left(\frac{y_0}{y_0-y_+}\right) \\ &\quad - \mathrm{Li}_2\!\left(\frac{y_0-1}{y_0-y_+}\right) + \mathrm{Li}_2\!\left(\frac{y_0}{y_0-y_-}\right) - \mathrm{Li}_2\!\left(\frac{y_0-1}{y_0-y_-}\right), \end{aligned} \tag{A.94}$$

while for $M^2 > 4m_{\tilde{q}}^2$ we get

$$\begin{aligned} f_C(M^2, m_{\tilde{q}}^2, m_{\tilde{g}}^2) \;&=\; \frac{\pi^2}{3} + \mathrm{Li}_2\!\left(\frac{y_0-1}{y_0-y_1}\right) - \mathrm{Li}_2\!\left(\frac{y_0}{y_0-y_1}\right) \\ &\quad + \mathrm{Li}_2\!\left(\frac{y_0}{y_0-y_+}\right) + \mathrm{Li}_2\!\left(\frac{y_0-y_+}{y_0-1}\right) + \frac{1}{2}\left[\ln\left(\frac{y_0-1}{y_0-y_+}\right) + i\pi\right]^2 \\ &\quad + \mathrm{Li}_2\!\left(\frac{y_0}{y_0-y_-}\right) + \mathrm{Li}_2\!\left(\frac{y_0-y_-}{y_0-1}\right) + \frac{1}{2}\left[\ln\left(\frac{y_0-1}{y_0-y_-}\right) - i\pi\right]^2. \end{aligned} \tag{A.95}$$

In the special case of equal masses, $m_{\tilde{g}} = m_{\tilde{q}}$, these results simplify significantly. We then obtain

$$c_{V,\mathrm{SUSY}}^{(1)} = C_F\left[3 - f_B(M^2, m_{\tilde{q}}^2) + \frac{2m_{\tilde{q}}^2}{M^2}\, f_C(M^2, m_{\tilde{q}}^2, m_{\tilde{q}}^2)\right], \tag{A.96}$$

where (with $x = 4m_{\tilde{q}}^2/M^2$ as before)

$$\begin{aligned} f_C(M^2, m_{\tilde{q}}^2, m_{\tilde{q}}^2) \;&=\; -2\arctan^2\frac{1}{\sqrt{x-1}}\,; \quad x \ge 1\,, \\ f_C(M^2, m_{\tilde{q}}^2, m_{\tilde{q}}^2) \;&=\; \frac{1}{2}\left(\ln\frac{1+\sqrt{1-x}}{1-\sqrt{1-x}} - i\pi\right)^2; \quad x < 1\,. \end{aligned} \tag{A.97}$$

A.7. Renormalization Constants for stop-pair production

In this appendix we summarize the renormalization constants needed to renormalize the hard function for stop-pair production:

$$\Delta Z_q \;=\; -\frac{g_s^2}{2} C_F\left(\frac{1}{\varepsilon} + \ln\frac{\mu_R^2}{m_{\tilde{q}}^2}\right) + \frac{g_s^2}{2} C_F\left[\frac{m_{\tilde{q}}^2 - 3m_{\tilde{g}}^2}{2(m_{\tilde{g}}^2 - m_{\tilde{q}}^2)} + \frac{m_{\tilde{g}}^4}{(m_{\tilde{g}}^2 - m_{\tilde{q}}^2)^2}\ln\frac{m_{\tilde{g}}^2}{m_{\tilde{q}}^2}\right], \tag{A.98}$$

$$
\begin{aligned}
\Delta Z_{\tilde{t}_1} &= -g_s^2 C_F \Big[\frac{1}{\varepsilon} + \ln\frac{\mu_R^2}{m_{\tilde{t}_1}^2} + B_{0\,f}(m_{\tilde{t}_1}^2, m_t^2, m_{\tilde{g}}^2) \\
&\qquad -B_0'(m_{\tilde{t}_1}^2, m_t^2, m_{\tilde{g}}^2)\left(m_t^2 + m_{\tilde{g}}^2 - m_{\tilde{t}_1}^2 - 2m_t m_{\tilde{g}}\sin(2\alpha)\right)\Big], \qquad \text{(A.99)}
\end{aligned}
$$

$$
\begin{aligned}
\Delta Z_g &= \frac{g_s^2}{2}\Big(-\frac{\frac{2}{3}C_A + \frac{1}{3}N_l + 1}{\varepsilon} + \frac{2}{3}C_A \log\frac{m_{\tilde{g}}^2}{\mu_R^2} + \frac{N_l}{3}\log\frac{m_{\tilde{q}}^2}{\mu_R^2} \\
&\qquad +\frac{2}{3}\log\frac{m_t^2}{\mu_R^2} + \frac{1}{6}\log\frac{m_{\tilde{t}_1}^2}{\mu_R^2} + \frac{1}{6}\log\frac{m_{\tilde{t}_2}^2}{\mu_R^2}\Big), \qquad \text{(A.100)}
\end{aligned}
$$

$$
\begin{aligned}
\Delta Z_{g_s} &= -\frac{g_s^2}{2}\Big(\frac{3C_A - N_l - 1}{\varepsilon} + \frac{2}{3}C_A \log\frac{m_{\tilde{g}}^2}{\mu_R^2} + \frac{N_l}{3}\log\frac{m_{\tilde{q}}^2}{\mu_R^2} \\
&\qquad +\frac{2}{3}\log\frac{m_t^2}{\mu_R^2} + \frac{1}{6}\log\frac{m_{\tilde{t}_1}^2}{\mu_R^2} + \frac{1}{6}\log\frac{m_{\tilde{t}_2}^2}{\mu_R^2}\Big), \qquad \text{(A.101)}
\end{aligned}
$$

$$
\begin{aligned}
\Delta Z_{m_{\tilde{t}_1}} &= 2C_F g_s^2 \left(\frac{2m_t^2 + 2m_{\tilde{g}}^2 - m_{\tilde{t}_1}^2 - 2m_t m_{\tilde{g}}\sin(2\alpha)}{\varepsilon}\right) \\
&\quad +2C_F g_s^2 \left(m_t^2 + m_{\tilde{g}}^2 + m_t^2 \log\frac{\mu_R^2}{m_t^2} + m_{\tilde{g}}^2 \log\frac{\mu_R^2}{m_{\tilde{g}}^2}\right) \\
&\quad +2C_F g_s^2 \left(B_{0\,f}(m_{\tilde{t}_1}^2, m_t^2, m_{\tilde{g}}^2) + \log\frac{\mu_R^2}{m_{\tilde{t}_1}^2}\right)\left(m_t^2 + m_{\tilde{g}}^2 - m_{\tilde{t}_1}^2 - 2m_t m_{\tilde{g}}\sin(2\alpha)\right) \\
&\quad +g_s^2 C_F m_{\tilde{t}_1}^2 \left(\frac{3}{\varepsilon} + 7 + 3\log\frac{\mu_R^2}{m_{\tilde{t}_1}^2}\right) - g_s^2 C_F \cos^2(2\alpha) m_{\tilde{t}_1}^2 \left(1 + \frac{1}{\varepsilon} + \log\frac{\mu_R^2}{m_{\tilde{t}_1}^2}\right) \\
&\quad -g_s^2 C_F \sin^2(2\alpha) m_{\tilde{t}_2}^2 \left(1 + \frac{1}{\varepsilon} + \log\frac{\mu_R^2}{m_{\tilde{t}_2}^2}\right), \qquad \text{(A.102)}
\end{aligned}
$$

where μ_R is the renormalization scale and $\varepsilon = (4-d)/2$. In the above expressions the scale dependence is explicit, therefore the loop function $B_{0\,f}(m_{\tilde{t}_1}^2, m_t^2, m_{\tilde{g}}^2)$ is intended to be evaluated at the scale $\mu_R^2 = m_{\tilde{t}_1}^2$. The subscript f refers to the finite part, $\mathcal{O}(\varepsilon^0)$, of the loop function $B_0(m_{\tilde{t}_1}^2, m_t^2, m_{\tilde{g}}^2)$. ΔZ_q, ΔZ_g and $\Delta Z_{\tilde{t}_1}$ are respectively the quark, gluon and stop wave function renormalization constants. ΔZ_{g_s} is the renormalization constant for the coupling g_s and $\Delta Z_{m_{\tilde{t}_1}}$ is the mass counter term.

A.8. NLO Soft Function Formulas for stop-pair production

In this appendix we collect the results of the calculation of the NLO soft function in PIM kinematics [9] and in 1PI kinematics [10].

Since the soft functions depend on the plus distributions, it is more convenient to work with the Laplace-transformed functions. They are defined as

$$\begin{aligned}\tilde{\boldsymbol{s}}\left(L,\mu\right) &= \int_0^\infty d\omega \exp\left(-\frac{\omega}{e^{\gamma_E}\mu e^{L/2}}\right)\boldsymbol{W}\left(\omega,\mu\right)\,,\\ &= \hat{\boldsymbol{W}}\left(x_0=\frac{-2i}{e^{\gamma_E}\mu e^{L/2}},\mu\right)\,.\end{aligned} \tag{A.103}$$

In Eq. (A.103) we omitted the dependence of the soft functions on the PIM or 1PI kinematic variables and on the heavy particle masses, as well as the subscripts $q\bar{q}$ or gg indicating the channel. The equality in the second line of Eq. (A.103) was proven in [5] and follows from the functional form of the position space Wilson loops [103].

The expansion of $\tilde{\boldsymbol{s}}$ in powers of the strong coupling constant is

$$\tilde{\boldsymbol{s}} = \tilde{\boldsymbol{s}}^{(0)} + \frac{\alpha_s}{4\pi}\tilde{\boldsymbol{s}}^{(1)} + \left(\frac{\alpha_s}{4\pi}\right)^2\tilde{\boldsymbol{s}}^{(2)} + \mathcal{O}(\alpha_s^3)\,. \tag{A.104}$$

At leading order the soft functions are the same both in PIM and 1PI kinematics:

$$\tilde{\boldsymbol{s}}^{(0)}_{q\bar{q}} = \begin{pmatrix} N & 0 \\ 0 & \frac{C_F}{2}\end{pmatrix}\,, \qquad \tilde{\boldsymbol{s}}^{(0)}_{gg} = \begin{pmatrix} N & 0 & 0 \\ 0 & \frac{N}{2} & 0 \\ 0 & 0 & \frac{N^2-4}{2N}\end{pmatrix}\,. \tag{A.105}$$

The bare soft function at one-loop order in position space, can be written in d-dimensions as

$$\hat{\boldsymbol{W}}^{(1,k)}_{\rm bare}(\varepsilon,x_0,\mu) = \sum_{ij}\boldsymbol{w}_{ij}\mathcal{I}^k_{ij}(\varepsilon,x_0,\mu)\,,\quad (k=\text{PIM},1\text{PI})\,, \tag{A.106}$$

where $\varepsilon=(4-d)/2$. The matrices $\boldsymbol{w}_{ij}$ are related to the products of color generators and are the same for both kinematics. In the quark annihilation channel they are

$$\boldsymbol{w}^{q\bar{q}}_{12} = \boldsymbol{w}^{q\bar{q}}_{34} = -\frac{C_F}{4N}\begin{pmatrix} 4N^2 & 0 \\ 0 & -1\end{pmatrix}\,,$$

$$\boldsymbol{w}^{q\bar{q}}_{33} = \boldsymbol{w}^{q\bar{q}}_{44} = \frac{C_F}{2}\begin{pmatrix} 2N & 0 \\ 0 & C_F\end{pmatrix}\,,$$

$$\boldsymbol{w}^{q\bar{q}}_{13} = \boldsymbol{w}^{q\bar{q}}_{24} = -\frac{C_F}{2}\begin{pmatrix} 0 & 1 \\ 1 & 2C_F-\frac{N}{2}\end{pmatrix}\,,$$

$$\boldsymbol{w}_{14}^{q\bar{q}} = \boldsymbol{w}_{23}^{q\bar{q}} = -\frac{C_F}{2N}\begin{pmatrix} 0 & -N \\ -N & 1 \end{pmatrix}, \tag{A.107}$$

while for the gluon fusion channel one finds

$$\boldsymbol{w}_{12}^{gg} = -\frac{1}{4}\begin{pmatrix} 4N^2 & 0 & 0 \\ 0 & N^2 & 0 \\ 0 & 0 & N^2-4 \end{pmatrix},$$

$$\boldsymbol{w}_{34}^{gg} = -\begin{pmatrix} C_F N & 0 & 0 \\ 0 & -\frac{1}{4} & 0 \\ 0 & 0 & -\frac{N^2-4}{4N^2} \end{pmatrix},$$

$$\boldsymbol{w}_{33}^{gg} = \boldsymbol{w}_{44}^{gg} = \frac{C_F}{2N}\begin{pmatrix} 2N^2 & 0 & 0 \\ 0 & N^2 & 0 \\ 0 & 0 & N^2-4 \end{pmatrix},$$

$$\boldsymbol{w}_{13}^{gg} = \boldsymbol{w}_{24}^{gg} = -\frac{1}{8}\begin{pmatrix} 0 & 4N & 0 \\ 4N & N^2 & N^2-4 \\ 0 & N^2-4 & N^2-4 \end{pmatrix},$$

$$\boldsymbol{w}_{14}^{gg} = \boldsymbol{w}_{23}^{gg} = -\frac{1}{8}\begin{pmatrix} 0 & -4N & 0 \\ -4N & N^2 & -(N^2-4) \\ 0 & -(N^2-4) & N^2-4 \end{pmatrix}. \tag{A.108}$$

The functions $\mathcal{I}_{ij}^{i}$ are integrals over the soft gluon phase space. In PIM kinematics one finds $\mathcal{I}_{11}^{\mathrm{PIM}} = \mathcal{I}_{22}^{\mathrm{PIM}} = 0$ and

$$\mathcal{I}_{12}^{\mathrm{PIM}} = -\left(\frac{2}{\varepsilon^2} + \frac{2}{\varepsilon}L_0 + L_0^2 + \frac{\pi^2}{6}\right),$$

$$\mathcal{I}_{33}^{\mathrm{PIM}} = \mathcal{I}_{44}^{\mathrm{PIM}} = \frac{2}{\varepsilon} + 2L_0 - \frac{2}{\beta_t}\ln x_s\,,$$

$$\mathcal{I}_{34}^{\mathrm{PIM}} = -\frac{1+x_s^2}{1-x_s^2}\left[\left(\frac{2}{\varepsilon} + 2L_0\right)\ln x_s - \ln^2 x_s + 4\ln x_s\ln(1-x_s) + 4\mathrm{Li}_2(x_s) - \frac{2\pi^2}{3}\right],$$

$$\mathcal{I}_{13}^{\mathrm{PIM}} = \mathcal{I}_{24}^{\mathrm{PIM}} = -\left[\frac{1}{2}\left(L_0 - \ln\frac{(1+y_t)^2 x_s}{(1+x_s)^2}\right)^2 + \frac{\pi^2}{12} + 2\mathrm{Li}_2\left(\frac{1-x_s y_t}{1+x_s}\right) + 2\mathrm{Li}_2\left(\frac{x_s-y_t}{1+x_s}\right)\right],$$

$$\mathcal{I}_{14}^{\mathrm{PIM}} = \mathcal{I}_{23}^{\mathrm{PIM}} = \mathcal{I}_{13}(y_t \to z_u)\,, \tag{A.109}$$

where $x_s = (1-\beta_{\tilde{t}_1})/(1+\beta_{\tilde{t}_1})$, $y_t = -\hat{t}_1/m_{\tilde{t}_1}^2 - 1$, $z_u = -\hat{u}_1/m_{\tilde{t}_1}^2 - 1$, and

$$L_0 = \ln\left(-\frac{\mu^2 x_0^2 e^{2\gamma_E}}{4}\right). \tag{A.110}$$

In 1PI kinematics one finds $\mathcal{I}_{11}^{\rm 1PI} = \mathcal{I}_{22}^{\rm 1PI} = 0$ and

$$\begin{aligned}
\mathcal{I}_{12}^{\rm 1PI} &= -\left[\frac{2}{\varepsilon^2} + \frac{2}{\varepsilon}\left(L_0 - \ln\frac{\hat{s}' m_{\tilde{t}_1}^2}{\hat{t}_1'\hat{u}_1'}\right) + \left(L_0 - \ln\frac{\hat{s}' m_{\tilde{t}_1}^2}{\hat{t}_1'\hat{u}_1'}\right)^2 + \frac{\pi^2}{6} + 2\mathrm{Li}_2\left(1 - \frac{\hat{s}' m_{\tilde{t}_1}^2}{\hat{t}_1'\hat{u}_1'}\right)\right], \\
\mathcal{I}_{33}^{\rm 1PI} &= \frac{2}{\varepsilon} + 2L_0 - \frac{2(1+\beta_{\tilde{t}_1}^2)}{\beta_{\tilde{t}_1}}\ln x_s\,, \\
\mathcal{I}_{44}^{\rm 1PI} &= \frac{2}{\varepsilon} + 2L_0 + 4\,, \\
\mathcal{I}_{14}^{\rm 1PI} = \mathcal{I}_{24}^{\rm 1PI} &= -\frac{1}{\varepsilon^2} - \frac{1}{\varepsilon}L_0 - \frac{1}{2}L_0^2 - \frac{\pi^2}{12}\,, \\
\mathcal{I}_{13}^{\rm 1PI} &= -\left[\frac{1}{\varepsilon^2} + \frac{1}{\varepsilon}\left(L_0 - 2\ln\frac{\hat{t}_1'}{\hat{u}_1'}\right) + \frac{1}{2}\left(L_0 - 2\ln\frac{\hat{t}_1'}{\hat{u}_1'}\right)^2 + \frac{\pi^2}{12}\right. \\
&\qquad \left. + 2\mathrm{Li}_2\left(1 - \frac{\hat{t}_1}{\hat{u}_1' x_s}\right) + 2\mathrm{Li}_2\left(1 - \frac{\hat{t}_1' x_s}{\hat{u}_1'}\right)\right], \\
\mathcal{I}_{23}^{\rm 1PI} &= \mathcal{I}_{13}'\,(\hat{t}_1 \leftrightarrow \hat{u}_1)\,, \\
\mathcal{I}_{34}^{\rm 1PI} &= \frac{1+\beta_{\tilde{t}_1}^2}{2\beta_{\tilde{t}_1}}\left[-\frac{2}{\varepsilon}\ln x_s - 2L_0\ln x_s + 2\ln^2 x_s - 4\ln x_s\ln(1-x_s^2) - 2\mathrm{Li}_2(x_s^2) + \frac{\pi^2}{3}\right].
\end{aligned} \tag{A.111}$$

Bibliography

[1] G. F. Sterman, *Summation of Large Corrections to Short Distance Hadronic Cross-Sections*, *Nucl. Phys.* **B281** (1987) 310. 8, 67, 83

[2] S. Catani and L. Trentadue, *Resummation of the QCD Perturbative Series for Hard Processes*, *Nucl. Phys.* **B327** (1989) 323. 8, 67, 83

[3] T. Becher, M. Neubert and B. D. Pecjak, *Factorization and momentum-space resummation in deep- inelastic scattering*, *JHEP* **01** (2007) 076 [hep-ph/0607228]. 8, 144, 145

[4] T. Becher and M. Neubert, *Threshold resummation in momentum space from effective field theory*, *Phys.Rev.Lett.* **97** (2006) 082001 [hep-ph/0605050]. 8, 86

[5] T. Becher, M. Neubert and G. Xu, *Dynamical Threshold Enhancement and Resummation in Drell- Yan Production*, *JHEP* **07** (2008) 030 [0710.0680]. 8, 10, 34, 67, 75, 79, 81, 83, 85, 86, 87, 88, 150

[6] V. Ahrens, T. Becher, M. Neubert and L. L. Yang, *Renormalization-Group Improved Prediction for Higgs Production at Hadron Colliders*, *Eur.Phys.J.* **C62** (2009) 333–353 [0809.4283]. 8, 34, 88

[7] V. Ahrens, T. Becher, M. Neubert and L. L. Yang, *Origin of the Large Perturbative Corrections to Higgs Production at Hadron Colliders*, *Phys.Rev.* **D79** (2009) 033013 [0808.3008]. 8, 34

[8] T. Becher and M. D. Schwartz, *Direct photon production with effective field theory*, *JHEP* **02** (2010) 040 [0911.0681]. 8, 147

[9] V. Ahrens, A. Ferroglia, M. Neubert, B. D. Pecjak and L. L. Yang, *Renormalization-Group Improved Predictions for Top-Quark Pair Production at Hadron Colliders*, *JHEP* **09** (2010) 097 [1003.5827]. 8, 10, 34, 88, 99, 100, 103, 105, 106, 110, 112, 113, 118, 150

[10] V. Ahrens, A. Ferroglia, M. Neubert, B. D. Pecjak and L.-L. Yang, *RG-improved single-particle inclusive cross sections and forward-backward asymmetry in $t\bar{t}$ production at hadron colliders*, *JHEP* **09** (2011) 070 [1103.0550]. 8, 10, 34, 99, 100, 105, 106, 110, 113, 114, 116, 118, 150

[11] M. Beneke, P. Falgari and C. Schwinn, *Threshold resummation for pair production of coloured heavy (s)particles at hadron colliders*, *Nucl.Phys.* **B842** (2011) 414–474 [1007.5414]. 8, 101

[12] M. Beneke, P. Falgari, S. Klein and C. Schwinn, *Hadronic top-quark pair production with NNLL threshold resumption*, *Nucl.Phys.* **B855** (2012) 695–741 [1109.1536]. 8

[13] P. Falgari, C. Schwinn and C. Wever, *NLL soft and Coulomb resummation for squark and gluino production at the LHC*, *JHEP* **1206** (2012) 052 [1202.2260]. 8, 101

[14] H. Baer, B. Harris and M. H. Reno, *Next-to-leading order slepton pair production at hadron colliders*, *Phys.Rev.* **D57** (1998) 5871–5874 [hep-ph/9712315]. 9, 82

[15] W. Beenakker, M. Klasen, M. Kramer, T. Plehn, M. Spira *et. al.*, *The Production of charginos/neutralinos and sleptons at hadron colliders*, *Phys.Rev.Lett.* **83** (1999) 3780–3783 [hep-ph/9906298]. 9, 82, 85, 96

[16] A. Djouadi and M. Spira, *SUSY-QCD corrections to Higgs boson production at hadron colliders*, *Phys.Rev.* **D62** (2000) 014004 [hep-ph/9912476]. 9, 82

[17] G. Bozzi, B. Fuks and M. Klasen, *Threshold resummation for slepton-pair production at hadron colliders*, *Nucl.Phys.* **B777** (2007) 157–181 [hep-ph/0701202]. 9, 83, 85, 96

[18] W. Beenakker, M. Kramer, T. Plehn, M. Spira and P. Zerwas, *Stop production at hadron colliders*, *Nucl.Phys.* **B515** (1998) 3–14 [hep-ph/9710451]. 9, 99, 104, 108

[19] J. Wess and B. Zumino, *A Lagrangian Model Invariant Under Supergauge Transformations*, *Phys.Lett.* **B49** (1974) 52. 11

[20] J. Wess and B. Zumino, *Supergauge Transformations in Four-Dimensions*, *Nucl.Phys.* **B70** (1974) 39–50. 11

[21] S. P. Martin, *A Supersymmetry primer*, hep-ph/9709356. 12, 26, 28, 29

[22] A. Djouadi, *The Anatomy of electro-weak symmetry breaking. II. The Higgs bosons in the minimal supersymmetric model*, *Phys.Rept.* **459** (2008) 1–241 [hep-ph/0503173]. 12

[23] H. P. Nilles, *Supersymmetry, Supergravity and Particle Physics*, *Phys.Rept.* **110** (1984) 1–162. 14

[24] R. Haag, J. T. Lopuszanski and M. Sohnius, *All Possible Generators of Supersymmetries of the s Matrix*, *Nucl.Phys.* **B88** (1975) 257. 14

[25] S. R. Coleman and J. Mandula, *All possible symmetries of the S matrix*, *Phys.Rev.* **159** (1967) 1251–1256. 14

[26] R. A. Flores and M. Sher, *Higgs Masses in the Standard, Multi-Higgs and Supersymmetric Models*, *Annals Phys.* **148** (1983) 95. 31

[27] K. Inoue, A. Kakuto, H. Komatsu and S. Takeshita, *Low-Energy Parameters and Particle Masses in a Supersymmetric Grand Unified Model*, *Prog.Theor.Phys.* **67** (1982) 1889. 31

[28] C. W. Bauer, S. Fleming and M. E. Luke, *Summing Sudakov logarithms in $B \to X_s\gamma$ in effective field theory*, *Phys.Rev.* **D63** (2000) 014006 [hep-ph/0005275]. 33

[29] C. W. Bauer, S. Fleming, D. Pirjol and I. W. Stewart, *An effective field theory for collinear and soft gluons: Heavy to light decays*, *Phys. Rev.* **D63** (2001) 114020 [hep-ph/0011336]. 33

[30] C. W. Bauer and I. W. Stewart, *Invariant operators in collinear effective theory*, *Phys.Lett.* **B516** (2001) 134–142 [hep-ph/0107001]. 33

[31] C. W. Bauer, D. Pirjol and I. W. Stewart, *Soft-Collinear Factorization in Effective Field Theory*, *Phys. Rev.* **D65** (2002) 054022 [hep-ph/0109045]. 33

[32] M. Beneke, A. P. Chapovsky, M. Diehl and T. Feldmann, *Soft-collinear effective theory and heavy-to-light currents beyond leading power*, *Nucl. Phys.* **B643** (2002) 431–476 [hep-ph/0206152]. 33

[33] M. Beneke and T. Feldmann, *Multipole-expanded soft-collinear effective theory with non-abelian gauge symmetry*, *Phys. Lett.* **B553** (2003) 267–276 [hep-ph/0211358]. 33, 44, 55, 57

[34] R. J. Hill and M. Neubert, *Spectator interactions in soft-collinear effective theory. ((U))*, *Nucl. Phys.* **B657** (2003) 229–256 [hep-ph/0211018]. 33, 62

[35] T. Becher, *Lectures on Soft-Collinear Effective Theory*, *http://www.becher.itp.unibe.ch/scet/index.html*. 33

[36] T. Becher, A. Broggio and A. Ferroglia, *Introduction to Soft-Collinear Effective Theory*, *in preparation*. 33

[37] T. Becher and M. D. Schwartz, *A Precise determination of α_s from LEP thrust data using effective field theory*, *JHEP* **0807** (2008) 034 [0803.0342]. 34

[38] T. Becher, G. Bell and S. Marti, *NNLO soft function for electroweak boson production at large transverse momentum*, *JHEP* **1204** (2012) 034 [1201.5572]. 34

[39] V. Ahrens, T. Becher, M. Neubert and L. L. Yang, *Updated Predictions for Higgs Production at the Tevatron and the LHC*, *Phys.Lett.* **B698** (2011) 271–274 [1008.3162]. 34

[40] V. Ahrens, A. Ferroglia, M. Neubert, B. D. Pecjak and L. L. Yang, *Threshold expansion at order α_s^4 for the t-tbar invariant mass distribution at hadron colliders*, *Phys. Lett.* **B687** (2010) 331–337 [0912.3375]. 34

[41] A. Ferroglia, B. D. Pecjak and L. L. Yang, *Soft-gluon resummation for boosted top-quark production at hadron colliders*, *Phys.Rev.* **D86** (2012) 034010 [1205.3662]. 34

[42] M. Beneke and V. A. Smirnov, *Asymptotic expansion of Feynman integrals near threshold*, *Nucl. Phys.* **B522** (1998) 321–344 [hep-ph/9711391]. 34

[43] V. A. Smirnov, *Applied asymptotic expansions in momenta and masses*, *Springer Tracts Mod. Phys.* **177** (2002) 1–262. 34, 38

[44] B. Jantzen, *Foundation and generalization of the expansion by regions*, *JHEP* **1112** (2011) 076 [1111.2589]. 38

[45] M. Bohm, A. Denner and H. Joos, *Gauge theories of the strong and electroweak interaction*, . Stuttgart, Germany: Teubner (2001) 784 p. 54

[46] P. A. Baikov, K. G. Chetyrkin, A. V. Smirnov, V. A. Smirnov and M. Steinhauser, *Quark and gluon form factors to three loops*, *Phys. Rev. Lett.* **102** (2009) 212002 [0902.3519]. 64

[47] T. Gehrmann, E. W. N. Glover, T. Huber, N. Ikizlerli and C. Studerus, *The quark and gluon form factors to three loops in QCD through to $O(\epsilon^2)$*, *JHEP* **11** (2010) 102 [1010.4478]. 64

[48] D. E. Soper, *Parton distribution functions*, *Nucl. Phys. Proc. Suppl.* **53** (1997) 69–80 [hep-lat/9609018]. 70

[49] A. V. Belitsky, *Two-loop renormalization of Wilson loop for Drell-Yan production*, *Phys. Lett.* **B442** (1998) 307–314 [hep-ph/9808389]. 76

[50] S. Dawson, E. Eichten and C. Quigg, *Search for supersymmetric particles in hadron-hadron collisions*, *Phys.Rev.* **D31** (1985) 1581. 82

[51] P. Chiappetta, J. Soffer and P. Taxil, *Spin asymmetries for scalar leptons from W and Z decay in $p\bar{p}$ collisions*, *Phys.Lett.* **B162** (1985) 192. 82

[52] F. del Aguila and L. Ametller, *On the detectability of sleptons at large hadron colliders*, *Phys.Lett.* **B261** (1991) 326–333. 82

[53] H. Baer, C.-h. Chen, F. Paige and X. Tata, *Detecting sleptons at hadron colliders and supercolliders*, *Phys.Rev.* **D49** (1994) 3283–3290 [hep-ph/9311248]. 82

[54] G. Altarelli, R. Ellis and G. Martinelli, *Large perturbative corrections to the Drell-Yan process in QCD*, *Nucl.Phys.* **B157** (1979) 461. 82

[55] R. Hamberg, W. van Neerven and T. Matsuura, *A complete calculation of the order α_s^2 correction to the Drell-Yan K factor*, *Nucl.Phys.* **B359** (1991) 343–405. 82

[56] R. V. Harlander and W. B. Kilgore, *Next-to-next-to-leading order Higgs production at hadron colliders*, *Phys.Rev.Lett.* **88** (2002) 201801 [hep-ph/0201206]. 82

[57] C. Anastasiou, L. J. Dixon, K. Melnikov and F. Petriello, *Dilepton rapidity distribution in the Drell-Yan process at NNLO in QCD*, *Phys.Rev.Lett.* **91** (2003) 182002 [hep-ph/0306192]. 82, 85, 96

[58] C. Anastasiou, L. J. Dixon, K. Melnikov and F. Petriello, *High precision QCD at hadron colliders: electroweak gauge boson rapidity distributions at NNLO*, *Phys.Rev.* **D69** (2004) 094008 [hep-ph/0312266]. 82

[59] K. Melnikov and F. Petriello, *The W boson production cross section at the LHC through $\mathcal{O}(\alpha_s^2)$*, *Phys.Rev.Lett.* **96** (2006) 231803 [hep-ph/0603182]. 82

[60] K. Melnikov and F. Petriello, *Electroweak gauge boson production at hadron colliders through $\mathcal{O}(\alpha_s^2)$*, *Phys.Rev.* **D74** (2006) 114017 [hep-ph/0609070]. 82

[61] S. Dittmaier and M. Huber, *Radiative corrections to the neutral-current Drell-Yan process in the Standard Model and its minimal supersymmetric extension*, *JHEP* **1001** (2010) 060 [0911.2329]. 82, 85

[62] G. F. Sterman and W. Vogelsang, *Threshold resummation and rapidity dependence*, *JHEP* **0102** (2001) 016 [hep-ph/0011289]. 83

[63] V. Ravindran, J. Smith and W. van Neerven, *QCD threshold corrections to di-lepton and Higgs rapidity distributions beyond N^2LO*, *Nucl.Phys.* **B767** (2007) 100–129 [hep-ph/0608308]. 83

[64] V. Ravindran and J. Smith, *Threshold corrections to rapidity distributions of Z and $W^{\pm}$ bosons beyond N^2LO at hadron colliders*, *Phys.Rev.* **D76** (2007) 114004 [0708.1689]. This paper is dedicated to the memory of W.L.G.A.M. van Neerven. 83

[65] A. Broggio, M. Neubert and L. Vernazza, *Soft-gluon resummation for slepton-pair production at hadron colliders*, *JHEP* **1205** (2012) 151 [1111.6624]. 83

[66] T. Becher and M. Neubert, *Drell-Yan production at small q_T, transverse parton distributions and the collinear anomaly*, *Eur. Phys. J.* **C71** (2011) 1665 [1007.4005]. 84

[67] G. Bozzi, B. Fuks and M. Klasen, *Joint resummation for slepton pair production at hadron colliders*, *Nucl.Phys.* **B794** (2008) 46–60 [0709.3057]. 85

[68] T. Gehrmann, T. Huber and D. Maitre, *Two-loop quark and gluon form-factors in dimensional regularisation*, *Phys.Lett.* **B622** (2005) 295–302 [hep-ph/0507061]. 86

[69] T. Gehrmann, E. Glover, T. Huber, N. Ikizlerli and C. Studerus, *Calculation of the quark and gluon form factors to three loops in QCD*, *JHEP* **1006** (2010) 094 [1004.3653]. 86

[70] A. Martin, W. Stirling, R. Thorne and G. Watt, *Parton distributions for the LHC*, *Eur.Phys.J.* **C63** (2009) 189–285 [0901.0002]. 87

[71] A. Martin, W. Stirling, R. Thorne and G. Watt, *Uncertainties on α_s in global PDF analyses and implications for predicted hadronic cross sections*, *Eur.Phys.J.* **C64** (2009) 653–680 [0905.3531]. 87

[72] J. A. Aguilar-Saavedra, A. Ali, B. C. Allanach, R. L. Arnowitt, H. A. Baer *et. al.*, *Supersymmetry parameter analysis: SPA convention and project*, *Eur.Phys.J.* **C46** (2006) 43–60 [hep-ph/0511344]. 92

[73] B. Allanach, M. Battaglia, G. Blair, M. S. Carena, A. De Roeck *et. al.*, *The Snowmass points and slopes: Benchmarks for SUSY searches*, *Eur.Phys.J.* **C25** (2002) 113–123 [hep-ph/0202233]. 92

[74] W. Beenakker, R. Hopker and M. Spira, *PROSPINO: A Program for the production of supersymmetric particles in next-to-leading order QCD*, hep-ph/9611232. 99, 109, 119

[75] W. Hollik, M. Kollar and M. K. Trenkel, *Hadronic production of top-squark pairs with electroweak NLO contributions*, *JHEP* **0802** (2008) 018 [0712.0287]. 99

[76] M. Beccaria, G. Macorini, L. Panizzi, F. Renard and C. Verzegnassi, *Stop-antistop and sbottom-antisbottom production at LHC: A One-loop search for model parameters dependence*, *Int.J.Mod.Phys.* **A23** (2008) 4779–4810 [0804.1252]. 99

[77] W. Beenakker, R. Hopker, M. Spira and P. Zerwas, *Squark and gluino production at hadron colliders*, *Nucl.Phys.* **B492** (1997) 51–103 [hep-ph/9610490]. 99

[78] W. Beenakker, S. Brensing, M. Kramer, A. Kulesza, E. Laenen *et. al.*, *Supersymmetric top and bottom squark production at hadron colliders*, *JHEP* **1008** (2010) 098 [1006.4771]. 99, 101

[79] N. Kidonakis, E. Laenen, S. Moch and R. Vogt, *Sudakov resummation and finite order expansions of heavy quark hadroproduction cross-sections*, *Phys.Rev.* **D64** (2001) 114001 [hep-ph/0105041]. 101

[80] J. C. Collins, D. E. Soper and G. F. Sterman, *Factorization of Hard Processes in QCD*, *Adv.Ser.Direct.High Energy Phys.* **5** (1988) 1–91 [hep-ph/0409313]. 101

[81] T. Becher and M. Neubert, *On the Structure of Infrared Singularities of Gauge-Theory Amplitudes*, *JHEP* **06** (2009) 081 [0903.1126]. 106

[82] T. Becher and M. Neubert, *Infrared singularities of QCD amplitudes with massive partons*, *Phys. Rev.* **D79** (2009) 125004 [0904.1021]. [Erratum-ibid.D80:109901,2009]. 106, 146

[83] A. Ferroglia, M. Neubert, B. D. Pecjak and L. L. Yang, *Two-loop divergences of massive scattering amplitudes in non-abelian gauge theories*, *JHEP* **11** (2009) 062 [0908.3676]. 106, 107, 112

[84] P. Nogueira, *Automatic Feynman graph generation*, *J.Comput.Phys.* **105** (1993) 279–289. 108

[85] A. Denner, H. Eck, O. Hahn and J. Kublbeck, *Compact Feynman rules for Majorana fermions*, *Phys.Lett.* **B291** (1992) 278–280. 108

[86] A. Denner, H. Eck, O. Hahn and J. Kublbeck, *Feynman rules for fermion number violating interactions*, *Nucl.Phys.* **B387** (1992) 467–484. 108

[87] J. Vermaseren, *New features of FORM*, math-ph/0010025. 108

[88] M. Veltman, *Diagrammatica*, . 108

[89] C. Studerus, *Reduze-Feynman Integral Reduction in C++*, *Comput.Phys.Commun.* **181** (2010) 1293–1300 [0912.2546]. 109

[90] A. von Manteuffel and C. Studerus, *Reduze 2 - Distributed Feynman Integral Reduction*, 1201.4330. 109

[91] G. Passarino and M. Veltman, *One Loop Corrections for e+ e- Annihilation Into mu+ mu- in the Weinberg Model*, *Nucl.Phys.* **B160** (1979) 151. 109

[92] T. Hahn and M. Perez-Victoria, *Automatized one loop calculations in four-dimensions and D-dimensions*, *Comput.Phys.Commun.* **118** (1999) 153–165 [hep-ph/9807565]. 109

[93] R. K. Ellis and G. Zanderighi, *Scalar one-loop integrals for QCD*, *JHEP* **0802** (2008) 002 [0712.1851]. 109

[94] A. van Hameren, *OneLOop: For the evaluation of one-loop scalar functions*, *Comput.Phys.Commun.* **182** (2011) 2427–2438 [1007.4716]. 109

[95] S. AbdusSalam, B. Allanach, H. Dreiner, J. Ellis, U. Ellwanger *et. al.*, *Benchmark Models, Planes, Lines and Points for Future SUSY Searches at the LHC*, *Eur.Phys.J.* **C71** (2011) 1835 [1109.3859]. 114, 115, 118, 121, 122

[96] V. Ahrens, A. Ferroglia, M. Neubert, B. D. Pecjak and L. L. Yang, *Precision predictions for the t+t(bar) production cross section at hadron colliders*, *Phys.Lett.* **B703** (2011) 135–141 [1105.5824]. 116, 117

[97] M. Neubert *Eur.Phys.J.* **C40** (2005) 165–186 [hep-ph/0408179]. 144

[98] S. Moch, J. A. M. Vermaseren and A. Vogt, *The three-loop splitting functions in QCD: The non-singlet case*, *Nucl. Phys.* **B688** (2004) 101–134 [hep-ph/0403192]. 145

[99] S. Moch, J. A. M. Vermaseren and A. Vogt, *The quark form factor at higher orders*, *JHEP* **08** (2005) 049 [hep-ph/0507039]. 145, 146

[100] G. Korchemsky and A. Radyushkin, *Renormalization of the Wilson Loops Beyond the Leading Order*, *Nucl.Phys.* **B283** (1987) 342–364. 146

[101] G. Korchemsky and A. Radyushkin, *Infrared factorization, Wilson lines and the heavy quark limit*, *Phys.Lett.* **B279** (1992) 359–366 [hep-ph/9203222]. 146

[102] N. Kidonakis, *Two-loop soft anomalous dimensions and NNLL resummation for heavy quark production*, *Phys.Rev.Lett.* **102** (2009) 232003 [0903.2561]. 146

[103] G. Korchemsky and G. Marchesini, *Resummation of large infrared corrections using Wilson loops*, *Phys.Lett.* **B313** (1993) 433–440. 150